

# INAUGURAL-DISSERTATION

zur Erlangung der Doktorwürde  
der Naturwissenschaftlich-Mathematischen Gesamtfakultät  
der  
RUPRECHT-KARLS-UNIVERSITÄT  
HEIDELBERG

vorgelegt von  
**Dipl. Math. Alexandra Köthe**  
aus Potsdam-Babelsberg

Tag der mündlichen Prüfung:.....



---

# Hysteresis-driven pattern formation in Reaction-Diffusion-ODE models

---

Gutachter: Prof. Dr. Anna Marciniak-Czochra

.....



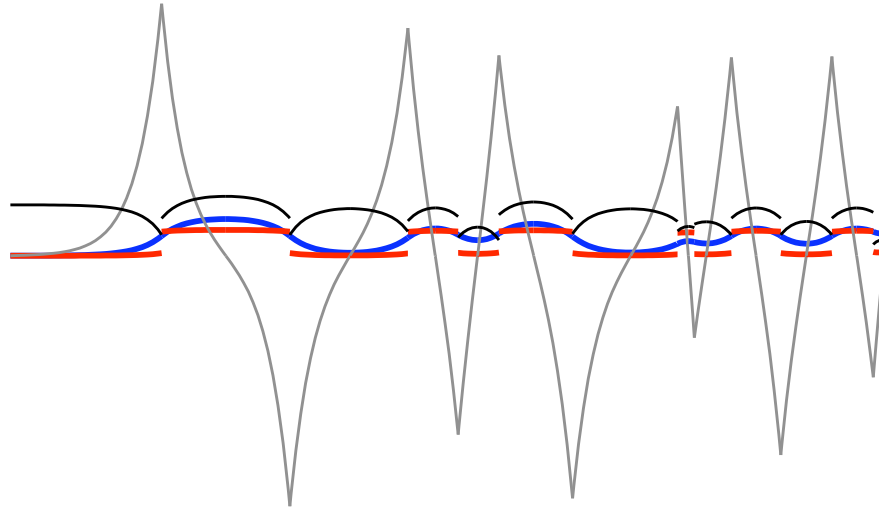


Figure: An irregular solution of the generic model in the hysteresis case with several jumps



To My Parents



## Abstract

Processes containing multistability and switching play an important role in cell signalling. Coupled to cell-to-cell communication of diffusing ligands such processes may give rise to spatial pattern in biological systems. This leads to a new type of mathematical models consisting of nonlinear partial differential equations of diffusion, transport and reactions coupled with dynamical systems controlling the transitions.

In this thesis we propose a model consisting of one reaction-diffusion equation with homogeneous Neumann boundary conditions coupled to one ordinary differential equation containing bistability in the kinetic functions. We analyse the ability of our model to produce patterns. Therefore, we compare two cases of the model, where one does include the hysteresis effect and the second one does not.

We show that the model without hysteresis in the kinetic functions is not able to describe pattern formation, because all spatially inhomogeneous stationary solutions are unstable.

Furthermore, we prove that the model including hysteresis possesses an infinite number of stationary solutions. There are monotone and periodic solutions. Moreover, we prove the existence of irregular solutions, which, restricted to certain intervals, consist of different monotone ones. All stationary solutions are discontinuous in one component. Furthermore, we show under which conditions on the parameters a plurality of these solutions is stable.

Since the mechanism for pattern formation in our model is different from the usual Turing mechanism, patterns do not evolve spontaneously from small perturbations, but they need a sufficiently strong external signal for their emergence. In terms of our model we prove that there is coexistence of different patterns for the same set of parameters, with the final pattern strongly depending on the initial perturbation.



## Zusammenfassung

Prozesse mit Multistabilität und Switches spielen eine wichtige Rolle in intrazellulärer Signalübertragung. Gekoppelt mit Kommunikation zwischen Zellen durch diffundierende Liganden führen solche Prozesse zur Bildung räumlicher Muster in biologischen Systemen. Dies führt zu einer neuen Klasse mathematischer Modelle bestehend aus nichtlinearen partiellen Differentialgleichungen für Diffusion, Transport und Reaktionen gekoppelt mit dynamischen Systemen, die die Übergänge kontrollieren.

In dieser Arbeit stellen wir ein Modell vor, das aus einer Reaktions-Diffusionsgleichung mit homogenen Neumann-Randbedingungen gekoppelt mit einer gewöhnlichen Differentialgleichung mit Bistabilität in den kinetischen Funktionen besteht. Wir untersuchen die Fähigkeit des Modells Musterbildungsprozesse zu beschreiben. Wir vergleichen eine Variante des Modells mit Bistabilität und Hysterese mit einer mit Bistabilität, aber ohne Hysterese.

Wir zeigen, dass das Modell ohne Hysterese nicht in der Lage ist, Musterbildung zu beschreiben, da alle räumlich inhomogenen stationären Lösungen instabil sind.

Des Weiteren beweisen wir in dieser Arbeit, dass das Modell mit Hysterese unendlich viele stationäre Lösungen besitzt. Es gibt monotone sowie periodische Lösungen. Außerdem beweisen wir die Existenz von irregulären Lösungen, die eingeschränkt auf gewisse Intervalle monotone Lösungen sind. Alle stationären Lösungen sind unstetig in einer Komponente. Außerdem untersuchen wir, unter welchen Bedingungen für die Parameter eine Vielzahl dieser Lösungen stabil ist.

Da der Mechanismus für Musterbildung in unserem Modell sich vom üblichen Turing-Mechanismus unterscheidet, entstehen Muster nicht aus kleinen Störungen, sondern benötigen ein ausreichend starkes externes Signal für ihre Entstehung. Wir beweisen, dass es in unserem Modell Koexistenz verschiedener Muster für den gleichen Satz von Parametern gibt, wobei das finale Muster stark von der Ausgangsstörung des Systems abhängt.

## Acknowledgements

First of all I would like to thank my supervisor Prof. Dr. Anna Marciniak-Czochra. She introduced me to the field of mathematical biology and in particular to reaction-diffusion systems. She gave me the opportunity to work on the presented topic and supported me during the time of my thesis.

I am grateful for the support of Prof. Izumi Takagi. I thank him for teaching me a lot about layer positions and the SLEP method. I am very happy that I could visit him in Sendai and enjoyed my stay there very much.

I thank Prof. Grzegorz Karch for giving me fruitful advice to my work. I thank him for giving me the opportunity to come to Wroclaw and to work on the stability of discontinuous solutions. Moreover, he made me realise that it is worth to investigate irregular solutions.

I thank Franziska Knauer, Marcel Mohr and Dr. Andreas Rüdinger for proofreading this thesis and giving me useful suggestions how to improve it.

I thank my parents for supporting me during the whole time of my studies.

Last but not least, I thank Krzysztof for believing in me when I did not.

This work was financed by the Starting grant IDEAS of European Research Council. “Multiscale mathematical modelling of dynamics of structure formation in cell systems”

# Contents

<b>Abstract</b>	<b>i</b>
<b>Zusammenfassung</b>	<b>iii</b>
<b>Acknowledgements</b>	<b>iv</b>
<b>Contents</b>	<b>v</b>
<b>List of Figures</b>	<b>vii</b>
<b>1 Introduction</b>	<b>1</b>
1.1 Pattern formation in developmental biology . . . . .	1
1.2 The model organism Hydra . . . . .	3
1.3 Bistability and hysteresis in cell signalling . . . . .	5
1.4 Outline of the thesis . . . . .	6
<b>2 Presentation of the model and basic properties</b>	<b>11</b>
2.1 Presentation of the generic model . . . . .	11
2.2 Stability of constant steady states . . . . .	18
2.3 Global existence of solutions . . . . .	20
2.4 Global attractors for the kinetic system . . . . .	32
2.5 Summary . . . . .	38
<b>3 Instability of stationary solutions for the bistable case</b>	<b>41</b>
3.1 Construction of stationary solutions . . . . .	41
3.2 Instability of stationary solutions . . . . .	55
3.3 Summary . . . . .	59
<b>4 Construction and stability of discontinuous stationary solutions</b>	<b>61</b>
4.1 Phase plane analysis . . . . .	61
4.2 The potential . . . . .	66
4.3 The time-maps . . . . .	68

---

4.4	Stability of discontinuous stationary solutions . . . . .	77
4.5	Summary . . . . .	91
<b>5</b>	<b>Properties of stationary solutions</b>	<b>93</b>
5.1	Dependence of the jump . . . . .	93
5.2	The layer position depending on the jump . . . . .	102
5.3	The role of the diffusion coefficient . . . . .	108
5.4	Irregular solutions . . . . .	119
5.5	Summary . . . . .	141
<b>6</b>	<b>Summary and Outlook</b>	<b>143</b>
<b>A</b>	<b>Models for pattern formation in Hydra</b>	<b>147</b>
A.1	Activator-inhibitor model . . . . .	147
A.2	Receptor-based models . . . . .	147
	<b>Bibliography</b>	<b>149</b>

# List of Figures

1.1	The grafting experiment for Hydra . . . . .	4
2.1	Typical configurations of the zero sets of the kinetic functions . . . . .	14
2.2	The functions $q_H(u)$ and $q_T(u)$ with critical values $u_H^{cr}$ and $u_T^{cr}$ . . . . .	18
2.3	The phase plane divided into five subareas. . . . .	34
2.4	The phase plane for the kinetic system. . . . .	36
2.5	Simulations of the generic model in the hysteresis case for different initial conditions. . . . .	39
3.1	A stationary solution of the generic system in the bistable case. . . . .	42
3.2	The phase plane in the bistable case. . . . .	44
3.3	The potential $Q$ in the bistable case . . . . .	45
3.4	The time-maps in the bistable case. . . . .	53
3.5	Two kinetic functions in the bistable case. . . . .	54
3.6	Simulations of the generic model in the bistable case. . . . .	57
4.1	Phase planes for $\frac{1}{\gamma}U_{xx} + q_H(U) = 0$ and $\frac{1}{\gamma}U_{xx} + q_T(U) = 0$ 'glued' together at $\bar{u}$ . . . . .	63
4.2	A monotone increasing solution of $\frac{1}{\gamma}U_{xx} + q_{\bar{u}}(U) = 0$ . . . . .	64
4.3	A possible configuration of kinetic functions $f$ and $g$ , together with the function $F$ and the potential $Q_{\bar{u}}$ for increasing values of $\bar{u}$ . . . . .	67
4.4	The time-maps in the hysteresis case. . . . .	76
4.5	Simulations of the generic model in the hysteresis case for different types of perturbations of a stationary solution. . . . .	78
4.6	Simulations of the generic model in the hysteresis case for admissible kinetic functions. . . . .	88
4.7	Simulations of the generic model in the hysteresis case for admissible kinetic functions. . . . .	89
4.8	Simulations of the generic model in the hysteresis case for admissible kinetic functions. . . . .	90
4.9	Simulations of the generic model in the hysteresis case for kinetic functions which are not admissible. . . . .	90

---

5.1	The potential $Q(\bar{u}, u)$ in the hysteresis case. . . . .	94
5.2	Plots $u_0(\bar{u})$ and $u_e(\bar{u})$ as function of the jump $\bar{u}$ for kinetic functions possessing a value $u^*$ . . . . .	98
5.3	Plots of $u_0(\bar{u})$ and $u_e(\bar{u})$ as function of the jump $\bar{u}$ for kinetic functions not possessing a value $u^*$ . . . . .	99
5.4	The layer position $\bar{x}(\bar{u})$ is decreasing as function of the jump $\bar{u}$ . . . . .	107
5.5	Simulations of stationary solutions for different diffusion coefficients. . . . .	109
5.6	A periodic stationary solution with six modes . . . . .	120
5.7	Overlapping phase planes of $\frac{1}{\gamma}U_{xx} + q_H(U) = 0$ and $\frac{1}{\gamma}U_{xx} + q_T(U) = 0$ with trajectories for periodic and irregular solutions. . . . .	121
5.8	An irregular solution with three jumps. . . . .	123
5.9	Overlapping phase planes of $\frac{1}{\gamma}U_{xx} + q_H(U) = 0$ and $\frac{1}{\gamma}U_{xx} + q_T(U) = 0$ with trajectories which cannot be connected. . . . .	127
5.10	Irregular solutions with five jumps for admissible kinetic functions with $u^*$ . . . . .	133
5.11	Irregular solutions with five jumps for admissible kinetic functions with $u^*$ . . . . .	134
5.12	Irregular solutions with five jumps for admissible kinetic functions with $Q(\bar{u}, u_2) < 0$ . . . . .	135
5.13	Irregular solutions with five jumps for admissible kinetic functions with $Q(\bar{u}, u_2) > 0$ . . . . .	136
5.14	Simulations of the generic model in the hysteresis case for admissible kinetic functions with $u^*$ . . . . .	139
5.15	Simulations of the generic model in the hysteresis case for admissible kinetic functions with $Q(\bar{u}, u_2) < 0$ . . . . .	139
5.16	Simulations of the generic model in the hysteresis case for admissible kinetic functions with $Q(\bar{u}, u_2) > 0$ . . . . .	140
5.17	Simulations of the generic model in the hysteresis case which simulate the grafting experiments for Hydra. . . . .	141

# Chapter 1

## Introduction

This work is devoted to the mathematical analysis of a model for pattern formation in biological systems. It is motivated by a model for pattern formation in Hydra and includes bistability and hysteresis in its kinetic functions. We explain in the following the importance of mathematical modelling to understand pattern formation in developmental biology, in particular of the model organism Hydra. Moreover, we highlight the significance of bistability and hysteresis in cell signalling and how it can be modelled mathematically.

### 1.1 Pattern formation in developmental biology

Pattern formation is a widely occurring process in nature. There is an astonishing variety of structures arising in physical, chemical and biological systems. They range from sand dunes to animal coat markings, and from precipitation patterns in chemical reactions to bacterial colonies [Bal12] [HJ80].

To understand the principles underlying these processes mathematical modelling is crucial and has helped to identify relevant mechanisms.

Pattern formation in biological systems plays a key role in development of organisms. Here a spatial pattern is related to symmetry breaking what means a process where the embryo loses homogeneity and cells develop specialisation. This is one of the crucial issues in development together with growth regulation and the right timing of these events [Lew08].

Recent research in molecular biology has identified a huge amount of information concerning gene regulatory networks, signalling cascades and metabolic pathways. The next step is to understand how signals, exchanged inside and between cells, drive the formation of macroscopic pattern that we observe. We aim to figure out how the biochemical machinery is used for control of the behaviour of living cells [Lan11].

Basically, there exist two approaches how to apply modelling to investigate biochemical mechanisms. In the *bottom-up* approach one starts with knowledge how the parts of the system are connected to each other and infers the possible behaviour of the system. The underlying strategy is that it is only possible to understand the functioning of a system if one understands the functioning of its components and interactions. In the *top-down* approach one starts with the knowledge of the desired behaviour and constructs a system that fulfils this behaviour. Starting with such high-level representation allows to comprehend the building blocks of biochemical networks and guides the search for suitable components [TA07].

The most famous mechanism for pattern formation in biological systems is a top-down approach going back to Alan Turing [Tur51]. The Turing mechanism needs two diffusing molecules with different diffusion coefficients which react with each other. Turing identified conditions on the nonlinear interactions under which diffusion destabilises a stable spatially homogeneous stationary solution and may lead to the formation of heterogeneous structures. Turing also introduced the notation of a “morphogen”, a diffusing molecule determining the morphology of the embryo. The concentration of a morphogen is supplying “positional information” to the cells based on which cell fate decisions are made.

A well known implementation of this mechanism is the activator-inhibitor model of Gierer and Meinhardt [GM72]. Models based on Turings mechanism have been used to describe skin pigmentation patterning in fish [KA95], the establishment of the right-left asymmetry in vertebrates by the Nodal/Lefty system [Ham12], the creation of the Sog-Gradient related to dorsal-ventral polarity in *Drosophila* embryos, and many others [Mur03] [KM10].

The Turing mechanism has been very successfully used to describe biological pattern formation. But, for many biological systems it is still an open question which molecules should play the role, for example of the activator or the inhibitor. Moreover, models implementing the Turing mechanism are able to describe *de novo* pattern formation. Above a critical number of cells, they lose their homogeneity and start differentiation processes. This happens spontaneously and the final pattern does not depend on the initial perturbation.

In reality there is another kind of mechanism leading to pattern formation which plays an important role. This mechanism is due to some external signal triggering the differentiation. The signal can be set up by the maternal individual, for example the Bicoid gradient in *Drosophila* embryos, [GWM<sup>+</sup>07] or it originates from another group of cells, for example the Spemann organizer in amphibians [Nie01]. The signal must be sufficiently strong to generate patterns. The Turing mechanism cannot describe pattern formation which is set up by some external signal.

Thus, it is becoming more clear that morphogens alone are not sufficient for sup-

plying positional information in a robust and precise manner. Therefore additional or alternative mechanisms involving interactions among cells are supposed to be crucial [KW07].

Besides classical reaction-diffusion equations, the class of receptor-based models consisting of reaction-diffusion equations coupled to ODEs are very promising for explaining pattern formation. Pattern formation in such models can be due to the Turing mechanism [MC03] but a variety of other mechanisms is possible as well. Recently, criteria which are leading to unstable pattern have been studied in [MCKS13] for a certain class of kinetic functions.

## 1.2 The model organism Hydra

The fresh water polyp Hydra is the motivating example for our work. It is an evolutionary old organism and is known for its high regenerative and inductive capacities. Therefore, it has served as a model organism for developmental biology for several years [Gal12].

Hydra has a 5 to 15 mm long, tubular body with a whorl of tentacles surrounding the mouth at the upper end and a disk-shaped organ for adhesion at the lower end. The axial pattern is subdivided into a head, a gastric region, a budding zone, a stalk and a foot. The upper part of the head is called hypostome.

Hydra tissue is in a state of constant growth and tissue replacement, therefore axial patterning processes are permanently active, not only during development.

There are two kind of basic experiments which should be explained by every theory of pattern formation in Hydra.

**Cutting experiments:** The experiment consists of cutting a Hydra into parts.

One observes that all pieces of the Hydra body column having a minimal size regenerate and form a normal Hydra. By cutting at different levels, one can see that the same cells can form different parts of the body depending on their position along the body axis. Thus, cutting experiments suggest that there is a “positional information” telling the cells their position. Regeneration is without growth, thus, axial patterning processes reorganise the tissue.

**Grafting experiments:** The experiment consists of a transplantation of tissue from one Hydra to another one. The outcome of the experiment depends on the change of position along the body axis. If the change is sufficiently big, the transplantation yields the formation of a secondary body axis (Fig. 1.1). Using ink a difference between the hypostome and upper parts of the body axis has been shown. Grafting of hypostome tissue leads to the formation a secondary body axis, which consists mainly of host tissue. Grafting of upper

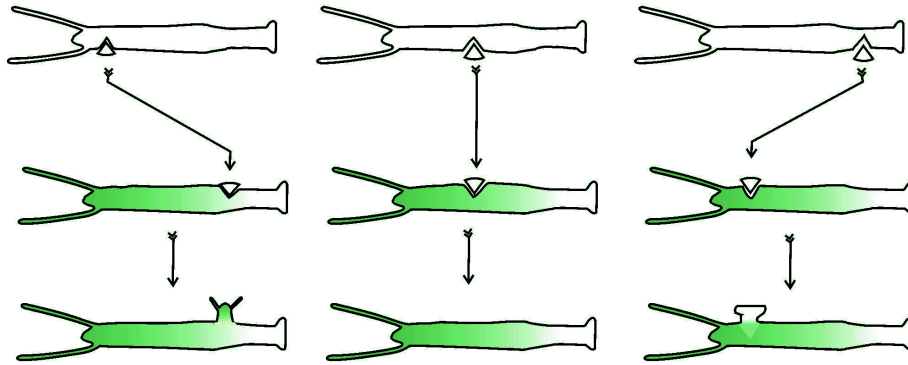


Figure 1.1: The grafting experiment for Hydra [Courtesy of W. Müller.]

parts of the body axis leads to the formation of a secondary body axis, which consists mainly of donor tissue [BB02]. Thus, the hypostome has the capacity to induce the fate of neighboring cells. The body axis has a self-organising capacity.

These experiments gave rise to the question how the positional information is transmitted to the cells and how the self-organising and inducing capacities are obtained.

One common theory is claiming the existence of two morphogen gradients set up by the hypostome - the head activation gradient and the head inhibition gradient - as well as a head organiser which leads to the formation of the hypostome [BGRB05] [BB02].

The questions related to the astonishing abilities of Hydra have motivated several mathematical models. Gierer and Meinhardt developed a model (see Appendix A.1 for the model equations) for the head activator and the head inhibitor which code the positional information for the cells [GM72]. The model allows to describe the self-organising capacities of Hydra, but fails to explain the grafting experiments. Different pattern in models based on the Turing mechanism are usually obtained due to growth of the domain.

In [SMJ95] a receptor-based model for pattern formation in Hydra has been introduced. It is based on the idea that positional information is provided by the density of bound receptors.

This idea has been further developed in [MC03] and [MC06] (see Appendix A.2), where several models consisting of reaction-diffusion equations coupled with ordinary differential equations have been proposed. These models describe binding and dissociation of diffusing ligands to receptors. The model including a hysteretic de-

pendence of the production of ligands on the amount of ligands present in a steady-state can explain head formation as well as the grafting experiments. Without hysteresis in the production rates for ligands and enzyme, the grafting experiments cannot be explained [MC03].

### 1.3 Bistability and hysteresis in cell signalling

The receptor-based model which could most suitably explain the axial patterning process in Hydra included hysteresis and bistability in its kinetic functions. Both processes are connected and play an important role in cell signalling for a variety of biological systems.

Bistability and hysteresis are important mechanisms which are relevant in biological systems to generate oscillations, switches between discrete states and to remember transient stimuli [AFS04]. They can create an all-or-non-response and transform a graded input signal into a discontinuous output. Moreover, it makes processes irreversible, which is of particular importance in development [FX01].

Bistability (or more general multistability) is a phenomenon taking place in systems which toggle between two (or more) stable equilibrium points. Between the stable ones there is an unstable intermediate equilibrium point working as a threshold. A mechanical example is a ball rolling between two different valley basins.

Hysteresis was first described for magnetic materials. It refers to a system where the output does not only depend on the input, but also on the history of the system. There may be different responses to the same input depending on the history of the system. In systems with bistability the system state often has a hysteretic dependence of a parameter involved. Below and above a certain range for the parameter there is only one stable steady state, but in the intermediate region the system state depends on the history.

One important example is the lactose operon in *Escheria Coli*. The allolactose, a sugar molecule, binds to the lactose repressor which, finally, leads to the blocking of a set of genes, the operon. The ordinary differential equation describing the dynamics of the intracellular concentration of allolactose shows a bistability and the extracellular concentration of allolactose has a hysteretic dependence of the intracellular concentration in the steady-state [LK99].

In [QX10] a model with hysteresis for calcium-mediated ciliary beat frequency was proposed. The efficiency of clearance of the mammalian airway is determined by the tip velocity of cilia on the inner surface of the airway and the degree of co-operative activity between cilia. Both are enhanced by increases in the ciliary beat frequency, which is related to intracellular  $\text{Ca}^{2+}$  concentration.

Another well-studied example is the *Xenopus* oocyte maturation [SMC<sup>+</sup>03] and early embryonic cell cycle of the frog *Xenopus laevis*, where hysteresis and bistability have been detected in the Cyclin-induced activation of Cdc2 [PSJ03].

Bistability was also found in Dpp-receptor interactions during *Drosophila* dorsal-ventral patterning [WF05] or in cell-fate choices in the *Drosophila* eye [GTDR10].

From the mathematical point of view it has been shown that bistability might occur in systems of ordinary differential equations containing a positive feedback loop or a mutually inhibitory feedback loop. A symmetrical set-up combining both kind of loops was shown to make it substantially easier to generate a robust bistable response [Fer08]. For more complicated systems conditions for the existence of bistability have been analysed in [AFS04].

In [Wil09] the smallest chemical reaction with bistability was presented. Using only the law of mass action, the minimal number of reactants, reactions and ordinary differential equations was determined. This clarified that three conditions are necessary for bistability: positive feedback, a mechanism to filter out small stimuli and a mechanism to prevent explosions.

Biological processes are regulated by non-linear intra-cellular processes which may be described by ordinary differential equations. Coupling such processes to cell-to-cell communication of diffusing signalling factors leads to spatial models of partial differential equations which also may include bistability and hysteresis.

A reaction-diffusion model with hysteresis for bacterial growth pattern has been proposed in [HJP83].

In [LVH<sup>+</sup>08] a reaction-diffusion model of Hunchback transcription with Bicoid cooperative binding and Hunchback selfregulation was used to show that bistability generates hunchback Expression sharpness in the *Drosophila* embryo.

A bisubstrate kinetic system with substrate inhibition embedded in a metabolic network may show hysteresis behaviour. Under certain conditions pattern which are not of Turing-type emerge [Kle98].

In [GT12] a reaction-diffusion equation involving a discontinuous hysteresis operator was analysed. It was shown the uniqueness time-dependent solutions for a certain class of initial conditions called transverse functions.

## 1.4 Outline of the thesis

The receptor-based model for pattern formation in *Hydra* proposed in [MC06] showed in numerical simulations the desired outcome which might explain patterning processes in *Hydra*. But, due to its size (two reaction-diffusion equations coupled with

four ordinary differential equations) it is difficult to analyse mathematically. On this account, we present in this thesis a reduced version of the receptor-based model with hysteresis (see Appendix A.2 for the models equations) which is called the *generic model*. The advantage of the generic model is that the kinetic functions are chosen in such a way that we are able to perform analytical investigations and do not have to rely exclusively on numerical experiments.

The generic model consists of one reaction-diffusion equation coupled with one ordinary differential equation and describes the dynamics of diffusing molecules. The model is a top-down approach to comprehend biological pattern formation in Hydra. The variable  $x$  corresponds to the position along the body axis of Hydra and  $u(t, x)$  is the concentration of a ligand at position  $x$  and time  $t$ . The production rate  $v$  of the ligands is modeled by an ordinary differential equation with bistability, which may be a macroscopic description of a more complicated biochemical network. Qualitatively, the shape of the kinetic functions in the steady-state is the same as for the original model in [MC06].

The equations of the generic model read

$$\begin{aligned} u_t &= \frac{1}{\gamma} u_{xx} + f(u, v) = \frac{1}{\gamma} u_{xx} + \alpha v - \beta u && \text{for } x \in (0, 1), t \in (0, \infty], \\ v_t &= g(u, v) = u - (a_2 v^3 + a_1 v^2 + a_0 v) && \text{for } x \in (0, 1), t \in (0, \infty]. \end{aligned}$$

These equations are supplemented with an initial condition and homogeneous Neumann boundary conditions for  $u$ .

This thesis is focused on the analysis of the generic model. We compare two cases of our model, one with bistability and a hysteretic dependence of the production rate of the concentration of the molecule in the steady state and the second one with bistability, but without hysteresis. We address the question of existence, uniqueness and stability of nonhomogeneous stationary solutions.

In **Chapter 2**, we introduce the model and identify suitable ranges for the parameters to obtain both cases of the model.

The model admits global-in-time nonnegative and bounded solutions and it does not exhibit diffusion-driven instability. Hence, all observed patterns are generated by a mechanism which is essentially different from the Turing mechanism.

As a first step to understand the mechanism for pattern formation in the generic model, we investigate the kinetic system and prove the existence of two stable steady states and one saddle. The stable manifold of the saddle represents a separatrix, i.e., trajectories starting on one side of the stable manifold are attracted by one of the stable steady states and those starting on the other side are attracted by the other one. We do not observe any essential difference between the two cases of the model. Therefore, heuristically we expect pattern formation in both cases provided

the initial condition has values on both sides of the stable manifold.

**Chapter 3** considers the behaviour of the model with bistability in the kinetic functions but without the hysteresis effect. We construct monotone and periodic stationary solutions by phase plane analysis, which are twice continuously differentiable. Analysing the spectrum of the system linearised at a stationary solution, we prove that all spatially inhomogeneous stationary solutions are unstable.

Primary ideas of Section 3.2 have been published in [MCK13]

In **Chapter 4**, we construct monotone stationary solutions of the model incarnating the hysteresis effect. Other than in the model without hysteresis it is not possible to construct solutions which are twice continuously differentiable. We choose a “jump value” which defines a switch between two branches of  $g = 0$ . For every jump there is a unique monotone increasing stationary solution. This is shown by the analysis of the time-map related to the equation. Every solution has a discontinuity in one component called the “layer position”.

Next, we address the problem of stability of stationary solutions. We show the asymptotic stability of solutions fulfilling a certain condition with respect to  $L^\infty$  perturbations. The discontinuity of the stationary solution causes that the application of spectral analysis to the linearised system is not possible. Therefore, a new method using the semigroup representation of the solution is developed. We obtain conditions for the parameters of the kinetic function and for the jump that lead to the formation of stable pattern.

Simulations of the time-dependent system suggest that the layer position of a stable stationary solution is set up by the choice of an initial condition. The layer position is determining the final pattern selection.

**Chapter 5** is motivated by the question how the layer position depends on the jump and the diffusion coefficient. The aim is to understand for which kinetic functions which choices of initial conditions lead to stable pattern.

Therefore, we consider all functions involved in the analysis of stationary solutions as functions of the jump. We show that for the same conditions on the jumps which lead to stable stationary solutions, the layer position is monotone decreasing as a function of the jump. Moreover, this function has a steep slope at a certain value  $u^*$ , such that both local maxima of the potential are equal. For the jump  $u^*$ , the stationary solution has an interior transition layer, whereas it has a boundary transition layer in all other cases. To better understand this behaviour, we showed that the layer position is moving more to the boundary for decreasing diffusion coefficient.

Hence, for kinetic functions such that there is a value  $u^*$ , a big range of layer positions is obtained for a very small interval of jumps near  $u^*$ . If, moreover,  $u^*$  lies in the

interval of jumps leading to stable stationary solutions, we obtain for a big variety of initial conditions stable stationary solutions.

Finally, we construct all possible stationary solutions of the problem. Besides periodic ones, there is another class of solutions which we call irregular. They are composed out of monotone solutions which may have different jumps. We discuss their existence as well as their layer positions. Importantly, we show under which conditions an irregular solution exists with a prescribed set of layer positions depending on the diffusion coefficient.



# Chapter 2

## Presentation of the model and basic properties

### 2.1 Presentation of the generic model

We study the system

$$\begin{aligned}u_t &= \frac{1}{\gamma}u_{xx} + f(u, v) \\v_t &= g(u, v)\end{aligned}\tag{2.1}$$

for  $x \in (0, 1)$ ,  $t > 0$  with homogeneous Neumann boundary condition for  $u$

$$u_x(t, 0) = u_x(t, 1) = 0\tag{2.2}$$

and initial conditions

$$u(0, x) = u_0(x) \quad v(0, x) = v_0(x).\tag{2.3}$$

The kinetic functions are chosen to be

$$\begin{aligned}f(u, v) &= \alpha v - \beta u, \\g(u, v) &= u - p(v),\end{aligned}\tag{2.4}$$

where  $\alpha, \beta$  are positive constants and  $p(v)$  is a polynomial of degree three with only one real root at  $v = 0$ . We assume that there are three intersection points of  $f = 0$  and  $g = 0$  with nonnegative coordinates

$$S_0 = (0, 0), S_1 = (u_1, v_1) \quad \text{and} \quad S_2 = (u_2, v_2).\tag{2.5}$$

This system is called the **generic model**. We will distinguish two cases of the kinetic functions and use the following terminology:

**Bistable case:** The polynomial  $p(v)$  is monotone increasing.

**Hysteresis case:** The polynomial  $p(v)$  is nonmonotone. In this case we denote by  $H = (u_H, v_H) = (p(v_H), v_H)$  the local maximum of  $v \mapsto p(v)$  and by  $T = (u_T, v_T) = (p(v_T), v_T)$  the local minimum of  $v \mapsto p(v)$ . Moreover, we assume that the coordinates of  $H$  and  $T$  are positive and that  $\lim_{v \rightarrow +\infty} p(v) = +\infty$  holds.

We will show in Section 2.2 that both cases show bistability. Thus, the bistable case refers to a model with bistability, but without hysteresis, whereas the hysteresis case refers to a models with both, bistability and hysteresis.

The generic model in the hysteresis case can be seen as a reduced version of the receptor-based model with hysteresis of Marciniak-Czochra [MC06] (cf. Appendix A.2 for the model equations). We focus on the behaviour of the ligand concentration in this model. Using a quasi-steady-state approximation the six-component model can be reduced to equations of the form (2.1) with  $u$  denoting the concentration of the ligands and  $v$  the production rate of the ligands.  $x$  corresponds to the position along the Hydra body axis and if the concentration of ligands is above some threshold, there is the formation of a head. The properties of the kinetic functions for this reduced model are the following: The kinetic system shows bistability. The function  $f(u, v)$  is growing in  $v$  and decaying in  $u$ . Moreover, in the steady state the production rate has a hysteretic dependence on the concentration of ligands. This means that  $g(u, v) = 0$  is S-shaped.

Our aim is to capture these properties of the receptor-based model, but with kinetic functions which are as simple as possible. Therefore, we choose  $f$  as a linear function which is growing in  $v$  and decaying in  $u$ . The term  $-\beta u$  refers to the decay of ligands and  $\alpha v$  to its production. The simplest way of obtaining a function  $g$ , such that  $g(u, v) = 0$  is S-shaped, is by taking a polynomial of degree three, which is nonmonotone.

As also a monotone polynomial of degree three can lead to a bistable system, but without the hysteresis effect, we investigate the generic model for monotone and nonmonotone polynomials. This allows us to grasp the key features of pattern formation in such a system.

**Remark 2.1.1.** *In the remainder of this thesis, we will state our choice of kinetic functions by noting the function  $f(u, v)$  and the polynomial  $p(v)$ .*

First, we derive the parameter spaces leading to each of the cases.

**Proposition 2.1.2.** *In both, the bistable and the hysteresis case, the coefficients of the polynomial  $p(v) = a_2 v^3 + a_1 v^2 + a_0 v$  and the straight line  $f(u, v) = \alpha v - \beta u$  satisfy*

$$a_2 > 0, a_1 < 0, a_0 > \frac{\alpha}{\beta} \quad \text{and} \quad a_1^2 > 4a_2 \left( a_0 - \frac{\alpha}{\beta} \right).$$

Furthermore, in the bistable case the condition

$$0 < \frac{a_1^2}{a_0 a_2} < 3$$

has to be fulfilled, whereas in the hysteresis case the condition

$$3 < \frac{a_1^2}{a_0 a_2} < 4$$

is necessary.

*Proof.* First, we notice that the polynomial  $p(v)$  has no constant term, as we assume that  $p(0) = 0$ . Moreover, we observe that  $\lim_{v \rightarrow \infty} p(v) = +\infty$  holds in the hysteresis case as well as in the bistable case, which induces that the leading coefficient  $a_2$  of  $p(v)$  has to be positive.

We choose the coefficients to ensure the existence of three different intersection points  $S_0, S_1$  and  $S_2$ . These points are solutions of  $f(u, v) = 0$  and  $g(u, v) = 0$ , therefore the  $v$ -coordinates of the intersection points are solutions of the following equation

$$p(v) - \frac{\alpha}{\beta}v = a_2 v \cdot \left( v^2 + \frac{a_1}{a_2}v + \frac{1}{a_2} \left( a_0 - \frac{\alpha}{\beta} \right) \right) = 0. \quad (2.6)$$

The polynomial  $v^2 + \frac{a_1}{a_2}v + \frac{1}{a_2} \left( a_0 - \frac{\alpha}{\beta} \right)$  has two solutions with positive real parts if its trace  $\frac{a_1}{a_2}$  is negative and its determinant  $\frac{1}{a_2} \left( a_0 - \frac{\alpha}{\beta} \right)$  is positive. This yields the condition  $a_1 < 0$  and  $a_0 > \frac{\alpha}{\beta}$ . These solutions are real if the discriminant  $\frac{1}{4a_2^2} \left( a_1^2 - 4a_2 \left( a_0 - \frac{\alpha}{\beta} \right) \right)$  is positive, which leads to the condition  $a_1^2 > 4a_2 \left( a_0 - \frac{\alpha}{\beta} \right)$ .

We have already shown that  $a_0$  and  $a_2$  are positive and therefore the condition  $0 < \frac{a_1^2}{a_0 a_2}$  holds. Next, we calculate the derivative  $p'(v) = 3a_2 v^2 + 2a_1 v + a_0$  and its discriminant  $4a_1^2 - 4 \cdot 3a_2 a_0$ . In the bistable case, we want  $p(v)$  to be monotone, hence the discriminant has to be negative and we obtain the condition  $\frac{a_1^2}{a_0 a_2} < 3$ .

In the hysteresis case, we want  $p'(v)$  to have zeros and therefore the discriminant has to be positive, which leads to  $\frac{a_1^2}{a_0 a_2} > 3$ . Moreover, we want  $p(v)$  to have exactly one zero which is at  $v = 0$  and therefore the polynomial  $a_2 v^2 + a_1 v + a_0$  is supposed to have no real zeros. This induces that the discriminant  $a_1^2 - 4a_0 a_2$  has to be negative. Hence  $\frac{a_1^2}{a_0 a_2} < 4$  holds.  $\square$

**Lemma 2.1.3.** *The coordinates of the intersection points  $S_0, S_1$  and  $S_2$  are given by*

$$v_0 = 0 \quad \text{and} \quad v_{1/2} = \frac{1}{2a_2} \left( -a_1 \pm \sqrt{a_1^2 - 4a_2 \left( a_0 - \frac{\alpha}{\beta} \right)} \right) \quad (2.7)$$

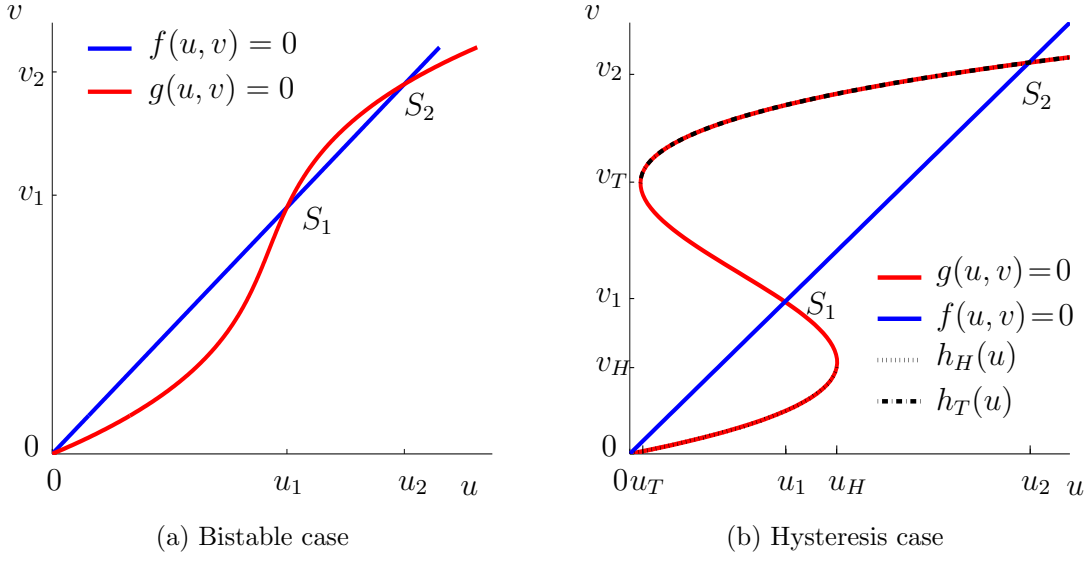


Figure 2.1: Typical configurations of the zero sets of the kinetic functions.

and

$$u_i = \frac{\alpha}{\beta} v_i \quad \text{for } i = 0, 1, 2.$$

Moreover, in the hysteresis case the coordinates of  $H$  and  $T$  are given by

$$v_T = \frac{-a_1 + \sqrt{a_1^2 - 3a_0a_2}}{3a_2} \quad \text{and} \quad v_H = \frac{-a_1 - \sqrt{a_1^2 - 3a_0a_2}}{3a_2}, \quad (2.8)$$

respectively, and  $u_H = p(v_H)$  and  $u_T = p(v_T)$ , respectively. Finally, the polynomial  $p(v)$  has an inflection point  $W = (u_W, v_W)$ , where the coordinates are given by

$$v_W = -\frac{a_1}{3a_2} \quad \text{and} \quad u_W = p(v_W). \quad (2.9)$$

*Proof.* The  $v$ -coordinate of the intersection points is determined by  $p(v) = \frac{\alpha}{\beta}v$ . Thus, we calculate the roots of  $v(a_2v^2 + a_1v + a_0 - \frac{\alpha}{\beta}) = 0$  which are given by (2.7). Then the  $u$ -coordinate is given by  $u = \frac{\alpha}{\beta}v$ .

The  $v$ -coordinate of  $H$  and  $T$  are the roots of the derivative  $p'(v) = 3a_2v^2 + 2a_1v + a_0$ , which are given by (2.8). Whereas the inflection point is the root of the second derivative  $p''(v) = 6a_2v + 2a_1$ , which is (2.9).  $\square$

The main difference between the bistable and the hysteresis case is the different behaviour of the kinetic function  $g$  concerning invertibility.

**Notation:** In the bistable case, the equation  $p(v) = u$  can be inverted globally and we call the inverse function  $h$ , i.e.,

$$p(v) = u \iff h(u) = v.$$

In the hysteresis case, the equation  $p(v) = u$  has three solution branches, i. e.,

$$p(v) = u \iff \begin{cases} v = h_H(u) & \text{when } v \in (-\infty, v_H] \text{ and } u \in [-\infty, u_H], \\ v = h_T(u) & \text{when } v \in [v_T, \infty) \text{ and } u \in [u_T, \infty), \\ v = h_0(u) & \text{when } v \in [v_T, v_H] \text{ and } u \in [u_T, u_H]. \end{cases}$$

In Figure 2.1a we see the typical shape of the zero sets  $f = 0$  and  $g = 0$  in the bistable case and in Figure 2.1b we see the typical configuration in the hysteresis case with the local inverse functions  $h_H$  and  $h_T$ . We remark that we omit the solution branch  $h_0$  in the plot, because it does not play a role in the further analysis.

**Remark 2.1.4.** *The hysteresis case got its name from the fact that  $u = p(v)$  cannot be solved in a unique way. For  $u \in (u_T, u_H)$ , we always have three choices for  $v$  fulfilling  $u = p(v)$ . Therefore the choice depends on the history of the system.*

For the construction of stationary solutions in Chapter 3 and 4 we will need the following functions.

**Definition:** In the bistable case, we denote by  $q$  the function defined by

$$q(u) = f(u, h(u)) \quad \text{for all } u \in \mathbb{R}.$$

In the hysteresis case we denote by  $q_H$  and  $q_T$  the functions defined by

$$q_H(u) = f(u, h_H(u)) \quad \text{for } u < u_H$$

and

$$q_T(u) = f(u, h_T(u)) \quad \text{for } u_T > u.$$

We investigate the behaviour of these functions, which will be needed later on.

**Lemma 2.1.5.** *The derivative  $p'(v)$  of the polynomial in the hysteresis case is positive for  $v \in (-\infty, v_H) \cup (v_T, \infty)$  and negative for  $v \in (v_H, v_T)$ . The second derivative  $p''(v)$  of the polynomial is negative for  $v < v_W$  and positive for  $v > v_W$ .*

*The functions  $h_H$  and  $h_T$  are continuously differentiable. The derivative  $h'_H(u)$  is positive for all  $u < u_H$  and the derivative  $h'_T(u)$  is positive for all  $u > u_T$ . Moreover, in the limit it holds*

$$\lim_{u \rightarrow u_H} h'_H(u) = \infty \quad \text{and} \quad \lim_{u \rightarrow u_T} h'_T(u) = \infty$$

*Proof.* The first part of the lemma is clear, because  $v_H$  and  $v_T$  are by definition the zeros of  $p'$  and, furthermore, we know that  $\lim_{v \rightarrow \infty} p(v) = \infty$ . The second derivative  $p''(v) = 6a_2v + 2a_1$  is a straight line with positive slope, because  $a_2 > 0$  (see Proposition 2.1.2). Its zero fulfills  $6a_2v + 2a_1 = 0$  which leads to  $v = v_W$  (see 2.1.3).

For the results concerning  $h_T$  and  $h_H$ , we use the chain rule to obtain  $h'_H(u) = \frac{1}{p'(h_H(u))}$  and  $h'_T(u) = \frac{1}{p'(h_T(u))}$ . Therefore,  $h_H$  is continuously differentiable, because  $p$  is a polynomial. For  $u < u_H$ , we have  $h_H(u) < v_H$  and thus  $p'(h_H(u)) > 0$  and the derivative is well-defined. Moreover,

$$\lim_{u \rightarrow u_H} h'_H(u) = \lim_{u \rightarrow u_H} \frac{1}{p'(h_H(u))} = \frac{1}{p'(v_H)} = \frac{1}{0} = \infty.$$

For  $h'_T(u)$  we obtain the result using a similar argument.  $\square$

**Lemma 2.1.6.** *The functions  $q, q_H$  and  $q_T$  are continuously differentiable.*

*Proof.* Differentiability has been shown in Lemma 2.1.5 for  $h_H$  and  $h_T$ . For  $h$  it follows from  $h'(u) = \frac{1}{p'(h(u))} > 0$ .

The function  $f$  is continuously differentiable, because it is linear. Thus,  $q, q_H$  and  $q_T$  are continuously differentiable as composition of continuously differentiable functions.  $\square$

**Definition:** For the generic model in the hysteresis case, we call **critical values** the values which fulfil

$$q'_H(u_H^{cr}) = 0 \quad \text{and} \quad q'_T(u_T^{cr}) = 0.$$

**Lemma 2.1.7.** *The critical values can be calculated by*

$$u_H^{cr} = p(v_H^{cr}) \quad \text{and} \quad u_T^{cr} = p(v_T^{cr}).$$

Here,  $v_H^{cr} < v_T^{cr}$  are the solutions of the quadratic equation

$$p'(v) = \frac{\alpha}{\beta}.$$

Thus, the critical values are unique and it holds

$$u_H^{cr} < u_H \quad \text{and} \quad u_T^{cr} > u_T.$$

*Proof.* By definition,  $q_H(u) = f(u, h_H(u)) = \alpha h_H(u) - \beta u$ . Thus, the derivative is calculated by

$$q'_H(u) = \alpha h'_H(u) - \beta = \alpha \frac{1}{p'(h_H(u))} - \beta.$$

Therefore,  $q'_H(u) = 0$  corresponds to  $p'(v) = \frac{\alpha}{\beta}$  where  $v = h_H(u)$ . This is a quadratic equation

$$3a_2v^2 + 2a_1v + (a_0 - \frac{\alpha}{\beta}) = 0 \quad (2.10)$$

which has the solutions

$$v_H^{cr} = \frac{-a_1 - \sqrt{a_1^2 - 3a_2(a_0 - \frac{\alpha}{\beta})}}{3a_2} \quad \text{and} \quad v_T^{cr} = \frac{-a_1 + \sqrt{a_1^2 - 3a_2(a_0 - \frac{\alpha}{\beta})}}{3a_2}.$$

The discriminant  $a_1^2 - 3a_2(a_0 - \frac{\alpha}{\beta})$  of the quadratic equation (2.10) is positive, because of Proposition 2.1.2. Using the formula (2.8) for  $v_H$  and  $v_T$  in Lemma 2.1.3 we obtain  $v_H^{cr} < v_H$  and  $v_T^{cr} > v_T$ . Using that  $p$  is monotone increasing for  $v < v_H$  and  $v > v_T$ , we obtain the result.  $\square$

**Remark 2.1.8.** *The the order relation between  $u_H^{cr}$  and  $u_T^{cr}$  depends strongly on the kinetic functions (compare Figure 2.2). We will show in Section 4.4 that the most interesting situation occurs, if the critical values fulfill*

$$u_T^{cr} < u_H^{cr}.$$

**Lemma 2.1.9.** *The derivative  $q'_H(u)$  is negative for  $u < u_H^{cr}$  and positive for  $u \in (u_H^{cr}, u_H)$ . The derivative  $q'_T(u)$  is negative for  $u > u_T^{cr}$  and positive for  $u \in (u_T, u_T^{cr})$ . In particular, it holds*

$$q'_H(0) < 0 \quad \text{and} \quad q'_T(u_2) < 0.$$

*Proof.* The only zero of  $q'_H$  is given by  $u_H^{cr}$ . We calculate the second derivative

$$q''_H(u) = -\frac{\alpha p''(h_H(u))}{(p'(h_H(u)))^3} = -\frac{\alpha(6a_2h_H(u) + 2a_1)}{(p'(h_H(u)))^3},$$

which is positive for all  $u < u_W$ , thus in particular for all  $u < u_H$ . Therefore,  $q'_H(u)$  is positive for  $u < u_H^{cr}$  and negative for  $u > u_H^{cr}$ . For  $q'_T$  we argue similarly.  $\square$

**Lemma 2.1.10.** *The function  $q_H(u)$  is negative for all  $u \in (0, u_H)$ , whereas  $q_T(u)$  is positive for all  $u \in (u_T, u_2)$ .*

*Proof.* Replacing  $u = p(v)$ , we obtain  $q_H(p(v)) = \alpha v - \beta p(v)$  and  $q_T(p(v)) = \alpha v - \beta p(v)$ . Thus, the only zeros of  $q_H$  and  $q_T$  can be at the  $u$ -coordinates of the intersection points. Therefore, 0 is the only zero of  $q_H$ , because  $u_1$  and  $u_2$  are not in the domain of definition of  $q_H$ . Similarly, only  $u_2$  is a zero of  $q_T$ . Together with Lemma 2.1.9 we obtain the result.  $\square$

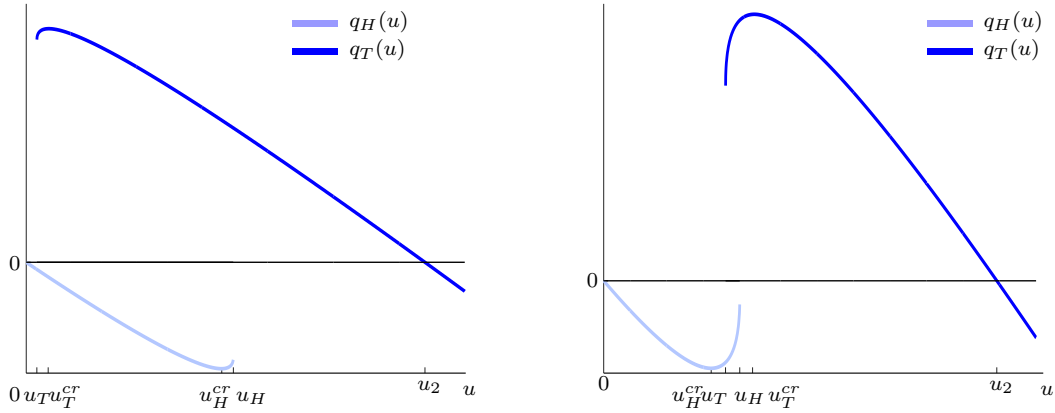


Figure 2.2: The functions  $q_H(u)$  and  $q_T(u)$  for different kinetic functions in the hysteresis case. The length of the interval  $[u_T, u_H]$ , as well as the relative position of the critical values  $u_H^{cr}$  and  $u_T^{cr}$  depends on the kinetic functions.

**Remark 2.1.11.** *Let us now explain that the configuration of the zero sets of  $f$  and  $g$  is the most symmetric if the intersection point  $S_1$  equals the inflection point  $W$ , that is*

$$u_1 = u_W \quad \text{and} \quad v_1 = v_W. \quad (2.11)$$

*This is the case when the ratio  $\frac{\alpha}{\beta}$  is chosen such that*

$$u_W = p(v_W) \stackrel{!}{=} \frac{\alpha}{\beta} v_W$$

*holds true.*

*A polynomial of degree three is point symmetric with respect to the inflection point. Therefore, condition (2.11) induces that the coordinates of  $S_2$  are given by  $v_2 = 2v_1$  and  $u_2 = 2u_1$ . Furthermore, the area enclosed by  $f = 0$  and  $g = 0$  is the same between  $S_0$  and  $S_1$  as well as between  $S_1$  and  $S_2$ , but with a different sign.*

## 2.2 Stability of constant steady states

In this section we discuss stability properties of constant solutions (2.5) for system (2.1). We show that  $S_0$  and  $S_2$  are always stable, whereas  $S_1$  is unstable. On the one hand, this shows bistability of the generic model. Moreover, the model does not show diffusion-driven instability, which is a necessary condition for the mechanism of pattern formation developed by Alan Turing.

**Lemma 2.2.1.** *In both, bistable and hysteresis, case the steady states  $S_0$  and  $S_2$  are asymptotically stable solutions of the kinetic system*

$$u_t = f(u, v) \quad v_t = g(u, v). \quad (2.12)$$

The steady state  $S_1$ , on the contrary, is a saddle.

*Proof.* The Jacobian matrix at a steady state  $(\bar{u}, \bar{v})$  has the following form

$$J(\bar{u}, \bar{v}) = \begin{pmatrix} f_u(\bar{u}, \bar{v}) & f_v(\bar{u}, \bar{v}) \\ g_u(\bar{u}, \bar{v}) & g_v(\bar{u}, \bar{v}) \end{pmatrix} = \begin{pmatrix} -\beta & \alpha \\ 1 & -p'(\bar{v}) \end{pmatrix}. \quad (2.13)$$

Hence, we calculate

$$\det J(\bar{u}, \bar{v}) = \beta \left( p'(\bar{v}) - \frac{\alpha}{\beta} \right) \quad \text{and} \quad \text{Tr } J(\bar{u}, \bar{v}) = -(\beta + p'(\bar{v})).$$

As  $\frac{\alpha}{\beta}$  is the slope of  $f(u, v) = 0$  solved with respect to  $v$ , we have  $p'(0) > \frac{\alpha}{\beta} > 0, p'(v_2) > \frac{\alpha}{\beta} > 0$ . Hence  $\det J(S_0) > 0$  and  $\det J(S_2) > 0$ , whereas the trace is negative for both steady states. Therefore, the linearisation of the generic model at  $S_0$  and  $S_2$  has only negative eigenvalues.

For  $S_1$  we have to distinguish between the hysteresis and the bistable case. In the hysteresis case it holds  $p'(v_1) < 0$ , hence  $\det J(S_1) < 0$ . In the bistable case it holds  $p'(v_1) > 0$ , but still  $p'(v_1) < \frac{\alpha}{\beta}$  and also  $\det J(S_1) < 0$ . Therefore, the linearisation at  $S_1$  has one positive and one negative eigenvalue.  $\square$

**Theorem 2.2.2.** *The homogeneous steady states  $S_0, S_2$  are linearly stable as solutions of the generic model (2.1) in the bistable case and in the hysteresis case.*

*Proof.* We consider the linearisation of equation (2.1) at a steady state  $(\bar{u}, \bar{v})$

$$\begin{pmatrix} \tilde{u}_t \\ \tilde{v}_t \end{pmatrix} = \begin{pmatrix} \frac{1}{\gamma} \tilde{u}_{xx} \\ 0 \end{pmatrix} + J(\bar{u}, \bar{v}) \cdot \begin{pmatrix} \tilde{u} \\ \tilde{v} \end{pmatrix} =: L \cdot \begin{pmatrix} \tilde{u} \\ \tilde{v} \end{pmatrix}$$

with boundary conditions  $\tilde{u}_x(0) = \tilde{u}_x(1) = 0$ .

The eigenvalue equation  $L \begin{pmatrix} \varphi \\ \psi \end{pmatrix} = \lambda \begin{pmatrix} \varphi \\ \psi \end{pmatrix}$  with boundary condition  $\varphi_x(0) = \varphi_x(1) = 0$  leads to the system

$$\begin{aligned} \frac{1}{\gamma} \varphi'' - (\beta + \lambda) \varphi + \alpha \psi &= 0 \\ \varphi - (p'(\bar{v}) + \lambda) \psi &= 0. \end{aligned} \quad (2.14)$$

We denote  $\phi_n = \cos(n\pi x)$ , the  $n$ -th eigenfunction of  $-\frac{d^2}{dx^2}$  with homogeneous Neumann boundary conditions corresponding to the eigenvalue  $\omega_n^2 = \left(\frac{n}{\pi}\right)^2$ . The vector

$\begin{pmatrix} \varphi \\ \psi \end{pmatrix} = \begin{pmatrix} C_1 \phi_n \\ C_2 \phi_n \end{pmatrix}$  with  $C_1, C_2 \in \mathbb{R}$  is a solution of system (2.14) provided

$$\det(L_n - \lambda E_2) = 0.$$

Here, the matrix  $L_n$  is given by

$$L_n = \begin{pmatrix} -\frac{\omega_n^2}{\gamma} - \beta & \alpha \\ 1 & -p'(\bar{v}) \end{pmatrix}.$$

Hence, the spectrum of  $L$ ,  $\text{spec}(L)$ , consists of solutions of the quadratic equation

$$0 = \lambda^2 + (\beta + p'(\bar{v}) + \frac{1}{\gamma}\omega_n^2)\lambda + \beta p'(\bar{v}) - \alpha + \frac{1}{\gamma}\omega_n^2 p'(\bar{v})$$

for every  $n \in \mathbb{N}$ .

The solutions are all negative. This can be checked by calculation of the trace and of the determinant of  $L_n$ . As  $S_0$  and  $S_2$  are stable solutions of the kinetic system, it holds  $\text{Tr } J(\bar{u}, \bar{v}) < 0$  for both steady states and therefore

$$\text{Tr } L_n = \text{Tr } J(\bar{u}, \bar{v}) - \frac{1}{\gamma}\omega_n^2 < 0.$$

Furthermore,  $\det J(\bar{u}, \bar{v}) > 0$  for  $S_0$  and  $S_2$  and therefore

$$\det L_n = \det J(\bar{u}, \bar{v}) + \frac{1}{\gamma}\omega_n^2 p'(\bar{v}) > 0.$$

because  $p'(0) > 0$  and  $p'(v_2) > 0$  for the hysteresis and the bistable case.  $\square$

**Remark 2.2.3.** *The steady state  $S_1$  is unstable as solution of the kinetic system and hence also for the reaction-diffusion system.*

## 2.3 Global existence of solutions

In this section, we show existence and uniqueness of nonnegative global-in-time solutions of the generic model (2.1) - (2.3) in both the bistable and the hysteresis case for all bounded and nonnegative initial conditions.

There are different types of solutions which depend basically on the regularity of the initial conditions and the nonlinearity. We refer to [MC04] for a review about existence theorems for mild, weak and classical solutions for reaction-diffusion equations coupled with ordinary differential equations.

In Chapter 3, we show that stationary solutions of the generic system in the bistable case are in  $C^2([0, 1])$ . Therefore, it is suitable in this context to consider classical solutions of the time-dependent system.

**Remark 2.3.1.** *The kinetic function  $f(u, v) = \alpha v - \beta u$  is linear, thus globally Lipschitz continuous, and  $g(u, v) = u - p(v)$  is  $C^\infty(\mathbb{R}^2)$ , thus locally Lipschitz continuous.*

**Theorem 2.3.2.** *For initial data  $u_0, v_0 \in C^1([0, 1])$  fulfilling the compatibility condition  $\frac{d}{dx}u_0(0) = \frac{d}{dx}u_0(1) = 0$  the generic model (2.1) - (2.3) has a unique classical solution  $(u(t, x), v(t, x)) \in C^1((0, T]; C^2([0, 1])) \times C^1([0, T]; C([0, 1]))$  in both the hysteresis and the bistable case.*

*Proof.* For a proof of the existence of classical solutions for systems with reaction-diffusion-equations coupled with ordinary differential equation and Neumann boundary conditions, we refer to [Nak12]. The proof uses a representation of the solution with Green's function and Picard iterations.  $\square$

However, in the hysteresis case, we will see in Chapter 4 that a stationary solution  $(U(x), V(x))$  is given by a function  $U(x)$  being only once differentiable and a function  $V(x)$  which is even discontinuous. Thus, we need to consider solutions  $(u, v)$  such that for a fixed  $t$   $u(t, \cdot)$  and  $v(t, \cdot)$  are in suitable function spaces, e.g. Lebesgue or Sobolev spaces.

We review the theory presented in [Bre10] to solve evolution equations. In the following, we consider a Hilbert space  $H$  be with scalar product  $(\cdot, \cdot)$  and norm  $\|\cdot\|$ .

**Definition:** Let  $A : \mathcal{D}(A) \subset H \rightarrow H$  be a linear unbounded operator with domain  $\mathcal{D}(A) = \{u \in H \mid A(u) \in H\}$ .  $A$  is called **monotone** if

$$(Av, v) \geq 0 \quad \text{for all } v \in \mathcal{D}(A).$$

$A$  is called **maximal monotone** if it additionally holds that the range of  $A$  plus the identity is equal to the Hilbert space, i.e.  $R(A + I) = H$ .

**Proposition 2.3.3.** *Let  $A$  be a maximal monotone operator. Then  $\mathcal{D}(A)$  is dense in  $H$ .*

*Proof.* We refer to [Bre10, Proposition 7.1]  $\square$

**Definition:** The operator  $A$  is called **symmetric** if it holds

$$(Au, v) = (u, Av) \quad \text{for all } u, v \in \mathcal{D}(A).$$

$A$  is called **self-adjoint** if

$$A^* = A,$$

where  $A^*$  is the adjoint operator defined by  $(Au, v) = (u, A^*v)$  for all  $u \in \mathcal{D}(A)$ . For a self-adjoint operator it holds  $\mathcal{D}(A^*) = \mathcal{D}(A)$ .

**Proposition 2.3.4.** *Let  $A$  be a maximal monotone symmetric operator. Then  $A$  is self-adjoint.*

*Proof.* We refer to [Bre10, Proposition 7.6].  $\square$

**Theorem 2.3.5** (Hille-Yosida). *Let  $A$  be a maximal monotone self-adjoint operator. Then for all  $u_0 \in H$ , there is a unique function*

$$u \in C([0, \infty); H) \cap C^1((0, \infty); H) \cap C((0, \infty); \mathcal{D}(A))$$

*which is a solution of the homogeneous Cauchy problem*

$$\frac{d}{dt}u + Au = 0 \quad \text{for } t \in (0, \infty), \quad (2.15)$$

$$u(0) = u_0. \quad (2.16)$$

*Moreover, it holds*

$$\|u(t)\| \leq \|u_0\| \quad \text{and} \quad \left\| \frac{d}{dt}u(t) \right\| = \|Au(t)\| \leq \frac{1}{t}\|u_0\| \quad \text{for all } t > 0.$$

*Proof.* We refer to [Bre10, Theorem 7.7].  $\square$

**Definition:** A family of linear operators  $\{S(t)\}_{t \geq 0}$  is called a **strongly continuous semigroup of contractions** if it holds

- i) for all  $t \geq 0$  the mapping  $S(t) : H \rightarrow H$  is a linear continuous operator and it holds  $\|S(t)u\| \leq \|u\|$  for all  $u \in H$ ,
- ii)  $S(0) = I$  and  $S(t_1 + t_2) = S(t_1)S(t_2)$  for all  $t_1, t_2 \geq 0$ ,
- iii)  $\lim_{t \rightarrow 0, t \geq 0} \|S(t)u - u\| = 0$  for all  $u \in H$  such that the limit exists.

The generator  $A$  of  $S(t)$  is the operator defined by

$$\mathcal{D}(A) = \left\{ u \in H \mid \lim_{t \rightarrow 0, t \geq 0} \frac{S(t)u - u}{t} \text{ exists} \right\}$$

$$Au = \lim_{t \rightarrow 0, t \geq 0} \frac{S(t)u - u}{t} \quad \text{for } u \in \mathcal{D}(A).$$

**Proposition 2.3.6.** *Let  $A$  be a maximal monotone self-adjoint operator. Then, it holds for all  $u \in H$*

$$\int_0^t S(s)u ds \in \mathcal{D}(A) \quad \text{and} \quad S(t)u \in \mathcal{D}(A).$$

*Proof.* The first part can be found in [Paz83, Theorem 2.4], the second part is in the proof of [Bre10, Theorem 7.7].  $\square$

**Definition:** For  $t \geq 0$ , we define

$$\begin{aligned} S_A(t) : H &\rightarrow H \\ u_0 &\mapsto u(t), \end{aligned}$$

where  $u(t)$  is the solution of problem (2.15)- (2.16).  $\{S_A(t)\}_{t \geq 0}$  is a family of linear operators which is called the **semigroup generated by  $A$** .

**Proposition 2.3.7.** *The family of linear operators  $\{S_A(t)\}_{t \geq 0}$  is a strongly continuous semigroup of contractions.*

*Proof.* See [Bre10, Chapter 7, Remark 5]. □

**Remark 2.3.8.** *Let  $A$  be a maximal monotone symmetric operator and  $\lambda \in \mathbb{R}$ . Then, solving the problem*

$$\begin{aligned} \frac{d}{dt}u + Au + \lambda u &= 0 && \text{for } t \in (0, \infty), \\ u(0) &= u_0 \end{aligned}$$

*can be reduced to solving the problem*

$$\begin{aligned} \frac{d}{dt}v + Av &= 0 && \text{for } t \in (0, \infty), \\ v(0) &= u_0 \end{aligned}$$

*by setting  $v(t) = e^{\lambda t}u(t)$ .*

**Theorem 2.3.9.** *Let  $A$  be a maximal monotone self-adjoint operator. Then, for all  $u_0 \in H$  and all  $f \in C([0, T]; H)$ , there is a unique function*

$$u \in C([0, T]; H) \cap C^1((0, T]; H) \cap C((0, T]; \mathcal{D}(A))$$

*which is a solution of the inhomogeneous Cauchy problem*

$$\begin{aligned} \frac{d}{dt}u(t) + Au(t) &= f(t) && \text{for } t \in [0, T], \\ u(0) &= u_0. \end{aligned}$$

*Moreover,  $u$  is given by the formula*

$$u(t) = S_A(t)u_0 + \int_0^t S_A(t-s)f(s)ds, \tag{2.17}$$

*where  $S_A(t)$  is the semigroup of linear operators generated by  $A$ .*

*Proof.* This is shown in [Bre10, Theorem 7.10] for  $f \in C^1([0, T]; H)$ . But, we observe that if we assume less time regularity  $f \in C([0, T]; H)$  the solution given by (2.17) still belongs to the desired function spaces.  $\square$

Now, we cast our problem into this context to be able to apply Theorem 2.3.9.

**Notation:** We denote the Sobolev space incorporating the Neumann boundary condition of the generic problem (2.1) - (2.3) by

$$H_N^2(0, 1) := \{u \in H^2(0, 1) \mid u_x(0) = u_x(1) = 0\}.$$

**Proposition 2.3.10.** *The unbounded operator  $A : L^2(0, 1) \rightarrow L^2(0, 1)$  defined by*

$$\begin{aligned} \mathcal{D}(A) &= H_N^2(0, 1), \\ Au &:= -\frac{1}{\gamma}u_{xx} + \beta u \quad \text{for } u \in \mathcal{D}(A) \end{aligned}$$

*with positive constants  $\gamma, \beta \in \mathbb{R}$  is a maximal monotone self-adjoint operator and it generates a strongly continuous semigroup denoted by  $S(t)$  which fulfils the estimate*

$$\|S(t)u\|_{L^2(0,1)} \leq e^{-\beta t} \|u\|_{L^2(0,1)} \quad (2.18)$$

*for all  $u \in L^2(0, 1)$ .*

*Proof.* The proof can be found in [Bre10, Theorem 10.1] for Dirichlet boundary conditions, but we repeat it here for completeness.

i)  $A$  is monotone, because for all  $u \in \mathcal{D}(A)$  it holds

$$(Au, u)_{L^2(0,1)} = \int_0^1 \left(-\frac{1}{\gamma}u_{xx} + \beta u\right)u dx = \frac{1}{\gamma} \int_0^1 u_x^2 dx + \beta \int_0^1 u^2 dx \geq 0.$$

ii)  $A$  is maximal monotone because it holds  $R(I + A) = L^2(0, 1)$ , which is equivalent to the existence of a solution  $u \in \mathcal{D}(A)$  for all  $f \in L^2(0, 1)$  of the equation

$$-\frac{1}{\gamma}u_{xx} + (\beta + 1)u = f.$$

This follows from the standard theory for elliptic differential equations and can be found e.g. in [Bre10, Theorem 9.26].

iii)  $A$  is self-adjoint. Using Proposition 2.3.4 it is enough to show that  $A$  is symmetric. Indeed for all  $u, v \in \mathcal{D}(A)$  it holds

$$\begin{aligned} (Au, v)_{L^2(0,1)} &= \int_0^1 \left(-\frac{1}{\gamma}u_{xx} + \beta u\right)v dx = \frac{1}{\gamma} \int_0^1 u_x v_x dx + \beta \int_0^1 uv dx, \\ (u, Av)_{L^2(0,1)} &= \int_0^1 u \left(-\frac{1}{\gamma}v_{xx} + \beta v\right) dx = \frac{1}{\gamma} \int_0^1 u_x v_x dx + \beta \int_0^1 uv dx, \end{aligned}$$

thus  $(Au, v)_{L^2(0,1)} = (u, Av)_{L^2(0,1)}$ .

- iv) We use that the operator  $\tilde{A} := -\frac{1}{\gamma}u_{xx}$  with  $\mathcal{D}(\tilde{A}) = \mathcal{D}(A)$  is maximal monotone and self-adjoint. Therefore, Proposition 2.3.7 yields that the associated semigroup  $S_{\tilde{A}}(t)$  fulfils  $\|S_{\tilde{A}}(t)u\|_{L^2(0,1)} \leq \|u\|_{L^2(0,1)}$ . With Remark 2.3.8 we obtain the stronger estimate (2.18).

□

**Proposition 2.3.11** (Local-in-time existence of solutions). *Let  $(u_0, v_0) \in L^2(0, 1)^2$ . Then there exists  $T_0 > 0$  such that the initial value problem (2.1)- (2.3) has a unique solution*

$$u \in C([0, T_0]; L^2(0, 1)) \cap C^1((0, T_0]; L^2(0, 1)) \cap C((0, T_0]; H_N^2(0, 1))$$

and

$$v \in C^1([0, T_0]; L^2(0, 1))$$

given by

$$u(t, x) = S(t)u_0(x) + \int_0^t S(t-s)\alpha v(s, x)ds, \quad (2.19)$$

$$v(t, x) = v_0(x) + \int_0^t (u(s, x) - p(v(s, x)))ds, \quad (2.20)$$

where  $S(t)$  is the semigroup defined in Proposition 2.3.10. Moreover, it holds

$$u \in L^2(0, T_0; H^1(0, 1))$$

and for all  $0 < T \leq T_0$  the following equation holds

$$\begin{aligned} \frac{1}{2}\|u(T, \cdot)\|_{L^2(0,1)}^2 + \frac{1}{\gamma} \int_0^T \|u_x(t, \cdot)\|_{L^2(0,1)}^2 dt + \beta \int_0^T \|u(t, \cdot)\|_{L^2(0,1)}^2 dt \\ = \frac{1}{2}\|u_0\|_{L^2(0,1)}^2 + \alpha \int_0^T (u(t, \cdot), v(t, \cdot))_{L^2(0,1)} dt. \end{aligned} \quad (2.21)$$

*Proof.* For some  $0 < T < \infty$ , which will be determined later, we consider the Banach space

$$X(T) := C([0, T]; L^2(0, 1)) \times C([0, T]; L^2(0, 1))$$

endowed with the norm

$$\|(u, v)\|_{X(T)} = \max\{\|u\|_{C([0,T];L^2(0,1))}, \|v\|_{C([0,T];L^2(0,1))}\}$$

where

$$\|u\|_{C([0,T];L^2(0,1))} = \max_{0 \leq t \leq T} \{ \|u(t, \cdot)\|_{L^2(0,1)} \}.$$

We define an operator  $\mathcal{B} : X(T) \rightarrow X(T)$ . Given  $(u, v) \in X(T)$ , we set

$$h_1(t, x) = \alpha v(t, x)$$

and observe that  $h_1 \in C([0, T]; L^2(0, 1))$ . Because of Proposition 2.3.10, the operator  $Au = -\frac{1}{\gamma}u_{xx} + \beta u$  fulfils the requirements of Theorem 2.3.9 and the inhomogeneous evolution equation

$$\frac{\partial}{\partial t} w_1(t, x) - \frac{1}{\gamma} (w_1)_{xx}(t, x) + \beta w_1(t, x) = h_1(t, x) \quad \text{for } t > 0, \quad (2.22)$$

$$w_1(0, x) = u_0(x) \quad (2.23)$$

with the boundary condition  $(w_1)_x(t, 0) = (w_1)_x(t, 1) = 0$  has a unique solution  $w_1 \in C([0, T]; L^2(0, 1))$  given by

$$w_1(t, x) = S(t)u_0(x) + \int_0^t S(t-s)h_1(s, x)ds. \quad (2.24)$$

Next, we set

$$h_2(t, x) = g(u(t, x), v(t, x))$$

and observe

$$h_2 \in C([0, T]; L^2(0, 1))$$

that because of continuity of  $g$ .

The equation

$$\frac{\partial}{\partial t} w_2(t, x) = h_2(t, x)$$

for fixed  $x \in [0, 1]$  with initial condition  $w_2(0, x) = v_0(x)$  has a unique solution  $w_2(t, x)$  given by the integral

$$w_2(t, x) = v_0(x) + \int_0^t h_2(s, x)ds. \quad (2.25)$$

Thus,  $w_2(t, x) \in C^1([0, T]; L^2(0, 1))$ .

Now, we define the operator

$$\begin{aligned} \mathcal{B} : X(T) &\rightarrow X(T) \\ (u, v) &\mapsto (w^1, w^2) = w \end{aligned}$$

and show that  $\mathcal{B}$  is a strict contraction. To do so, let  $w = \mathcal{B}(u, v)$  and  $\tilde{w} = \mathcal{B}(\tilde{u}, \tilde{v})$  and set  $h_1 = \alpha v$ ,  $h_2 = g(u, v)$ ,  $\tilde{h}_1 = \alpha \tilde{v}$ ,  $\tilde{h}_2 = g(\tilde{u}, \tilde{v})$ . We show that for a suitably chosen time interval  $[0, T_0]$ , there exists a constant  $\theta < 1$  such that

$$\|w - \tilde{w}\|_{X(T_0)} = \|\mathcal{B}(u, v) - \mathcal{B}(\tilde{u}, \tilde{v})\|_{X(T_0)} < \theta \|(u, v) - (\tilde{u}, \tilde{v})\|_{X(T_0)}. \quad (2.26)$$

To prove this inequality, we subtract equation (2.24) for  $w_1$  from that for  $\tilde{w}_1$  and obtain

$$(w_1 - \tilde{w}_1)(t, x) = \int_0^t S(t-s)(h_1(s, x) - \tilde{h}_1(s, x)) ds.$$

Multiplying the previous equation by  $(w_1 - \tilde{w}_1)$  and integrating with respect to  $x$ , this yields an estimate of the  $L^2(0, 1)$  norm using the Cauchy-Schwarz inequality with  $\epsilon$

$$\begin{aligned} \|(w_1 - \tilde{w}_1)(t, \cdot)\|_{L^2(0,1)}^2 &= \int_0^1 \int_0^t S(t-s)((h_1 - \tilde{h}_1)(s, x)) ds ((w_1 - \tilde{w}_1)(t, x)) dx \\ &\leq \frac{1}{\epsilon} \left\| \int_0^t S(t-s)((h_1 - \tilde{h}_1)(s, \cdot)) ds \right\|_{L^2(0,1)}^2 + \epsilon \|(w_1 - \tilde{w}_1)(t, \cdot)\|_{L^2(0,1)}^2 \end{aligned}$$

Taking  $0 < \epsilon < 1$  and using the estimate (2.18), we obtain

$$\begin{aligned} (1 - \epsilon) \|(w_1 - \tilde{w}_1)(t, \cdot)\|_{L^2(0,1)}^2 &\leq \frac{1}{\epsilon} \int_0^t \|S(t-s)(h_1 - \tilde{h}_1)(s, \cdot)\|_{L^2(0,1)}^2 ds, \\ &\leq \frac{1}{\epsilon} \int_0^t e^{-\beta(t-s)} \|(h_1 - \tilde{h}_1)(s, \cdot)\|_{L^2(0,1)}^2 ds. \end{aligned}$$

Dividing by  $(1 - \epsilon)$  and taking the maximum over  $t \in [0, T]$  yields

$$\begin{aligned} \|w_1 - \tilde{w}_1\|_{C([0,T];L^2(0,1))}^2 &\leq \tilde{C}_1 \max_{t \in [0,T]} \left\{ \int_0^t e^{-\beta(t-s)} \|h_1(s, \cdot) - \tilde{h}_1(s, \cdot)\|_{L^2(0,1)}^2 ds \right\} \\ &\leq \tilde{C}_1 T \|h_1 - \tilde{h}_1\|_{C([0,T];L^2(0,1))}^2 \\ &= \tilde{C}_1 \alpha^2 T \|v - \tilde{v}\|_{C([0,T];L^2(0,1))}^2 \\ &= C_1 T \|v - \tilde{v}\|_{C([0,T];L^2(0,1))}^2. \end{aligned}$$

Thus, it holds

$$\|w_1 - \tilde{w}_1\|_{C([0,T];L^2(0,1))} \leq C_1 T \|(u, v) - (\tilde{u}, \tilde{v})\|_{X(T)}. \quad (2.27)$$

Now, we consider the equation  $(w_2)_t(t, \cdot) = h_2(t, \cdot)$  and  $(\tilde{w}_2)_t(t, \cdot) = \tilde{h}_2(t, \cdot)$  with initial conditions  $w_2(0, x) = \tilde{w}_2(0, x) = v_0(x)$ . Subtracting equation (2.25) for  $w_2$  and  $\tilde{w}_2$  from each other leads to

$$w_2(t, \cdot) - \tilde{w}_2(t, \cdot) = \int_0^t (h_2 - \tilde{h}_2)(s, \cdot) ds.$$

Multiplying the previous equation by  $(w_1 - \tilde{w}_1)$  and integrating with respect to  $x$ , it yields an estimate of the  $L^2(0, 1)$  norm using the Cauchy-Schwarz inequality with  $\epsilon$

$$\begin{aligned} \|(w^2 - \tilde{w}^2)(t, \cdot)\|_{L^2(0,1)}^2 &\leq \int_0^1 \int_0^t (h_2 - \tilde{h}_2)(s, x) ds (w^2 - \tilde{w}^2)(t, x) dx \\ &\leq \frac{1}{\epsilon} \left\| \int_0^t (g(u(s, \cdot), v(s, \cdot)) - g(\tilde{u}(s, \cdot), \tilde{v}(s, \cdot))) ds \right\|_{L^2(0,1)}^2 + \epsilon \|(w_2 - \tilde{w}_2)(t, \cdot)\|_{L^2(0,1)}^2 \end{aligned}$$

Taking  $0 < \epsilon < 1$  and using the Lipschitz-continuity of  $g$ , we obtain

$$(1-\epsilon) \|(w^2 - \tilde{w}^2)(t, \cdot)\|_{L^2(0,1)}^2 \leq \tilde{C}_2 \int_0^t \max\{\|u(s, \cdot) - \tilde{u}(s, \cdot)\|_{L^2(0,1)}^2, \|v(s, \cdot) - \tilde{v}(s, \cdot)\|_{L^2(0,1)}^2\} ds$$

Dividing by  $1 - \epsilon$  and taking the maximum over  $t \in [0, T]$  yields

$$\|w_2 - \tilde{w}_2\|_{C([0,T];L^2(0,1))}^2 \leq C_2 T \max\{\|u - \tilde{u}\|_{C([0,T];L^2(0,1))}^2, \|v - \tilde{v}\|_{C([0,T];L^2(0,1))}^2\},$$

thus

$$\|w_2 - \tilde{w}_2\|_{C([0,T];L^2(0,1))} \leq C_2 T \|(u, v) - (\tilde{u}, \tilde{v})\|_{X(T)} \quad (2.28)$$

Taking the maximum of equation (2.27) and (2.28) yields

$$\|(w_1, w_2) - (\tilde{w}_1, \tilde{w}_2)\|_{X(T)} \leq \max\{C_1 T, C_2 T\} \|(u, v) - (\tilde{u}, \tilde{v})\|_{X(T)}.$$

If  $T_0$  is chosen sufficiently small that holds  $\theta = \max\{C_1 T_0, C_2 T_0\} < 1$ , then the equation (2.26) holds and  $\mathcal{B}$  is a strict contraction. Using Banach's fixed point theorem (see [Eva08]) yields existence and uniqueness of a solution  $(u, v) \in C([0, T_0]; L^2(0, 1))^2$ .

We obtain better regularity results by bootstrapping. Because

$$\frac{\partial}{\partial t} v(t, x) = u(t, x) - p(v(t, x)) \in C([0, T_0]; L^2(0, 1)),$$

we obtain  $v \in C^1([0, T_0]; L^2(0, 1))$ . Moreover,  $\alpha v \in C^1([0, T_0]; L^2(0, 1))$ . Using Proposition 2.3.6 yields that  $\int_0^t S(t-s) \alpha v ds \in C((0, T_0]; H_N^2(0, 1))$  for  $t \geq 0$  and  $S(t)u_0(x) \in H_N^2(0, 1)$  for all  $t > 0$ . The representation (2.19) yields that

$$u \in C((0, T_0]; H_N^2(0, 1)).$$

Furthermore, this yields that  $\frac{1}{\gamma} \frac{\partial^2}{\partial x^2} u - \beta u \in C((0, T_0]; L^2(0, 1))$  and thus

$$\frac{\partial}{\partial t} u = \frac{1}{\gamma} \frac{\partial^2}{\partial x^2} u + \alpha v - \beta u \in C((0, T_0]; L^2(0, 1)).$$

Therefore, it holds  $u \in C^1((0, T_0]; L^2(0, 1))$ .

Finally, we show equation (2.21). To do so, we set  $\varphi(t) = \frac{1}{2}\|u(t, \cdot)\|_{L^2(0,1)}^2 \in C^1((0, T_0); \mathbb{R})$ . The derivative is calculated by

$$\begin{aligned} \frac{d}{dt}\varphi(t) &= (u(t, \cdot), \frac{\partial}{\partial t}u(t, \cdot))_{L^2(0,1)} \\ &= (u(t, \cdot), \frac{1}{\gamma}\frac{\partial^2}{\partial x^2}u(t, \cdot) + \alpha v(t, \cdot) - \beta u(t, \cdot))_{L^2(0,1)} \\ &= -\frac{1}{\gamma}\|\frac{\partial}{\partial x}u(t, \cdot)\|_{L^2(0,1)}^2 - \beta\|u(t, \cdot)\|_{L^2(0,1)}^2 + \alpha(u(t, \cdot), \alpha v(t, \cdot))_{L^2(0,1)}. \end{aligned}$$

For  $0 < \epsilon < T \leq T_0$ , it holds

$$\begin{aligned} \varphi(T) - \varphi(\epsilon) &= \int_{\epsilon}^T \frac{d}{dt}\varphi(t) dt \\ &= -\frac{1}{\gamma} \int_{\epsilon}^T \|\frac{\partial}{\partial x}u(t, \cdot)\|_{L^2(0,1)}^2 dt - \beta \int_{\epsilon}^T \|u(t, \cdot)\|_{L^2(0,1)}^2 dt \\ &\quad + \alpha \int_{\epsilon}^T (u(t, \cdot), \alpha v(t, \cdot))_{L^2(0,1)} dt. \end{aligned}$$

Taking the limit  $\lim_{\epsilon \rightarrow 0} \varphi(\epsilon) = \frac{1}{2}\|u_0\|_{L^2(0,1)}^2$ , we obtain equation (2.21) which yields that  $u \in L^2(0, T_0; H^1(0, 1))$ .  $\square$

To obtain global existence of solutions we show boundedness of solutions.

**Proposition 2.3.12.** *We choose values  $R_u$  and  $R_v$  subject to*

$$R_u > \max\{u_2, u_H\} \quad \text{and} \quad h_T(R_u) < R_v < \frac{\beta}{\alpha}R_u.$$

*Let  $(u_0, v_0) \in L^2(0, 1)^2$  and assume that  $(u, v)$  is a solution of the system (2.1) - (2.3) on a certain time interval  $[0, T]$ . If the initial conditions are bounded, i.e.  $u_0 \leq R_u$  and  $v_0 \leq R_v$ , then the solution stays bounded from above,*

$$u(t, x) \leq R_u \quad \text{and} \quad v(t, x) \leq R_v.$$

*Proof.* We use the method of Stampaccia as it can be found in [Bre10, Theorem 10.3]. Let  $G \in C^1(\mathbb{R})$  be a function fulfilling

- i)  $|G'(s)| \leq M$  for all  $s \in \mathbb{R}$  and some positive constant  $M$ ,
- ii)  $G'(s) > 0$  for all  $s > 0$  and
- iii)  $G(s) = 0$  for all  $s \leq 0$ .

We set  $H(s) = \int_0^s G(\tilde{s})d\tilde{s}$  for  $s \in \mathbb{R}$  and remark that  $G$  and  $H$  are positive for  $s > 0$ . We define the functions

$$\begin{aligned}\varphi_u(t) &= \int_0^1 H(u(t, x) - R_u)dx && \text{for } t \in [0, T], \\ \varphi_v(t) &= \int_0^1 H(v(t, x) - R_v)dx && \text{for } t \in [0, T]\end{aligned}$$

and verify that  $\varphi_u(0) = \varphi_v(0) = 0$  and  $\varphi_u(t) \geq 0$  as well as  $\varphi_v(t) \geq 0$  holds. Moreover, we observe that  $\varphi_u \in C([0, T_0]; L^2(0, 1)) \cap C^1((0, T_0]; L^2(0, 1)) \cap C((0, T_0]; H_N^2(0, 1)) \cap L^2(0, T_0; H^1(0, 1))$  and  $\varphi_v \in C^1([0, T_0]; L^2(0, 1))$ .

Now, we calculate the derivatives

$$\begin{aligned}\frac{d}{dt}\varphi_u(t) &= \int_0^1 G(u(t, x) - R_u) \cdot \frac{\partial}{\partial t}u(t, x)dx, \\ &= \int_0^1 G(u(t, x) - R_u) \cdot \left(\frac{1}{\gamma}u_{xx}(t, x) + f(u(t, x), v(t, x))\right)dx, \\ &= -\frac{1}{\gamma} \int_0^1 G'(u(t, x) - R_u)u_x^2(t, x)dx + \int_0^1 G(u(t, x) - R_u)f(u(t, x), v(t, x))dx. \\ \frac{d}{dt}\varphi_v(t) &= \int_0^1 G(v(t, x) - R_v) \cdot \frac{\partial}{\partial t}v(t, x)dx, \\ &= \int_0^1 G(v(t, x) - R_v) \cdot g(u(t, x), v(t, x))dx.\end{aligned}$$

We would like to show that  $\frac{d}{dt}\varphi_u(t) \leq 0$  and  $\frac{d}{dt}\varphi_v(t) \leq 0$  holds. Then, together with the observations made above, this yields  $\varphi_u \equiv \varphi_v \equiv 0$ . And by definition of the functions  $G$  and  $H$  this induces  $u(t, x) \leq R_u$  and  $v(t, x) \leq R_v$  as desired.

Indeed, we see that  $-\frac{1}{\gamma} \int_0^1 G'(u(t, x) - R_u)u_x^2(t, x)dx \leq 0$ , thus it remains to show that

$$\int_0^1 G(u(t, x) - R_u) \cdot (\alpha v(t, x) - \beta u(t, x))dx \leq 0, \quad (2.29)$$

$$\int_0^1 G(v(t, x) - R_v) \cdot (u(t, x) - p(v(t, x)))dx \leq 0. \quad (2.30)$$

For  $t = 0$  we have by assumption that  $G(u_0(x) - R_u) = 0$  and  $G(v_0(x) - R_v) = 0$ . Because of the time-continuity we assume that there is  $t_0$  and  $x_0$  such that  $u(t, x) \leq R_u$  and  $v(t, x) \leq R_v$  for all  $t < t_0$  and all  $x \in [0, 1]$ , but  $v(t_0, x_0) > R_v$ . Then  $u(t_0, x_0) - p(v(t_0, x_0)) \leq R_u - p(R_v) < 0$  and the integral (2.30) is negative. Similarly, if  $v(t, x) \leq R_v$  but  $u(t_0, x_0) > R_u$ , then it holds  $\alpha v(t_0, x_0) - \beta u(t_0, x_0) \leq \alpha R_v - \beta R_u < 0$  and the integral (2.29) is negative.  $\square$

**Proposition 2.3.13.** *Let  $(u_0, v_0) \in L^2(0, 1)^2$ . Assume that  $(u, v)$  is a solution of system (2.1)- (2.3) on a certain time interval  $[0, T]$ . If  $u_0$  and  $v_0$  are nonnegative, then the solution stays nonnegative.*

*Proof.* We use the same method as in Proposition 2.3.12 and the same definitions of  $G$  and  $H$ . We define the functions

$$\begin{aligned}\varphi_u(t) &= \int_0^1 H(-u(t, x)) dx && \text{for } t \in [0, T], \\ \varphi_v(t) &= \int_0^1 H(-v(t, x)) dx && \text{for } t \in [0, T]\end{aligned}$$

and we verify that  $\varphi_u(0) = \varphi_v(0) = 0$  and  $\varphi_u(t) \geq 0$  as well as  $\varphi_v(t) \geq 0$  holds. Moreover, we observe that  $\varphi_u \in C([0, T_0]; L^2(0, 1)) \cap C^1((0, T_0]; L^2(0, 1)) \cap C((0, T_0]; H_N^2(0, 1)) \cap L^2(0, T_0; H^1(0, 1))$  and  $\varphi_u \in C^1([0, T_0]; L^2(0, 1))$ .

Now, we calculate the derivatives

$$\begin{aligned}\frac{d}{dt}\varphi_u(t) &= \int_0^1 G(-u(t, x)) \cdot \left(-\frac{\partial}{\partial t}u(t, x)\right) dx \\ &= \int_0^1 G(-u(t, x)) \cdot \left(-\frac{1}{\gamma}u_{xx}(t, x) - f(u(t, x), v(t, x))\right) dx \\ &= -\frac{1}{\gamma} \int_0^1 G'(-u(t, x))u_x^2(t, x) dx - \int_0^1 G(-u(t, x))f(u(t, x), v(t, x)) dx \\ \frac{d}{dt}\varphi_v(t) &= \int_0^1 G(-v(t, x)) \cdot \left(-\frac{\partial}{\partial t}v(t, x)\right) dx \\ &= \int_0^1 G(-v(t, x)) \cdot \left(-g(u(t, x), v(t, x))\right) dx\end{aligned}$$

Using the same kind of argumentation as in the proof of Proposition 2.3.12, we show that  $\frac{d}{dt}\varphi_u(t) \leq 0$  and  $\frac{d}{dt}\varphi_v(t) \leq 0$  holds. Then  $u(t, x) \geq 0$  and  $v(t, x) \geq 0$ .

Indeed, we see that  $-\frac{1}{\gamma} \int_0^1 G'(-u(t, x))u_x^2(t, x) dx \leq 0$ , thus it remains to show that it holds

$$\int_0^1 G(-u(t, x))(\beta u(t, x) - \alpha v(t, x)) dx \leq 0 \quad (2.31)$$

$$\int_0^1 G(-v(t, x)) \cdot (p(v(t, x)) - u(t, x)) dx \leq 0. \quad (2.32)$$

For  $t = 0$  we have by assumption that  $G(-u_0(x)) = 0$  and  $G(-v_0(x)) = 0$ . Because of the time-continuity we assume that there is  $t_0$  and  $x_0$  such that  $u(t, x) \geq 0$  for all  $t < t_0$  and all  $x \in [0, 1]$ , but  $v(t_0, x_0) < 0$ . Then holds  $p(v(t_0, x_0)) - u(t_0, x_0) < 0$  and the integral (2.32) is negative. Similarly if  $v(t, x) \geq 0$  but  $u(t_0, x_0) < 0$  then it holds  $\beta u(t_0, x_0) - \alpha v(t_0, x_0) < 0$  and the integral (2.31) is negative.  $\square$

**Theorem 2.3.14** (Global existence of solutions). *Assume that the initial conditions  $(u_0, v_0) \in L^\infty(0, 1)^2$  are nonnegative. Then the generic model (2.1) - (2.3) has a unique, nonnegative solution  $(u, v)$  in both the hysteresis and the bistable case satisfying*

$$u \in C([0, \infty); L^\infty(0, 1)) \cap C^1((0, \infty); L^2(0, 1)) \cap C((0, \infty); H_N^2(0, 1))$$

and

$$v \in C^1([0, \infty); L^\infty(0, 1)).$$

Moreover, it holds

$$u \in L^2(0, \infty; H^1(0, 1)).$$

*Proof.* The solution constructed in Proposition 2.3.11 exists for all times  $T > 0$ . Indeed, because it is bounded from below and above it cannot tend to infinity and, therefore, it can be prolonged successively. Moreover, if we assume that the initial condition is bounded, it is an element of  $L^\infty(0, 1)$  and also the solutions  $u(t, \cdot)$  and  $v(t, \cdot)$  are bounded and therefore they are in  $L^\infty(0, 1)$ .  $\square$

## 2.4 Global attractors for the kinetic system

We have already seen in Subsection 2.2 that the kinetic system (2.12) has two stable steady states  $S_0$  and  $S_2$  and a saddle  $S_1$ . The Jacobian evaluated at the hyperbolic steady state  $S_1$  has a positive and a negative eigenvalue, therefore the kinetic system (2.12) has a one-dimensional stable manifold  $W^s$  and one-dimensional unstable manifold  $W^u$  at  $S_1$  (see Figure 2.4). We know as a special case of Theorem 2.3.14 that all solutions with nonnegative initial conditions  $(u_0, v_0)$  are bounded for all times  $T$  and stay nonnegative. Now, we show that for all initial conditions the solution will approach  $S_0$  or  $S_2$ , except those lying on the stable manifold of  $S_1$ .

First, we investigate the location of the stable manifold  $W^s$ . We use here similar arguments as stated in [Nak12].

**Proposition 2.4.1.** *The stable manifold  $W^s$  at the steady state  $S_1$  cuts the positive  $u$ -axis in one point  $(u^s, 0)$  in both the hysteresis and the bistable case.*

For simplicity of the following arguments, we divide the phase plane  $\mathbb{R}_+^2$  into five subareas which are bounded by the nullclines  $f = 0$  and  $g = 0$ , as one can see in Figure 2.3.

**Definition:** We define five open sets by

$$\begin{aligned}\mathcal{O}_0 &= \{(u, v) \in \mathbb{R}_+^2 \mid f(u, v) < 0, g(u, v) < 0, u < u_1\}, \\ \mathcal{O}_2^1 &= \{(u, v) \in \mathbb{R}_+^2 \mid f(u, v) > 0, g(u, v) > 0, u_1 < u < u_2\}, \\ \mathcal{O}_2^2 &= \{(u, v) \in \mathbb{R}_+^2 \mid f(u, v) < 0, g(u, v) < 0, u_2 < u\}, \\ \mathcal{A}_l &= \{(u, v) \in \mathbb{R}_+^2 \mid f(u, v) > 0, g(u, v) < 0\}, \\ \mathcal{A}_r &= \{(u, v) \in \mathbb{R}_+^2 \mid f(u, v) < 0, g(u, v) > 0\}.\end{aligned}$$

*Proof of Proposition 2.4.1.* We consider the Jacobian matrix  $J(u_1, v_1)$  of the kinetic system (2.12) evaluated at  $S_1$  (see equation (2.13)) and its eigenvalue equation for the negative eigenvalue  $\lambda < 0$

$$-\beta u_\lambda + \alpha v_\lambda = \lambda u_\lambda, \quad (2.33)$$

$$u_\lambda - p'(v_1)v_\lambda = \lambda v_\lambda. \quad (2.34)$$

Setting  $v_\lambda = 1$  in equation (2.34), we obtain

$$u_\lambda = \lambda + p'(v_1).$$

In the hysteresis case we have  $p'(v_1) < 0$  and thus  $u_\lambda < 0$ . For the bistable case we remark that  $\lambda$  is given by

$$\lambda = -\frac{\beta + p'(v_1)}{2} - \frac{\sqrt{(\beta + p'(v_1))^2 - 4(\beta p'(v_1) - \alpha)}}{2} < -(\beta + p'(v_1)).$$

The previous inequality holds because  $\det J(u_1, v_1) = (\beta p'(v_1) - \alpha)$  is negative (see Lemma 2.2.1). Thus, in the bistable case  $u_\lambda = \lambda + p'(v_1) < -(\beta + p'(v_1)) + p'(v_1) = -\beta$  is negative as well.

Now, observe that the scalar product of the eigenvector  $(u_\lambda \ 1)^T$  and the normal vector of  $f(u, v) = 0$  at  $S_1$  which is given by  $(f_u(u_1, v_1) \ f_v(u_1, v_1)) = (-\beta \ \alpha)$  equals

$$\begin{pmatrix} u_\lambda \\ 1 \end{pmatrix} \cdot \begin{pmatrix} -\beta \\ \alpha \end{pmatrix} = -\beta u_\lambda + \alpha = \lambda u_\lambda > 0.$$

Thus, the angle  $\theta_f$  between these vectors (see Figure 2.3) is smaller than  $\frac{\pi}{2}$ .

The scalar product of the eigenvector  $(u_\lambda \ 1)^T$  and the normal vector of  $g(u, v) = 0$  at  $S_1$  equals

$$\begin{pmatrix} u_\lambda \\ 1 \end{pmatrix} \cdot \begin{pmatrix} 1 \\ -p'(v_1) \end{pmatrix} = u_\lambda - p'(v_1) = \lambda < 0.$$

Thus, the angle  $\theta_g$  between those vectors is between  $\frac{\pi}{2}$  and  $\pi$ . Therefore the tangent vector of the stable manifold  $W^s$  at  $S_1$  in a neighborhood of  $S_1$  is included in the set  $\mathcal{A}_l \cup \mathcal{A}_r \cup \{S_1\}$  (compare Figure 2.3).

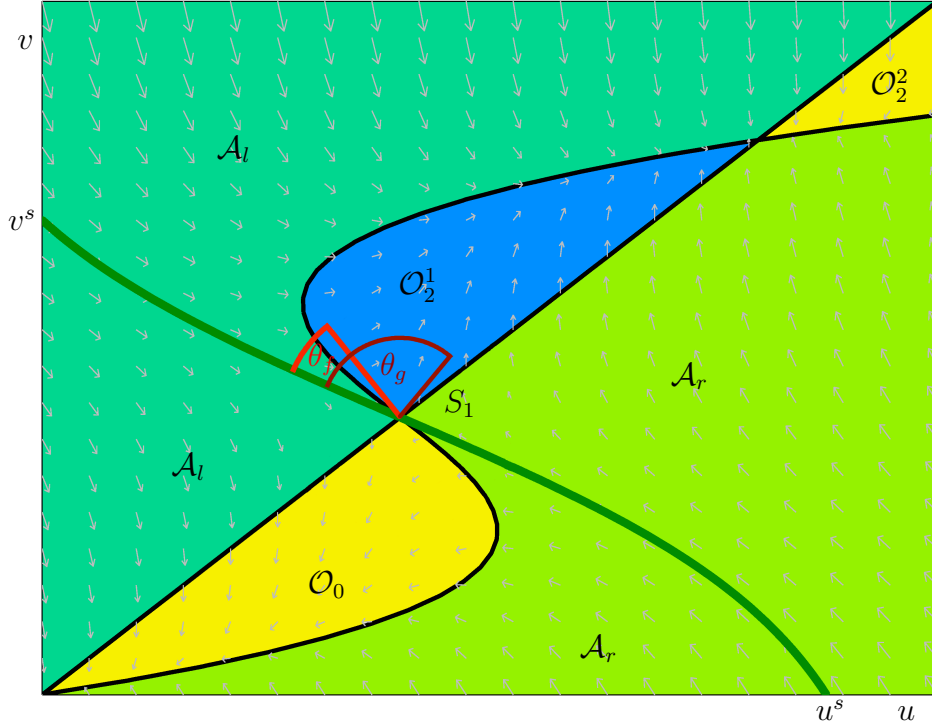


Figure 2.3: The phase plane for the kinetic system in the hysteresis case, divided by the nullclines into five subareas. The value  $\theta_f$  (resp.  $\theta_g$ ) denotes the angle between the eigenvector of the negative eigenvalue at  $S_1$  and the normal of  $f = 0$  (resp.  $g = 0$ ) at  $S_1$ . The stable manifold (darkgreen) cuts the  $u$ -axis in the point  $(u^s, 0)$  and the  $v$ -axis in  $(0, v^s)$ .

Next, we investigate the behavior of the time-reversed kinetic system, where we set  $\tilde{u}(t) = u(-t)$  and  $\tilde{v}(t) = v(-t)$

$$\begin{aligned} \frac{d}{dt} \tilde{u}(t) &= -f(\tilde{u}(t), \tilde{v}(t)), \\ \frac{d}{dt} \tilde{v}(t) &= -g(\tilde{u}(t), \tilde{v}(t)) \end{aligned}$$

for an initial condition  $(\tilde{u}_0, \tilde{v}_0) \in W^s \cap \mathcal{A}_r$  close to  $S_1$ . We will show that there is a time  $0 < T_0 < \infty$  such that holds  $(\tilde{u}(T_0), \tilde{v}(T_0)) = (u^s, 0)$  with  $u^s > 0$ .

In  $\mathcal{A}_r$  the vectorfield  $(-f, -g)$  is pointing down to the right. Thus, a trajectory cannot enter  $\mathcal{O}_2^1$  or  $\mathcal{O}_2^2$ . Moreover,  $(\tilde{u}(t), \tilde{v}(t))$  cannot cross the nullcline  $g(\tilde{u}, \tilde{v}) = 0$ , because the flux for the reversed system is pointing into  $\mathcal{A}_r$ .

Thus, we have to exclude the possibility that  $\tilde{u}(t)$  grows to infinity and  $\tilde{v}(t)$  does not cross  $v = 0$ . Therefore, we assume that there is a time  $T_{\max}$  such that  $\tilde{u}(t) \rightarrow \infty$  for  $t \rightarrow T_{\max}$  and  $\tilde{v}(t) > 0$  for all times  $t \in [0, T_{\max}]$ . But, then it necessarily holds

$T_{\max} = \infty$  because of

$$0 < \frac{d}{dt} \tilde{u}(t) = \beta \tilde{u}(t) - \alpha \tilde{v}(t) \leq \beta \tilde{u}(t),$$

which yields

$$\tilde{u}_0 \leq \tilde{u}(t) \leq \tilde{u}_0 + e^{\beta t}.$$

Moreover,  $\frac{d}{dt} \tilde{v}(t) < 0$  and thus  $0 < \tilde{v}(t) \leq \tilde{v}_0 < v_1$  for all  $t > 0$ . The polynomial  $p(v)$  attains its maximum in  $[0, v_1]$  at  $v_H$ . This leads to

$$\frac{d}{dt} \tilde{v}(t) = -g(\tilde{u}(t), \tilde{v}(t)) = -\tilde{u}(t) + p(\tilde{v}(t)) \leq -\tilde{u}(t) + p(v_H) = -\tilde{u}(t) + u_H.$$

We choose  $t_0 > 0$  big enough such that  $\tilde{u}(t_0) + u_H < -1$  holds. This is possible as  $\tilde{u}$  is growing to infinity. Then for  $t > t_0$  it holds

$$\tilde{v}(t) \leq \tilde{v}(t_0) - (t - t_0),$$

which is negative for  $t$  big enough. This yields the contradiction to the assumption.  $\square$

**Remark 2.4.2.** *Simulations suggest, that the stable manifold at  $S_1$  also cuts the positive  $v$ -axis in one point  $(0, v^s)$ . Because of the fast growing term  $v^3$ , we are not able to prove this.*

Using the previous Proposition, we see that the stable manifold  $W^s$  divides the phase plane  $\mathbb{R}_+^2$  into two disjoint and connected subsets  $\mathcal{U}_0, \mathcal{U}_2$  such that there is the cover

$$\mathbb{R}_+^2 = \{(u, v) \mid u \geq 0, v \geq 0\} = \mathcal{U}_0 \cup \mathcal{U}_2 \cup W^s.$$

The set  $\mathcal{U}_0$  contains  $S_0$  and is bounded whereas  $\mathcal{U}_2$  contains  $S_2$  and is unbounded.

A trajectory  $(u(t), v(t))$  with initial condition  $(u_0, v_0) \in W^s$  will approach  $S^1$  by definition of the stable manifold. For all other nonnegative initial condition one of the two other steady states will be approached.

**Proposition 2.4.3.** *A solution of the kinetic system (2.12) in both cases, hysteresis and bistable, with initial condition lying in  $\mathcal{U}_0$  (resp.  $\mathcal{U}_2$ ) tends for  $t \rightarrow \infty$  to  $S_0$  (resp. to  $S_2$ ).*

*Proof.* At first we remark that no trajectory can cross the stable manifold  $W^s$ . Together with the positivity of solutions, which follows as special case from Proposition 2.3.13, this yields that  $\mathcal{U}_0$  and  $\mathcal{U}_2$  are invariant sets.

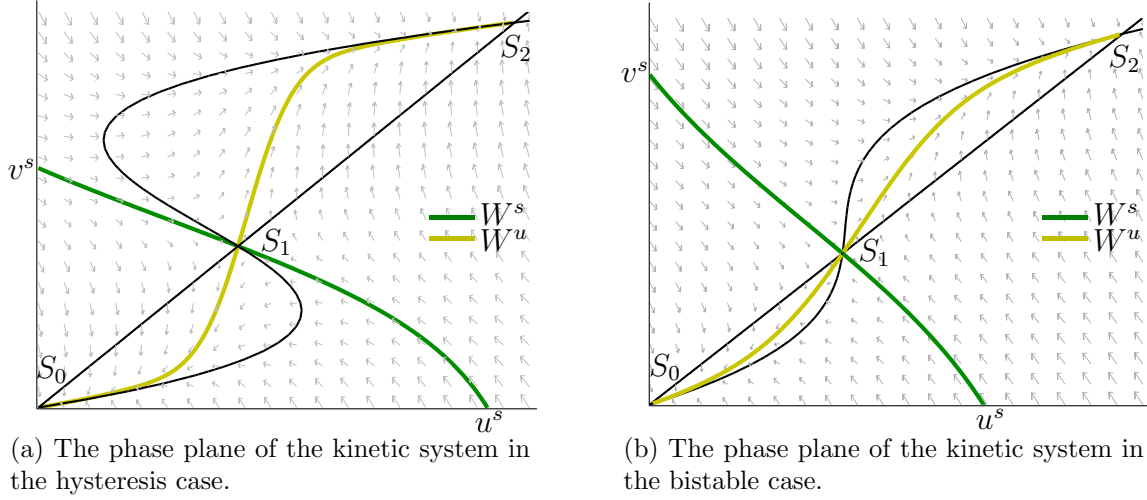


Figure 2.4: The phase plane for the kinetic system in the hysteresis and the bistable case. All trajectories starting below the stable manifold  $W^s$  of  $S_1$  tend for  $t \rightarrow \infty$  to  $S_0$  whereas those starting above tend to  $S_2$ .

In the following we denote sets

$$\begin{aligned} \mathcal{A}_{r,0} &= \mathcal{A}_r \cap \mathcal{U}_0 & \mathcal{A}_{l,0} &= \mathcal{A}_l \cap \mathcal{U}_0 \\ \mathcal{A}_{r,2} &= \mathcal{A}_r \cap \mathcal{U}_2 & \mathcal{A}_{l,2} &= \mathcal{A}_l \cap \mathcal{U}_2 \end{aligned}$$

and remark that holds

$$\mathcal{U}_0 = \mathcal{A}_{r,0} \cup \mathcal{A}_{l,0} \cup \overline{\mathcal{O}_0} \setminus \{S_0\} \quad \mathcal{U}_2 = \mathcal{A}_{r,2} \cup \mathcal{A}_{l,2} \cup \overline{\mathcal{O}_2^1} \setminus \{S_2\} \cup \overline{\mathcal{O}_2^2}$$

We show that solutions starting in  $\mathcal{O}_0$  (resp.  $\mathcal{O}_2^1, \mathcal{O}_2^2$ ) will tend to  $S_0$  (resp.  $S_2$ ) using the direct method of Lyapunov (see [RHL77]). Therefore, we define the function

$$F_0(u, v) = u^2 + v^2 \geq 0$$

which fulfils  $F_0(0, 0) = 0$  and

$$\frac{d}{dt} F_0(u(t), v(t)) = 2uu_t + 2vv_t.$$

In the set  $\mathcal{O}_0$  it holds  $u, v > 0$  as well as  $u_t = f(u, v) < 0$  and  $v_t = g(u, v) < 0$ , hence  $\frac{d}{dt} F_0(u(t), v(t)) < 0$  for all  $(u, v) \in \mathcal{O}_0$ . Thus,  $F_0$  is a Lyapunov function for the set  $\mathcal{O}_0$  and shows that  $S_0$  is an attractor for all  $(u, v) \in \mathcal{O}_0$ .

Similarly, we define the function

$$F_2^1(u, v) = (u - u_2)^2 + (v - v_2)^2 \geq 0$$

which fulfils  $F_2^1(u_2, v_2) = 0$  and

$$\frac{d}{dt}F_2^1(u(t), v(t)) = 2(u - u_2)u_t + 2(v - v_2)v_t.$$

In  $\mathcal{O}_2^1$  we have  $u < u_2, v < v_2$  and  $u_t, v_t > 0$ , hence  $\frac{d}{dt}F_2^1(u(t), v(t)) < 0$  for all  $(u, v) \in \mathcal{O}_2^1$ .

For  $\mathcal{O}_2^2$  we set  $F_2^2(u, v) = F_2^1(u, v)$  and observe that we have  $u > u_2, v > v_2$  and  $u_t, v_t < 0$ , hence  $\frac{d}{dt}F_2^2(u(t), v(t)) < 0$  for all  $(u, v) \in \mathcal{O}_2^2$ .

Next, we show that all trajectories starting in the first quadrant but not on  $W^s$  will reach one of the sets  $\mathcal{O}_0, \mathcal{O}_2^1, \mathcal{O}_2^2$ .

In the set  $\mathcal{A}_{r,0}$  the flux is pointing above to the right. Because a trajectory cannot leave  $\mathcal{U}_0$  it has to enter  $\mathcal{O}_0$  at some time  $t$ . In  $\mathcal{A}_{l,0}$  the flux is pointing down to the left and again a trajectory starting there has to enter  $\mathcal{O}_0$  at some time  $t$ . The same argumentation applies for the sets  $\mathcal{A}_{r,2}$  and  $\mathcal{A}_{l,2}$ .  $\square$

In [Nak12] it was shown for a similar model that solutions of the time-dependent system with initial conditions such that it holds

$$\left( \min_{x \in [0,1]} u_0(x), \min_{x \in [0,1]} v_0(x) \right) \in \mathcal{U}_0 \quad \text{and} \quad \left( \max_{x \in [0,1]} u_0(x), \max_{x \in [0,1]} v_0(x) \right) \in \mathcal{U}_0$$

will approach the constant solution  $S_0$  for  $t \rightarrow \infty$ . Similarly if

$$\left( \min_{x \in [0,1]} u_0(x), \min_{x \in [0,1]} v_0(x) \right) \in \mathcal{U}_2 \quad \text{and} \quad \left( \max_{x \in [0,1]} u_0(x), \max_{x \in [0,1]} v_0(x) \right) \in \mathcal{U}_2$$

then it holds  $\lim_{t \rightarrow \infty} (u(t, x), v(t, x)) = S_2$ .

We will not prove this here. But, we observe this behaviour in simulations. Moreover, we observe in simulations that for initial conditions fulfilling the weaker condition  $(u_0(x), v_0(x)) \in \mathcal{U}_0$  (resp.  $\mathcal{U}_2$ ) for all  $x \in [0, 1]$  the solution  $(u(t, x), v(t, x))$  will approach  $S_0$  (resp.  $S_2$ ).

Hence, we expect pattern formation in such system for initial conditions such that there are at least two disjoint intervals  $I_1, I_2 \subset [0, 1]$  with  $(u_0(x), v_0(x)) \in \mathcal{U}_0$  for  $x \in I_1$  and  $(u_0(x), v_0(x)) \in \mathcal{U}_2$  for  $x \in I_2$ .

**Example 2.4.4.** *We consider the generic model in the hysteresis case for kinetic functions  $f(u, v) = 1.4v - u$  and  $p(v) = v^3 - 6.3v^2 + 10v$ . The saddle of the kinetic system has the coordinates  $S_1 = (u_1, v_1) = (2.8, 2)$ . We perform simulations for the initial condition*

$$u_0(x) = \begin{cases} 2.79 & \text{for } x \leq 0.4 \\ 2.81 & \text{for } x > 0.4 \end{cases} \quad \text{and} \quad v_0(x) = 2. \quad (2.35)$$

The slope of stable manifold  $W^s$  at  $S_1$  is negative, thus for  $x \leq 0.4$  the initial condition  $(u_0(x), v_0(x))$  lies below  $W^s$ , whereas it is above for  $x > 0.4$ . Although the initial condition is almost constant, this is enough to produce a pattern. Compare Figure 2.5b and 2.5c.

Moreover, we perform simulations for initial conditions lying entirely in the set  $\mathcal{U}_0$  and  $\mathcal{U}_2$ , resp., a situation where we do not expect pattern formation.

The initial condition  $u_0(x) = 6x$  and  $v_0(x) = -\frac{1}{4}u_0(x) + \frac{5}{2}$  corresponds in the phase plane (Figure 2.5a) to the blue line and lies below the stable manifold. Therefore, the time-dependent solutions approaches the steady state  $S_0 = (0, 0)$ , as one can see in Figure 2.5d.

Similarly, the initial condition  $u_0(x) = 7x$  and  $v_0(x) = -\frac{2}{7}u_0(x) + 3$ , which corresponds in the phase plane to the red line and lies above the stable manifold. The solution approaches the steady state  $S_2 = (u_2, v_2) = (6.02, 4.3)$  as one can see in Figure 2.5e

## 2.5 Summary

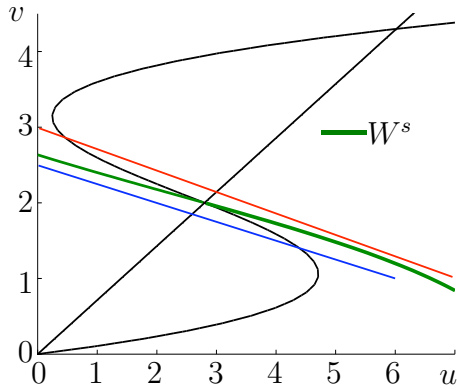
We introduced the generic model which consists of one reaction-diffusion equation coupled with one ordinary differential equation supplemented with homogeneous Neumann boundary conditions and bounded and nonnegative initial conditions. We showed the existence of nonnegative global-in-time solutions for this model.

We distinguish between two cases of the generic model. In the bistable case, the kinetic functions are monotone increasing, whereas in the hysteresis case there are overlapping branches of the nullclines.

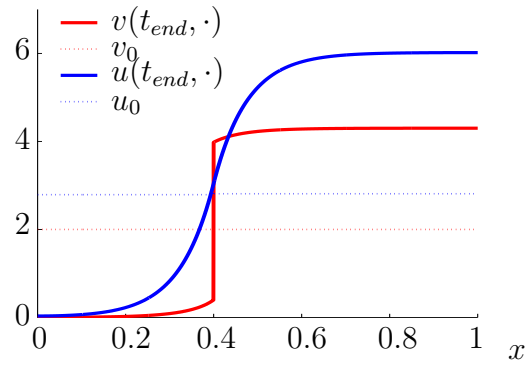
We investigated the kinetic system for both cases, where we did not observe any significant difference. Both systems show bistability which means they possess two stable steady states and one saddle in between. The stable manifold of the saddle is a separatrix for the kinetic system. This means that for initial conditions on one side of the separatrix the solutions will tend to one steady state and for initial conditions on the other side of the separatrix the solutions will tend to the other steady state.

We are interested in the ability of the generic model to produce patterns. We showed that it does not exhibit diffusion-driven instabilities. Thus, if the model allows pattern formation, then the mechanism cannot be of Turing-type, the most frequently used mechanism for biological pattern formation.

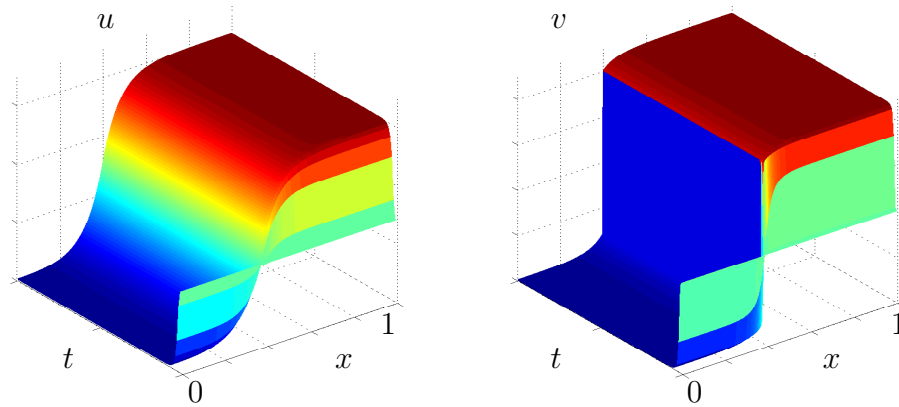
The results for the kinetic system suggests that the generic model might allow pattern formation for both cases, with the final pattern strongly depending on the initial conditions. We do not expect pattern that arise spontaneously from small perturbations.



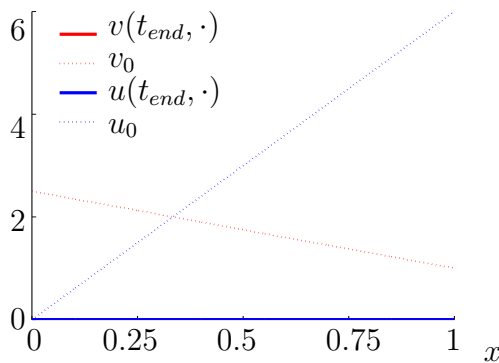
(a) The phase plane of the kinetic system with the stable manifold  $W^s$  and initial conditions lying entirely above (red line) and below (blue line), resp.,  $W^s$ .



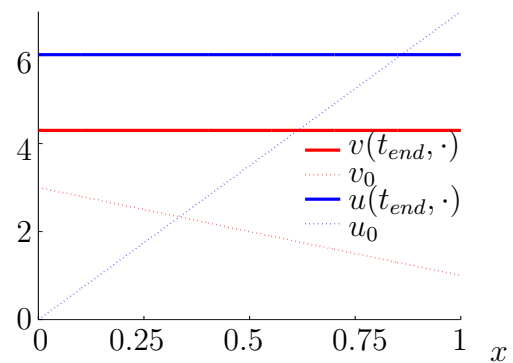
(b) Simulations for the initial condition given by (2.35) lead to the formation of a nonhomogeneous stationary solution.



(c) Simulations for initial conditions given by (2.35) lead to the formation of a nonhomogeneous stationary solution.



(d) Simulations for initial condition corresponding to the blue line in the phase plane (a), lying entirely below the separatrix



(e) Simulations for initial condition corresponding to the red line in the phase plane (a), lying entirely above the separatrix

Figure 2.5: Simulations of the generic model in the hysteresis case for initial conditions with different position relative to the separatrix  $W^s$ .



# Chapter 3

## Instability of stationary solutions for the bistable case

In this chapter we study system (2.1) in the bistable case. We construct non-homogeneous stationary solutions which do not bifurcate from homogeneous ones. Moreover, we show that there is no pattern formation possible in the bistable system by showing that all nonhomogeneous stationary solutions are unstable.

### 3.1 Construction of stationary solutions

The stationary solutions of (2.1) are solutions of

$$\begin{aligned} 0 &= \frac{1}{\gamma}U_{xx} + f(U, V), \\ 0 &= g(U, V) \end{aligned} \tag{3.1}$$

for  $x \in (0, 1)$  with the homogeneous Neumann boundary condition for  $U$ .

We recall that in the bistable case the equation  $u = p(v)$  can be uniquely solved with respect to  $v$  and we call  $h$  the inverse function.

To simplify the notation we denote the value

$$\gamma_0 := \frac{\pi^2}{\alpha h'(u_1) - \beta} \tag{3.2}$$

where  $u_1$  is the  $u$ -coordinate of the unstable homogeneous steady state  $S_1$ .

**Theorem 3.1.1.** *There is a monotone increasing nonhomogeneous stationary solution  $(U(x), V(x)) \in C^2([0, 1])^2$  of the generic model (2.1) in the bistable case for all diffusion coefficients  $\frac{1}{\gamma}$  with  $\gamma > \gamma_0$ .*

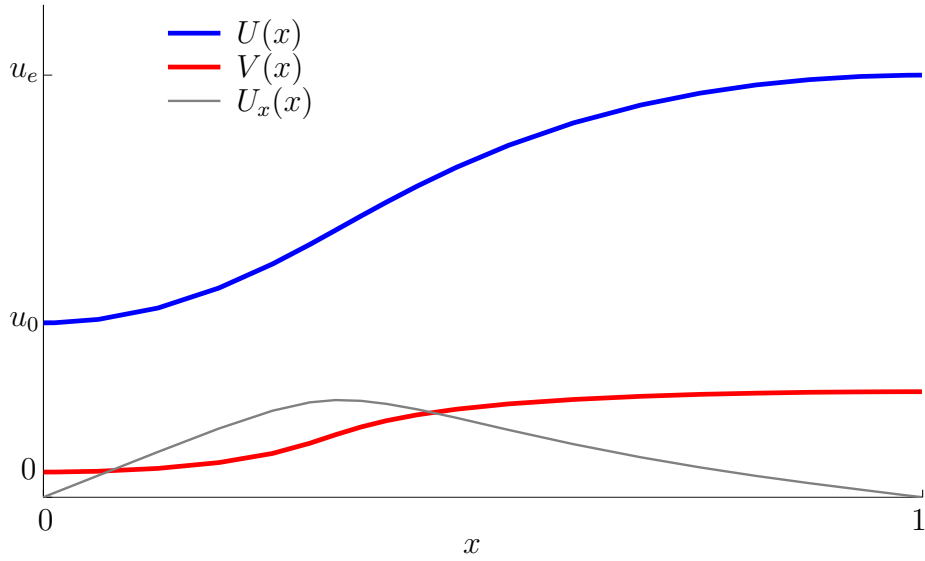


Figure 3.1: A stationary solution  $(U(x), V(x))$  of system (2.1) together with the derivative  $U_x(x)$ .

**Definition:** Let  $k \in \mathbb{N}$  and  $k \geq 2$ . We call a function  $U \in C([0, 1])$  a **periodic function** on  $[0, 1]$  with  $k$  modes if  $U(x)$  is monotone on  $[0, \frac{1}{k}]$  and

$$U(x) = \begin{cases} U(x - \frac{2j}{k}) & \text{for } x \in [\frac{2j}{k}, \frac{2j+1}{k}] \\ U(\frac{2j+2}{k} - x) & \text{for } x \in [\frac{2j+1}{k}, \frac{2j+2}{k}] \end{cases} \quad (3.3)$$

for every  $j \in \{0, 1, 2, \dots\}$  such that  $2j + 2 \leq k$ .

**Corollary 3.1.2.** *There is a monotone decreasing nonhomogeneous stationary solution  $(U(x), V(x)) \in C^2([0, 1])^2$  of system (2.1) in the bistable case for all diffusion coefficients  $\frac{1}{\gamma}$  with  $\gamma > \gamma_0$ .*

*Furthermore, there is a nonhomogeneous stationary solution  $(U(x), V(x)) \in C^2([0, 1])^2$  of system (2.1) in the bistable case which is periodic with  $k$  modes for all diffusion coefficients  $\frac{1}{\gamma}$  with  $\gamma > k^2\gamma_0$ .*

In summary, we obtain for every diffusion coefficient a finite number of stationary solutions, three homogeneous ones and at least  $2 \lfloor \sqrt{\frac{\gamma}{\gamma_0}} \rfloor$  nonhomogeneous ones.

*Proof of Corollary 3.1.2.* For the first part of the Corollary, we construct a monotone increasing solution  $(\tilde{U}(x), \tilde{V}(x))$  of (3.1) using Theorem 3.1.1. Then we set

$$U(x) = \tilde{U}(1 - x) \quad V(x) = \tilde{V}(1 - x)$$

which are monotone decreasing functions by definition. Moreover, because of

$$g(U, V) = g(\tilde{U}, \tilde{V}) = 0 \quad \text{and} \quad \frac{1}{\gamma}U_{xx} + f(U, V) = (-1)^2 \frac{1}{\gamma}\tilde{U}_{xx} + f(\tilde{U}, \tilde{V}) = 0,$$

$(U(x), V(x))$  is a solution of system (3.1).

For the second part of the Corollary, we construct a monotone (increasing or decreasing) solution  $(\tilde{U}(x), \tilde{V}(x))$  of system (3.1) for the diffusion coefficient  $\frac{k^2}{\gamma}$ . This is possible since  $\gamma > k^2\gamma_0$ . Now, we define the functions

$$U(x) = \tilde{U}(kx) \quad V(x) = \tilde{V}(kx) \quad \text{for } x \in [0, \frac{1}{k}]$$

which we continue periodically for  $x \in [0, 1]$  by formula (3.3)  $U(x)$  and  $V(x)$  are periodic with  $k$  modes by construction. Moreover,  $(U(x), V(x))$  is a solution of system (3.1) for the diffusion coefficient  $\frac{1}{\gamma}$  as

$$g(U, V) = g(\tilde{U}, \tilde{V}) = 0$$

and

$$\frac{1}{\gamma}U_{xx}(x) + f(U(x), V(x)) = \frac{k^2}{\gamma}\tilde{U}_{xx}(kx) + f(\tilde{U}(kx), \tilde{V}(kx)) = 0.$$

□

For the proof of Theorem 3.1.1 we proceed by a standard method for solving boundary value problems of second order ordinary differential equation. An introduction to this topic can be found in [For10], for a more detailed analysis we refer to [Ver10] or [Sch90].

For solving problem (3.1), we remind that equation  $g(U, V) = 0$  can be uniquely solved with respect to  $V$ . Hence, we plug  $V = h(U)$  into the first equation of (3.1). We now observe that a solution  $(U(x), V(x))$  of problem (3.1) is given by a solution of

$$0 = \frac{1}{\gamma}U_{xx}(x) + q(U(x)), \tag{3.4}$$

for  $x \in [0, 1]$  with  $U_x(0) = U_x(1) = 0$  and  $V(x) = h(U(x))$ . Here,  $q(u) = \alpha h(u) - \beta u$ , as defined in Section 2.1.

We want to construct a solution in the phase plane. We observe that equation (3.4) is equivalent to the system

$$\begin{aligned} U_x &= W, \\ W_x &= -\gamma q(U). \end{aligned} \tag{3.5}$$

To construct a monotone increasing solution of the boundary value problem (3.4), we need to connect a point  $(u_0, 0)$  with a point  $(u_e, 0)$ , where  $u_e > u_0$ , by a trajectory  $(U, W)$  which has to be such that  $W(x) > 0$  for all  $x \in (0, 1)$  (cf. Figure

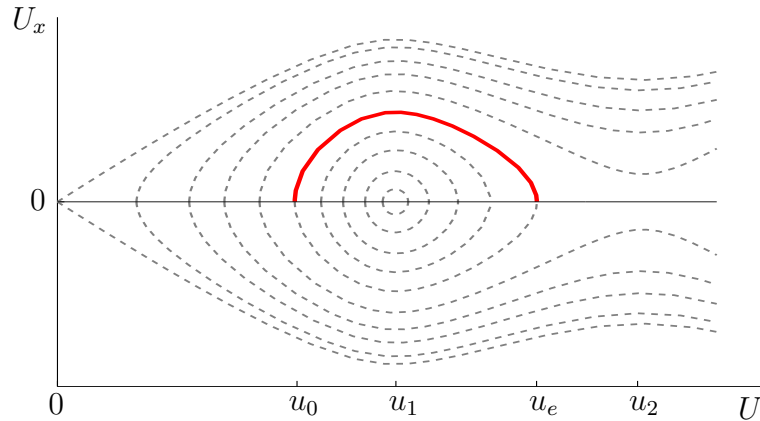


Figure 3.2: The phase plane in the bistable case with a trajectory connecting  $(u_0, 0)$  with  $(u_e, 0)$

3.2.). We see that for all values  $u_0$  problem (3.5) together with the initial condition  $(U(0), W(0)) = (u_0, 0)$  has a unique solution  $(U(x, u_0), W(x, u_0))$ . Hence, we have to choose  $u_0$ , such that  $W(1, u_0) = 0$  and  $U(1, u_0) = u_e$  holds.

To find the appropriate value  $u_0$ , we define the potential associated to equation (3.4).

**Definition:** The function  $Q$ , which is defined by

$$Q(u) := \int_0^u q(\tilde{u})d\tilde{u}$$

is called the **potential** of equation (3.4).

By definition the potential fulfils  $Q'(u) = q(u)$  and  $Q(0) = 0$ . Moreover, it is continuous. Using the change of variables  $v = h(u)$ , we obtain  $Q(u) = F(h(u))$ , where

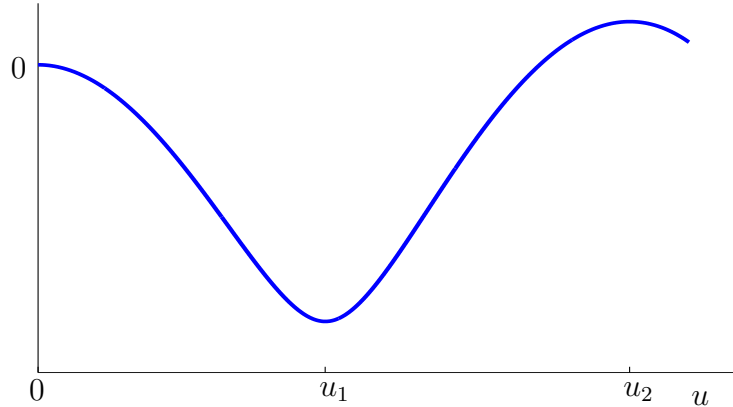
$$F(v) = \int_0^v (\alpha\tilde{v} - \beta p(\tilde{v}))p'(\tilde{v})d\tilde{v},$$

is a polynomial of degree 6 having a double zero at  $v = 0$ .

We can calculate the derivative

$$\frac{d}{dv}F(v) = (\alpha v - \beta p(v))p'(v),$$

which has zeros  $0, v_1, v_2$ . Since the leading coefficient  $-\frac{\beta a_2^2}{2}$  of  $F$  is negative,  $Q(u)$  has a minimum at  $u_1$  and maxima at  $0$  and  $u_2$ . See Figure 3.3 for a possible behaviour of the potential  $Q(u)$ .

Figure 3.3: The potential  $Q$  in the bistable case

Multiplying equation (3.4) by  $U_x$  and integrating over  $x$  leads to

$$0 = \frac{1}{\gamma} U_{xx} U_x + q(U) U_x, \quad (3.6)$$

$$0 = \frac{1}{\gamma} \int \frac{d}{dx} \left( \frac{U_x^2}{2} \right) dx + \int q(U) dU. \quad (3.7)$$

For  $U$  being a solution of (3.4), we see that for all  $x \in [0, 1]$  the condition

$$\frac{1}{\gamma} \frac{U_x^2(x)}{2} + Q(U(x)) = \text{constant} \quad (3.8)$$

has to be fulfilled. The left-hand side of (3.8) is called the “first integral” of system (3.4). In a physical context the constant corresponds to the total energy of the system and  $Q(U(x))$  the potential energy (see [Arn06]).

The homogeneous Neumann boundary condition at  $x = 0$  and  $x = 1$  induces that this constant equals

$$Q(u_0) = Q(u_e). \quad (3.9)$$

This, furthermore, determines the connection between  $u_0$  and  $u_e$ .

Because of the shape of  $Q$  it is possible to find values  $0 < u_0 < u_1 < u_e < u_2$  fulfilling the above condition such that  $Q(u) < Q(u_0)$  for all  $u \in (u_0, u_e)$ .

**Definition:** We call  $I = (u_{\min}, u_{\max})$  with  $0 \leq u_{\min}$  and  $u_{\max} \leq u_2$  the maximal interval such that for all  $u_0 \in I \setminus \{u_1\}$  there exists a unique value  $u_e \in I$  with  $u_e \neq u_0$ , such that  $Q(u_0) = Q(u_e)$  holds.

**Lemma 3.1.3.** *If the potential  $Q(u_2)$  at the  $u$ -coordinate of the intersection point  $S_2$  is nonnegative, then  $u_{\min} = 0$  and  $u_{\max} \in (u_1, u_2]$  is defined by  $Q(u_{\max}) = 0$ . If  $Q(u_2) \leq 0$ , then  $u_{\max} = u_2$  and  $u_{\min} \in [0, u_1)$  is defined by  $Q(u_{\min}) = Q(u_2)$ . In particular, if  $Q(u_2) = 0$ , then  $I = (0, u_2)$ .*

*Proof.* The values 0 and  $u_2$  are the local maxima of  $Q(u)$ . Hence, we only need to figure out at which of those values the potential is smaller. This provides the assertion of the lemma, having in mind that  $Q(0) = 0$ .  $\square$

**Remark 3.1.4.** *The case  $Q(u_2) = 0$  signifies that the area between the graph of  $q(u)$  and the  $u$ -axis is the same between 0 and  $u_1$ , as well as between  $u_1$  and  $u_2$  but with different sign. By Remark 2.1.11 this corresponds to  $u_1 = u_W$  and therefore  $q(u)$  is point symmetric around  $u_1$ .*

So far there are many possible choices of the value  $u_0$  and  $u_e$ . To assure that a solution connecting  $u_0$  and  $u_e$  is a solution on the interval  $[0, 1]$ , we consider the so-called “time-map” (see [Sch90] for a detailed exposition concerning time-maps).

**Definition:** We define the **time-map**  $T(u_0)$  as minimal “time”  $x$  needed for a trajectory of the phase plane associated to system (3.5) starting at  $(u_0, 0)$  to reach the  $u$ -axis again.

$$\begin{aligned} \mathcal{D}(T) &:= \{u_0 \in \mathbb{R} \mid \exists x > 0 \text{ with } W(x, u_0) = 0 \text{ and } u_0 < U(x, u_0)\}, \\ T(u_0) &:= \min\{x > 0 \mid W(x, u_0) = 0\}, \text{ for } u_0 \in \mathcal{D}(T). \end{aligned}$$

**Lemma 3.1.5.** *The domain of definition for the time-map is given by*

$$\mathcal{D}(T) := (u_{\min}, u_1).$$

*Proof.* Finding  $x > 0$  such that  $W(x, u_0) = 0$  requires  $U(x, u_0) = u_e$ . Hence, we have to choose  $u_0$  such that there is  $u_e$  with  $Q(u_0) = Q(u_e)$ . This is by definition the interval  $I = (u_{\min}, u_{\max})$ . Furthermore, we require that  $u_0 < u_e$ , hence  $\mathcal{D}(T) = (u_{\min}, u_1)$ .  $\square$

**Proposition 3.1.6.** *The time-map can be calculated by the formula*

$$T(u_0) = \frac{1}{\sqrt{2\gamma}} \int_{u_0}^{u_e} \frac{du}{\sqrt{Q(u_0) - Q(u)}}.$$

*Proof.* We deduce from (3.8) the differential equation

$$U_x = \pm \sqrt{2\gamma(Q(u_0) - Q(U(x)))}.$$

We choose the positive branch, as we are interested in a monotone increasing solution  $U(x)$ , and solve the equation by separation of variables. Hence, we obtain a formula for  $x$  in terms of  $U(x)$

$$x = \frac{1}{\sqrt{2\gamma}} \int_{u_0}^{U(x)} \frac{du}{\sqrt{Q(u_0) - Q(u)}}.$$

In particular, we deduce the formula for the time-map.  $\square$

**Proposition 3.1.7.** *The start value  $u_0$  of a monotone increasing solution of equation (3.4) is determined by*

$$T(u_0) = 1.$$

**Theorem 3.1.8.** *The mapping  $u_0 \mapsto T(u_0)$  is well-defined for all  $u_0 \in \mathcal{D}(T)$ . Furthermore, it is continuously differentiable with range  $(\frac{\pi}{\sqrt{\gamma Q''(u_1)}}, \infty)$ .*

This is a standard result and can be found for example in [Sch90]. We will give here a direct proof without using results on time-maps of problem (3.1) with Dirichlet boundary conditions.

*Proof.* As the potential  $Q(u)$  has a local minimum at  $u_1$ , it is convenient to split the integral defining  $T(u_0)$  at  $u_1$  into two parts. Referring to the first part of the integral as

$$T_1(u_0) = \frac{1}{\sqrt{2\gamma}} \int_{u_0}^{u_1} \frac{du}{\sqrt{Q(u_0) - Q(u)}}$$

and to the second part as

$$T_2(u_e) = \frac{1}{\sqrt{2\gamma}} \int_{u_1}^{u_e} \frac{du}{\sqrt{Q(u_e) - Q(u)}},$$

we obtain the representation

$$T(u_0) = T_1(u_0) + T_2(u_e(u_0)),$$

where the dependence  $u_e(u_0)$  is determined by  $Q(u_0) = Q(u_e)$ .

We divide the proof of the theorem into three steps. After showing the continuity of the time-map, we investigate its well-definedness and the behaviour for  $u_0$  near  $u_{\min}$ . The last step is devoted to the behaviour of the mapping for  $u_0$  near  $u_1$ .

**Continuity:** The time-map  $T(u_0)$  is implicitly defined by

$$W(T(u_0), u_0) = 0.$$

Furthermore, we know by definition that  $u_1 < U(T(u_0), u_0) = u_e < u_2$  and we calculate

$$\frac{\partial}{\partial x} W(T(u_0), u_0) = \frac{\partial^2}{\partial x^2} U(T(u_0), u_0) = \gamma q(U(T(u_0), u_0)) = \gamma q(u_e) > 0.$$

Hence, using the implicit function theorem, we obtain that  $T(u_0)$  has the same regularity as  $W(x, u_0)$ . But,  $q(u)$  is at least  $C^1$  (see 2.1.6) and therefore  $W \in C^1$  as well by the standard regularity theorem for ODEs (see [Chi00]).

**Well-definedness and behaviour near  $u_{\min}$ :** The integral  $T_1(u_0)$  is improper, because the denominator is zero for  $u = u_0$ . Therefore, we choose  $\delta > 0$  small, split the integral and investigate its behaviour near  $u_0$ .

$$T_1(u_0) = \frac{1}{\sqrt{2\gamma}} \int_{u_0}^{u_0+\delta} \frac{du}{\sqrt{Q(u_0) - Q(u)}} + \frac{1}{\sqrt{2\gamma}} \int_{u_0+\delta}^{u_1} \frac{du}{\sqrt{Q(u_0) - Q(u)}}.$$

The second integral is proper, so we have to investigate the first one. We remind that  $Q(u) = F(h(u))$  with  $F$  being a polynomial of degree 6 with a double zero at  $v = 0$ . We write  $c_n$  for the coefficient in front of the monomial  $v^n$  in  $F(v)$ . As  $v_0 := h(u_0)$  is a zero of  $F(v_0) - F(v)$ , we can factor out  $(v - v_0)$  to find an approximation of  $Q(u_0) - Q(u)$  near  $u_0$ .

$$\begin{aligned} F(v_0) - F(v) &= (c_6 v_0^6 + c_5 v_0^5 + c_4 v_0^4 + c_3 v_0^3 + c_2 v_0^2) \\ &\quad - (c_6 v^6 + c_5 v^5 + c_4 v^4 + c_3 v^3 + c_2 v^2) \\ &= (v_0 - v) [c_6(v_0^5 + v_0^4 v + v_0^3 v^2 + v_0^2 v^3 + v_0 v^4 + v^5) + \\ &\quad c_5(v_0^4 + v_0^3 v + v_0^2 v^2 + v_0 v^3 + v^4) + \\ &\quad c_4(v_0^3 + v_0^2 v + v_0 v^2 + v^3) + c_3(v_0^2 + v_0 v + v^2) + c_2(v_0 + v)] \\ &\approx (v_0 - v)(6c_6 v_0^5 + 5c_5 v_0^4 + 4c_4 v_0^3 + 3c_3 v_0^2 + 2c_2 v_0) \\ &=: (v_0 - v)(-1) \text{pol}(v_0) \end{aligned}$$

As  $F(v_0) - F(v)$  is positive for  $v > v_0$ , but  $v$  close to  $v_0$ , the expression  $\text{pol}(v_0)$  is positive and tends to zero for  $v_0 \rightarrow 0$ . Furthermore,  $\text{pol}(v_0)$  does not depend on  $v = h(u)$  anymore, so we can pull the term out of the integral and obtain

$$\int_{u_0}^{u_0+\delta} \frac{du}{\sqrt{F(h(u_0)) - F(h(u))}} \approx \frac{1}{\sqrt{\text{pol}(h(u_0))}} \int_{u_0}^{u_0+\delta} \frac{du}{\sqrt{h(u) - h(u_0)}}.$$

Now, we carry out the change of variables  $u = p(v)$  and use the notation  $v_\delta = h(u_0 + \delta)$  and  $v_0 = h(u_0)$  to write

$$\int_{u_0}^{u_0+\delta} \frac{du}{\sqrt{h(u_0) - h(u)}} = \int_{v_0}^{v_\delta} \frac{p'(v)dv}{\sqrt{v - v_0}}.$$

As  $p$  is a polynomial of degree 3 we use three times integration by parts and obtain

$$\int_{u_0}^{u_0+\delta} \frac{du}{\sqrt{h(u) - h(u_0)}} = 2p'(v_\delta)(v_\delta - v_0)^{\frac{1}{2}} - \frac{4}{3}p''(v_\delta)(v_\delta - v_0)^{\frac{3}{2}} + \frac{8}{15}p'''(v_\delta)(v_\delta - v_0)^{\frac{5}{2}}.$$

We check that the expression on the right hand side is positive. By assumption  $p'(v) > 0$  for all  $v$ ,  $p''(v) = 6a_2v + 2a_1$  is a monotone increasing straight line with positive zero at  $v = -\frac{a_1}{3a_2}$ , cf. Proposition 2.1.2. Therefore,  $p''(v_\delta) < 0$  for  $v_0$  and  $\delta$  small enough. Finally,  $p'''(v) = 6a_2$  is a positive constant. For  $\delta$  small we use the approximation  $h(u_0 + \delta) \approx h(u_0) + h'(u_0)\delta$  and conclude that

$$\lim_{\delta \rightarrow 0} (v_0 - v_\delta) = \lim_{\delta \rightarrow 0} h'(u_0)\delta = 0.$$

Therefore, the integral  $T_1(u_0)$  is well-defined.

Furthermore, we define the constants  $c_1, c_2, c_3$  for a fixed  $\delta > 0$  and  $u_0 > 0$

$$c_1 = 2p'(0) \approx p'(v_\delta) > 0,$$

$$c_2 = p''(0) \approx -\frac{4}{3}p''(v_\delta) > 0$$

and

$$c_3 = \frac{8}{15}p'''(0) = \frac{8}{15}p'''(0)6a_2 = \frac{8}{15}p'''(v_\delta) > 0.$$

Therefore,

$$\int_{u_0}^{u_0+\delta} \frac{du}{\sqrt{F(h(u_0)) - F(h(u))}} \approx \frac{\sqrt{\delta h'(u_0)}}{\sqrt{\text{pol}(h(u_0))}} (c_1 + c_2\delta h'(u_0) + c_3\delta^2 h'(u_0)^2)$$

and we conclude that if  $u_{\min} = 0$  then

$$\lim_{u_0 \rightarrow 0} T_1(u_0) = \infty,$$

because  $\text{pol}(h(u_0))$  tends to zero for  $u_0 \rightarrow 0$ , whereas the numerator tends to a positive constant. If  $u_{\min} > 0$  then  $\text{pol}(h(u_0))$  does not tend to zero and

$$\lim_{u_0 \rightarrow u_{\min}} T_1(u_0) = \text{constant} < \infty.$$

The integral  $T_2(u_e)$  is improper at  $u = u_e$ . For showing well-definedness, we can argue similarly as for  $T_1(u_0)$ . If  $u_{\max} = u_2$ , then by a similar argument as for  $T_1(u_0)$ , we can show that

$$\lim_{u_e \rightarrow u_2} T_2(u_e) = \infty.$$

But, if  $u_{\max} < u_2$ , then

$$\lim_{u_e \rightarrow u_{\max}} T_2(u_e) = \text{constant} < \infty.$$

Finally, we know by Lemma 3.1.3 that either  $u_{\min} = 0$  or  $u_{\max} = u_2$ . Hence, we conclude that

$$\begin{aligned} \lim_{u_0 \rightarrow u_{\min}} T(u_0) &= \lim_{u_0 \rightarrow u_{\min}} T_1(u_0) + \lim_{u_0 \rightarrow u_{\min}} T_2(u_e(u_0)) \\ &= \lim_{u_0 \rightarrow u_{\min}} T_1(u_0) + \lim_{u_e \rightarrow u_{\max}} T_2(u_e) \\ &= \infty. \end{aligned}$$

**Behaviour near  $u_1$ :** For investigating the behaviour of the time-map integrals for  $u_0 \rightarrow u_1$ , we use the Taylor expansion of  $Q$  near  $u_1$  remarking that  $u_1$  is a local minimum

$$Q(u) \approx Q(u_1) + \frac{1}{2}(u - u_1)^2 Q''(u_1).$$

Furthermore, we use the change of variables  $u = (u_1 - u_0)t + u_0$  to get rid of  $u_0$  and  $u_1$  as integration limits. For  $\sqrt{2\gamma}T_1(u_0)$ , we obtain

$$\begin{aligned} \lim_{u_0 \rightarrow u_1} \int_{u_0}^{u_1} \frac{du}{\sqrt{Q(u_0) - Q(u)}} &= \lim_{u_0 \rightarrow u_1} \int_0^1 \frac{(u_1 - u_0)dt}{\sqrt{Q(u_0) - Q((u_1 - u_0)t + u_0)}} \\ &= \lim_{u_0 \rightarrow u_1} \sqrt{\frac{2}{Q''(u_1)}} \int_0^1 \frac{(u_1 - u_0)dt}{\sqrt{(u_1 - u_0)^2 - (u_1 - u_0)^2(t-1)^2}} \\ &= \sqrt{\frac{2}{Q''(u_1)}} \int_0^1 \frac{dt}{\sqrt{-t(t-2)}} \\ &= \sqrt{\frac{2}{Q''(u_1)}} \int_{-1}^0 \frac{ds}{\sqrt{1-s^2}}. \end{aligned}$$

Evaluating the primitive  $\int \frac{ds}{\sqrt{1-s^2}} = \arcsin(s)$ , yields

$$\lim_{u_0 \rightarrow u_1} \int_{u_0}^{u_1} \frac{du}{\sqrt{Q(u_0) - Q(u)}} = -\sqrt{\frac{2}{Q''(u_1)}} (\arcsin(0) - \arcsin(-1)) = \sqrt{\frac{2}{Q''(u_1)}} \frac{\pi}{2}.$$

Because of the continuity of the potential and the relation  $Q(u_0) = Q(u_e)$ , we see that  $u_e \rightarrow u_1$  when  $u_0 \rightarrow u_1$ . Hence, we find by a similar calculation as for  $T_1(u_0)$  that

$$\lim_{u_e \rightarrow u_1} \sqrt{2\gamma} T_2(u_e) = \lim_{u_e \rightarrow u_1} \int_{u_1}^{u_e} \frac{du}{\sqrt{Q(u_e) - Q(u)}} = \frac{\pi}{\sqrt{2Q''(u_1)}}$$

holds true. Putting this together we see that

$$\lim_{u_0 \rightarrow u_1} T(u_0) = \frac{1}{\sqrt{2\gamma}} \left( \frac{\pi}{\sqrt{2Q''(u_1)}} + \frac{\pi}{\sqrt{2Q''(u_1)}} \right) = \frac{\pi}{\sqrt{\gamma Q''(u_1)}}.$$

Therefore, we conclude that the range of  $T$  is given by

$$\left( \frac{\pi}{\sqrt{\gamma Q''(u_1)}}, \infty \right).$$

□

*Proof of Theorem 3.1.1.* We constructed a solution connecting  $u_0 \in (u_{\min}, u_1)$  and  $u_e \in (u_1, u_{\max})$  requiring that  $Q(u_0) = Q(u_e)$  holds. This is a solution on the interval  $x \in [0, 1]$  if and only if  $T(u_0) = 1$ . Theorem 3.1.8 yields that  $T$  is a continuous mapping with range  $\left( \frac{\pi}{\sqrt{\gamma Q''(u_1)}}, \infty \right)$ . Observing that 1 is in the range if  $\frac{\pi^2}{Q''(u_1)} < \gamma$  and that

$$Q''(u_1) = \alpha h'(u_1) - \beta > 0,$$

we obtain the condition  $\gamma_0 = \frac{\pi^2}{\alpha h'(u_1) - \beta} < \gamma$  for the existence of a monotone increasing solution. □

For investigating the monotonicity of the time-map we need to know how  $u_e$  depends on  $u_0$ .

**Lemma 3.1.9.** *The derivative of  $u_e$  with respect to  $u_0$  is given by*

$$\frac{d}{du_0} u_e(u_0) = \frac{q(u_0)}{q(u_e)} < 0.$$

*Proof.* Derivating equation (3.9) with respect to  $u_0$  yields the result. □

**Remark 3.1.10.** *Monotonicity of the time-map induces that the monotone increasing solution of equation (3.1) constructed in Theorem 3.1.1 is unique. Simulations (See Figure 3.4) suggest that the time-map  $T(u_0)$  is monotone decreasing for all*

possible kinetic functions in the bistable case.

We observe that if

$$\frac{d}{du_0}T_1(u_0) < 0 \quad (3.10)$$

and

$$\frac{d}{du_e}T_2(u_e) > 0 \quad (3.11)$$

then

$$\begin{aligned} \frac{d}{du_0}T(u_0) &= \frac{d}{du_0}T_1(u_0) + \frac{d}{du_e}T_2(u_e) \cdot \frac{d}{du_0}u_e(u_0) \\ &= \frac{d}{du_0}T_1(u_0) + \frac{d}{du_e}T_2(u_e) \cdot \frac{q(u_0)}{q(u_e)} < 0 \end{aligned} \quad (3.12)$$

holds.

Unfortunately equations (3.10) and (3.11) do not seem to be true in general as one can see in Figure 3.4b and 3.4k. But, at least (3.10) or (3.11) is always true.

**Proposition 3.1.11.** *The derivatives of the time-maps in the bistable case have the form*

$$T_1'(u_0) = -\frac{q(u_0)}{\sqrt{2\gamma(Q(u_0) - Q(u_1))}} \int_{u_0}^{u_1} \left( \frac{(Q(u) - Q(u_1))q'(u)}{q(u)^2} - \frac{1}{2} \right) \frac{du}{\sqrt{Q(u_0) - Q(u)}} \quad (3.13)$$

and

$$T_2'(u_e) = -\frac{q(u_e)}{\sqrt{2\gamma(Q(u_e) - Q(u_1))}} \int_{u_1}^{u_e} \left( \frac{(Q(u) - Q(u_1))q'(u)}{q(u)^2} - \frac{1}{2} \right) \frac{du}{\sqrt{Q(u_e) - Q(u)}}. \quad (3.14)$$

*Proof.* Requiring that  $q(u)$  is monotone in a neighborhood of  $u_1$ , this has been shown by Loud in [Lou59]. Indeed, because of  $q'(u_1) > 0$  the assumption holds.  $\square$

**Proposition 3.1.12.** *For the generic model in the bistable case fulfilling the condition  $Q(u_2) \geq 0$ , it holds  $\frac{d}{du_0}T_1(u_0) < 0$ . For the generic model in the bistable case fulfilling the condition  $Q(u_2) \leq 0$  it holds  $\frac{d}{du_e}T_2(u_e) > 0$ . In particular, if  $Q(u_2) = 0$  then it holds  $T'(u_0) < 0$ .*

*Proof.* We shown that the integrand of the derivative of the time-map given by Proposition 3.1.11 is positive. Therefore, we denote the function

$$l(u) = \frac{(Q(u) - Q(u_1))q'(u)}{q(u)^2} - \frac{1}{2}$$

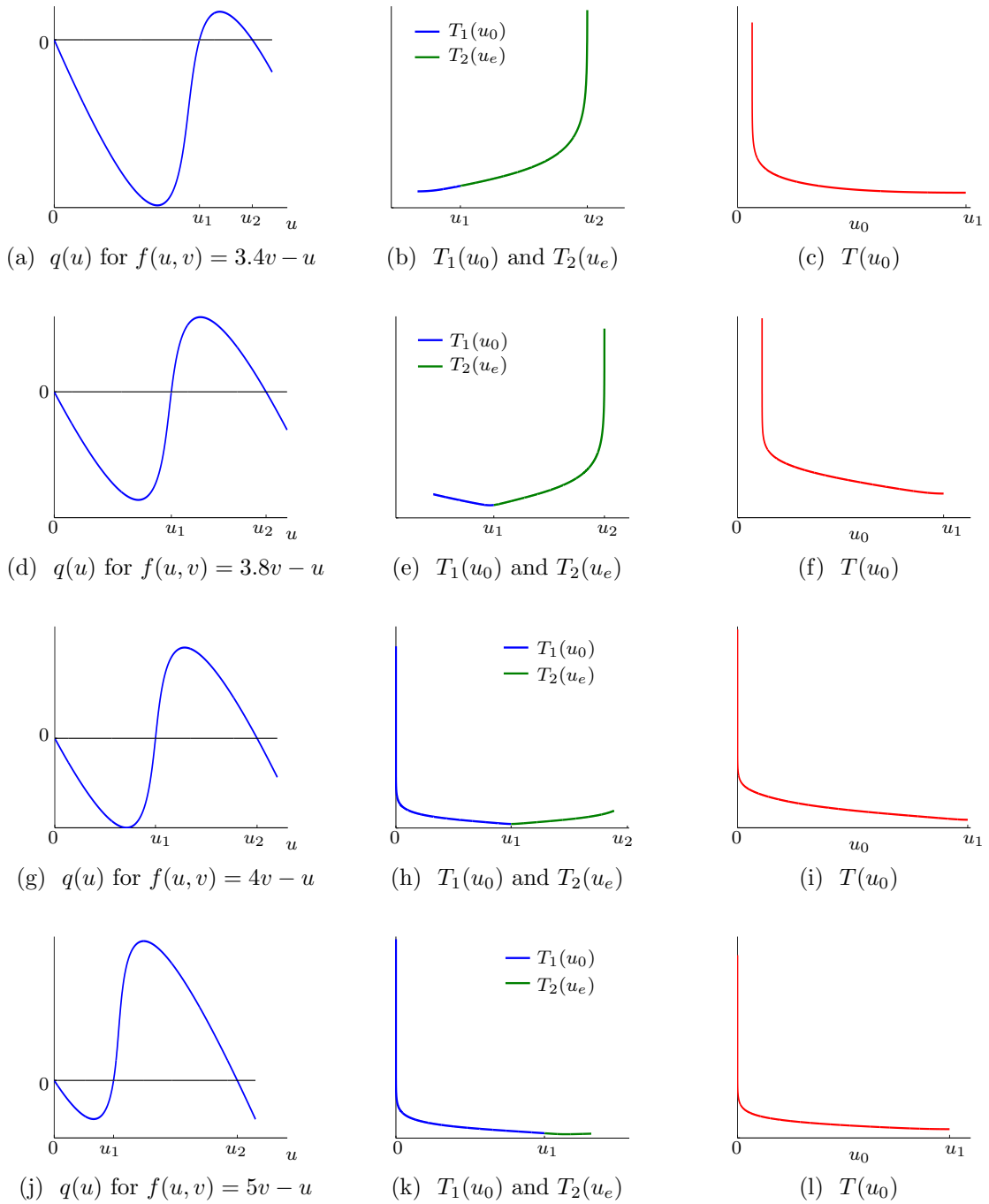
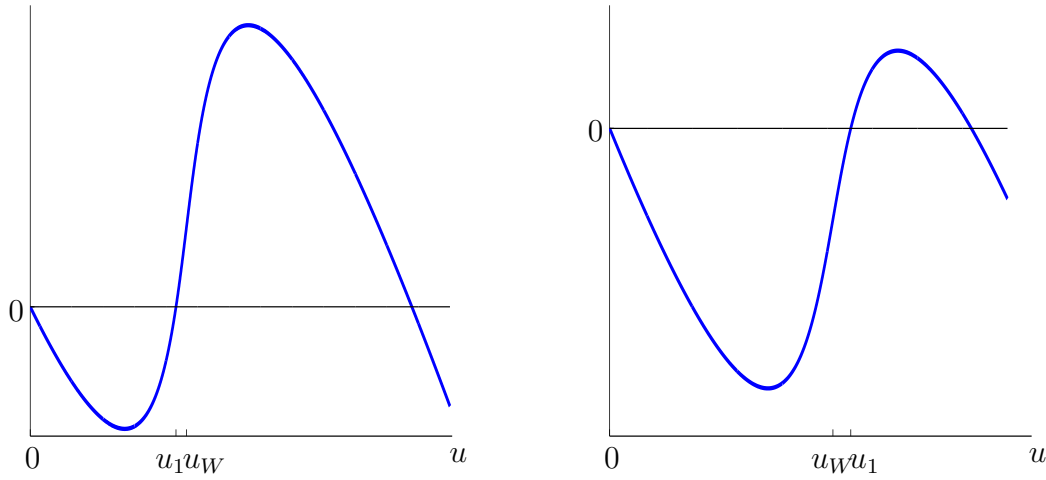


Figure 3.4: Simulations of time-maps for different kinetic functions. We fix  $p(v) = v^3 - 5.2v^2 + 10v$  and  $\beta = 1$  but vary  $\alpha$  in  $f(u, v) = \alpha v - \beta u$ . In the first column, we plot the function  $q(u) = f(u, h(u))$ , in the second column we have the corresponding time-maps  $T_1(u_0)$  and  $T_2(u_e)$ , whereas in the third column there is the total time-map  $T(u_0) = T_1(u_0) + T_2(u_e(u_0))$ . We observe that  $\frac{d}{du_0}T(u_0) < 0$  holds even if either  $\frac{d}{du_0}T_1(u_0) < 0$  or  $\frac{d}{du_e}T_2(u_e) > 0$  is not fulfilled.



(a)  $f(u, v) = 5v - u$ . The potential at  $u_2$  is positive and hence  $u_1 < u_W$ . (b)  $f(u, v) = 4v - u$ . The potential at  $u_2$  is negative and hence  $u_W < u_1$ .

Figure 3.5: Two kinetic functions in the bistable case. The polynomial  $p(v) = v^3 - 5v^2 + 10v$  is the same in both simulation. We vary  $f$  to have a different potential at  $u_2$ , which changes the relative position of  $u_1$  and  $u_W$ .

and calculate

$$\frac{d}{du} (q(u)^2 l(u)) = (Q(u) - Q(u_1)) q''(u).$$

This leads together with  $q(u)^2 l(u)|_{u=u_1} = 0$  to

$$q(u)^2 l(u) = \int_{u_1}^u (Q(\tilde{u}) - Q(u_1)) q''(\tilde{u}) d\tilde{u}. \quad (3.15)$$

For all  $u \in (u_0, u_e) \subset I$  we know that  $Q(u) - Q(u_1) \geq 0$ . Hence, the sign of  $l(u)$  is determined by the sign of  $q''(u)$ . Using the chain rule we obtain

$$q''(u) = \alpha h''(u) = -\alpha \frac{p''(h(u))}{p'(h(u))^3}.$$

By assumption in the bistable case,  $p'(v) > 0$  for all  $v$ . Hence, the sign of  $q''(u)$  depends only on  $p''(v) = 3a_2 v + 2a_1$ . We can see that the only zero of  $p''(h(u))$  is given by  $u = u_W$ , which is the  $u$ -coordinate of the inflection point  $W$  (see Lemma 2.1.3). We remind that  $a_1 < 0$ , hence  $p''(h(u)) < 0$  for all  $u < u_W$  and  $p''(h(u)) > 0$  for all  $u > u_W$ .

Observing that  $u_1 = u_W$  if and only if  $Q(u_2) = 0$  (see Remark 2.1.11 and Remark 3.1.4), we can establish a connection between the potential at  $u_2$  and the derivative of the time-maps.

If  $Q(u_2) \leq 0$ , then  $u_W \leq u_1$  and we obtain that

$$q''(u) \leq 0 \quad \text{for all } u \in [u_1, u_e].$$

This leads to  $l(u) \leq 0$  and using representation (3.14) to  $T_2'(u_e) > 0$  remarking that  $\frac{q(u_e)}{Q(u_e)-Q(u_1)} > 0$ .

In a similar fashion we see that if  $Q(u_2) \geq 0$ , then  $u_W \geq u_1$  and

$$q''(u) \geq 0 \quad \text{for all } u \in [u_0, u_1]$$

which leads as well to  $l(u) \leq 0$  because we integrate backwards in equation (3.15). Finally, we obtain  $T_1'(u_0) < 0$  using representation (3.13) together with the observation  $\frac{q(u_0)}{(Q(u_0)-Q(u_1))} < 0$ .  $\square$

### 3.2 Instability of stationary solutions

In this section we will show that there is no pattern formation possible in the system (2.1) in the bistable case. The proof is similar to the proof of nonexistence of stable pattern for one-dimensional reaction-diffusion systems with homogeneous Neumann boundary conditions (see for example [MC04]).

**Theorem 3.2.1.** *There exists no stable nonhomogeneous stationary solution  $(U, V)$  of the generic model (2.1) in the bistable case.*

In the proof we use the Sturm comparison principle, whose proof can be found in [MU78] and in [JK99].

**Theorem 3.2.2** (Sturm comparison principle). *Let  $\phi_1$  and  $\phi_2$  be non-trivial solutions of the equations*

$$\begin{aligned} Du_{xx} + q_1(x)u &= 0 \quad \text{and} \\ Du_{xx} + q_2(x)u &= 0, \end{aligned}$$

*respectively, for  $x \in [0, 1]$  and  $D > 0$ . We assume that the functions  $q_1$  and  $q_2$  are continuous on  $[0, 1]$  and that*

$$q_1(x) \leq q_2(x)$$

*holds for all  $x \in [0, 1]$ .*

*Then between any two consecutive zeros  $x_1$  and  $x_2$  of  $\phi_1$ , there exists at least one zero of  $\phi_2$  unless  $q_1(x) \equiv q_2(x)$  on  $[0, 1]$ .*

*Proof of Theorem 3.2.1.* We consider system (2.1) linearised at  $(U(x), V(x))$

$$\begin{pmatrix} \tilde{u}_t \\ \tilde{v}_t \end{pmatrix} = \begin{pmatrix} \frac{1}{\gamma} \tilde{u}_{xx} \\ 0 \end{pmatrix} + \begin{pmatrix} -\beta & \alpha \\ 1 & -p'(V(x)) \end{pmatrix} \cdot \begin{pmatrix} \tilde{u} \\ \tilde{v} \end{pmatrix} =: \mathcal{L} \cdot \begin{pmatrix} \tilde{u} \\ \tilde{v} \end{pmatrix}$$

with boundary conditions  $\tilde{u}_x(0) = \tilde{u}_x(1) = 0$ .

The eigenvalue equation

$$\mathcal{L} \begin{pmatrix} \varphi \\ \psi \end{pmatrix} = \lambda \begin{pmatrix} \varphi \\ \psi \end{pmatrix}$$

with boundary condition  $\varphi_x(0) = \varphi_x(1) = 0$  reads

$$\begin{aligned} \frac{1}{\gamma} \varphi_{xx} - (\beta + \lambda) \varphi + \alpha \psi &= 0 \\ \varphi - (p'(V(x)) + \lambda) \psi &= 0. \end{aligned} \tag{3.16}$$

We denote the function

$$r(\lambda, x) := \frac{\alpha}{\lambda + p'(V(x))} - \beta$$

and define the operator depending on  $\lambda$

$$\begin{aligned} \mathcal{D}(A(\lambda)) &= H_N^2(0, 1), \\ A(\lambda) : \varphi &\mapsto \frac{1}{\gamma} \varphi_{xx} + r(\lambda, x) \varphi. \end{aligned}$$

As  $p'(V(x)) > 0$  for all  $x \in [0, 1]$ , we observe that for  $\lambda \geq 0$  the eigenvalue problem (3.16) is equivalent to the equation

$$A(\lambda) \varphi = \lambda \varphi.$$

Let us first explain that there exists  $C > 0$  independent of  $\lambda \geq 0$  such that

$$|r(\lambda, x)| \leq C$$

for all  $x \in [0, 1]$ . Indeed, the denominator  $\lambda + p'(V(x))$  is positive and linearly growing in  $\lambda$ . Therefore,  $r(\lambda, x)$  is decaying in  $\lambda$  and it holds

$$\frac{\alpha}{\lambda + p'(V(x))} - \beta \leq \frac{\alpha}{p'(V(x))} - \beta = r(0, x) \leq \frac{\alpha}{\kappa} - \beta =: C,$$

where  $\kappa = \min_{x \in [0, 1]} p'(V(x))$ . We observe that in the bistable case by assumption  $\kappa > 0$  holds. Furthermore,  $\frac{\alpha}{\kappa} - \beta > 0$ , which is clear as this is necessary to have 3 intersection points. Now, we argue in the same way as it was done in [MC04] for the instability of nonhomogeneous solutions of a single reaction-diffusion equation

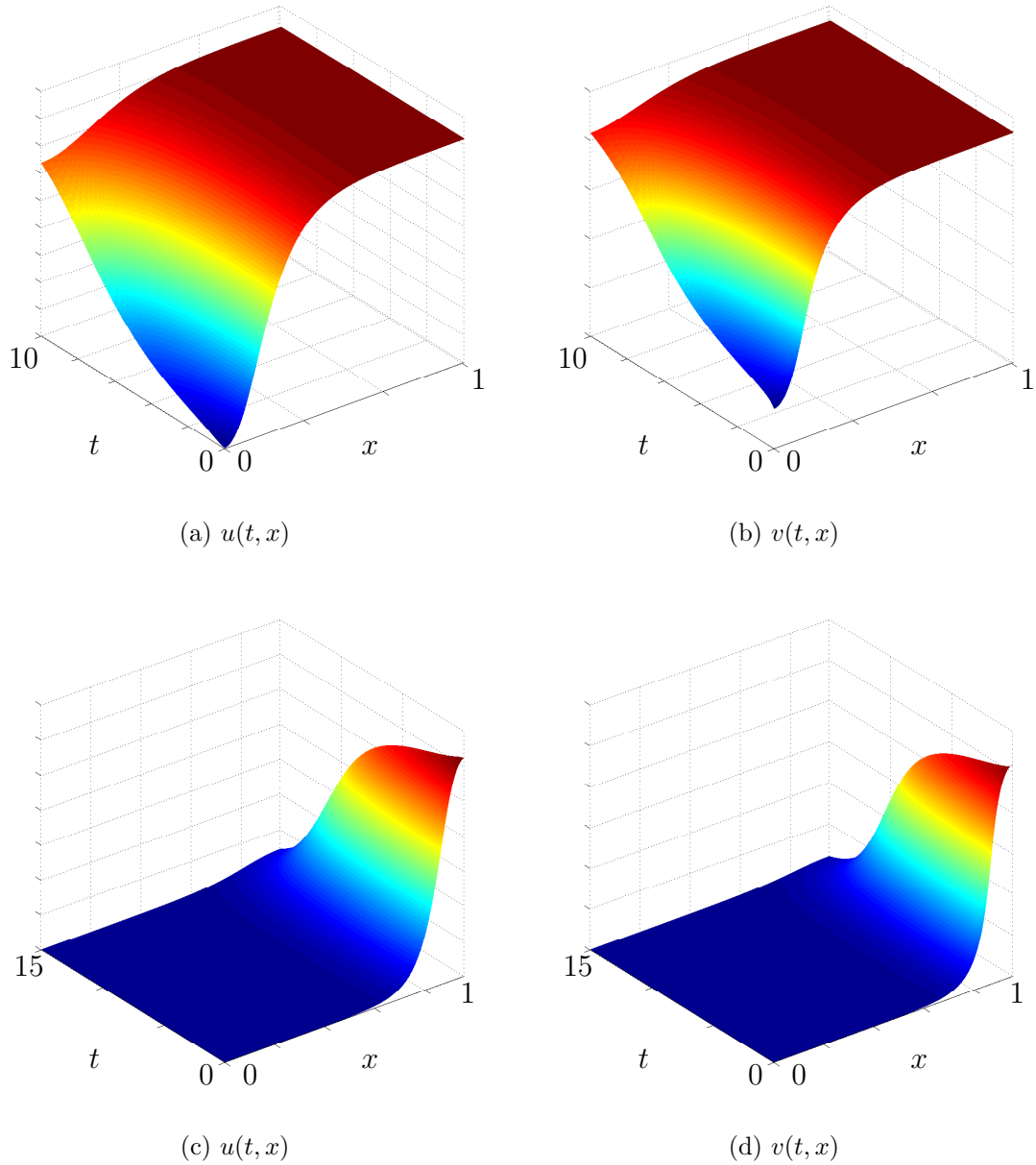


Figure 3.6: Two simulations of the generic model in the bistable case. The polynomial is  $p(v) = v^3 - 4.6v^2 + 10v$ , for the upper panel  $f(u, v) = 5v - u$  which leads to a negative value of  $Q(u_2)$ , whereas in the lower one  $f(u, v) = 5.5v - u$  which leads to a positive value of  $Q(u_2)$ . The initial condition is in both cases a small perturbation of the respective steady state solution.

with homogeneous Neumann boundary conditions. We denote by  $\mu_0(\lambda)$  the largest eigenvalue of the Neumann problem

$$A(\lambda)\varphi = \mu(\lambda)\varphi \quad \text{and} \quad \varphi_x(0) = \varphi_x(1) = 0,$$

and by  $\nu_0(\lambda)$  the largest eigenvalue of the Dirichlet problem

$$A(\lambda)\varphi = \nu(\lambda)\varphi \quad \text{and} \quad \varphi(0) = \varphi(1) = 0.$$

Using the Sturm comparison principle we can show that

$$\mu_0(\lambda) > \nu_0(\lambda)$$

holds. Indeed,  $\mu_0(\lambda) \leq \nu_0(\lambda)$  yields

$$q_2(x) := r(\lambda, x) - \mu_0(\lambda) \geq r(\lambda, x) - \nu_0(\lambda) =: q_1(x).$$

By definition the principal eigenfunction of the Dirichlet problem is of one sign and has its only zeros at  $x = 0$  and  $x = 1$ . Hence, from the Sturm comparison principle, we obtain that the principal eigenfunction corresponding to the Neumann problem has a zero in  $(0, 1)$ , but this is impossible because the principal eigenfunction is of one sign (see [Smo83]).

Next, we remark that  $U_x(x)$  is an eigenfunction for the eigenvalue 0 of the Dirichlet problem by derivating equation (3.4)

$$\begin{aligned} 0 &= \frac{1}{\gamma}(U_x)_{xx} + q'(U)U_x = \frac{1}{\gamma}(U_x)_{xx} + \alpha h'(U)U_x - \beta U_x \\ &= \frac{1}{\gamma}(U_x)_{xx} + \left(\alpha \frac{1}{p'(V)} - \beta\right)U_x = A(0)U_x. \end{aligned}$$

Therefore,  $\nu(0) \geq 0$  and hence  $\mu(0) > 0$ .

Furthermore, we know that  $\mu(\lambda)$  depends continuously on  $\lambda$  and can be calculated by

$$\mu(\lambda) = \sup_{\varphi \in W^{1,2}(0,1), \|\varphi\|_2=1} \left[ -\frac{1}{\gamma} \langle \varphi_x, \varphi_x \rangle + \langle r(\lambda, x)\varphi, \varphi \rangle \right]. \quad (3.17)$$

We obtain

$$-\int_0^1 \frac{1}{\gamma} \varphi_x \varphi_x dx + \int_0^1 r(\lambda, x) \varphi^2 dx \leq -\int_0^1 \frac{1}{\gamma} \varphi_x \varphi_x dx + \int_0^1 C \varphi^2 dx \leq C. \quad (3.18)$$

Therefore,  $\mu(\lambda)$  is bounded and, hence there exists a value  $\bar{\lambda} > 0$  fulfilling  $\mu(\bar{\lambda}) = \bar{\lambda}$ . This induces the existence of an eigenfunction  $\bar{\varphi} \neq 0$  satisfying

$$A(\bar{\lambda})\bar{\varphi} = \mu(\bar{\lambda})\bar{\varphi} = \bar{\lambda}\bar{\varphi} \quad \text{with} \quad \bar{\varphi}_x(0) = \bar{\varphi}_x(1) = 0,$$

which proves the existence of a positive eigenvalue of problem (3.16).  $\square$

### 3.3 Summary

We showed that the generic model in the bistable case admits for every diffusion coefficient  $\frac{1}{\gamma}$  with  $\gamma > \gamma_0$  a monotone increasing stationary solution. The steady state equation reduces to one differential equation of elliptic type with continuous right hand side. We constructed a monotone increasing and a monotone decreasing solution as well as periodic solutions of the problem. Simulations of the time-map related to the steady state equation suggest that the monotone increasing solution is unique. Thus, for every diffusion there is a finite number of stationary solutions. The smaller the diffusion coefficient is the more solutions there are.

Next, we showed that all these spatially inhomogeneous stationary solutions are unstable as solutions of the reaction-diffusion system. Thus, there is no pattern formation in the generic model in the bistable case. This was not expected from the observation of the kinetic system. Therefore, bistability in such system is not enough to produce stable patterns.



# Chapter 4

## Construction and stability of discontinuous stationary solutions

In the previous chapter, we showed that bistability in the kinetic system is not sufficient to obtain stable pattern formation in the generic system (2.1). Therefore, we turn our attention to the hysteresis case now. In the hysteresis case the kinetic functions show bistability and, moreover, in the steady state there is a hysteretic dependence of  $v$  from  $u$ .

We construct nonhomogeneous stationary solutions using the same method as for the bistable case together with the ideas presented in [Gri91]. We show that there is an infinite number of monotone increasing stationary solutions for every diffusion coefficient, which have a discontinuous  $v$ -component.

Then, we derive a condition under which a stationary solution is stable with respect to small  $L^\infty(0, 1)$  perturbations.

### 4.1 Phase plane analysis

The stationary solutions of system (2.1) are solutions of

$$\begin{aligned} 0 &= \frac{1}{\gamma} U_{xx} + f(U, V), \\ 0 &= g(U, V), \end{aligned} \tag{4.1}$$

for  $x \in [0, 1]$  and with the homogeneous Neumann boundary condition for  $U$ .

To construct a solution, we proceed in a similar fashion as in the bistable case: We solve  $g(U, V) = 0$  with respect to  $V$  and to plug this into the first equation of (4.1). We remind that equation  $g(U, V) = 0$  has 3 local solution branches, but as the unstable homogeneous steady state  $S_1$  is on the middle branch, we can only expect

stable solutions of equation (4.1) by plugging the outer branches  $V = h_T(U)$  and  $V = h_H(U)$  into the first equation. Hence, we would like to solve the equation

$$\frac{1}{\gamma}U_{xx} + q_H(U) = 0 \quad (4.2)$$

or

$$\frac{1}{\gamma}U_{xx} + q_T(U) = 0, \quad (4.3)$$

both on the interval  $[0, 1]$  with boundary condition  $U_x(0) = U_x(1) = 0$ . Here,  $q_i(U) = f(U, h_i(U))$ , for  $i = H, T$  (compare Section 2.1). We observe that equations (4.2) and (4.3) are equivalent to the system

$$\begin{aligned} U_x &= W, \\ W_x &= -\gamma q_i(U) \end{aligned} \quad (4.4)$$

for  $i = H$  and  $i = T$ , respectively. To construct a monotone increasing solution of the boundary value problem, we need to connect a point  $(u_0, 0)$  with a point  $(u_e, 0)$ , where  $u_e > u_0$ , by a trajectory  $(U, W)$ , which has to be such that  $W(x) > 0$  for all  $x \in (0, 1)$ .

We show that it is not possible to construct a solution of problem (4.1) by plugging in just one solution branch of  $g(U, V) = 0$  into the equation with diffusion.

**Proposition 4.1.1.** *Neither the boundary value problem (4.2) nor (4.3), both with homogeneous Neumann boundary condition*

$$U_x(0) = U_x(1) = 0,$$

*has a nonconstant solution.*

*Proof.* We know that in the phase plane (4.4) a solution has to connect the point  $(u_0, 0)$  with the point  $(u_e, 0)$ . By definition, it holds that  $q_H(0) = 0$  and  $-q_H(U) > 0$  for  $U \in (0, u_H)$  (Lemma 2.1.10). That means that the flux at the point  $(u_0, 0)$  always points upwards and to the right. Consequently, a solution starting at  $(u_0, 0)$  for  $0 < u_0$  never reaches the  $U$ -axis again.

Similarly,  $q_T(u_2) = 0$  and  $-q_T(U) < 0$  for  $U \in (u_T, u_2)$ . Hence, all orbits ending at  $(u_e, 0)$  with  $u_e < u_2$  have started at some point with positive  $W$ -component.  $\square$

As it is not sufficient to plug in one branch of  $g(U, V) = 0$ , we try to use both branches. We observe that the phase planes associated to the systems (4.4) overlap for  $u \in (u_H, u_T)$ . Heuristically, to construct a solution, we choose a value  $\bar{u} \in (u_H, u_T)$  and 'glue' the phase planes (4.2) and (4.3) together at  $\bar{u}$ .

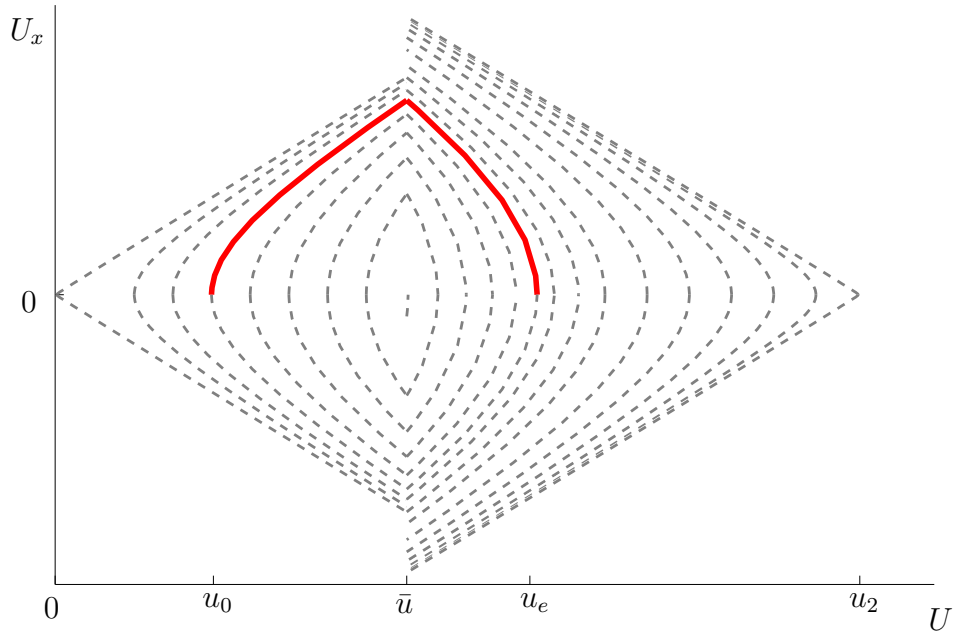


Figure 4.1: Phase planes for  $\frac{1}{\gamma}U_{xx} + q_H(U) = 0$  and  $\frac{1}{\gamma}U_{xx} + q_T(U) = 0$  'glued' together at  $\bar{u}$ . The red trajectory connects the points  $(u_0, 0)$  and  $(u_e, 0)$ .

**Definition:** We denote by  $q_{\bar{u}}$  the function with discontinuity at  $\bar{u}$  defined by

$$q_{\bar{u}}(u) = \begin{cases} q_H(u) & \text{when } u \leq \bar{u} \\ q_T(u) & \text{when } u > \bar{u}. \end{cases}$$

**Definition:** A function  $U(x) \in H_N^2(0, 1)$  is called a **weak solution** of the boundary value problem

$$\frac{1}{\gamma}U_{xx} + q_{\bar{u}}(U) = 0 \quad \text{with } U_x(0) = U_x(1) = 0, \tag{4.5}$$

if for all  $\varphi \in C^\infty([0, 1])$  it holds

$$\frac{1}{\gamma} \int_0^1 U(x)\varphi_{xx}(x)dx + \int_0^1 q_{\bar{u}}(U(x))\varphi(x)dx = 0.$$

**Definition:** A pair of functions  $(U(x), V(x))$  is called a **solution with jump at  $\bar{u}$**  of the stationary problem (4.1), if  $U(x) \in C^1([0, 1])$  is a weak solution of the problem (4.5). The function  $V(x) \in L^\infty(0, 1)$  is given for almost all  $x \in [0, 1]$  by

$$V(x) = \begin{cases} h_H(U(x)) & \text{if } U(x) \leq \bar{u} \\ h_T(U(x)) & \text{if } U(x) > \bar{u}. \end{cases}$$

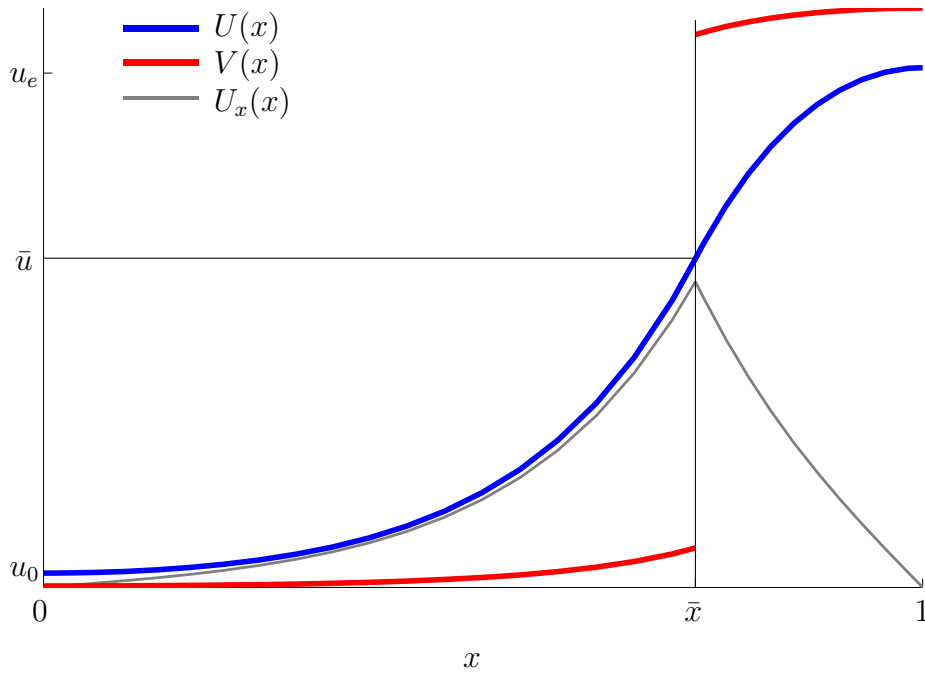


Figure 4.2: A monotone increasing stationary solution with jump at  $\bar{u}$  of the generic model in the hysteresis case.  $U(x)$  is connecting  $u_0$  and  $u_e$  and is a  $C^1$  solution of  $\frac{1}{\gamma}U_{xx} + q_{\bar{u}}(U) = 0$ . The derivative  $U_x(x)$  is continuous, but not differentiable, whereas  $V(x)$  is discontinuous.

**Definition:** The values  $0 < \bar{x} < 1$ , where  $U(\bar{x}) = \bar{u}$  holds are called the **layer positions** of the solution  $(U(x), V(x))$ .

**Remark 4.1.2.** *It is indeed possible to construct solutions of problem (4.5) which are differentiable. In fact, for  $x$  such that  $U(x) < \bar{u}$  the function  $U(x)$  is a classical solution of  $\frac{1}{\gamma}U_{xx} + q_H(U) = 0$  and therefore  $C^2$ . Similarly,  $U(x)$  is a classical solution of  $\frac{1}{\gamma}U_{xx} + q_T(U) = 0$  for  $x$  such that  $U(x) > \bar{u}$ . Moreover, we will see that it is possible to connect these branches such that  $U(x) \in C^1([0, 1])$  holds.*

*The function  $V(x)$  has by definition the same regularity as  $U(x)$  except for  $x$  such that  $U(x) = \bar{u}$ , where it is necessarily discontinuous.*

The main theorem of this chapter reads:

**Theorem 4.1.3.** *There is a unique monotone increasing nonhomogeneous stationary solution  $(U(x), V(x))$  of the generic model (2.1) in the hysteresis case for all diffusion coefficients  $\frac{1}{\gamma}$  with  $\gamma > 0$  and with jump at  $\bar{u}$  for every  $\bar{u} \in (u_T, \min(u_H, u_2))$ .*

**Corollary 4.1.4.** *There is a unique monotone decreasing nonhomogeneous stationary solution  $(U(x), V(x))$  with jump at  $\bar{u} \in (u_T, \min(u_H, u_2))$  of system (2.1) in the hysteresis case for all diffusion coefficients  $\frac{1}{\gamma}$ .*

*Proof of Corollary 4.1.4.* The proof of existence is identically to the one in the bistable case, compare Corollary 3.1.2. The uniqueness follows from the uniqueness of the monotone increasing solution.  $\square$

Theorem 4.1.3 and Corollary 4.1.4 will be the basis for the construction of all stationary solutions of the generic system, which will be done in Section 5.4.

To construct a solution we observe that the right-hand side of the system

$$\begin{aligned} U_x &= W, \\ W_x &= -\gamma q_H(U) \end{aligned} \tag{4.6}$$

is Lipschitz-continuous. Therefore, the initial value problem  $(U(0), W(0)) = (u_0, 0)$  solved forward has a unique solution for all  $u_0 \in (0, u_H)$ . We call this solution  $(U_H(x, u_0), W_H(x, u_0))$ . Similarly, the right-hand side of the system

$$\begin{aligned} U_x &= W, \\ W_x &= -\gamma q_T(U) \end{aligned} \tag{4.7}$$

is Lipschitz-continuous. Hence, the initial value problem  $(U(0), W(0)) = (u_e, 0)$  solved backwards has for all  $u_e \in [u_T, u_2]$  a unique solution, which we call  $(U_T(x, u_e), W_T(x, u_e))$ . Now, we fix the jump  $\bar{u}$  and search for values  $u_0, u_e$  and the layer position  $\bar{x} \in (0, 1)$  such that

$$U_H(\bar{x}, u_0) = \bar{u} = U_T(\bar{x}, u_e)$$

holds. Furthermore, we require that  $U$  is continuously differentiable and therefore

$$W_H(\bar{x}, u_0) = W_T(\bar{x}, u_e)$$

has to be fulfilled.

Then, the monotone increasing solution of system (4.5) is given by

$$U(x) = \begin{cases} U_H(x, u_0) & \text{for } x \leq \bar{x}, \\ U_T(x, u_e) & \text{for } x > \bar{x}, \end{cases}$$

for suitable values of  $u_0, u_e$  and the layer position  $\bar{x}$ .

We emphasise that  $u_0, u_e$  and  $\bar{x}$  depend on the diffusion coefficient  $\frac{1}{\gamma}$  and the jump  $\bar{u}$ . We analyse this dependence in more detail in Chapter 5. In the remainder of the current chapter we consider diffusion coefficient and jump as fixed.

## 4.2 The potential

To find the appropriate values for  $u_0$  and  $u_e$ , we define the potential.

**Definition:** The function  $Q_{\bar{u}}$ , which is defined by

$$Q_{\bar{u}}(u) = \int_0^u q_{\bar{u}}(\tilde{u}) d\tilde{u}$$

is called the **potential** of equation (4.5).

By definition  $Q_{\bar{u}}$  is continuous for all  $u$  but it is not differentiable in  $\bar{u}$ , because its derivative  $q_{\bar{u}}(u)$  is not continuous in  $\bar{u}$ . Furthermore, it fulfils  $Q'_{\bar{u}}(u) = q_{\bar{u}}(u)$  and  $Q_{\bar{u}}(0) = 0$ .

Using the change of variables  $\tilde{v} \mapsto p(\tilde{v}) = \tilde{u}$  we obtain that  $Q_{\bar{u}}(u)$  can be written in the form

$$Q_{\bar{u}}(u) = \begin{cases} F(h_H(u)) & \text{if } u \leq \bar{u}, \\ F(h_H(\bar{u})) - F(h_T(\bar{u})) + F(h_T(u)) & \text{if } u > \bar{u}, \end{cases} \quad (4.8)$$

with  $F$  defined by

$$F(v) = \int_0^v f(p(\tilde{v}), \tilde{v}) p'(\tilde{v}) d\tilde{v},$$

a polynomial of degree 6 having a double zero at  $v = 0$ . We can calculate the derivative

$$\frac{d}{dv} F(v) = (\alpha v - \beta p(v)) p'(v),$$

which has zeros  $0, v_H, v_1, v_T, v_2$ . Observing that the leading coefficient  $-\frac{\beta a_2^2}{2}$  of  $F$  is negative, we see that  $F(v)$  has local minima at  $v_T$  and  $v_H$ . The jump  $\bar{u}$  is in the interval  $[u_T, u_H]$  and therefore it holds  $h_H(\bar{u}) \leq v_H$ . Consequently  $Q_{\bar{u}}$  is monotonically decreasing for  $u \in [0, \bar{u}]$ . Moreover, it holds  $v_T \leq h_T(\bar{u})$ , but it is not clear if also  $h_T(\bar{u}) < v_2$  holds. Hence, we have to distinguish between two cases (see Figure 4.3):

- If  $\bar{u} < u_2$  then  $h_T(\bar{u}) < v_2$  and  $Q_{\bar{u}}$  is monotone increasing on  $[\bar{u}, u_2]$  and monotone decreasing on  $[u_2, \infty]$ .
- If  $\bar{u} \geq u_2$  then  $h_T(\bar{u}) \geq v_2$  and  $Q_{\bar{u}}$  is monotone decreasing on  $\mathbb{R}_{\geq 0}$ .

Proceeding as in the bistable case in (3.6), we obtain the first integral of the system (4.5) which is given by

$$\frac{1}{\gamma} \frac{U_x^2(x)}{2} + Q_{\bar{u}}(U(x)) = \text{constant}. \quad (4.9)$$

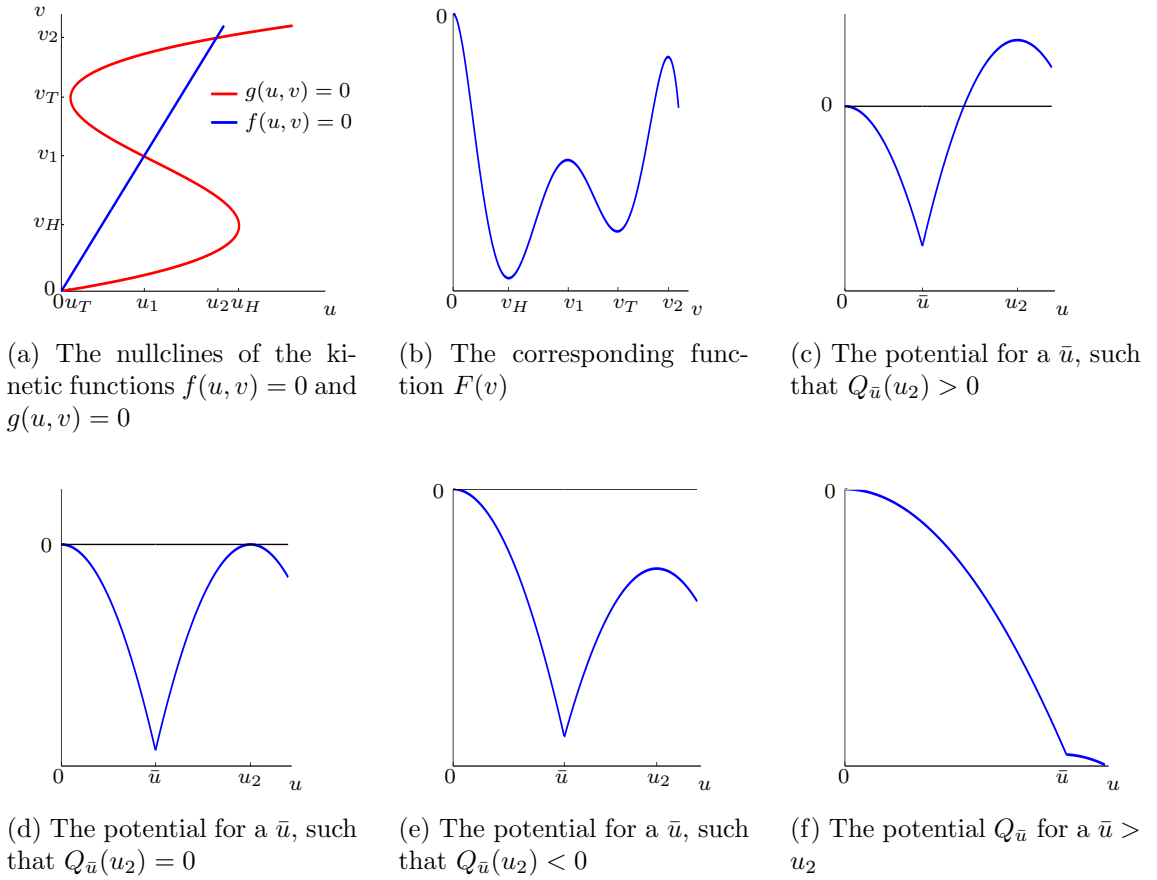


Figure 4.3: A possible configuration of kinetic functions  $f$  and  $g$  together with the function  $F$  and the potential  $Q_{\bar{u}}$  for increasing values of  $\bar{u}$ . We see that the value  $Q_{\bar{u}}(u_2)$  is decreasing. Here  $u_2 < u_H$  and we see that the potential has no local minimum at  $\bar{u}$ , if  $\bar{u} > u_2$ .

The Neumann boundary condition at  $x = 0$  and  $x = 1$  determines this constant to be

$$Q_{\bar{u}}(u_0) = Q_{\bar{u}}(u_e). \tag{4.10}$$

If we choose  $\bar{u}$  in the interval  $(u_T, \min(u_H, u_2))$  the potential  $Q_{\bar{u}}$  has a minimum at  $u = \bar{u}$ . Therefore, it is possible to find values  $0 < u_0 < \bar{u} < u_e < u_2$  fulfilling condition (4.10) and such that  $Q_{\bar{u}}(u) < Q_{\bar{u}}(u_0)$  for all  $u \in (u_0, u_e)$ .

**Definition:** We call  $I_{\bar{u}} = (u_{\min}, u_{\max})$  with  $0 \leq u_{\min}$  and  $u_{\max} \leq u_2$ , the maximal interval such that for all  $u_0 \in I \setminus \{\bar{u}\}$  there exists a unique value  $u_e \in I_{\bar{u}}$  with  $u_e \neq u_0$  fulfilling  $Q_{\bar{u}}(u_0) = Q_{\bar{u}}(u_e)$ .

The interval  $I_{\bar{u}}$  depends on the sign of the potential at the  $u$ -coordinate of the intersection point  $S_2$  and can be calculated in the same way as it was done in the bistable case. (compare Lemma 3.1.3.)

**Lemma 4.2.1.** *If  $Q_{\bar{u}}(u_2) \geq 0$  then  $u_{\min} = 0$  and  $u_{\max} \in (\bar{u}, u_2]$  is defined by  $Q_{\bar{u}}(u_{\max}) = 0$ . If  $Q_{\bar{u}}(u_2) \leq 0$  then  $u_{\max} = u_2$  and  $u_{\min} \in [0, \bar{u})$  is defined by  $Q_{\bar{u}}(u_{\min}) = Q_{\bar{u}}(u_2)$ . In particular if  $Q_{\bar{u}}(u_2) = 0$ , then  $I_{\bar{u}} = (0, u_2)$ .*

### 4.3 The time-maps

To see if a monotone increasing solution connecting some values of  $u_0$  and  $u_e$  is a solution of the stationary problem on the interval  $[0, 1]$ , we have to verify that the “time”  $x$  needed to go from  $u_0$  to  $u_e$  is equal to one. We proceed similar as in the bistable case and define the time-maps following [Sch90]. But, unlike the bistable case, the time-map in the hysteresis case tends to zero for  $u_0 \rightarrow \bar{u}$ . Moreover, we prove monotonicity of the time-map.

**Definition:** We define  $T_1^{\bar{u}}(u_0)$  as “time”  $x$  a forward orbit in the phase plane associated to system (4.6) starting at  $(u_0, 0)$  needs to reach the  $u = \bar{u}$  axis for the first time.

$$\begin{aligned} \mathcal{D}(T_1^{\bar{u}}) &:= \{u_0 \in (-\infty, u_H) \mid \exists x > 0 \text{ with } U_H(x, u_0) = \bar{u} \text{ and } W_H(x, u_0) > 0\}, \\ T_1^{\bar{u}}(u_0) &:= \min\{x \in [0, \infty) \mid U_H(x, u_0) = \bar{u}\} \quad \text{for } u_0 \in \mathcal{D}(T_1^{\bar{u}}). \end{aligned}$$

We define  $T_2^{\bar{u}}(u_e)$  as “time”  $x$  a backward orbit in the phase plane associated to system (4.7) starting at  $(u_e, 0)$  needs to reach the  $u = \bar{u}$  axis for the first time.

$$\begin{aligned} \mathcal{D}(T_2^{\bar{u}}) &:= \{u_e \in (u_T, \infty) \mid \exists x < 1 \text{ with } U_T(x, u_e) = \bar{u} \text{ and } W_T(x, u_e) > 0\}, \\ T_2^{\bar{u}}(u_e) &:= 1 - \max\{x \in [-\infty, 1] \mid U_T(x, u_e) = \bar{u}\} \quad \text{for } u_e \in \mathcal{D}(T_2^{\bar{u}}). \end{aligned}$$

Furthermore, we define the sum of the time-maps  $T_1^{\bar{u}}$  and  $T_2^{\bar{u}}$ , the total time-map

$$\begin{aligned} \mathcal{D}(T_{\bar{u}}) &:= \{u_0 \in \mathcal{D}(T_1^{\bar{u}}) \mid \exists u_e \text{ with } Q_{\bar{u}}(u_0) = Q_{\bar{u}}(u_e)\}, \\ T_{\bar{u}}(u_0) &:= T_1^{\bar{u}}(u_0) + T_2^{\bar{u}}(u_e(u_0)) \quad \text{for } u_0 \in \mathcal{D}(T_{\bar{u}}). \end{aligned}$$

**Remark 4.3.1.** *We could have defined  $T_2^{\bar{u}}(u_e)$  as well as the “time”  $x$  a forward orbit starting at  $U(0) = \bar{u}$  and ending at  $(u_e, 0)$ . But, we wanted the definition to be consistent with the definition of the trajectory  $U_T(x, u_e)$ .*

**Lemma 4.3.2.** *The domain of definition for the time-map is then given by*

$$\mathcal{D}(T_1^{\bar{u}}) = (0, \bar{u}), \mathcal{D}(T_2^{\bar{u}}) = (\bar{u}, u_2) \quad \text{and} \quad \mathcal{D}(T_{\bar{u}}) = (u_{\min}, \bar{u}).$$

*Proof.* For  $u_0 \leq 0$  a trajectory starting at  $(u_0, 0)$  has a decreasing  $U$ -component and will therefore not reach  $U = \bar{u} > 0$ . For  $u_0 > 0$  the  $U$ -component is increasing, hence we have to choose  $u_0 < \bar{u}$  to be able to reach  $\bar{u}$  in positive 'time'  $x$ . We argue similarly for  $\mathcal{D}(T_2^{\bar{u}})$ . Moreover, we remark that  $\mathcal{D}(T_{\bar{u}}) = \mathcal{D}(T_1^{\bar{u}}) \cap I_{\bar{u}}$  which leads to the assertion of the lemma.  $\square$

**Remark 4.3.3.** *Another way of defining the time-map is to choose  $u_e$  as independent variable by setting*

$$\begin{aligned} \mathcal{D}(\tilde{T}_{\bar{u}}) &:= \{u_e \in \mathcal{D}(T_2^{\bar{u}}) \mid \exists u_0 \text{ with } Q_{\bar{u}}(u_0) = Q_{\bar{u}}(u_e)\}, \\ \tilde{T}_{\bar{u}}(u_e) &:= T_1^{\bar{u}}(u_0(u_e)) + T_2^{\bar{u}}(u_e) \quad \text{for } u_e \in \mathcal{D}(\tilde{T}_{\bar{u}}). \end{aligned}$$

Now, the domain of definition is given by  $\mathcal{D}(\tilde{T}_{\bar{u}}) = (\bar{u}, u_{\max})$ .  
The connection between  $T_{\bar{u}}$  and  $\tilde{T}_{\bar{u}}$  is given by

$$T_{\bar{u}}(u_0) := \tilde{T}_{\bar{u}}(u_e(u_0)),$$

where  $u_0, u_e \in I_{\bar{u}}$  and it holds  $Q(\bar{u}, u_e(u_0)) = Q(\bar{u}, u_0)$ .

The "time" a monotone increasing solution needs to connect  $u_0$  with  $u_e(u_0)$  is the same a monotone decreasing solutions needs to connect  $u_e(u_0)$  with  $u_0$ . This follows from the symmetry of the phaseplane (Fig. 4.1) with respect to the  $u$ -axis.

**Proposition 4.3.4.** *The value  $u_0$  which equals  $U(0)$  for a monotone increasing solution  $U(x)$  with jump at  $\bar{u}$  on the interval  $[0, 1]$  is determined by*

$$T_{\bar{u}}(u_0) = 1.$$

Furthermore, the layer position  $\bar{x}$  is given by

$$\bar{x} = T_1^{\bar{u}}(u_0).$$

*Proof.* This follows from the definition of the time-maps.  $\square$

**Corollary 4.3.5.** *The layer position of a monotone decreasing solution with jump at  $\bar{u}$  is given by*

$$\bar{x} = T_2(\bar{u}, u_0),$$

where  $u_0 := U(0) > \bar{u}$ .

*Proof.* A monotone decreasing solution  $(U(x), V(x))$  is constructed from a monotone decreasing solution  $(\tilde{U}(x), \tilde{V}(x))$  by setting

$$U(x) = \tilde{U}(1-x) \quad \text{and} \quad V(x) = \tilde{V}(1-x).$$

Hence, the layer position is given by

$$1 - T_1(\bar{u}, \tilde{U}(0)) = T_2(\bar{u}, \tilde{U}(1)) = T_2(\bar{u}, U(0)).$$

$\square$

**Proposition 4.3.6.** *The time-maps can be calculated by the following formulas*

$$T_1^{\bar{u}}(u_0) = \frac{1}{\sqrt{2\gamma}} \int_{u_0}^{\bar{u}} \frac{du}{\sqrt{F(h_H(u_0)) - F(h_H(u))}}$$

and

$$T_2^{\bar{u}}(u_e) = \frac{1}{\sqrt{2\gamma}} \int_{\bar{u}}^{u_e} \frac{du}{\sqrt{F(h_T(u_e)) - F(h_T(u))}}.$$

*Proof.* The proof is the same as in the bistable case (compare Proposition 3.1.6.). The difference is that we split the integral at  $\bar{u}$  from the beginning and we use formula (4.8) for the potential.  $\square$

**Theorem 4.3.7.** *The mapping*

$$u_0 \mapsto T_1^{\bar{u}}(u_0)$$

*is well-defined, continuously differentiable for all  $u_0 \in (0, \bar{u})$  and has the range  $(0, \infty)$ . Similarly the mapping*

$$u_e \mapsto T_2^{\bar{u}}(u_e)$$

*is well-defined, continuously differentiable for all  $u_e \in (\bar{u}, u_2)$  and has the range  $(0, \infty)$ .*

*Proof.* The proof of continuity, differentiability, well-definedness and the behaviour of  $T_1^{\bar{u}}(u_0)$  for  $u_0 \rightarrow 0$ , respectively the behaviour of  $T_2^{\bar{u}}(u_e)$  for  $u_e \rightarrow u_2$  is the same as in the bistable case and can be found in the proof of Theorem 3.1.8. We remark that different to the bistable case, there is a priori no connection between  $T_1^{\bar{u}}$  and  $T_2^{\bar{u}}$ . Therefore

$$\lim_{u_0 \rightarrow 0} T_1^{\bar{u}}(u_0) = \infty \quad \text{and} \quad \lim_{u_e \rightarrow u_2} T_2^{\bar{u}}(u_e) = \infty$$

holds independently of the sign of  $Q_{\bar{u}}(u_2)$ .

For investigating the behaviour of the time-map integral  $T_1^{\bar{u}}$  for  $u_0 \rightarrow \bar{u}$ , we use the Taylor expansion of  $Q_{\bar{u}}$  near  $\bar{u}$  from the left remarking that  $q_{\bar{u}}(u) = q_H(u)$  for  $u \leq \bar{u}$

$$Q_{\bar{u}}(u) = F(h_H(u)) \approx F(h_H(\bar{u})) + q_H(\bar{u})(u - \bar{u}).$$

Furthermore, we carry out the change of variables  $u = (\bar{u} - u_0)t + u_0$  to get rid of  $u_0$  as bound of integration

$$T_1^{\bar{u}}(u_0) = \frac{1}{\sqrt{2\gamma}} \int_0^1 \frac{(\bar{u} - u_0)dt}{\sqrt{F(h_H(u_0)) - F(h_H((\bar{u} - u_0)t + u_0))}}. \quad (4.11)$$

We calculate the limit

$$\begin{aligned}
\lim_{u_0 \rightarrow \bar{u}} T_1^{\bar{u}}(u_0) &= \lim_{u_0 \rightarrow \bar{u}} \frac{1}{\sqrt{2\gamma}} \int_0^1 \frac{(\bar{u} - u_0)dt}{\sqrt{q_H(\bar{u})(u_0 - \bar{u}) - q_H(\bar{u})((\bar{u} - u_0)t + u_0 - \bar{u})}} \\
&= \lim_{u_0 \rightarrow \bar{u}} \frac{1}{\sqrt{2\gamma}} \int_0^1 \frac{(\bar{u} - u_0)dt}{\sqrt{q_H(\bar{u})(u_0 - \bar{u})t}} \\
&= \lim_{u_0 \rightarrow \bar{u}} \frac{1}{\sqrt{2\gamma}} \frac{\sqrt{\bar{u} - u_0}}{\sqrt{q_H(\bar{u})}} \int_0^1 \frac{1}{\sqrt{t}} dt \\
&= \lim_{u_0 \rightarrow \bar{u}} \frac{1}{\sqrt{2\gamma}} \frac{\sqrt{\bar{u} - u_0}}{\sqrt{q_H(\bar{u})}} 2 = 0.
\end{aligned}$$

For investigating the behaviour of the time-map integral  $T_2^{\bar{u}}$  for  $u_e \rightarrow \bar{u}$ , we use the Taylor expansion of  $Q_{\bar{u}}$  near  $\bar{u}$  from the right

$$\begin{aligned}
Q_{\bar{u}}(u) &= F(h_H(\bar{u})) - F(h_T(\bar{u})) + F(h_T(u)) \\
&\approx F(h_H(\bar{u})) - F(h_T(\bar{u})) + F(h_T(\bar{u})) + q_T(\bar{u})(u - \bar{u}) \\
&= F(h_H(\bar{u})) + q_T(\bar{u})(u - \bar{u})
\end{aligned}$$

Furthermore, we carry out the change of variables  $u = (u_e - \bar{u})t + \bar{u}$  to get rid of  $u_e$  as bound of integration

$$T_2^{\bar{u}}(u_0) = \frac{1}{\sqrt{2\gamma}} \int_0^1 \frac{(u_e - \bar{u})dt}{\sqrt{F(h_T(u_e)) - F(h_T((u_e - \bar{u})t + \bar{u}))}} \quad (4.12)$$

and we can calculate in a similar way as for  $T_1^{\bar{u}}(u_0)$  that

$$\lim_{u_e \rightarrow \bar{u}} T_2^{\bar{u}}(u_e) = 0$$

holds. □

**Remark 4.3.8.** *We conclude that the behaviour of the time-map near the minimum of the potential is different then in the bistable case. The difference lies in the fact that the potential in the bistable case is differentiable at its minimum, whereas it is not in the hysteresis case. Therefore, in the hysteresis case it is enough to use the Taylor expansion until the first order term, whereas we need the second order term in the bistable case.*

Finally, we show uniqueness of a monotone increasing solution of problem (4.1) with jump at  $\bar{u}$ . To prove this we need the following representation of the derivatives of the time-maps.

**Proposition 4.3.9.** *The time-maps are differentiable and the derivatives have the following form*

$$\frac{d}{du_0} T_1^{\bar{u}}(u_0) = \frac{-\frac{1}{\sqrt{2\gamma}} q_H(u_0)}{Q_{\bar{u}}(u_0) - Q_{\bar{u}}(\bar{u})} \int_{u_0}^{\bar{u}} \left( \frac{(Q_{\bar{u}}(u) - Q_{\bar{u}}(\bar{u})) q'_H(u)}{q_H(u)^2} - \frac{1}{2} \right) \frac{du}{\sqrt{Q_{\bar{u}}(u_0) - Q_{\bar{u}}(u)}} \quad (4.13)$$

and

$$\frac{d}{du_e} T_2^{\bar{u}}(u_e) = \frac{-\frac{1}{\sqrt{2\gamma}} q_T(u_e)}{Q_{\bar{u}}(u_e) - Q_{\bar{u}}(\bar{u})} \int_{\bar{u}}^{u_e} \left( \frac{(Q_{\bar{u}}(u) - Q_{\bar{u}}(\bar{u})) q'_T(u)}{q_T(u)^2} - \frac{1}{2} \right) \frac{du}{\sqrt{Q_{\bar{u}}(u_e) - Q_{\bar{u}}(u)}}. \quad (4.14)$$

*Proof.* Differentiability has already been show in Theorem 4.3.7. To show the representation of the derivatives we use the results from Loud in [Lou59]. The essential assumption  $q_{\bar{u}}(\bar{u}) = 0$  is not fulfilled in the hysteresis case. Therefore, we repeat Louds proof in our notation and show that the formula given by Loud still holds true.

In Theorem 1 in [Lou59] Loud shows that the derivative of  $T_2^{\bar{u}}(u_e)$  can be written in the form

$$\frac{d}{du_e} T_2(u_e) = \frac{1}{\sqrt{2\gamma} \sqrt{Q_{\bar{u}}(u_e) - Q_{\bar{u}}(\bar{u})}} - \frac{1}{2\sqrt{2\gamma}} \int_{\bar{u}}^{u_e} \frac{q_T(u_e) - q_T(u)}{(Q_{\bar{u}}(u_e) - Q_{\bar{u}}(u))^{\frac{3}{2}}} du \quad (4.15)$$

Now, let be  $\bar{u} < a < b < u_e$  and observe that it holds

$$\begin{aligned} \int_a^b \frac{q_T(b) du}{(Q_{\bar{u}}(u_e) - Q_{\bar{u}}(u))^{\frac{3}{2}}} &= \frac{1}{Q_{\bar{u}}(u_e) - Q_{\bar{u}}(\bar{u})} \int_a^b \frac{q_T(b) du}{\sqrt{Q_{\bar{u}}(u_e) - Q_{\bar{u}}(u)}} \\ &\quad + \frac{1}{Q_{\bar{u}}(u_e) - Q_{\bar{u}}(\bar{u})} \int_a^b \frac{q_T(b)(Q_{\bar{u}}(u) - Q_{\bar{u}}(\bar{u})) du}{(Q_{\bar{u}}(u_e) - Q_{\bar{u}}(u))^{\frac{3}{2}}}. \end{aligned}$$

Using a clever integration by parts of the second integral with

$$v(u) = \frac{q_T(b)(Q_{\bar{u}}(u) - Q_{\bar{u}}(\bar{u}))}{q_T(u)} \quad \text{and} \quad w'(u) = \frac{q_T(u)}{(Q_{\bar{u}}(u_e) - Q_{\bar{u}}(u))^{\frac{3}{2}}},$$

hence

$$v'(u) = q_T(b) \left( 1 - \frac{(Q_{\bar{u}}(u) - Q_{\bar{u}}(\bar{u})) q'_T(u)}{q_T(u)^2} \right) \quad \text{and} \quad w(u) = \frac{2}{\sqrt{Q_{\bar{u}}(u_e) - Q_{\bar{u}}(u)}}$$

yields

$$\begin{aligned} \int_a^b \frac{q_T(b)du}{(Q_{\bar{u}}(u_e) - Q_{\bar{u}}(u))^{\frac{3}{2}}} &= \frac{Q_{\bar{u}}(b) - Q_{\bar{u}}(\bar{u})}{Q_{\bar{u}}(u_e) - Q_{\bar{u}}(\bar{u})} \frac{2}{\sqrt{Q_{\bar{u}}(u_e) - Q_{\bar{u}}(b)}} \\ &\quad - \frac{Q_{\bar{u}}(a) - Q_{\bar{u}}(\bar{u})}{Q_{\bar{u}}(u_e) - Q_{\bar{u}}(\bar{u})} \frac{q_T(b)}{q_T(a)} \frac{2}{\sqrt{Q_{\bar{u}}(u_e) - Q_{\bar{u}}(a)}} \\ &\quad + \frac{2q_T(b)}{Q_{\bar{u}}(u_e) - Q_{\bar{u}}(\bar{u})} \int_a^b \left( \frac{(Q_{\bar{u}}(u) - Q_{\bar{u}}(\bar{u}))q'_T(u)}{q_T(u)^2} - \frac{1}{2} \right) \frac{du}{\sqrt{Q_{\bar{u}}(u_e) - Q_{\bar{u}}(u)}}. \end{aligned}$$

Furthermore, we integrate by substitution

$$\int_a^b \frac{q_T(u)du}{(Q_{\bar{u}}(u_e) - Q_{\bar{u}}(b))^{\frac{3}{2}}} = \frac{2}{\sqrt{Q_{\bar{u}}(u_e) - Q_{\bar{u}}(b)}} - \frac{2}{\sqrt{Q_{\bar{u}}(u_e) - Q_{\bar{u}}(a)}}$$

which yields

$$\begin{aligned} \int_a^b \frac{q_T(b) - q_T(u)}{(Q_{\bar{u}}(u_e) - Q_{\bar{u}}(u))^{\frac{3}{2}}} du &= \frac{2}{\sqrt{Q_{\bar{u}}(u_e) - Q_{\bar{u}}(a)}} - \frac{2\sqrt{Q_{\bar{u}}(u_e) - Q_{\bar{u}}(b)}}{Q_{\bar{u}}(u_e) - Q_{\bar{u}}(\bar{u})} \\ &\quad - \frac{Q_{\bar{u}}(a) - Q_{\bar{u}}(\bar{u})}{Q_{\bar{u}}(u_e) - Q_{\bar{u}}(\bar{u})} \frac{q_T(b)}{q_T(a)} \frac{2}{\sqrt{Q_{\bar{u}}(u_e) - Q_{\bar{u}}(a)}} \\ &\quad + \frac{2q_T(b)}{Q_{\bar{u}}(u_e) - Q_{\bar{u}}(\bar{u})} \int_a^b \left( \frac{(Q_{\bar{u}}(u) - Q_{\bar{u}}(\bar{u}))q'_T(u)}{q_T(u)^2} - \frac{1}{2} \right) \frac{du}{\sqrt{Q_{\bar{u}}(u_e) - Q_{\bar{u}}(u)}} \end{aligned} \quad (4.16)$$

Finally, we let tend  $a \rightarrow \bar{u}$  and  $b \rightarrow u_e$  and obtain

$$\begin{aligned} \int_{\bar{u}}^{u_e} \frac{q_T(u_e) - q_T(u)}{(Q_{\bar{u}}(u_e) - Q_{\bar{u}}(u))^{\frac{3}{2}}} du &= \frac{2}{\sqrt{Q_{\bar{u}}(u_e) - Q_{\bar{u}}(\bar{u})}} \\ &\quad + \frac{2q_T(u_e)}{Q_{\bar{u}}(u_e) - Q_{\bar{u}}(\bar{u})} \int_{\bar{u}}^{u_e} \left( \frac{(Q_{\bar{u}}(u) - Q_{\bar{u}}(\bar{u}))q'_T(u)}{q_T(u)^2} - \frac{1}{2} \right) \frac{du}{\sqrt{Q_{\bar{u}}(u_e) - Q_{\bar{u}}(u)}}. \end{aligned}$$

Together with representation (4.15) this integral leads to the formula in the proposition. In a similar fashion we deduce the result for  $\frac{d}{du_0} T_1^{\bar{u}}(u_0)$ .

We remark that Loud assumes the function  $q_{\bar{u}}$  to be continuous with zero  $q_{\bar{u}}(\bar{u}) = 0$ . Therefore, he requires that  $\lim_{a \rightarrow \bar{u}, b \rightarrow 0} \frac{q_T(a)}{q_T(b)} = 0$  holds in equation (4.16). In our case just the nominator but not the denominator is zero, hence the term is zero without further assumptions.  $\square$

**Theorem 4.3.10.** *We consider the generic model in the hysteresis case. For all jumps  $\bar{u} \in (u_T, \min(u_H, u_2))$  the derivative of the time-map  $T_{\bar{u}}$  is negative, i.e.,*

$$\frac{d}{du_0} T_{\bar{u}}(u_0) < 0.$$

Moreover, the derivatives of  $T_1^{\bar{u}}$  and  $T_2^{\bar{u}}$  have the following signs

$$\frac{d}{du_0} T_1^{\bar{u}}(u_0) < 0 \quad \text{and} \quad \frac{d}{du_e} T_2^{\bar{u}}(u_e) > 0.$$

*Proof.* We start by showing  $\frac{d}{du_0} T_1^{\bar{u}}(u_0) < 0$ . To this end we use Proposition 4.3.9 showing that the derivative of the time-map has an integral representation (4.13) which we rewrite in the form

$$\frac{d}{du_0} T_1^{\bar{u}}(u_0) = -\frac{q_H(u_0)}{\sqrt{2\gamma(Q_{\bar{u}}(u_0) - Q_{\bar{u}}(\bar{u}))}} \cdot \int_{u_0}^{\bar{u}} l_H(u) \frac{du}{\sqrt{Q_{\bar{u}}(u_0) - Q_{\bar{u}}(u)}}$$

with a function  $l_H$  defined by

$$l_H(u) = \frac{(Q_{\bar{u}}(u) - Q_{\bar{u}}(\bar{u}))q'_H(u)}{q_H(u)^2} - \frac{1}{2}.$$

We observe that for all  $u \in (u_0, \bar{u})$  it holds  $Q_{\bar{u}}(u) - Q_{\bar{u}}(\bar{u}) \geq 0$ . This leads together with Lemma 2.1.10 to the positivity of  $-\frac{q_H(u_0)}{\sqrt{2\gamma(Q_{\bar{u}}(u_0) - Q_{\bar{u}}(\bar{u}))}}$ . Thus, it remains to show that  $l_H$  is negative for  $u \in [u_0, \bar{u}]$ .

Therefore, we multiply  $l_H$  by the square of  $q_H$  and calculate the derivative

$$\frac{d}{du} (q_H(u)^2 l_H(u)) = (Q_{\bar{u}}(u) - Q_{\bar{u}}(\bar{u}))q''_H(u)$$

which leads together with

$$q_H(u)^2 l_H(u)|_{u=\bar{u}} = -\frac{1}{2}q_H(\bar{u})^2 =: C_H < 0$$

to the representation

$$q_H(u)^2 l_H(u) = C_H + \int_{\bar{u}}^u (Q_{\bar{u}}(\tilde{u}) - Q_{\bar{u}}(\bar{u}))q''_H(\tilde{u})d\tilde{u} = C_H - \int_u^{\bar{u}} (Q_{\bar{u}}(\tilde{u}) - Q_{\bar{u}}(\bar{u}))q''_H(\tilde{u})d\tilde{u}.$$

To see that this expression is negative, it remains to show that  $q''_H(u) = \alpha h''_H(u) = -\alpha \frac{p''(h_H(u))}{p'(h_H(u))^3}$  is of positive sign. Lemma 2.1.5 yields that for all  $u \in (u_0, \bar{u})$  it holds  $p'(h_H(u)) > 0$  as well as  $p''(h_H(u)) < 0$ . Hence, we obtain  $l_H(u) < 0$ , which proves  $\frac{d}{du_0} T_1^{\bar{u}}(u_0) < 0$ .

We use the same reasoning for showing that  $\frac{d}{du_e} T_2^{\bar{u}}(u_e) > 0$ . The derivative is given by the integral representation (4.14) which we rewrite as

$$\frac{d}{du_e} T_2^{\bar{u}}(u_e) = -\frac{q_T(u_e)}{\sqrt{2\gamma(Q_{\bar{u}}(u_e) - Q_{\bar{u}}(\bar{u}))}} \cdot \int_{\bar{u}}^{u_e} l_T(u) \frac{du}{\sqrt{Q_{\bar{u}}(u_e) - Q_{\bar{u}}(u)}}$$

using the function

$$l_T(u) = \frac{(Q_{\bar{u}}(u) - Q_{\bar{u}}(\bar{u}))q'_T(u)}{q_T(u)^2} - \frac{1}{2}.$$

We observe that  $-\frac{q_T(u_e)}{\sqrt{2\gamma}(Q_{\bar{u}}(u_e) - Q_{\bar{u}}(\bar{u}))}$  is negative, because of Lemma 2.1.10. Therefore, it remains to show the negativity of  $l_T$ .

We obtain the representation

$$q_T(u)^2 l_T(u) = C_T + \int_{\bar{u}}^u (Q_{\bar{u}}(\tilde{u}) - Q_{\bar{u}}(\bar{u}))q''_T(\tilde{u})d\tilde{u}$$

using

$$\frac{d}{du} (q_T(u)^2 l_T(u)) = (Q_{\bar{u}}(u) - Q_{\bar{u}}(\bar{u}))q''_T(u)$$

and

$$q_T(u)^2 l_T(u)|_{u=\bar{u}} = -\frac{1}{2}q_T(\bar{u})^2 =: C_T < 0.$$

For all  $u \in (\bar{u}, u_e)$  it holds that  $Q_{\bar{u}}(u) - Q_{\bar{u}}(\bar{u}) \geq 0$ , hence we have to show that  $q''_T(u) = \alpha h''_T(u) = -\alpha \frac{p''(h_T(u))}{p'(h_T(u))^3} < 0$  holds. Indeed, Lemma 2.1.5 shows that for all  $u \in (\bar{u}, u_e)$  it holds  $p'(h_T(u)) > 0$  as well as  $p''(h_T(u)) > 0$ , which proves  $\frac{d}{du_e} T_2^{\bar{u}}(u_e) > 0$ .

To accomplish the proof, we deduce similarly as in the bistable case (cf. Lemma 3.1.9)

$$\frac{d}{du_0} u_e(u_0) = \frac{q_H(u_0)}{q_T(u_e)} < 0. \quad (4.17)$$

by derivating equation (4.10) with respect to  $u_0$ . Therefore,

$$\begin{aligned} \frac{d}{du_0} T_{\bar{u}}(u_0) &= \frac{d}{du_0} T_1^{\bar{u}}(u_0) + \frac{d}{du_e} T_2^{\bar{u}}(u_e) \cdot \frac{d}{du_0} u_e(u_0) \\ &= \frac{d}{du_0} T_1^{\bar{u}}(u_0) + \frac{d}{du_e} T_2^{\bar{u}}(u_e) \cdot \frac{q_H(u_0)}{q_T(u_e)} < 0. \end{aligned} \quad (4.18)$$

□

Now, we finish the proof of Theorem 4.1.3, which states the existence of a unique monotone increasing solution of equation (4.5) for all diffusion coefficients.

*Proof of Theorem 4.1.3.* We have constructed a solution connecting  $u_0 < \bar{u} < u_e$  requiring that  $Q_{\bar{u}}(u_0) = Q_{\bar{u}}(u_e)$  holds. This is possible when  $Q_{\bar{u}}(u)$  has a local minimum at  $\bar{u}$  which is the case for all  $\bar{u} \in (u_T, \min(u_H, u_2))$ . Furthermore, the constructed solution is a solution on the interval  $x \in [0, 1]$  if  $T_{\bar{u}}(u_0) = 1$ .

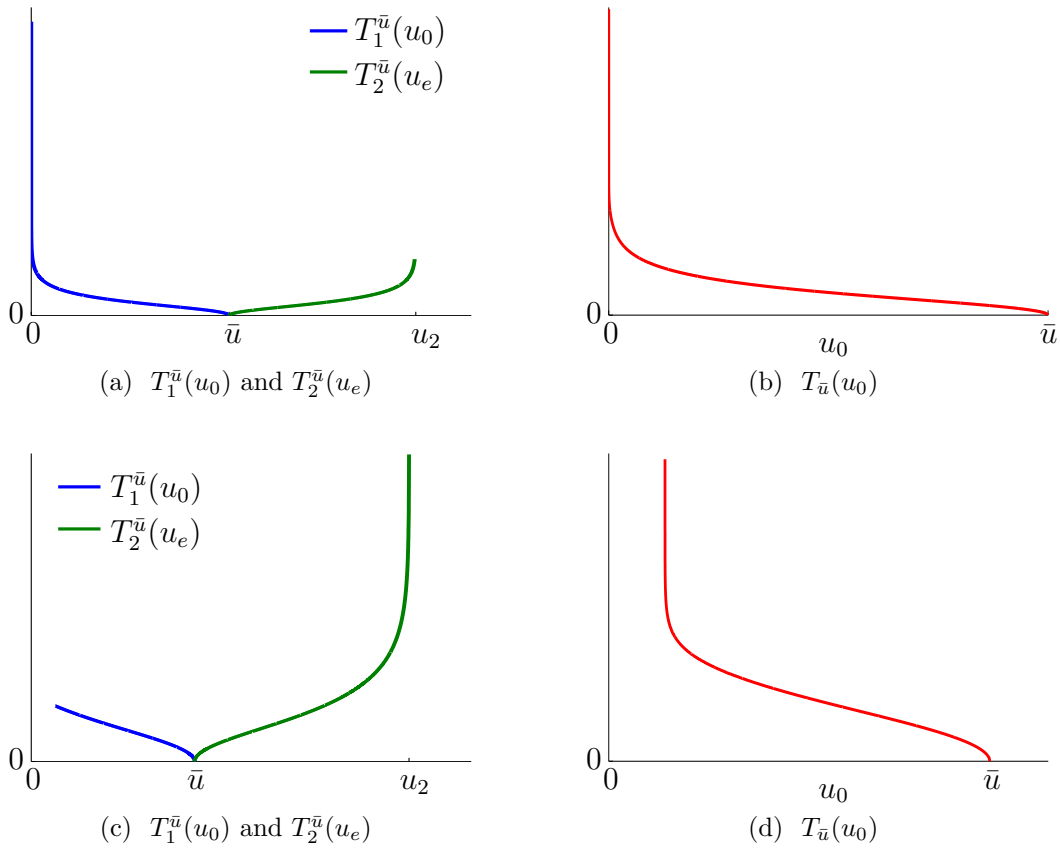


Figure 4.4: The time-maps in the hysteresis case. The upper row shows simulations for the polynomial  $p(v) = v^3 - 6.2v^2 + 10v$ , the line  $f(u, v) = 2v - u$  and jump  $\bar{u} = 4.5$ , whereas in the lower row we chose  $p(v) = v^3 - 6v^2 + 10v$ ,  $f(u, v) = 1.8v - u$  and  $\bar{u} = 3.6$ .

We remark that the simulations for  $T_1^{\bar{u}}$  and  $T_2^{\bar{u}}$  are only computed on the interval  $(u_{\min}, \bar{u})$  and  $(\bar{u}, u_{\max})$ , respectively. We see that  $T_1^{\bar{u}}$  is decreasing, whereas  $T_2^{\bar{u}}$  is increasing, which leads to  $\frac{d}{du_0} T_{\bar{u}}(u_0) < 0$ . Furthermore, we observe that  $\lim_{u_0 \rightarrow \bar{u}} T_{\bar{u}}(u_0) = 0$  in contrast to the bistable case.

It suffices to show that  $T_{\bar{u}}(u_0)$  is a continuous mapping with range  $(0, \infty)$ .

$T_{\bar{u}}$  is continuous as sum and composition of continuous functions. Because of the continuity of  $Q_{\bar{u}}$  we conclude that  $u_0 \rightarrow \bar{u}$  implies  $u_e \rightarrow \bar{u}$  and, therefore,

$$\lim_{u_0 \rightarrow \bar{u}} T_{\bar{u}}(u_0) = \lim_{u_0 \rightarrow \bar{u}} T_1^{\bar{u}}(u_0) + \lim_{u_e \rightarrow \bar{u}} T_2^{\bar{u}}(u_e) = 0.$$

Finally, we know that by Lemma 4.2.1 that either  $u_{\min} = 0$  or  $u_{\max} = u_2$  holds true

and therefore

$$\lim_{u_0 \rightarrow u_{\min}} T_{\bar{u}}(u_0) = \lim_{u_0 \rightarrow u_{\min}} T_1^{\bar{u}}(u_0) + \lim_{u_e \rightarrow u_{\max}} T_2^{\bar{u}}(u_e) = \infty,$$

because either the first or the second limit is infinite.

Therefore, we obtain that  $T_{\bar{u}}$  is continuous with range  $(0, \infty)$  and, hence, for all diffusion coefficients  $\frac{1}{\gamma}$  it is possible to find  $u_0$  such that  $T_{\bar{u}}(u_0) = 1$ . This value is unique because of Theorem 4.3.10, which accomplishes the existence of a unique monotone increasing stationary solution of system (2.1).  $\square$

## 4.4 Stability of discontinuous stationary solutions

In this section we derive a condition for the stability of stationary solutions of the generic model (2.1) in the hysteresis case.

A standard approach to show stability of stationary solutions is based on linear stability analysis (see for example [Smo83], [Hen93]). However, the linear stability analysis cannot be applied to discontinuous steady states.

In [ATH84] the stability of discontinuous steady states was analysed by excluding the discontinuities. We use a new approach to show stability by applying a direct method based on estimates.

We have to pay attention with respect to what kind of perturbations a stationary solution can be stable. The generic model in the hysteresis case admits an infinite number of monotone increasing stationary solutions. Simulations (see Figure 2.5) suggest that the stationary solution which is selected strongly depends on the initial conditions. For this reason it is suitable to consider stability in  $L^\infty(0, 1)$  sense. A perturbation which is small in  $L^\infty(0, 1)$  cannot move a point on the stationary solution  $(U(x), V(x))$  lying on one side of the separatrix to the other side. In contrast, a perturbation which is small in  $L^2(0, 1)$  may have high values on some small interval leading to another stationary solution. Thus, a stationary solutions which is stable in  $L^\infty(0, 1)$  sense might be unstable with respect to  $L^2(0, 1)$ -perturbations.

**Example 4.4.1.** *To show the difference between perturbations in  $L^2(0, 1)$  and  $L^\infty(0, 1)$ , we consider the generic model in the hysteresis case for the kinetic functions  $f(u, v) = 1.4v - u$  and  $p(v) = v^3 - 6.3v^2 + 10v$ . Let  $(U(x), V(x))$  be a monotone increasing stationary solution with layer position at  $\bar{x} = 0.4$  (see Figure 4.5a).*

*At first, we add to  $(U(x), V(x))$  a random perturbation  $(\varphi_0(x), \psi_0(x))$  fulfilling  $\|\varphi_0\|_{L^\infty(0,1)} = \|\psi_0\|_{L^\infty(0,1)} = 0.4$ . We see in Figure 4.5b that the solution of system (2.1) with initial condition  $(U(x) + \varphi_0(x), V(x) + \psi_0(x))$  approaches  $(U(x), V(x))$ .*

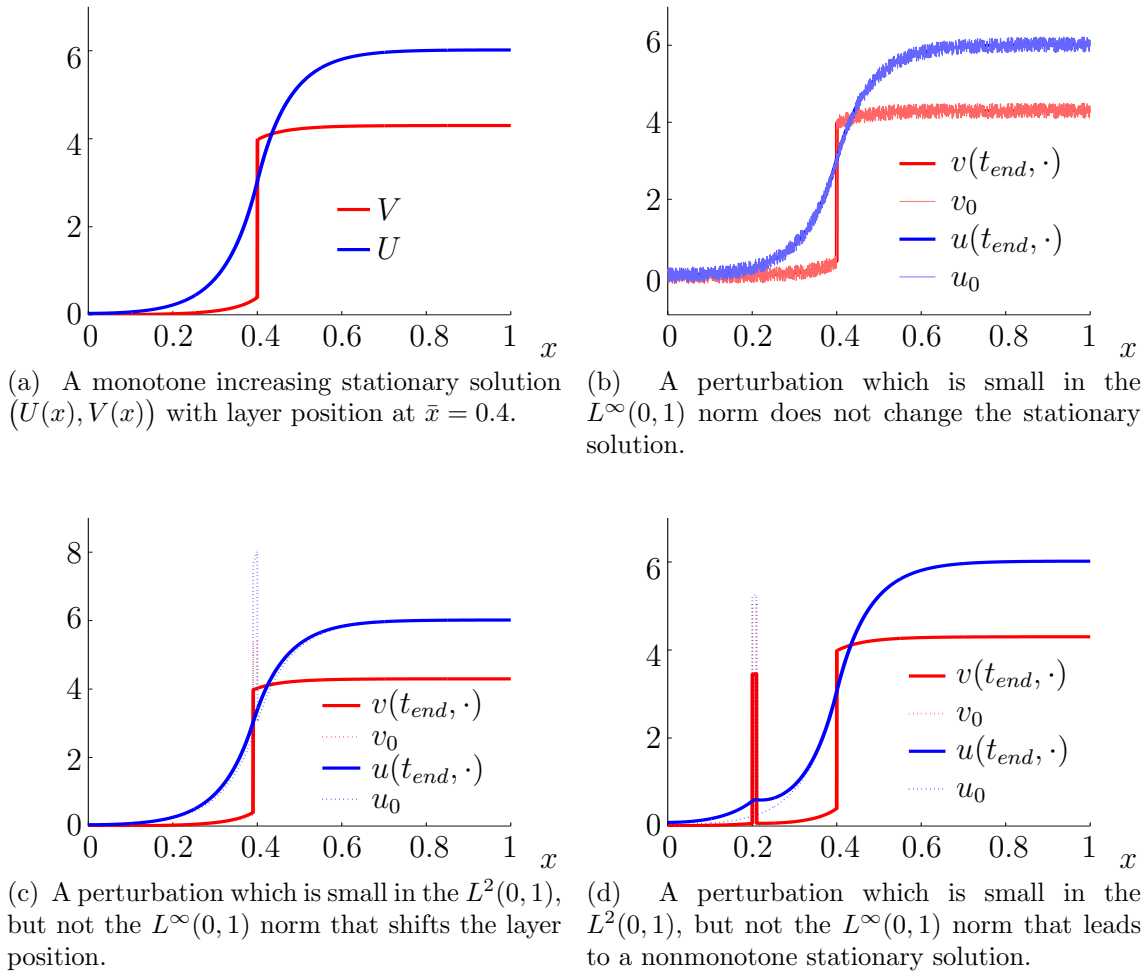


Figure 4.5: Simulations of the generic model in the hysteresis case for different types of perturbations of a stationary solution. The plots show the initial condition (dotted lines) and the approached stationary solution (continuous lines) after a sufficiently big time  $t_{end}$ .

Next, we perturb with the step function

$$\varphi_0(x) = \psi_0(x) = \begin{cases} 5 & \text{for } x \in [0.39, 0.4] \\ 0 & \text{else.} \end{cases}$$

This perturbation is small in  $L^2(0, 1)$  because  $\|\varphi_0\|_{L^2(0,1)} = 5 \cdot 0.01 = 0.05$ , but it is big in  $L^\infty(0, 1)$ , where we obtain  $\|\varphi_0\|_{L^\infty(0,1)} = 5$ . We see in Figure 4.5c that the simulation leads to a stationary solution with layer position  $\bar{x} = 0.39$ .

Finally, the perturbation

$$\varphi_0(x) = \psi_0(x) = \begin{cases} 5 & \text{for } x \in [0.19, 0.2] \\ 0 & \text{else} \end{cases}$$

with norm  $\|\varphi_0\|_{L^2(0,1)} = 0.05$  and  $\|\varphi_0\|_{L^\infty(0,1)} = 5$ , leads to a stationary solution which is not monotone anymore.

Let  $(U(x), V(x)) \in H_N^2(0, 1) \times L^\infty(0, 1)$  be a nonhomogeneous stationary solution of system (2.1). We denote  $(u, v)$  a small nonlinear perturbation of the stationary solution in the  $L^\infty(0, 1)$ -norm, i.e.

$$u(t, x) = U(x) + \varphi(t, x), \quad (4.19)$$

$$v(t, x) = V(x) + \psi(t, x) \quad (4.20)$$

with  $(\varphi, \psi) \in C([0, \infty]; L^\infty(0, 1) \times L^\infty(0, 1))$ .

We assume that

$$\operatorname{ess\,inf}_{x \in [0,1]} p'(V(x)) := K > \frac{\alpha}{\beta}, \quad (4.21)$$

is fulfilled, which we call the **stability condition**.

We show in the following that a stationary solution fulfilling assumption (4.21) is asymptotically stable as a solution of the reaction-diffusion system.

**Notation:** For simplicity we write in this section  $\|\cdot\|_\infty$  for the norm  $\|\cdot\|_{L^\infty(0,1)}$ .

We start with a technical result.

**Lemma 4.4.2.** *For every real constant  $c > 0$  it holds*

$$\lim_{t \rightarrow \infty} \int_0^t e^{-c(t-s)} ds = \frac{1}{c}.$$

*Proof.* We calculate the integral

$$\int_0^t e^{-c(t-s)} ds = \left[ \frac{1}{c} e^{-c(t-s)} \right]_0^t = \frac{1}{c} (1 - e^{-ct})$$

and obtain that

$$\lim_{t \rightarrow \infty} \frac{1}{c} (1 - e^{-ct}) = \frac{1}{c}$$

holds true. □

First, we consider a linearised system, where  $\varphi, \psi$  are small linear perturbations given by (4.19)

$$\varphi_t(t, x) = \frac{1}{\gamma} \varphi_{xx}(t, x) + \alpha \psi(t, x) - \beta \varphi(t, x), \quad t > 0, x \in [0, 1] \quad (4.22)$$

$$\psi_t(t, x) = \varphi(t, x) - p'(V(x))\psi(t, x) \quad t > 0, x \in [0, 1]. \quad (4.23)$$

**Proposition 4.4.3.** *The linear system (4.22)-(4.23) with bounded initial condition  $\varphi(0, x) = \varphi_0(x) \in L^\infty(0, 1)$  and  $\psi(0, x) = \psi_0(x) \in L^\infty(0, 1)$  and boundary condition  $\varphi_x(t, 0) = \varphi_x(t, 1) = 0$  has a unique bounded solution*

$$(\varphi, \psi) \in C([0, \infty]; L^\infty(0, 1) \times L^\infty(0, 1))$$

given by

$$\varphi(t, x) = S(t)\varphi_0(x) + \alpha \int_0^t S(t-s)\psi(s, x)ds, \quad (4.24)$$

$$\psi(t, x) = e^{-tp'(V(x))}\psi_0(x) + \int_0^t e^{-(t-s)p'(V(x))}\varphi(s, x)ds. \quad (4.25)$$

Here,  $S(t)$  is the semigroup generated by the operator

$$\mathcal{D}(A) = \{u \in W^{2,\infty}(0, 1) \mid u_x(0) = u_x(1) = 0\}, \quad (4.26)$$

$$Au := \frac{1}{\gamma}u_{xx} - \beta u \quad \forall u \in \mathcal{D}(A) \quad (4.27)$$

which fulfils the estimate

$$\|S(t)\varphi_0\|_\infty \leq e^{-\beta t}\|\varphi_0\|_\infty. \quad (4.28)$$

*Proof.* Replacing  $L^2(0, 1)$  by  $L^\infty(0, 1)$ , the proof can be performed in a similar way as for Theorem 2.3.14.  $\square$

**Theorem 4.4.4** (Linearised Stability). *Let  $(\varphi, \psi) \in C([0, \infty]; L^\infty(0, 1) \times L^\infty(0, 1))$  be a solution of system (4.22)-(4.23), then it holds*

$$\limsup_{t \rightarrow \infty} (\|\varphi(t, \cdot)\|_\infty, \|\psi(t, \cdot)\|_\infty) \rightarrow (0, 0).$$

*Proof.* Using the integral representation (4.24) and (4.25) we estimate the  $L^\infty(0, 1)$ -norm of the solution by

$$\|\varphi(t, \cdot)\|_\infty \leq e^{-t\beta}\|\varphi_0\|_\infty + \alpha \int_0^t e^{-\beta(t-s)}\|\psi(s, \cdot)\|_\infty ds \quad (4.29)$$

and

$$\|\psi(t, \cdot)\|_\infty \leq e^{-tK} \|\psi_0\|_\infty + \int_0^t e^{-K(t-s)} \|\varphi(s, \cdot)\|_\infty ds. \quad (4.30)$$

In the next step, we define

$$\Phi^L := \limsup_{t \rightarrow \infty} \|\varphi(t, \cdot)\|_\infty \quad \text{and} \quad \Psi^L := \limsup_{t \rightarrow \infty} \|\psi(t, \cdot)\|_\infty. \quad (4.31)$$

It holds  $\Phi^L < \infty$  and  $\Psi^L < \infty$ , because  $\varphi$  and  $\psi$  are bounded by Theorem 4.4.3. Moreover, equation (4.29) yields the estimate

$$\Phi^L \leq \limsup_{t \rightarrow \infty} e^{-t\beta} \|\varphi_0\|_\infty + \alpha \Psi^L \limsup_{t \rightarrow \infty} \int_0^t e^{-\beta(t-s)} ds.$$

Using Lemma 4.4.2 we obtain

$$0 \leq \Phi^L \leq \frac{\alpha}{\beta} \Psi^L. \quad (4.32)$$

Similarly, we deduce from equation (4.30)

$$\Psi^L \leq \limsup_{t \rightarrow \infty} e^{-tK} \|\psi_0\|_\infty + \Phi^L \limsup_{t \rightarrow \infty} \int_0^t e^{-K(t-s)} ds$$

and again by Lemma 4.4.2 we obtain

$$0 \leq \Psi^L \leq \frac{1}{K} \Phi^L. \quad (4.33)$$

Finally, the estimates (4.32) and (4.33) lead to

$$0 \leq \left(\frac{\alpha}{\beta} - K\right) \Phi^L.$$

Because of the stability condition (4.21) it holds  $\frac{\alpha}{\beta} - K \leq 0$ , which induces  $\Phi^L = 0$ . From estimate (4.33), we obtain  $\Psi^L = 0$  as well. This shows that a linear perturbation in  $L^\infty(0, 1)$  of a stationary solution decays to zero.  $\square$

Next, we investigate the behaviour of the system under nonlinear perturbations. We show at first that for sufficiently small initial perturbations the perturbations stay small. Then we will show in Theorem 4.4.8 that they decay to zero.

**Lemma 4.4.5.** *The nonlinear perturbation*

$$(\varphi, \psi) \in C([0, \infty]; L^\infty(0, 1) \times L^\infty(0, 1))$$

*is a solution of the system*

$$\varphi_t(t, x) = \frac{1}{\gamma} \varphi_{xx}(t, x) + \alpha \psi(t, x) - \beta \varphi(t, x), \quad t > 0, x \in [0, 1] \quad (4.34)$$

$$\psi_t(t, x) = \varphi(t, x) - p'(V(x))\psi(t, x) + R(x)\psi^2(t, x), \quad t > 0, x \in [0, 1] \quad (4.35)$$

*where  $R(x)$  is a bounded function.*

*Proof.* We use definition (4.19) to obtain

$$\begin{aligned}\varphi_t = u_t &= \frac{1}{\gamma}U_{xx} + \frac{1}{\gamma}\varphi_{xx} + \alpha(V + \psi) - \beta(U + \varphi) \\ &= \frac{1}{\gamma}\varphi_{xx} + \alpha\psi - \beta\varphi.\end{aligned}$$

Similarly, we find

$$\begin{aligned}\psi_t = v_t &= U + \varphi - p(V + \psi) \\ &= \varphi + p(V) - p(V + \psi) \\ &= \varphi + p'(V(x))\psi + p''(\theta(x))\psi^2,\end{aligned}$$

where we use the Taylor development of  $p(V(x))$  for  $x$  fixed with  $\theta(x)$  being the rest. Observe that  $\theta(x) \in (0, v_2)$  and that  $p''(v) = 6a_1v + 2a_2$  is bounded for  $v$  being in some interval. Hence, we conclude the proof by setting  $R(x) := p''(\theta(x))$  which is bounded.  $\square$

**Proposition 4.4.6.** *The nonlinear system (4.34)-(4.35) with bounded initial condition  $\varphi(0, x) = \varphi_0(x) \in L^\infty(0, 1)$  and  $\psi(0, x) = \psi_0(x) \in L^\infty(0, 1)$  and boundary condition  $\varphi_x(t, 0) = \varphi_x(t, 1) = 0$  has a unique bounded solution*

$$(\varphi, \psi) \in C([0, \infty]; L^\infty(0, 1) \times L^\infty(0, 1)).$$

given by

$$\varphi(t, x) = S(t)\varphi_0(x) + \alpha \int_0^t S(t-s)\psi(s, x)ds, \quad (4.36)$$

$$\begin{aligned}\psi(t, x) &= e^{-p'(V(x))t}\psi_0(x) + \int_0^t e^{-(t-s)p'(V(x))}\varphi(s, x)ds \\ &\quad + \int_0^t e^{-(t-s)p'(V(x))}R(x)\psi^2(s, x)ds.\end{aligned} \quad (4.37)$$

*Proof.* We refer to the proof of Proposition 4.4.3.  $\square$

**Theorem 4.4.7** (Nonlinear Stability). *If  $\varphi_0$  and  $\psi_0$  are initial perturbations of a stationary solution fulfilling assumption (4.21) with  $\|\varphi_0\|_\infty$  and  $\|\psi_0\|_\infty$  sufficiently small, then*

$$\|\varphi(t, \cdot)\|_\infty \quad \text{and} \quad \|\psi(t, \cdot)\|_\infty$$

*stay also small for all times  $t$ . More precisely, we set  $R_0 = \sup_{x \in [0, 1]} R(x)$ . Let the initial perturbations fulfil*

$$K\|\psi_0\|_\infty + \|\varphi_0\|_\infty \leq \frac{1}{4R_0} \left(K - \frac{\alpha}{\beta}\right)^2, \quad (4.38)$$

and

$$\|\psi_0\|_\infty \leq \frac{1}{2R_0} \left( K - \frac{\alpha}{\beta} \right) - \sqrt{\left( K - \frac{\alpha}{\beta} \right)^2 - 4R_0(K\|\psi_0\|_\infty + \|\varphi_0\|_\infty)} \quad (4.39)$$

then the following estimates hold

$$\begin{aligned} \|\varphi(t, \cdot)\|_\infty &\leq \|\varphi_0\|_\infty + \frac{\alpha}{\beta} \frac{1}{2R_0} \left( K - \frac{\alpha}{\beta} \right), \\ \|\psi(t, \cdot)\|_\infty &\leq \frac{1}{2R_0} \left( K - \frac{\alpha}{\beta} \right) \end{aligned}$$

for all  $t \in [0, \infty)$ .

*Proof.* We define increasing continuous functions

$$\Phi(t) := \sup_{0 \leq \tau \leq t} \|\varphi(\tau, \cdot)\|_\infty \quad \text{and} \quad \Psi(t) := \sup_{0 \leq \tau \leq t} \|\psi(\tau, \cdot)\|_\infty.$$

Using the integral representations (4.36), the estimate of the semigroup (4.28) and taking the supremum over  $\tau \in [0, t]$ , we obtain the estimate

$$\Phi(t) \leq \|\varphi_0\|_\infty + \alpha \int_0^t e^{-\beta(t-s)} \Psi(s) ds \quad (4.40)$$

and similarly using (4.37)

$$\Psi(t) \leq \|\psi_0\|_\infty + \int_0^t e^{-K(t-s)} \Phi(s) ds + R_0 \int_0^t e^{-K(t-s)} \Psi^2(s) ds. \quad (4.41)$$

Using that  $\Phi(t)$  and  $\Psi(t)$  are increasing by definition, estimate (4.40) leads together with Lemma 4.4.2 to

$$\begin{aligned} \Phi(t) &\leq \|\varphi_0\|_\infty + \alpha \Psi(t) \int_0^t e^{-\beta(t-s)} ds \\ &\leq \|\varphi_0\|_\infty + \frac{\alpha}{\beta} \Psi(t). \end{aligned} \quad (4.42)$$

Similarly, we obtain from (4.41) that holds

$$\begin{aligned} \Psi(t) &\leq \|\psi_0\|_\infty + \Phi(t) \int_0^t e^{-K(t-s)} ds + R_0 \Psi^2(t) \int_0^t e^{-K(t-s)} ds, \\ &\leq \|\psi_0\|_\infty + \frac{1}{K} \Phi(t) + \frac{1}{K} R_0 \Psi^2(t). \end{aligned} \quad (4.43)$$

Substituting equation (4.42) into equation (4.43) and multiplying by  $K$ , we obtain the estimate

$$0 \leq K\|\psi_0\|_\infty + \|\varphi_0\|_\infty + \left(\frac{\alpha}{\beta} - K\right)\Psi(t) + R_0\Psi^2(t). \quad (4.44)$$

The graph of

$$y \mapsto K\|\psi_0\|_\infty + \|\varphi_0\|_\infty + \left(\frac{\alpha}{\beta} - K\right)y + R_0y^2 \quad (4.45)$$

is a parabola which is positive at  $y = 0$ . As the linear term is negative by the stability condition (4.21), this parabola has zeros if the constant term  $K\|\psi_0\|_\infty + \|\varphi_0\|_\infty$  is small enough. Thus, because  $\Psi(t)$  is nonnegative for all times, it is bounded by the smallest zero of the parabola, provided  $\Psi(0) = \|\psi_0\|_\infty$ .

To be more precise, we calculate the discriminant of the parabola (4.45)

$$D = \left(K - \frac{\alpha}{\beta}\right)^2 - 4R_0(K\|\psi_0\|_\infty + \|\varphi_0\|_\infty).$$

Therefore, under the condition (4.38) the discriminant  $D$  is positive, which yields that the parabola has zeros, given by

$$y_{1/2} = \frac{1}{2R_0} \left(K - \frac{\alpha}{\beta} \pm \sqrt{D}\right).$$

The smallest zero is necessarily smaller than  $\frac{1}{2R_0} \left(K - \frac{\alpha}{\beta}\right)$ , which leads the bound for  $\Psi(t)$ . Together with equation (4.42), we obtain the bound for  $\Phi(t)$ .  $\square$

Finally, we prove asymptotic stability of stationary solutions in the hysteresis case with respect to nonlinear  $L^\infty(0, 1)$  perturbations. This means that a perturbation does not only stays bounded, it decays to zero.

**Theorem 4.4.8** (Asymptotic Stability). *Let  $(U(x), V(x))$  be a stationary solution fulfilling the stability condition (4.21). If  $\varphi_0$  and  $\psi_0$  are initial perturbations, which are sufficiently small, that means which fulfil the estimate (4.38), then for the nonlinear perturbation  $(\varphi, \psi)$  holds*

$$\left(\|\varphi(t, \cdot)\|_\infty, \|\psi(t, \cdot)\|_\infty\right) \rightarrow (0, 0)$$

for  $t \rightarrow \infty$ .

*Proof.* We define the values

$$\Phi^{NL} := \limsup_{t \rightarrow \infty} \|\varphi(t, \cdot)\|_\infty \quad \text{and} \quad \Psi^{NL} := \limsup_{t \rightarrow \infty} \|\psi(t, \cdot)\|_\infty,$$

which are finite because of Proposition 4.4.6.

Using the integral representation (4.36) for  $\varphi$  yields

$$\Phi^{NL} \leq \limsup_{t \rightarrow \infty} e^{-\beta t} \|\varphi_0\|_\infty + \alpha \Psi^{NL} \limsup_{t \rightarrow \infty} \int_0^t e^{-\beta(t-s)} ds.$$

Together with equation (4.28) and Lemma 4.4.2, we deduce that the inequality

$$\Phi^{NL} \leq \frac{\alpha}{\beta} \Psi^{NL} \quad (4.46)$$

holds. From (4.37) we deduce in the same way

$$\Psi^{NL} \leq \limsup_{t \rightarrow \infty} e^{-Kt} \|\psi_0\|_\infty + \Phi^{NL} \limsup_{t \rightarrow \infty} \int_0^t e^{-K(t-s)} ds + R_0 (\Psi^{NL})^2 \limsup_{t \rightarrow \infty} \int_0^t e^{-K(t-s)} ds$$

and, thus,

$$\Psi^{NL} \leq \frac{1}{K} \Phi^{NL} + \frac{R_0}{K} (\Psi^{NL})^2. \quad (4.47)$$

Using the inequalities (4.46) and (4.47) leads to

$$0 \leq \left(\frac{\alpha}{\beta} - K\right) \Psi^{NL} + R_0 (\Psi^{NL})^2.$$

We obtain that either  $\Psi^{NL} = 0$  or it fulfils the inequality  $0 \leq \left(\frac{\alpha}{\beta} - K\right) + R_0 \Psi^{NL}$ , which leads to  $\Psi^{NL} \geq \frac{1}{R_0} \left(K - \frac{\alpha}{\beta}\right)$ .

We know from Theorem 4.4.7 that for initial perturbations fulfilling (4.38), we have that  $\Psi^{NL} = \lim_{t \rightarrow \infty} \Psi(t) \leq \frac{1}{2R_0} \left(K - \frac{\alpha}{\beta}\right)$ , which contradicts  $\Psi^{NL} \geq \frac{1}{R_0} \left(K - \frac{\alpha}{\beta}\right)$ . Therefore,  $\Psi^{NL} = 0$  holds.  $\square$

The stability condition seems to be difficult to check, because it requires the knowledge of the stationary solution. But, we can translate it into a condition for the jump. Therefore, we remind that the critical values of a kinetic function are the zeros of  $q'_H$  and  $q'_T$ .

**Definition:** Kinetic functions in the hysteresis case are called **admissible**, if its critical values are such that holds

$$u_T^{cr} < u_H^{cr}.$$

We call a jump  $\bar{u}$  **admissible**, when it is in the interval  $\bar{u} \in (u_T^{cr}, u_H^{cr})$ .

**Corollary 4.4.9.** *We consider the generic model in the hysteresis case with admissible kinetic functions. Let  $(U(x), V(x))$  be a stationary solution with jump  $\bar{u}$  which is admissible, then  $(U(x), V(x))$  is asymptotically stable.*

*Proof.* By definition of a stationary solution with jump  $\bar{u}$ , the function  $V(x)$  is given by  $h_H(U(x))$  for  $x \in [0, 1]$  fulfilling  $U(x) \leq \bar{u}$ . Therefore, for those  $x$  the requirement  $p'(V(x)) > \frac{\alpha}{\beta}$  is equivalent to

$$q'_H(U(x)) = \alpha \frac{1}{p'(h_H(U(x)))} - \beta = \alpha \left( \frac{1}{p'(h_H(U(x)))} - \frac{\beta}{\alpha} \right) < 0.$$

And  $q'_H(U(x)) < 0$  holds exactly when  $U(x) < u_H^{cr}$  using Lemma 2.1.9. Therefore,  $\bar{u} < u_H^{cr}$  is necessary for fulfilling the stability condition.

Similarly, for  $x \in [0, 1]$  fulfilling  $U(x) > \bar{u}$  it holds  $V(x) = h_T(U(x))$  and the stability condition requires

$$q'_T(U(x)) = \alpha \frac{1}{p'(h_T(U(x)))} - \beta = \alpha \left( \frac{1}{p'(h_T(U(x)))} - \frac{\beta}{\alpha} \right) < 0.$$

Lemma 2.1.9 shows that  $q'_T(U(x)) < 0$  if  $u_T^{cr} < U(x)$ , hence we deduce  $u_T^{cr} < \bar{u}$ . Thus, by definition of an admissible jump the stability condition is fulfilled.  $\square$

In the following examples, we perform simulations of the generic model in the hysteresis case for different choices of kinetic functions and different initial conditions. We perform simulations for discontinuous initial conditions of type

$$u_0(x) = \begin{cases} 0.3 & \text{for } x \leq \bar{x}, \\ 6 & \text{for } x > \bar{x} \end{cases} \quad \text{and} \quad v_0(x) = \begin{cases} 0.5 & \text{for } x \leq \bar{x}, \\ 8 & \text{for } x > \bar{x}, \end{cases} \quad (4.48)$$

for different  $\bar{x}$ . The point  $(0.3, 0.5)$  is attracted by  $S_0$  and  $(6, 8)$  is attracted by  $S_2$  (Compare the phaseplane for these kinetic functions in Figure 2.5a). Moreover, we perform simulations for continuous initial conditions of type

$$u_0(x) = \begin{cases} 0.3 & x \leq \tilde{x}_1, \\ 0.3 + 5.7 \sin\left(\frac{\pi(x-\tilde{x}_1)}{2(\tilde{x}_2-\tilde{x}_1)}\right) & \tilde{x}_1 < x \leq \tilde{x}_2, \\ 6 & x > \tilde{x}_2 \end{cases} \quad (4.49)$$

$$v_0(x) = \begin{cases} 0.5 & x \leq \tilde{x}_1, \\ 0.5 + 7.5 \sin\left(\frac{\pi(x-\tilde{x}_1)}{2(\tilde{x}_2-\tilde{x}_1)}\right) & \tilde{x}_1 < x \leq \tilde{x}_2, \\ 8 & x > \tilde{x}_2 \end{cases} \quad (4.50)$$

The diffusion coefficient is  $\frac{1}{\gamma} = \frac{1}{200}$  in all simulations.

**Example 4.4.10.** We consider the admissible kinetic functions  $f(u, v) = 1.4v - u$  and  $p(v) = v^3 - 6.3v^2 + 10v$ . The maximal interval for  $\bar{u}$  is given by  $(u_T, \min(u_H, u_2)) = (0.24365, 4.7124)$  and the critical values are  $u_T^{cr} = 0.38264$  and  $u_H^{cr} = 4.5734$ . We

perform simulations for initial conditions of type (4.48) which are indicated by the dotted lines in Figure 4.6. For all choices of  $\bar{x}$  tested ( $\bar{x} = 0.3$  in Figure 4.6a and 4.6b,  $\bar{x} = 0.6$  in Figure 4.6e and  $\bar{x} = 0.95$  in Figure 4.6f), we observe a fast formation of a stable stationary solution having a layer position exactly where it has been prescribed by the initial conditions.

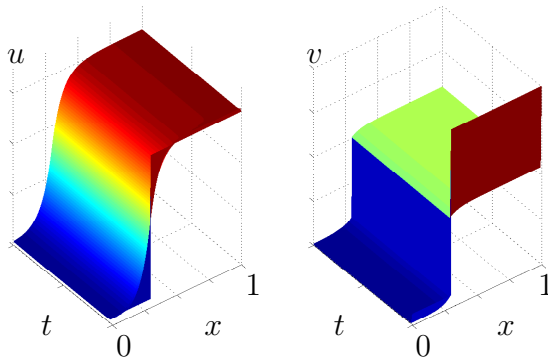
Moreover, we perform simulations for continuous initial conditions of type (4.49)-(4.50) for  $\tilde{x}_1 = 0.1, \tilde{x}_2 = 0.9$  (Figure 4.6c and 4.6d). We also obtained stable pattern for this kind of initial conditions. In the layer position of the approached stationary solution is approximately at  $\tilde{x} = 0.36$ . The value of the initial condition at this position is  $(u_0(\tilde{x}), v_0(\tilde{x})) \approx (1.9, 2.3)$ . This is a point lying on the stable manifold of the system (Compare the phaseplane in Figure 2.5a). We observe a similar behaviour for  $\tilde{x}_1 = 0.2, \tilde{x}_2 = 0.5$  in Figure 4.6g.

**Example 4.4.11.** We consider the admissible kinetic functions  $f(u, v) = 2.5v - u$  and  $p(v) = v^3 - 6v^2 + 10v$ . We calculate the interval  $(u_T, \min(u_H, u_2)) = (2.9113, 5.0887)$  and the critical values  $u_T^{cr} = 3.3876$  and  $u_H^{cr} = 4.6124$ . We obtain results that differ from those in example 4.4.10 for initial conditions of type (4.48). For  $\bar{x} = 0.4$  the simulation 4.7a shows a front moving to the left which is leading to the stationary solution  $S_2 = (10.56, 4.22)$  (see Figure 4.7b). But, for  $\bar{x} = 0.95$  we observe the formation of a stable stationary solution (Figure 4.7c and 4.7d).

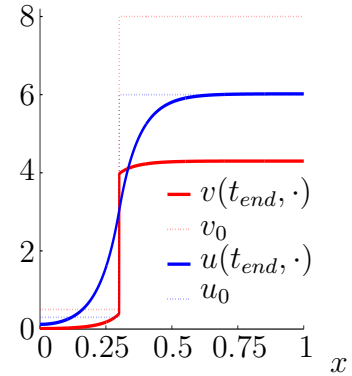
**Example 4.4.12.** We consider the admissible kinetic functions  $f(u, v) = 1.6v - u$  and  $p(v) = v^3 - 6v^2 + 10v$ . We calculate the interval  $(u_T, \min(u_H, u_2)) = (2.9113, 5.0887)$  and the critical values  $u_T^{cr} = 3.1236$  and  $u_H^{cr} = 4.8764$ . We obtain results that differ from those in example 4.4.10 for initial conditions of type (4.48). For  $\bar{x} = 0.8$  and  $\bar{x} = 0.4$  the simulation 4.7a shows a front moving to the right which is leading to the stationary solution  $S_0 = (0, 0)$  (see Figure 4.7b). But, for  $\bar{x} = 0.95$  we observe the formation of a stable stationary solution (Figure 4.7c and 4.7d).

**Example 4.4.13.** The kinetic functions  $f(u, v) = 2.53v - u$  and  $p(v) = v^3 - 5.8v^2 + 10v$  are not admissible, because  $u_T^{cr} = 4.9191 > 4.8421 = u_H^{cr}$ . However, for initial conditions of type (4.48) with  $\bar{x} = 0.2$  and  $\bar{x} = 0.4$ , we observe the formation of a stable stationary solution. For  $\bar{x} = 0.9$  the solution approaches the homogeneous solution  $S_0 = (0, 0)$  (Compare Figure 4.9).

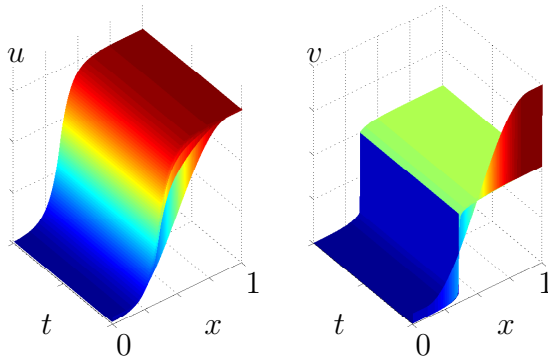
We deduce from the previous simulations that if a stable stationary solution is approached, its layer position is determined by the initial condition. For continuous initial conditions the layer position is at the value  $\bar{x}$  fulfilling  $(u_0(\bar{x}), v_0(\bar{x})) \in W^s$ . For discontinuous initial conditions the layer position is at the initial discontinuity providing that the values of the initial condition on both sides of the discontinuity are on different sides of the separatrix  $W^s$ .



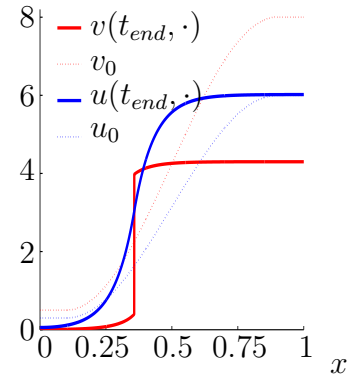
(a) The solution  $(u(t,x), v(t,x))$  for an initial condition of type (4.48) with  $\bar{x} = 0.3$  leads to a stable stationary solution.



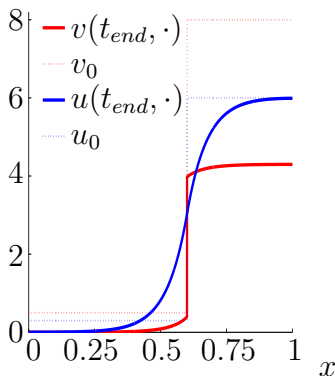
(b) The solution for the initial condition (4.48) with  $\bar{x} = 0.3$  evaluated at a sufficiently big time  $t_{end}$ .



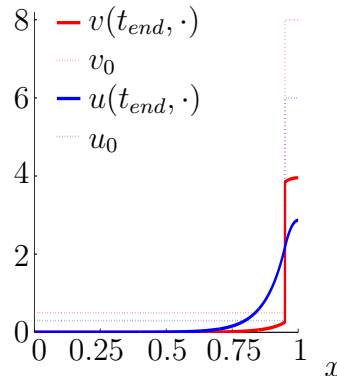
(c) The solution  $(u(t,x), v(t,x))$  for the continuous initial condition of type (4.49)-(4.50) with  $\bar{x}_1 = 0.1, \bar{x}_2 = 0.9$  leads to a stable stationary solution.



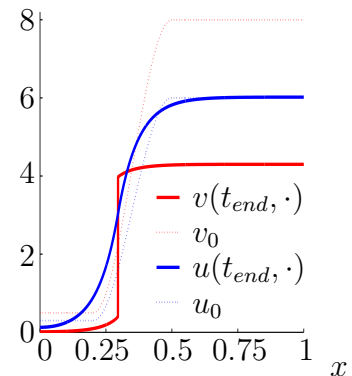
(d) The solution for the continuous initial condition of type (4.49)-(4.50) with  $\bar{x}_1 = 0.1, \bar{x}_2 = 0.9$  evaluated at a sufficiently big time  $t_{end}$ .



(e) The solution for the initial condition (4.48) with  $\bar{x} = 0.6$  evaluated at a sufficiently big time  $t_{end}$ .

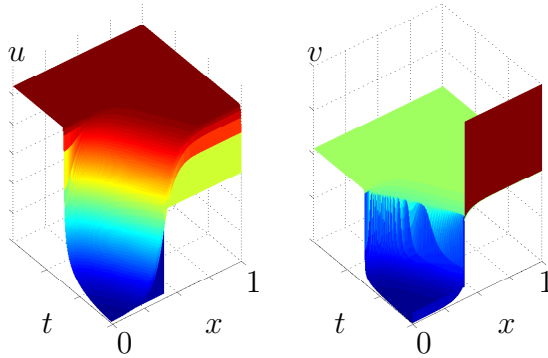


(f) The solution for the initial condition (4.48) with  $\bar{x} = 0.95$  evaluated at a sufficiently big time  $t_{end}$ .

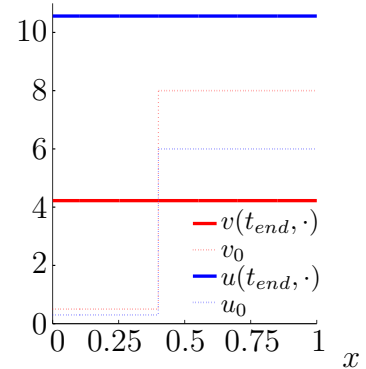


(g) The solution for the continuous initial condition of type (4.49)-(4.50) with  $\bar{x}_1 = 0.2, \bar{x}_2 = 0.5$  evaluated at a sufficiently big time  $t_{end}$ .

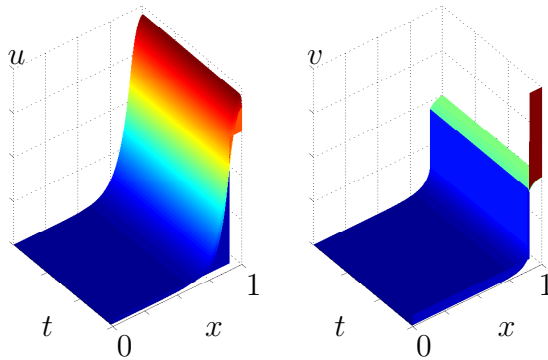
Figure 4.6: Simulations of the generic model in the hysteresis case for admissible kinetic functions  $f(u, v) = 1.4v - u$  and  $p(v) = v^3 - 6.3v^2 + 10v$  of example 4.4.10. All choices of initial conditions lead to the formation of a stable stationary solution. The layer position (where the red continuous line is perpendicular to the  $x$  axis) is determined by the initial conditions (dotted lines).



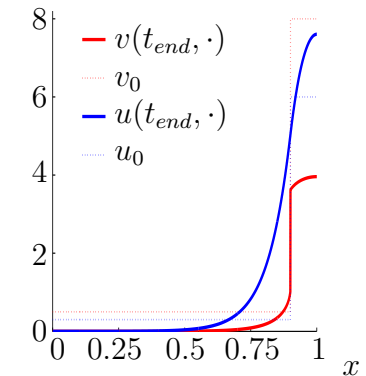
(a) The solution  $(u(t, x), v(t, x))$  for an initial condition of type (4.48) with  $\bar{x} = 0.4$  becomes constant after a certain time.



(b) The solution for the initial condition (4.48) with  $\bar{x} = 0.4$  evaluated at a sufficiently big time  $t_{end}$ .



(c) The solution  $(u(t, x), v(t, x))$  for an initial condition of type (4.48) with  $\bar{x} = 0.95$  leads to a stable stationary solution.

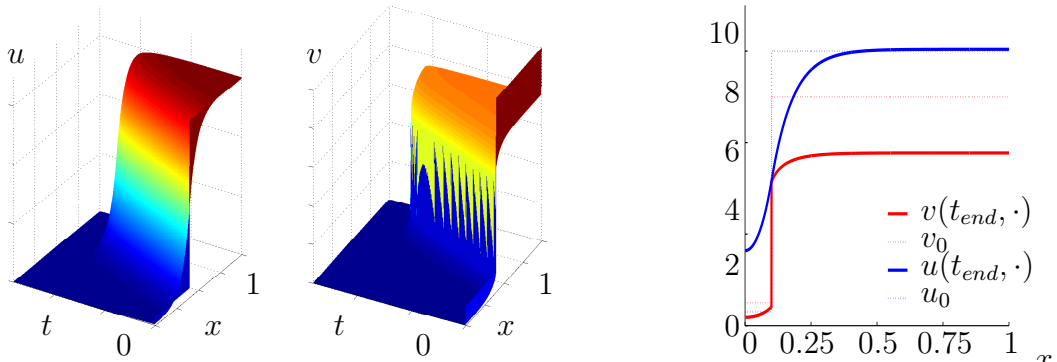


(d) The solution for the initial condition (4.48) with  $\bar{x} = 0.95$  evaluated at a sufficiently big time  $t_{end}$ .

Figure 4.7: Simulations of the generic model in the hysteresis case for admissible kinetic functions  $f(u, v) = 2.5v - u$  and  $p(v) = v^3 - 6v^2 + 10v$  of example 4.4.11.

Intuitively, one might expect that the formation of a stable stationary solution starting at an initial condition of type (4.48) is more probable for  $\bar{x}$  in the middle of the interval  $[0, 1]$ . But the simulations show that either, for a broad range of  $\bar{x}$ , we obtain a stable stationary solution or for  $\bar{x}$  lying close to one boundary.

The results of the simulations in the examples 4.4.11, 4.4.12 and 4.4.13 do not contradict Theorem 4.4.7 and Corollary 4.4.9. The initial condition is setting up the layer position  $\bar{x}$  of the stationary solution. But, we cannot say in advance, if there is a stationary solution with layer position  $\bar{x}$ . Moreover, if a stationary solution with



(a) The solution  $(u(t, x), v(t, x))$  for an initial condition of type (4.48) with  $\bar{x} = 0.4$  becomes constant after a certain time.

(b) The solution for the initial condition (4.48) with  $\bar{x} = 0.1$  evaluated at a sufficiently big time  $t_{end}$  leads to a stable stationary solution.

Figure 4.8: Simulations of the generic model in the hysteresis case for admissible kinetic functions  $f(u, v) = 1.6v - u$  and  $p(v) = v^3 - 6v^2 + 10v$  of example 4.4.12

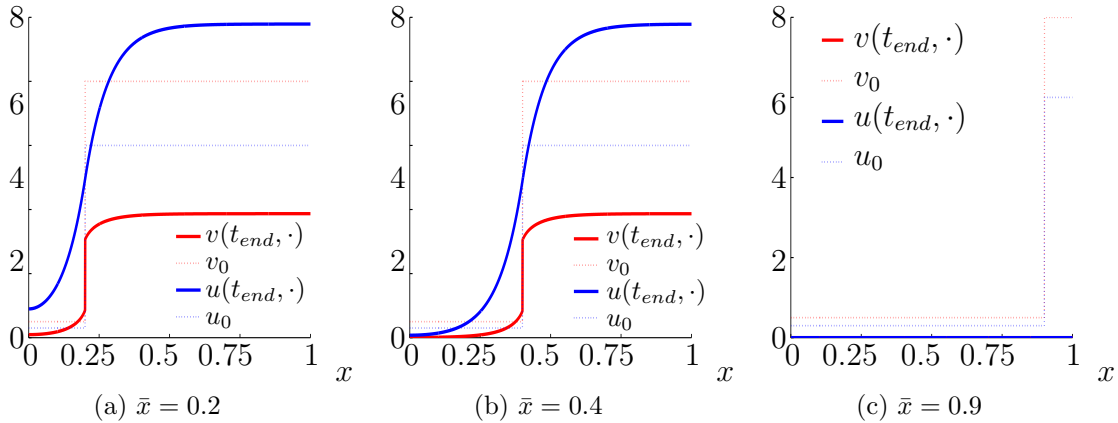


Figure 4.9: Simulations of the generic model in the hysteresis case for kinetic functions  $f(u, v) = 2.53v - u$  and  $p(v) = v^3 - 5.8v^2 + 10v$  of example 4.4.13 which are not admissible. The solution for the initial condition (4.48) with three different  $\bar{x}$  evaluated at a sufficient big time  $t_{end}$ .

layer position  $\bar{x}$  exists, we do not know if the corresponding jump  $\bar{u}$  is admissible. Furthermore, Corollary 4.4.9 is a sufficient condition for stability. We did not prove that it is a necessary condition. Apparently, there is another condition which is also important for stability which could be the explanation of Example 4.4.13.

## 4.5 Summary

We showed the existence of monotone increasing and monotone decreasing stationary solutions of the generic model in the hysteresis case. The steady state equation reduces to one differential equation of elliptic type with a discontinuous right hand side. The discontinuity is at the “jump”  $\bar{u}$ , which can be each value in the interval  $(u_T, \min(u_H, u_2))$ . For every jump and every diffusion coefficient there is a unique monotone increasing stationary solution. We proved this by analysing the range and the monotonicity of the time-maps associated to the stationary problem.

The stationary solutions in the hysteresis case differ from those in the bistable case. The  $u$ -component of the solution is continuously differentiable, whereas the  $v$ -component has a discontinuity at a value  $\bar{x}$ , which is called the layer position. Moreover, there is an infinite number of monotone increasing stationary solutions for every diffusion coefficient.

Furthermore, we introduced the notions of admissible kinetic functions and admissible jumps  $\bar{u} \in (u_T^{cr}, u_H^{cr})$ . We proved that a stationary solution with an admissible jump  $\bar{u}$  is asymptotically stable with respect to small perturbations in  $L^\infty(0, 1)$ . Simulations showed that the layer position of a stationary solution is set up by the initial condition. But, we observed significant differences between different admissible kinetic functions.

This is leading to the question how the layer position depends on the jump and which values  $\bar{x} \in [0, 1]$  are layer positions for stable stationary solutions depending on the choice of kinetic functions.



# Chapter 5

## Properties of stationary solutions

In the previous chapter, we showed for admissible jumps the stability of monotone solutions of the generic model in the hysteresis case. Simulations gave rise to the question for which choice of layer positions  $\bar{x}$ , we obtain a stationary solution with admissible jump  $\bar{u}$ .

Therefore, we consider in this chapter the potential, time-maps and the layer position  $\bar{x}$  as functions of the jump  $\bar{u}$ . We show that for admissible kinetic functions there is an interval of layer positions leading to a unique monotone increasing stationary solution which is stable. We identify a condition for the kinetic functions leading to a big interval of admissible layer positions. Moreover, we analyse the layer position for decreasing diffusion coefficient  $\frac{1}{\gamma}$ . We prove that for one certain choice of the jump, we obtain an interior transition layer, otherwise there is a boundary transition layer.

Finally, we use monotone solutions to construct more complicated stationary solutions. We introduce a definition of an irregular solution and we investigate their existence, uniqueness and stability.

### 5.1 Dependence of the jump

We aim to analyse the layer position  $\bar{x}$  as a function of the jump  $\bar{u}$ . To do so, we also have to consider all other values and functions involved in the stationary problem as depending on  $\bar{u}$ .

**Notation:** We denote the potential by

$$Q(\bar{u}, u) = \begin{cases} F(h_H(u)) & \text{for } u \leq \bar{u}, \\ F(h_H(\bar{u})) - F(h_T(\bar{u})) + F(h_T(u)) & \text{for } u > \bar{u}. \end{cases}$$

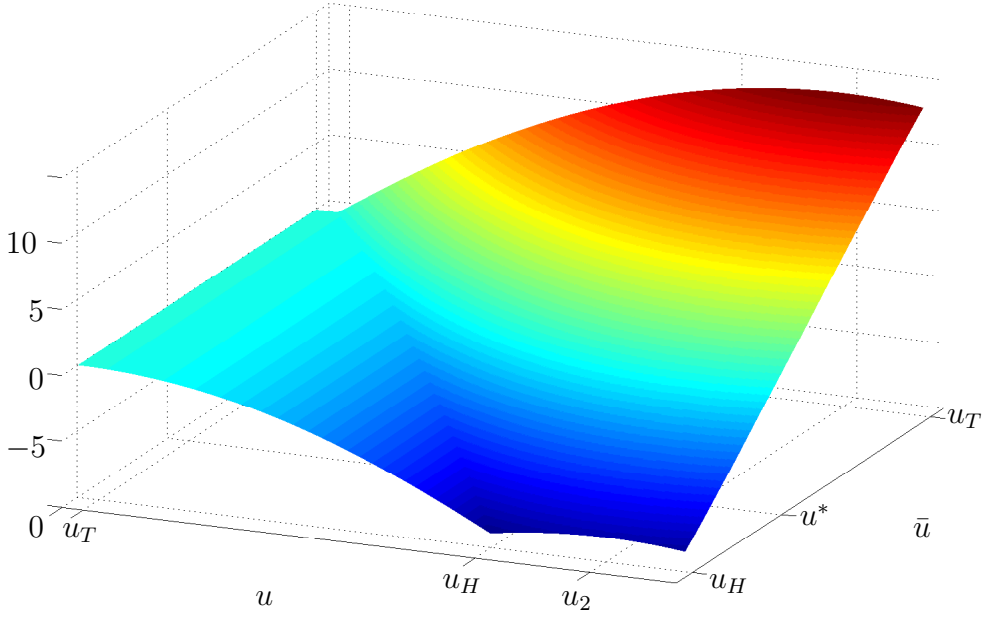


Figure 5.1: The potential  $Q(\bar{u}, u)$  for the kinetic functions  $p(v) = v^3 - 6.3v^2 + 10v$  and  $f(u, v) = 1.4v - u$ . It is continuous for all  $(\bar{u}, u)$ , but not differentiable at the line  $\bar{u} = u$ . Moreover, the local maximum  $Q(\bar{u}, u_2)$  is decaying for increasing  $\bar{u}$ .

**Proposition 5.1.1.** *The potential  $Q(\bar{u}, u)$  is continuous as function of  $\bar{u}$ . It is continuously differentiable with respect to  $\bar{u}$  for all  $\bar{u}$ , except at  $\bar{u} = u$ . The derivative of the potential with respect to  $\bar{u}$  has the following form*

$$\frac{\partial}{\partial \bar{u}} Q(\bar{u}, u) = \begin{cases} 0 & \text{for } u \leq \bar{u}, \\ q_H(\bar{u}) - q_T(\bar{u}) & \text{for } u > \bar{u}. \end{cases}$$

In particular, it holds

$$\frac{\partial}{\partial \bar{u}} Q(\bar{u}, u_2) = q_H(\bar{u}) - q_T(\bar{u}) < 0.$$

*Proof.* The potential  $Q(\bar{u}, u)$  is by definition continuous in  $\bar{u}$  for  $\bar{u} \neq u$ . But, for  $\bar{u} = u$  the term  $-F(h_T(\bar{u})) + F(h_T(u))$  cancels out and the limit is the same from both sides.

To calculate the derivative with respect to  $\bar{u}$  we observe that for  $u \leq \bar{u}$  then,  $Q(\bar{u}, u)$  is not depending on  $\bar{u}$ , hence the derivative is zero. For  $u > \bar{u}$  we calculate

$$\frac{\partial}{\partial \bar{u}} F(h_H(\bar{u})) = f(p(h_H(\bar{u}), h_H(\bar{u}))p'(h_H(\bar{u})) \cdot h'_H(\bar{u}) = f(\bar{u}, h_H(\bar{u})) = q_T(\bar{u})$$

and similarly  $\frac{\partial}{\partial \bar{u}} F(h_T(\bar{u})) = q_T(\bar{u})$  using the chain rule. This leads to  $\frac{\partial}{\partial \bar{u}} Q(\bar{u}, u) = q_H(\bar{u}) - q_T(\bar{u})$  for  $u > \bar{u}$ . Reminding that  $q_H(\bar{u}) < 0$  for  $\bar{u} \in (0, u_H)$  and  $q_T(\bar{u}) > 0$  for  $\bar{u} \in (u_T, u_2)$  (see Lemma 2.1.10), we obtain  $q_H(\bar{u}) - q_T(\bar{u}) < 0$ . Thus,  $\frac{\partial}{\partial \bar{u}} Q(\bar{u}, u)$  is not continuous for  $\bar{u} = u$ .  $\square$

**Definition:** In accordance with Lemma 4.2.1, we define the function  $u_{\min}(\bar{u})$  by setting  $u_{\min}(\bar{u}) = 0$  if  $Q(\bar{u}, u_2) \geq 0$ . In the case  $Q(\bar{u}, u_2) < 0$ , we define it implicitly by

$$Q(\bar{u}, u_{\min}(\bar{u})) = Q(\bar{u}, u_2), \quad (5.1)$$

where we choose the unique solution  $u_{\min}(\bar{u})$  in the interval  $(0, \bar{u})$ .

The function  $u_{\max}(\bar{u})$  is defined by  $u_{\max}(\bar{u}) = u_2$  if  $Q(\bar{u}, u_2) \leq 0$ . In the case  $Q(\bar{u}, u_2) > 0$ , we define it implicitly by

$$0 = Q(\bar{u}, 0) = Q(\bar{u}, u_{\max}(\bar{u})), \quad (5.2)$$

where we choose the unique solution  $u_{\max}(\bar{u})$  in the interval  $(\bar{u}, u_2)$ .

The value of the jump for which the sign of  $Q(\bar{u}, u_2)$  is changing, will play a pivotal role in the remainder of this thesis.

**Definition:** If there is a jump  $\bar{u} \in (u_T, \min(u_H, u_2))$  such that  $Q(\bar{u}, u_2) = 0$  holds, we denote this value  $u^*$ .

**Lemma 5.1.2.** *The potential at the  $u$ -coordinate of  $S_2$  is positive, if  $\bar{u} < u^*$  and negative if  $\bar{u} > u^*$ .*

*Proof.* This follows immediately from the negativity of the derivative  $\frac{\partial}{\partial \bar{u}} Q(\bar{u}, u_2) = q_H(\bar{u}) - q_T(\bar{u})$ .  $\square$

**Proposition 5.1.3.** *The functions  $u_{\min}(\bar{u})$  and  $u_{\max}(\bar{u})$  are continuous for all  $\bar{u}$  and continuously differentiable for all  $\bar{u}$  except at  $\bar{u} = u^*$ . The derivatives are given by*

$$\frac{d}{d\bar{u}} u_{\min}(\bar{u}) = \begin{cases} 0 & \text{for } \bar{u} \leq u^* \\ \frac{q_H(\bar{u}) - q_T(\bar{u})}{q_H(u_{\min}(\bar{u}))} > 0 & \text{for } \bar{u} > u^* \end{cases}$$

and

$$\frac{d}{d\bar{u}} u_{\max}(\bar{u}) = \begin{cases} \frac{q_T(\bar{u}) - q_H(\bar{u})}{q_T(u_{\max}(\bar{u}))} > 0 & \text{for } \bar{u} < u^* \\ 0 & \text{for } \bar{u} \geq u^*. \end{cases}$$

*Proof.* The functions  $u_{\min}(\bar{u})$  and  $u_{\max}(\bar{u})$  are continuous for  $\bar{u} \neq u^*$  because of the continuity of  $Q(\bar{u}, u)$  and the implicit function theorem.

For  $\bar{u} = u^*$ , we observe that  $Q(u^*, u_2) = 0$  yields  $u_{\min}(u^*) = 0$  and  $u_{\max}(u^*) = u_2$ . Thus, the limits from right and left agree for both functions.

For  $\bar{u} \leq u^*$  the function  $u_{\min}(\bar{u})$  is constant, thus it holds  $\frac{d}{d\bar{u}}u_{\min}(\bar{u}) = 0$ . To obtain the derivatives of  $u_{\min}(\bar{u})$  for  $\bar{u} > u^*$  we differentiate equation (5.1) with respect to  $\bar{u}$  which yields

$$\frac{d}{d\bar{u}}Q(\bar{u}, u_{\min}(\bar{u})) = \frac{d}{d\bar{u}}Q(\bar{u}, u_2). \quad (5.3)$$

$u_2$  does not depend on  $\bar{u}$  and therefore

$$\frac{d}{d\bar{u}}Q(\bar{u}, u_2) = \frac{\partial}{\partial \bar{u}}Q(\bar{u}, u_2) = q_H(\bar{u}) - q_T(\bar{u}) \quad (5.4)$$

holds. Moreover,

$$\begin{aligned} \frac{d}{d\bar{u}}Q(\bar{u}, u_{\min}(\bar{u})) &= \frac{\partial}{\partial \bar{u}}Q(\bar{u}, u_{\min}(\bar{u})) + \frac{d}{d\bar{u}}u_{\min}(\bar{u}) \cdot \frac{\partial}{\partial u}Q(\bar{u}, u_{\min}(\bar{u})) \\ &= 0 + \frac{d}{d\bar{u}}u_{\min}(\bar{u}) \cdot q_H(u_{\min}(\bar{u})), \end{aligned} \quad (5.5)$$

which yields the result by inserting (5.4) and (5.5) in equation (5.3) which is solved with respect to  $\frac{d}{d\bar{u}}u_{\min}(\bar{u})$ .

Similarly, for  $\bar{u} < u^*$ , we obtain by derivating equation (5.2)

$$\begin{aligned} 0 &= \frac{d}{d\bar{u}}Q(\bar{u}, u_{\max}(\bar{u})) = \frac{\partial}{\partial \bar{u}}Q(\bar{u}, u_{\max}(\bar{u})) + \frac{d}{d\bar{u}}u_{\max}(\bar{u}) \cdot \frac{\partial}{\partial u}Q(\bar{u}, u_{\max}(\bar{u})), \\ &= q_H(\bar{u}) - q_T(\bar{u}) + \frac{d}{d\bar{u}}u_{\max}(\bar{u}) \cdot q_T(u_{\max}(\bar{u})), \end{aligned}$$

which is then solved with respect to  $\frac{d}{d\bar{u}}u_{\max}(\bar{u})$ . For  $\bar{u} \geq u^*$  the function  $u_{\max}(\bar{u})$  is constant, thus  $\frac{d}{d\bar{u}}u_{\max}(\bar{u}) = 0$ .  $\square$

**Notation:** In the following we denote by  $u_0 \in (0, \bar{u})$ , respectively  $u_e \in (\bar{u}, u_2)$ , the values which are connected by a monotone increasing solution of

$$\frac{1}{\gamma}U_{xx} + q_{\bar{u}}(U) = 0 \quad (5.6)$$

with the homogenous Neumann boundary condition, on the interval  $[0, L]$  for some  $L > 0$ , which is determined by

$$L = T(\bar{u}, u_0).$$

Here, the time-map  $T$  is defined as sum

$$T(\bar{u}, u_0) = T_1(\bar{u}, u_0) + T_2(\bar{u}, u_e(\bar{u}, u_0)),$$

with

$$T_1(\bar{u}, u_0) = \frac{1}{\sqrt{2\gamma}} \int_{u_0}^{\bar{u}} \frac{du}{\sqrt{F(h_H(u_0)) - F(h_H(u))}},$$

and

$$T_2(\bar{u}, u_e) = \frac{1}{\sqrt{2\gamma}} \int_{\bar{u}}^{u_e} \frac{du}{\sqrt{F(h_T(u_e)) - F(h_T(u))}}.$$

The function  $u_e(\bar{u}, u_0)$  is implicitly given by

$$Q(\bar{u}, u_e(\bar{u}, u_0)) = Q(\bar{u}, u_0) \quad (5.7)$$

and leads to the value  $U(L) = u_e(\bar{u}, u_0)$  for a solution starting at  $U(0) = u_0$ . Moreover, we denote by  $u_0(\bar{u})$  the function which is implicitly determined by

$$T(\bar{u}, u_0(\bar{u})) = 1. \quad (5.8)$$

Finally, we set

$$u_e(\bar{u}) = u_e(\bar{u}, u_0(\bar{u})).$$

These two functions are the start and the end values for a monotone increasing solution of (5.6) on the interval  $[0, 1]$ .

**Proposition 5.1.4.** *The functions  $u_e(\bar{u}, u_0)$ ,  $T_1(\bar{u}, u_0)$ ,  $T_2(\bar{u}, u_e)$ ,  $T(\bar{u}, u_0)$ ,  $u_0(\bar{u})$  and  $u_e(\bar{u})$  are continuously differentiable as functions of  $\bar{u}$ .*

*The derivatives of these functions with respect to  $\bar{u}$  have the following form and sign.*

1.  $\frac{\partial}{\partial \bar{u}} u_e(\bar{u}, u_0) = \frac{q_T(\bar{u}) - q_H(\bar{u})}{q_T(u_e(\bar{u}, u_0))} > 0.$
2.  $\frac{\partial}{\partial \bar{u}} T_1(\bar{u}, u_0) = \frac{1}{\sqrt{2\gamma}} \frac{1}{\sqrt{F(h_H(u_0)) - F(h_H(\bar{u}))}} > 0.$
3.  $\frac{\partial}{\partial \bar{u}} T_2(\bar{u}, u_e) = \frac{1}{\sqrt{2\gamma}} \frac{-1}{\sqrt{F(h_T(u_e)) - F(h_T(\bar{u}))}} < 0.$
4.  $\frac{\partial}{\partial \bar{u}} T(\bar{u}, u_0) = \frac{q_T(\bar{u}) - q_H(\bar{u})}{q_T(u_e(\bar{u}, u_0))} \frac{\partial}{\partial u_e} T_2(\bar{u}, u_e(\bar{u}, u_0)) > 0.$
5.  $\frac{d}{d\bar{u}} u_0(\bar{u}) = \frac{q_H(\bar{u}) - q_T(\bar{u})}{q_T(u_e(\bar{u}))} \frac{\frac{\partial}{\partial u_e} T_2(\bar{u}, u_e(\bar{u}))}{\frac{\partial}{\partial u_0} T(\bar{u}, u_0(\bar{u}))} > 0.$
6.  $\frac{d}{d\bar{u}} u_e(\bar{u}) = \frac{q_T(\bar{u}) - q_H(\bar{u})}{q_T(u_e(\bar{u}))} \frac{\frac{\partial}{\partial u_0} T_1(\bar{u}, u_0(\bar{u}))}{\frac{\partial}{\partial u_0} T(\bar{u}, u_0(\bar{u}))} > 0.$

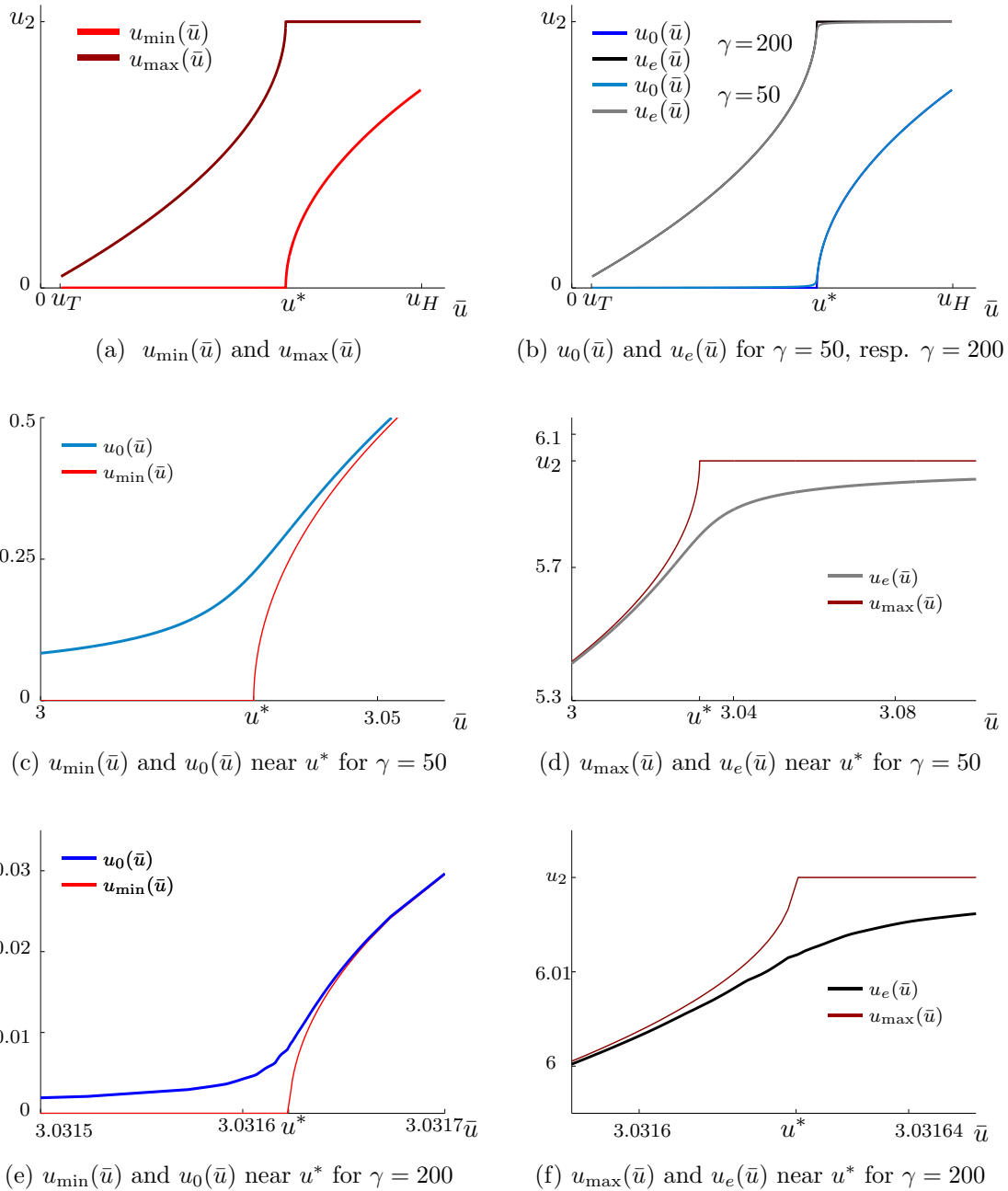


Figure 5.2: Plots of  $u_0(\bar{u})$  and  $u_e(\bar{u})$  as function of the jump  $\bar{u}$  for the kinetic functions  $p(v) = v^3 - 6.3v^2 + 10v$  and  $f(u, v) = 1.4v - u$ . The function  $u_0(\bar{u})$  is close to  $u_{\min}(\bar{u})$ , except in a neighborhood of  $u^*$ . This follows from the fact that  $u_0(\bar{u})$  is smooth at  $\bar{u} = u^*$ , whereas  $u_{\min}(\bar{u})$  is not. For increasing  $\gamma$  we see that  $u_0(\bar{u})$  is approaching  $u_{\min}(\bar{u})$ . The same holds for  $u_e(\bar{u})$  and  $u_{\max}(\bar{u})$ .

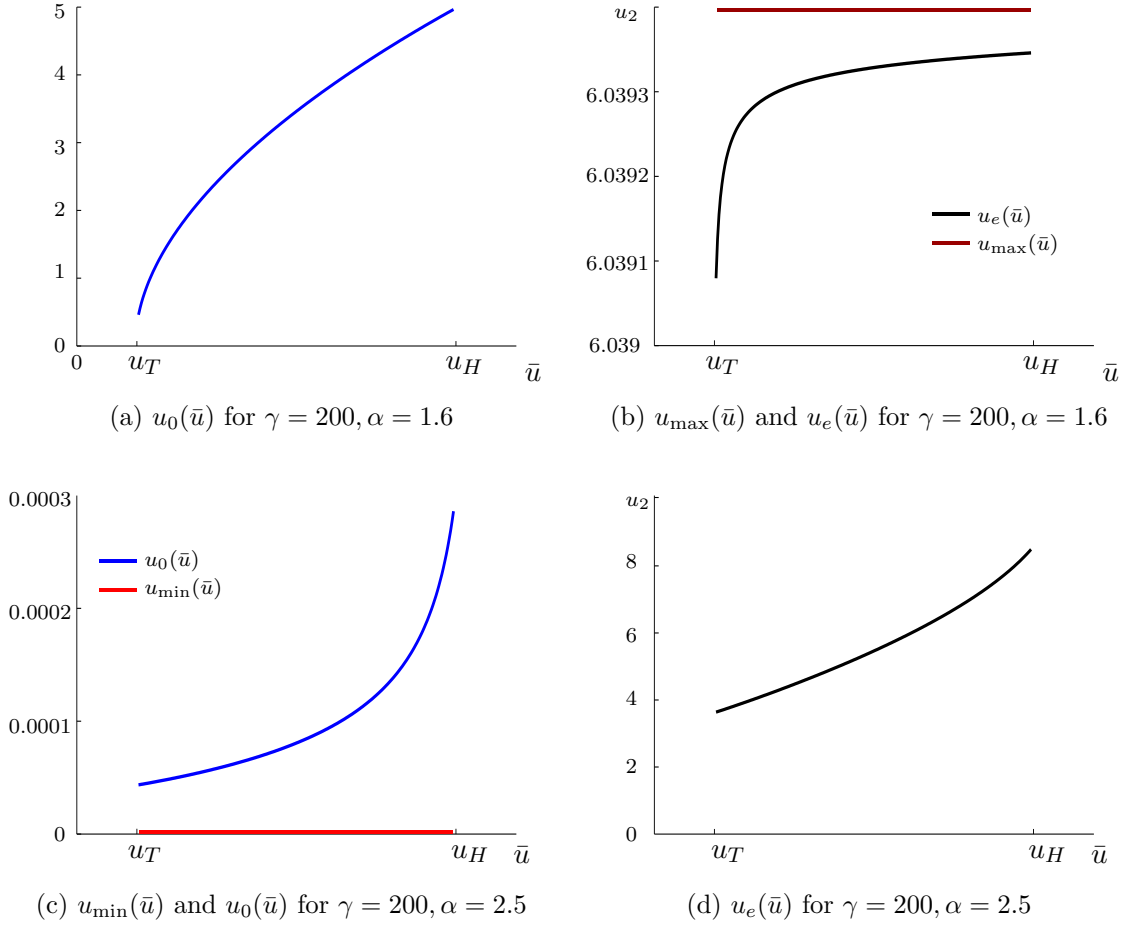


Figure 5.3: Plots of  $u_0(\bar{u})$  and  $u_e(\bar{u})$  as function of the jump  $\bar{u}$  for  $p(v) = v^3 - 6v^2 + 10v$  and  $f(u, v) = \alpha v - u$ , with two different  $\alpha$  such that there is no  $u^*$  with  $Q(u^*, u_2) = 0$ . For  $\alpha = 1.6$  the potential  $Q(\bar{u}, u_2)$  is negative for all  $\bar{u}$ . Thus,  $u_e$  is always close to  $u_2$  and varies only in the order of  $10^{-4}$ , whereas  $u_0$  varies between 0 and 5. We omit the plot of  $u_{\min}(\bar{u})$ , because there is no visible difference between  $u_0$  and  $u_{\min}$  on the scale used. For  $\alpha = 2.5$  the potential  $Q(\bar{u}, u_2)$  is positive for all  $\bar{u}$ . Thus,  $u_0$  is always close to 0 and varies only in the order of  $10^{-4}$ , whereas  $u_e$  varies from 4 to 10. We omit the plot of  $u_{\max}(\bar{u})$ , because there is no visible difference between  $u_e$  and  $u_{\max}$  on the scale used.

*Proof.* We observe that  $u_0, u_e \neq \bar{u}$  and, therefore,  $Q(\bar{u}, u_0)$ , respectively  $Q(\bar{u}, u_e)$  are differentiable, which yields differentiability and continuity of all functions.

The sign of the derivatives can be seen, reminding that  $q_H(u) < 0$  for  $u \in (0, u_H)$ ,  $q_T(u) > 0$  for  $u \in (u_T, u_2)$  (Lemma 2.1.10) and using Theorem 4.3.10 for the sign of the derivatives of the time-maps.

To calculate the derivatives, we use the implicit function theorem.

1. We consider  $u_0 < \bar{u}$  as fixed and observe that under this assumption

$$\frac{d}{d\bar{u}}Q(\bar{u}, u_0) = \frac{\partial}{\partial\bar{u}}Q(\bar{u}, u_0) = 0 \quad (5.9)$$

holds. When  $u_0 < \bar{u}$ , then  $u_e > \bar{u}$  and we calculate the derivative

$$\begin{aligned} \frac{d}{d\bar{u}}Q(\bar{u}, u_e(\bar{u}, u_0)) &= \frac{\partial}{\partial\bar{u}}Q(\bar{u}, u_e(\bar{u}, u_0)) + \frac{\partial}{\partial\bar{u}}u_e(\bar{u}, u_0) \cdot \frac{\partial}{\partial u_e}Q(\bar{u}, u_e(\bar{u}, u_0)) \\ &= q_H(\bar{u}) - q_T(\bar{u}) + \frac{\partial}{\partial\bar{u}}u_e(\bar{u}, u_0) \cdot q_T(u_e(\bar{u}, u_0)). \end{aligned} \quad (5.10)$$

The relation (5.7) yields

$$\frac{d}{d\bar{u}}Q(\bar{u}, u_0) = \frac{d}{d\bar{u}}Q(\bar{u}, u_e(\bar{u}, u_0)),$$

which leads to the result by inserting (5.9) and (5.10) and then solving this equation with respect to  $\frac{\partial}{\partial\bar{u}}u_e(\bar{u}, u_0)$ .

2. As  $\bar{u}$  appears only as integration limit of  $T_1(\bar{u}, u_0)$  this follows from derivating the integral.
3. We write at first  $T_2(\bar{u}, u_e) = -\frac{1}{\sqrt{2\gamma}} \int_{u_e}^{\bar{u}} \frac{du}{\sqrt{F(h_T(u_e)) - F(h_T(u))}}$  the rest follows from derivating the integral.
4. We consider  $u_0$  as fixed and calculate

$$\begin{aligned} \frac{\partial}{\partial\bar{u}}T(\bar{u}, u_0) &= \frac{\partial}{\partial\bar{u}}T_1(\bar{u}, u_0) + \frac{\partial}{\partial\bar{u}}T_2(\bar{u}, u_e(\bar{u}, u_0)) \\ &\quad + \frac{\partial}{\partial\bar{u}}u_e(\bar{u}, u_0) \cdot \frac{\partial}{\partial u_e}T_2(\bar{u}, u_e(\bar{u}, u_0)) \\ &= 0 + \frac{q_T(\bar{u}) - q_H(\bar{u})}{q_T(u_e(\bar{u}, u_0))} \cdot \frac{\partial}{\partial u_e}T_2(\bar{u}, u_e(\bar{u}, u_0)), \end{aligned}$$

where we have used that

$$\begin{aligned} &\frac{\partial}{\partial\bar{u}}T_1(\bar{u}, u_0) + \frac{\partial}{\partial\bar{u}}T_2(\bar{u}, u_e(\bar{u}, u_0)) \\ &= \frac{1}{\sqrt{2\gamma}} \frac{1}{\sqrt{F(h_H(u_0)) - F(h_H(\bar{u}))}} + \frac{1}{\sqrt{2\gamma}} \frac{-1}{\sqrt{F(h_T(u_e)) - F(h_T(\bar{u}))}} \\ &= \frac{1}{\sqrt{2\gamma}} \frac{1}{\sqrt{Q(\bar{u}, u_0) - Q(\bar{u}, \bar{u})}} - \frac{1}{\sqrt{2\gamma}} \frac{1}{\sqrt{Q(\bar{u}, u_e(\bar{u}, u_0)) - Q(\bar{u}, \bar{u})}} = 0 \end{aligned}$$

holds, because of (5.10).

5. We differentiate formula (5.8), which implicitly determines  $u_0(\bar{u})$ , with respect to  $\bar{u}$  and obtain

$$\frac{\partial}{\partial \bar{u}} T(\bar{u}, u_0(\bar{u})) + \frac{d}{d\bar{u}} u_0(\bar{u}) \frac{\partial}{\partial u_0} T(\bar{u}, u_0(\bar{u})) = 0.$$

This can be solved with respect to  $\frac{d}{d\bar{u}} u_0(\bar{u})$  and leads together with point 4. of this Proposition to

$$\frac{d}{d\bar{u}} u_0(\bar{u}) = -\frac{\frac{\partial}{\partial \bar{u}} T(\bar{u}, u_0(\bar{u}))}{\frac{\partial}{\partial u_0} T(\bar{u}, u_0(\bar{u}))} = \frac{q_H(\bar{u}) - q_T(\bar{u}) \frac{\partial}{\partial u_e} T_2(\bar{u}, u_e(\bar{u}))}{q_T(u_e(\bar{u})) \frac{\partial}{\partial u_0} T(\bar{u}, u_0(\bar{u}))}.$$

6. By definition, we have  $u_e(\bar{u}) = u_e(\bar{u}, u_0(\bar{u}))$ , which allows to use the chain rule to obtain

$$\begin{aligned} \frac{d}{d\bar{u}} u_e(\bar{u}, u_0(\bar{u})) &= \frac{\partial}{\partial \bar{u}} u_e(\bar{u}, u_0(\bar{u})) + \frac{d}{d\bar{u}} u_0(\bar{u}) \frac{\partial}{\partial u_0} u_e(\bar{u}, u_0(\bar{u})) \\ &= \frac{q_T(\bar{u}) - q_H(\bar{u})}{q_T(u_e(\bar{u}))} + \frac{q_H(\bar{u}) - q_T(\bar{u}) \frac{\partial}{\partial u_e} T_2(\bar{u}, u_e(\bar{u}))}{q_T(u_e(\bar{u})) \frac{\partial}{\partial u_0} T(\bar{u}, u_0(\bar{u}))} \frac{q_H(u_0(\bar{u}))}{q_T(u_e(\bar{u}))} \\ &= \frac{q_T(\bar{u}) - q_H(\bar{u})}{q_T(u_e(\bar{u}))^2 \frac{\partial}{\partial u_0} T(\bar{u}, u_0(\bar{u}))} \\ &\quad \cdot \left( q_T(u_e(\bar{u})) \frac{\partial}{\partial u_0} T(\bar{u}, u_0(\bar{u})) - q_H(u_0(\bar{u})) \frac{\partial}{\partial u_e} T_2(\bar{u}, u_e(\bar{u})) \right) \\ &= \frac{q_T(\bar{u}) - q_H(\bar{u})}{q_T(u_e(\bar{u}))^2 \frac{\partial}{\partial u_0} T(\bar{u}, u_0(\bar{u}))} \cdot \left( q_T(u_e(\bar{u})) \frac{\partial}{\partial u_0} T_1(\bar{u}, u_0(\bar{u})) \right) \\ &= \frac{q_T(\bar{u}) - q_H(\bar{u}) \frac{\partial}{\partial u_0} T_1(\bar{u}, u_0(\bar{u}))}{q_T(u_e(\bar{u})) \frac{\partial}{\partial u_0} T(\bar{u}, u_0(\bar{u}))}. \end{aligned}$$

We used here for the last step equation (4.17) and (4.18) to obtain

$$\begin{aligned} & q_T(u_e(\bar{u})) \frac{\partial}{\partial u_0} T(\bar{u}, u_0(\bar{u})) - q_H(u_0(\bar{u})) \frac{\partial}{\partial u_e} T_2(\bar{u}, u_e(\bar{u})) \\ &= q_T(u_e(\bar{u})) \left( \frac{\partial}{\partial u_0} T_1(\bar{u}, u_0(\bar{u})) + \frac{q_H(u_0(\bar{u}))}{q_T(u_e(\bar{u}))} \frac{\partial}{\partial u_e} T_2(\bar{u}, u_e(\bar{u})) \right) \\ &\quad - q_H(u_0(\bar{u})) \frac{\partial}{\partial u_e} T_2(\bar{u}, u_e(\bar{u})) \\ &= q_T(u_e(\bar{u})) \frac{\partial}{\partial u_0} T_1(\bar{u}, u_0(\bar{u})). \end{aligned}$$

□

**Remark 5.1.5.** In Figure 5.2 we remark a rectangular bend in the graph of  $u_{\min}(\bar{u})$ , resp.  $u_{\max}(\bar{u})$  at the value  $\bar{u} = u^*$ . We calculate

$$\lim_{\bar{u} \downarrow u^*} \frac{d}{d\bar{u}} u_{\min}(\bar{u}) = \frac{q_H(u^*) - q_T(u^*)}{\lim_{\bar{u} \rightarrow u^*} q_H(u_{\min}(\bar{u}))} = \frac{q_H(u^*) - q_T(u^*)}{q_H(0)} = \frac{q_H(u^*) - q_T(u^*)}{0} = \infty,$$

whereas

$$\lim_{\bar{u} \uparrow u^*} \frac{d}{d\bar{u}} u_{\min}(\bar{u}) = 0.$$

Thus, the graph of  $u_{\min}(\bar{u})$  is perpendicular at  $\bar{u} = u^*$ . Although  $u_0(\bar{u})$  approaches  $u_{\min}(\bar{u})$  for increasing  $\gamma$  it is continuously differentiable at  $\bar{u} = u^*$ . But, we see in Figure 5.2 that the slope  $\frac{d}{d\bar{u}} u_0(\bar{u})$  is changing strongly near  $u^*$ . An effect which is getting stronger for increasing  $\gamma$ .

The same is true for  $u_e(\bar{u})$  and  $u_{\max}(\bar{u})$ , because of

$$\lim_{\bar{u} \uparrow u^*} \frac{d}{d\bar{u}} u_{\max}(\bar{u}) = \frac{q_T(u^*) - q_H(u^*)}{\lim_{\bar{u} \rightarrow u^*} q_T(u_{\max}(\bar{u}))} = \frac{q_T(u^*) - q_H(u^*)}{q_T(u_2)} = \frac{q_H(u^*) - q_H(u^*)}{0} = \infty$$

and

$$\lim_{\bar{u} \downarrow u^*} \frac{d}{d\bar{u}} u_{\max}(\bar{u}) = 0.$$

## 5.2 The layer position depending on the jump

In this section, we investigate the layer position  $\bar{x}$  as function of  $\bar{u}$ . For admissible jumps, we prove the monotonicity of this function. This allows the definition of the admissible interval of layer positions, leading to a unique monotone increasing stationary solution which is stable.

**Definition:** The layer position  $\bar{x}(\bar{u})$  of a monotone increasing solution of (4.5) is given by

$$\bar{x}(\bar{u}) = T_1(\bar{u}, u_0(\bar{u})).$$

**Proposition 5.2.1.** The layer position  $\bar{x}(\bar{u})$  is continuous and its first derivative with respect to  $\bar{u}$  is given by

$$\begin{aligned} \frac{d}{d\bar{u}} \bar{x}(\bar{u}) &= \frac{1}{\sqrt{2\gamma}} \frac{1}{\sqrt{Q(\bar{u}, u_0(\bar{u})) - Q(\bar{u}, \bar{u})}} \\ &\quad + \frac{(q_H(\bar{u}) - q_T(\bar{u})) \frac{\partial}{\partial u_e} T_2(\bar{u}, u_e(\bar{u})) \frac{\partial}{\partial u_0} T_1(\bar{u}, u_0(\bar{u}))}{q_T(u_e(\bar{u})) \frac{\partial}{\partial u_0} T_1(\bar{u}, u_0(\bar{u})) + q_H(u_0(\bar{u})) \frac{\partial}{\partial u_e} T_2(\bar{u}, u_e(\bar{u}))}. \end{aligned}$$

This is a negative function for all  $\bar{u}$  fulfilling the conditions

$$q_H(u_0(\bar{u})) > q_H(\bar{u}) \tag{5.11}$$

and

$$q_T(u_e(\bar{u})) < q_T(\bar{u}). \quad (5.12)$$

*Proof.* The function  $\bar{x}(\bar{u})$  is continuous as composition of continuous functions. Derivating  $T_1(\bar{u}, u_0(\bar{u}))$  yields

$$\begin{aligned} \frac{d}{d\bar{u}}\bar{x}(\bar{u}) &= \frac{\partial}{\partial\bar{u}}T_1(\bar{u}, u_0(\bar{u})) + \frac{d}{d\bar{u}}u_0(\bar{u})\frac{\partial}{\partial u_0}T_1(\bar{u}, u_0(\bar{u})), \\ &= \frac{1}{\sqrt{2\gamma}E(\bar{u})} + \frac{q_H(\bar{u}) - q_T(\bar{u})}{q_T(u_e(\bar{u}))} \frac{\frac{\partial}{\partial u_e}T_2(\bar{u}, u_e(\bar{u})) \cdot \frac{\partial}{\partial u_0}T_1(\bar{u}, u_0(\bar{u}))}{\frac{\partial}{\partial u_0}T(\bar{u}, u_0(\bar{u}))}, \\ &= \frac{1}{\sqrt{2\gamma}E(\bar{u})} + \frac{(q_H(\bar{u}) - q_T(\bar{u})) \frac{\partial}{\partial u_e}T_2(\bar{u}, u_e(\bar{u})) \cdot \frac{\partial}{\partial u_0}T_1(\bar{u}, u_0(\bar{u}))}{q_T(u_e(\bar{u})) \frac{\partial}{\partial u_0}T_1(\bar{u}, u_0(\bar{u})) + q_H(u_0(\bar{u})) \frac{\partial}{\partial u_e}T_2(\bar{u}, u_e(\bar{u}))}, \end{aligned} \quad (5.13)$$

where we used Proposition 5.1.4 and equation (4.18). For simplicity of the exposition we wrote

$$E(\bar{u}) = \sqrt{F(h_H(u_0(\bar{u}))) - F(h_H(\bar{u}))} = \sqrt{Q(\bar{u}, u_0(\bar{u})) - Q(\bar{u}, \bar{u})}.$$

We multiply equation (5.13) by

$$q_T(u_e(\bar{u}))\frac{\partial}{\partial u_0}T_1(\bar{u}, u_0(\bar{u})) + q_H(u_0(\bar{u}))\frac{\partial}{\partial u_e}T_2(\bar{u}, u_e(\bar{u}))$$

and observe that this expression is negative because of Theorem 4.3.10. Therefore, showing the negativity of  $\frac{d}{d\bar{u}}\bar{x}(\bar{u})$  is equivalent to show the positivity of

$$\begin{aligned} &\frac{1}{\sqrt{2\gamma}E(\bar{u})}q_T(u_e(\bar{u}))\frac{\partial}{\partial u_0}T_1(\bar{u}, u_0(\bar{u})) + \frac{1}{\sqrt{2\gamma}E(\bar{u})}q_H(u_0(\bar{u}))\frac{\partial}{\partial u_e}T_2(\bar{u}, u_e(\bar{u})) \\ &+ (q_H(\bar{u}) - q_T(\bar{u}))\frac{\partial}{\partial u_e}T_2(\bar{u}, u_e(\bar{u}))\frac{\partial}{\partial u_0}T_1(\bar{u}, u_0(\bar{u})). \end{aligned} \quad (5.14)$$

Proposition 4.3.9 allows us to write the derivatives of the time-maps in the form

$$\begin{aligned} \frac{\partial}{\partial u_0}T_1(\bar{u}, u_0(\bar{u})) &= -\frac{q_H(u_0(\bar{u}))}{\sqrt{2\gamma}E(\bar{u})^2} \cdot \text{int}_H(u_0(\bar{u})), \\ \frac{\partial}{\partial u_e}T_2(\bar{u}, u_e(\bar{u})) &= -\frac{q_T(u_e(\bar{u}))}{\sqrt{2\gamma}E(\bar{u})^2} \cdot \text{int}_T(u_e(\bar{u})), \end{aligned}$$

where we denote by  $\text{int}_H(u_0)$  and  $\text{int}_T(u_e)$  the functions

$$\begin{aligned} \text{int}_H(u_0) &= \int_{u_0}^{\bar{u}} \left( \frac{(Q(\bar{u}, u) - Q(\bar{u}, \bar{u}))q'_H(u)}{q_H(u)^2} - \frac{1}{2} \right) \frac{du}{\sqrt{Q(\bar{u}, u_0) - Q(\bar{u}, u)}} < 0, \\ \text{int}_T(u_e) &= \int_{\bar{u}}^{u_e} \left( \frac{(Q(\bar{u}, u) - Q(\bar{u}, \bar{u}))q'_T(u)}{q_T(u)^2} - \frac{1}{2} \right) \frac{du}{\sqrt{Q(\bar{u}, u_e) - Q(\bar{u}, u)}} < 0. \end{aligned}$$

For better readability we write from now on only  $u_0$  and  $u_e$  and omit the dependencies of  $\bar{u}$ .

Using these representations of the derivatives of the time-maps we reformulate expression (5.14) as

$$\begin{aligned} & \frac{q_H(u_0)q_T(u_e)}{2\gamma E(\bar{u})^4} \left( (q_H(\bar{u}) - q_T(\bar{u})) \operatorname{int}_H(u_0) \operatorname{int}_T(u_e) - E(\bar{u}) \operatorname{int}_H(u_0) - E(\bar{u}) \operatorname{int}_T(u_e) \right) \\ &= \frac{q_H(u_0)q_T(u_e)}{2\gamma E(\bar{u})^4} \left( \operatorname{int}_T(u_e) (q_H(\bar{u}) \operatorname{int}_H(u_0) - E(\bar{u})) - \operatorname{int}_H(u_0) (q_T(\bar{u}) \operatorname{int}_T(u_e) + E(\bar{u})) \right). \end{aligned}$$

Remarking that  $q_H(u_0)q_T(u_e)$  is negative, the whole expression is positive, if the term in the brackets is negative. This is the case if

$$q_H(\bar{u}) \operatorname{int}_H(u_0) > E(\bar{u}) \quad (5.15)$$

and

$$-q_T(\bar{u}) \operatorname{int}_T(u_e) > E(\bar{u}) \quad (5.16)$$

holds.

For showing estimate (5.15), we investigate in detail the integral  $\operatorname{int}_H(u_0)$ . Therefore, we split the integrand into a suitable sum of two summands, which we abbreviate by  $\operatorname{int}_H^1$  and  $\operatorname{int}_H^2(u_0, \bar{u})$  with  $(u_0, \bar{u})$  indicating the bounds of integration.

$$\begin{aligned} \operatorname{int}_H(u_0) &= \int_{u_0}^{\bar{u}} \left( \frac{(Q(\bar{u}, u) - Q(\bar{u}, \bar{u}))q'_H(u)}{q_H(u)^2} - \frac{1}{2} \right) \frac{du}{\sqrt{Q(\bar{u}, u_0) - Q(\bar{u}, u)}}, \\ &= \int_{u_0}^{\bar{u}} \left( \frac{(Q(\bar{u}, u) - Q(\bar{u}, u_0) + Q(\bar{u}, u_0) - Q(\bar{u}, \bar{u}))q'_H(u)}{\sqrt{Q(\bar{u}, u_0) - Q(\bar{u}, u)}q_H^2(u)} - \frac{1}{2\sqrt{Q(\bar{u}, u_0) - Q(\bar{u}, u)}} \right) du, \\ &= \underbrace{\int_{u_0}^{\bar{u}} \left( \frac{-\sqrt{Q(\bar{u}, u_0) - Q(\bar{u}, u)}q'_H(u)}{q_H^2(u)} - \frac{1}{2\sqrt{Q(\bar{u}, u_0) - Q(\bar{u}, u)}} \right) du}_{\operatorname{int}_H^1} \\ &\quad + \underbrace{E(\bar{u})^2 \int_{u_0}^{\bar{u}} \frac{q'_H(u)}{\sqrt{Q(\bar{u}, u_0) - Q(\bar{u}, u)}q_H^2(u)} du}_{\operatorname{int}_H^2(u_0, \bar{u})} \end{aligned}$$

We calculate the integral  $\operatorname{int}_H^1$  using the fundamental theorem of calculus

$$\begin{aligned} \operatorname{int}_H^1 &= \int_{u_0}^{\bar{u}} \left( \frac{-\sqrt{Q(\bar{u}, u_0) - Q(\bar{u}, u)}q'_H(u)}{q_H^2(u)} - \frac{1}{2\sqrt{Q(\bar{u}, u_0) - Q(\bar{u}, u)}} \right) du, \\ &= \int_{u_0}^{\bar{u}} \frac{\partial}{\partial u} \left( \frac{\sqrt{Q(\bar{u}, u_0) - Q(\bar{u}, u)}}{q_H(u)} \right) du = \frac{E(\bar{u})}{q_H(\bar{u})}. \end{aligned} \quad (5.17)$$

For the integral  $\text{int}_H^2(u_0, \bar{u})$  we need a distinction of cases. We remind that there is the critical value  $u_H^{cr}$ , such that the derivative  $q'_H(u)$  is negative for  $u < u_H^{cr}$ , whereas it is positive for  $u > u_H^{cr}$ , see Lemma 2.1.9.

If  $\bar{u} \leq u_H^{cr}$  the integrand of  $\text{int}_H^2(u_0, \bar{u})$  is negative and we estimate

$$\begin{aligned} \text{int}_H^2(u_0, \bar{u}) &= E(\bar{u})^2 \int_{u_0}^{\bar{u}} \frac{q'_H(u)}{\sqrt{Q(\bar{u}, u_0) - Q(\bar{u}, u)} q_H^2(u)} du, \\ &\leq \frac{E(\bar{u})^2}{E(\bar{u})} \int_{u_0}^{\bar{u}} \frac{q'_H(u) du}{q_H^2(u)} = E(\bar{u}) \int_{u_0}^{\bar{u}} \frac{d}{du} \left( -\frac{1}{q_H(u)} \right) du, \\ &= E(\bar{u}) \left( \frac{1}{q_H(u_0)} - \frac{1}{q_H(\bar{u})} \right). \end{aligned} \quad (5.18)$$

We use here the estimate

$$\frac{1}{\sqrt{Q(\bar{u}, u_0) - Q(\bar{u}, u)}} > \frac{1}{\sqrt{Q(\bar{u}, u_0) - Q(\bar{u}, \bar{u})}} = \frac{1}{E(\bar{u})}, \quad (5.19)$$

which holds because  $Q(\bar{u}, u)$  is monotone decreasing in  $u$  for  $u \in (0, \bar{u})$ .

Furthermore,  $q_H$  is decreasing in the range  $\bar{u} \leq u_H^{cr}$ . Therefore, the inequality  $0 > q_H(u_0(\bar{u})) > q_H(\bar{u})$  always holds, which yields  $\frac{q_H(\bar{u})}{q_H(u_0(\bar{u}))} > 1$ . Hence, we obtain the estimate (5.15) by putting the results (5.17) and (5.18) for both integrals together

$$\begin{aligned} q_H(\bar{u}) \text{int}_H(u_0(\bar{u})) &= q_H(\bar{u}) (\text{int}_H^1 + \text{int}_H^2(u_0, \bar{u})), \\ &\geq q_H(\bar{u}) E(\bar{u}) \left( \frac{1}{q_H(\bar{u})} + \frac{1}{q_H(u_0(\bar{u}))} - \frac{1}{q_H(\bar{u})} \right), \\ &= E(\bar{u}) \frac{q_H(\bar{u})}{q_H(u_0(\bar{u}))} > E(\bar{u}). \end{aligned}$$

If  $\bar{u} > u_H^{cr}$  we split the integral  $\text{int}_H^2(u_0, \bar{u})$  at  $u_H^{cr}$  and denote in the brackets the bounds of integration

$$\text{int}_H^2(u_0, \bar{u}) = \text{int}_H^2(u_0, u_H^{cr}) + \text{int}_H^2(u_H^{cr}, \bar{u}).$$

We remark that for  $u \in [u_0, u_H^{cr}]$  the estimate

$$\frac{1}{\sqrt{Q(\bar{u}, u_0) - Q(\bar{u}, u)}} > \frac{1}{\sqrt{Q(\bar{u}, u_0) - Q(\bar{u}, u_H^{cr})}} = \frac{1}{E(u_H^{cr})} \quad (5.20)$$

holds. Furthermore, the derivative  $q'_H(u)$  is negative in this domain, thus the integral can be estimated in the same fashion as in the case  $\bar{u} \leq u_H^{cr}$ , compare (5.18):

$$\text{int}_H^2(u_0, u_H^{cr}) = E(\bar{u})^2 \int_{u_0}^{u_H^{cr}} \frac{q'_H(u)}{\sqrt{Q(\bar{u}, u_0) - Q(\bar{u}, u)} q_H^2(u)} du \leq \frac{E(\bar{u})^2}{E(u_H^{cr})} \left( \frac{1}{q_H(u_0)} - \frac{1}{q_H(u_H^{cr})} \right).$$

For  $u \in [u_H^{cr}, \bar{u}]$  the estimate

$$\frac{1}{\sqrt{Q(\bar{u}, u_0) - Q(\bar{u}, u)}} < \frac{1}{\sqrt{Q(\bar{u}, u_0) - Q(\bar{u}, u_H^{cr})}} = \frac{1}{E(u_H^{cr})}$$

holds in the opposite way compared to (5.20), but now  $q'_H(u) \geq 0$  and we estimate again similar as in (5.18):

$$\text{int}_H^2(u_H^{cr}, \bar{u}) = E(\bar{u})^2 \int_{u_H^{cr}}^{\bar{u}} \frac{q'_H(u)}{\sqrt{Q(\bar{u}, u_0) - Q(\bar{u}, u)} q_H^2(u)} du \leq \frac{E(\bar{u})^2}{E(u_H^{cr})} \left( \frac{1}{q_H(u_H^{cr})} - \frac{1}{q_H(\bar{u})} \right).$$

Thus, we obtain

$$\begin{aligned} q_H(\bar{u}) \text{int}_H(u_0(\bar{u})) &= q_H(\bar{u}) \left( \text{int}_H^1 + \text{int}_H^2(u_0, u_H^{cr}) + \text{int}_H^2(u_H^{cr}, \bar{u}) \right), \\ &\geq q_H(\bar{u}) \frac{E(\bar{u})}{q_H(\bar{u})} + q_H(\bar{u}) \frac{E(\bar{u})^2}{E(u_H^{cr})} \left( \frac{1}{q_H(u_0(\bar{u}))} - \frac{1}{q_H(u_H^{cr})} + \frac{1}{q_H(u_H^{cr})} - \frac{1}{q_H(\bar{u})} \right), \\ &= E(\bar{u}) + \frac{E(\bar{u})^2}{E(u_H^{cr})} \left( \frac{q_H(\bar{u})}{q_H(u_0(\bar{u}))} - 1 \right). \end{aligned}$$

Finally,  $\frac{E(\bar{u})}{E(u_H^{cr})} > 1$  holds by setting  $u = u_H^{cr}$  in estimate (5.19), if  $\bar{u} > u_H^{cr}$ . Because of assumption (5.11) the estimate  $\frac{q_H(\bar{u})}{q_H(u_0(\bar{u}))} > 1$  holds, thus we obtain

$$\begin{aligned} q_H(\bar{u}) \text{int}_H(u_0(\bar{u})) &\geq E(\bar{u}) + \frac{E(\bar{u})^2}{E(u_H^{cr})} \left( \frac{q_H(\bar{u})}{q_H(u_0(\bar{u}))} - 1 \right) \\ &> E(\bar{u}) + E(\bar{u}) \left( \frac{q_H(\bar{u})}{q_H(u_0(\bar{u}))} - 1 \right) \\ &= E(\bar{u}) \frac{q_H(\bar{u})}{q_H(u_0(\bar{u}))} > E(\bar{u}). \end{aligned}$$

To show the estimate (5.16) we argue in the same way, which accomplish the proof of this Proposition.  $\square$

**Lemma 5.2.2.** *If  $\bar{u}$  is admissible, then the requirements (5.11) and (5.12) of Proposition 5.2.1 are fulfilled.*

*Proof.* When  $\bar{u} \in (u_T^{cr}, u_H^{cr})$ , then it holds  $q'_H(u) < 0$  for all  $u \in (0, \bar{u})$  and  $q'_T(u) < 0$  for all  $u \in (\bar{u}, u_2)$ , which yields the conditions (5.11) and (5.12).  $\square$

It is possible to find kinetic functions which are not admissible, but meet the requirements (5.11) and (5.12). But, as we are mainly interested in stable stationary solutions, we do not investigate further this situation.

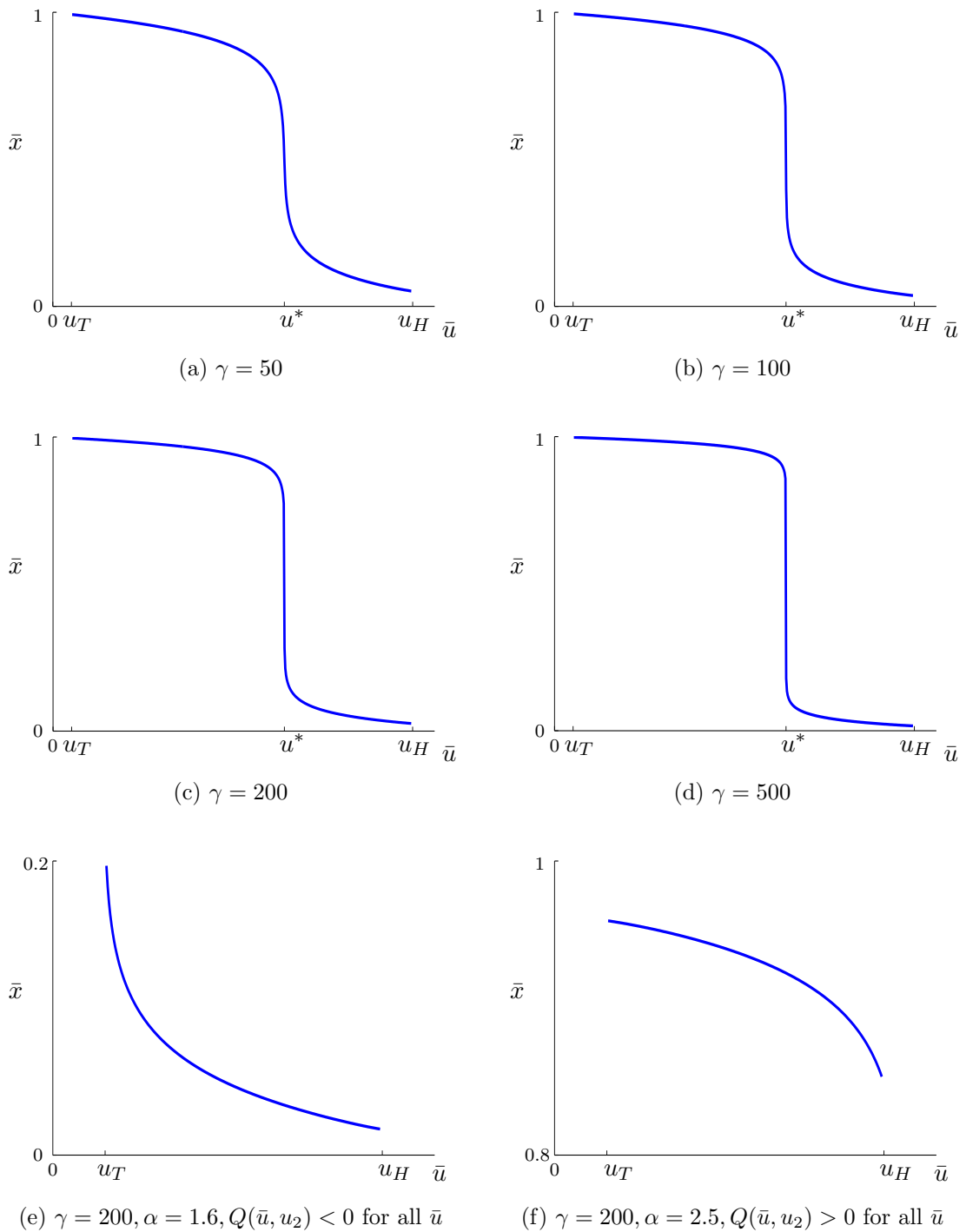


Figure 5.4: The layer position  $\bar{x}(\bar{u})$  is decreasing as function of the jump  $\bar{u}$ . The upper four plots are made for the kinetic functions  $p(v) = v^3 - 6.3v^2 + 10v$  and  $f(u, v) = 1.4v - u$  and for different diffusion coefficients  $\frac{1}{\gamma}$ . One can see that for increasing  $\gamma$  the range of values which is attained for  $\bar{u} \in (u^* - \epsilon, u^* + \epsilon)$  is getting larger. The last two plots are done for  $p(v) = v^3 - 6v^2 + 10v$  and  $f(u, v) = \alpha v - u$ , with two different  $\alpha$  such that there is no jump  $u^*$  with  $Q(u^*, u_2) = 0$ .

**Definition:** For admissible kinetic functions, we define

$$\bar{x}_{\min}^{cr} = T_1(u_H^{cr}, u_0(u_H^{cr})) \quad \text{and} \quad \bar{x}_{\max}^{cr} = T_1(u_T^{cr}, u_0(u_T^{cr}))$$

and call  $I^{cr} = (\bar{x}_{\min}^{cr}, \bar{x}_{\max}^{cr})$  the **admissible interval** for the layer position.

The admissible interval depends on the diffusion coefficient. For emphasising this dependence we sometimes write  $I^{cr}(\gamma)$ . This dependence will be analysed in more detail in Section 5.3.

**Theorem 5.2.3.** *We consider the generic model in the hysteresis case with admissible kinetic functions. There is for every value  $\bar{x} \in (\bar{x}_{\min}^{cr}, \bar{x}_{\max}^{cr})$  a unique monotone increasing solution of the stationary problem (4.1) with layer position  $\bar{x}$ .*

*Proof.* We consider the mapping

$$\begin{aligned} \bar{x} : (u_T^{cr}, u_H^{cr}) &\rightarrow (\bar{x}_{\min}^{cr}, \bar{x}_{\max}^{cr}) \\ \bar{u} &\mapsto \bar{x}(\bar{u}). \end{aligned}$$

Proposition 5.2.1 yields the continuity and the monotonicity of this mapping. Thus, it is invertible with monotone decreasing inverse function  $\bar{u}(\bar{x})$  defined for all  $\bar{x} \in (\bar{x}_{\min}^{cr}, \bar{x}_{\max}^{cr})$ . Therefore, there is a unique jump  $\bar{u}(\bar{x})$  and using Theorem 4.1.3 there is a unique monotone increasing stationary solution  $(U(x), V(x))$  with layer position  $\bar{x}$ .  $\square$

**Corollary 5.2.4.** *We consider the generic model in the hysteresis case with admissible kinetic functions. There is for every value  $\bar{x} \in (1 - \bar{x}_{\max}^{cr}, 1 - \bar{x}_{\min}^{cr})$  a unique monotone decreasing solution of the stationary problem (4.1) with layer position  $\bar{x}$ .*

*Proof.* We remind that the layer position of a monotone decreasing stationary solution is given by  $T_2(\bar{u}, u_e(\bar{u})) = 1 - \bar{x}(\bar{u})$ . This is a monotone increasing function because of Proposition 5.2.1 with the range  $(1 - \bar{x}_{\max}^{cr}, 1 - \bar{x}_{\min}^{cr})$ . Therefore, there is a unique jump  $\bar{u}(\bar{x})$  and a unique monotone decreasing stationary solution  $(U(x), V(x))$  with layer position  $\bar{x}$ .  $\square$

### 5.3 The role of the diffusion coefficient

Looking at Figure 5.4, we observe that for growing  $\gamma$  the layer position  $\bar{x}(\bar{u})$  approaches more and more the values 0 and 1, respectively, and is rapidly changing from 1 to 0 near  $u^*$ .

To proof this, we consider in this section the jump  $\bar{u}$  as fixed and investigate the layer position and its derivative  $\frac{d}{d\bar{u}}\bar{x}(u^*)$  for  $\gamma$  tending to infinity.

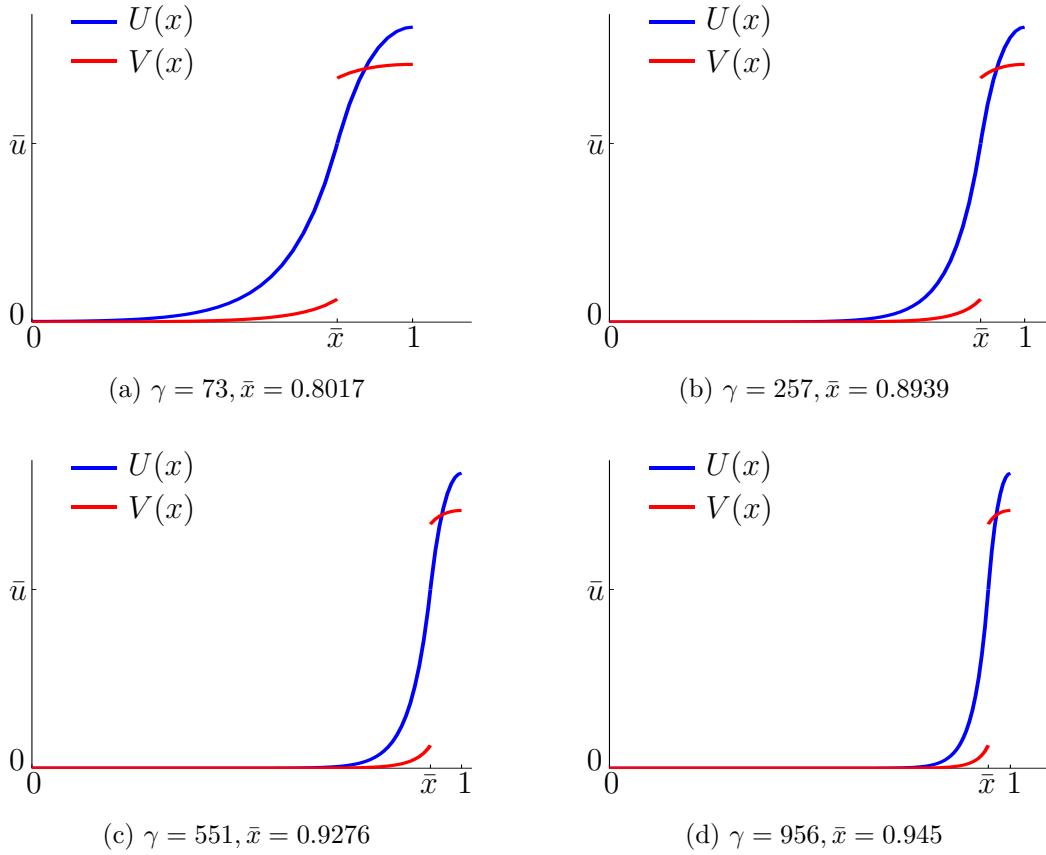


Figure 5.5: Simulations of stationary solutions with jump at  $\bar{u} = 2.9$  for different diffusion coefficients, but the same kinetic functions  $f(u, v) = 1.4v - u$  and  $g(u, v) = u - (v^3 - 6.3v^2 + 10v)$  with  $Q(\bar{u}, u_2) > 0$ . One can see that the layer position  $\bar{x}$  is moving towards 0 for increasing  $\gamma$ .

**Theorem 5.3.1.** *We consider the generic model in the hysteresis case and the jump  $\bar{u} \in (u_T, \min(u_H, u_2))$ . If  $Q(\bar{u}, u_2) > 0$  then the layer position  $\bar{x}$  of the monotone increasing solution  $(U(x), V(x))$  tends to 1 for  $\gamma \rightarrow \infty$ , whereas if  $Q(\bar{u}, u_2) < 0$  then  $\bar{x} \rightarrow 0$  for  $\gamma \rightarrow \infty$ .*

*Proof.* Multiplying the equation  $T_1(\bar{u}, u_0) + T_2(\bar{u}, u_e(u_0)) = 1$  by  $\sqrt{\gamma}$  yields

$$\frac{1}{\sqrt{2}} \int_{u_0}^{\bar{u}} \frac{du}{\sqrt{F(h_H(u_0)) - F(h_H(u))}} + \frac{1}{\sqrt{2}} \int_{\bar{u}}^{u_e} \frac{du}{\sqrt{F(h_T(u_e)) - F(h_T(u))}} = \sqrt{\gamma}. \quad (5.21)$$

If  $Q(\bar{u}, u_2) > 0$ , then  $I_{\bar{u}} = (0, u_{\max}(\bar{u}))$  with  $u_{\max}(\bar{u}) < u_2$ . Hence, for  $\gamma \rightarrow \infty$  then  $u_0 \rightarrow 0$ , whereas  $u_e \rightarrow u_{\max}(\bar{u})$  and, therefore, the integral  $\frac{1}{\sqrt{2}} \int_{u_0}^{\bar{u}} \frac{du}{\sqrt{F(h_H(u_0)) - F(h_H(u))}}$

tends to infinity by Theorem 4.3.7, whereas the second one is bounded

$$\frac{1}{\sqrt{2}} \int_{\bar{u}}^{u_e} \frac{du}{\sqrt{F(h_T(u_e)) - F(h_T(u))}} < \frac{1}{\sqrt{2}} \int_{\bar{u}}^{u_{\max}(\bar{u})} \frac{du}{\sqrt{F(h_T(u_e)) - F(h_T(u))}} < \infty.$$

Therefore, the layer position  $\bar{x} = T_1(\bar{u}, u_0)$  tends to 1 for  $\gamma$  tending to infinity. For  $Q(\bar{u}, u_2) < 0$ , we conclude similarly. Under this assumption  $I_{\bar{u}} = (u_{\min}(\bar{u}), u_2)$  with  $0 < u_{\min}(\bar{u})$ . Therefore, the first integral of (5.21) is bounded by the finite integral  $\frac{1}{\sqrt{2}} \int_{u_{\min}(\bar{u})}^{\bar{u}} \frac{du}{\sqrt{F(h_H(u_0)) - F(h_H(u))}}$ , whereas the second integral tends to infinity for  $\gamma \rightarrow \infty$ . Hence  $1 - \bar{x} = T_2(\bar{u}, u_e) \rightarrow 1$  and the layer position  $\bar{x}$  tends to zero.  $\square$

We apply this theorem for those layer position which are defining the admissible interval  $I^{cr} = (\bar{x}_{\min}^{cr}, \bar{x}_{\max}^{cr})$ . We determine the length of this interval depending on the diffusion coefficient  $\frac{1}{\gamma}$ .

**Corollary 5.3.2.** *We consider the generic model in the hysteresis case for admissible kinetic functions. If  $u^* \in (u_T^{cr}, u_H^{cr})$ , the admissible interval  $I^{cr}(\gamma)$  is getting bigger for  $\gamma \rightarrow \infty$ .*

*But, if  $u^* < u_T^{cr}$ , the admissible interval  $I^{cr}$  is getting smaller for increasing  $\gamma$  and it is close to 1. Similarly, if  $u^* > u_H^{cr}$ , the admissible interval  $I^{cr}$  is getting smaller for increasing  $\gamma$  and it is close to 0.*

**Example 5.3.3.** *We calculate in Table 5.1 the admissible interval  $I^{cr}(\gamma)$  using a Matlab program for the functions which have been used in the examples 4.4.10, 4.4.11 and 4.4.12.*

$f(u, v)$	$1.4v - u$	$1.6v - u$	$2.5v - u$
$p(v)$	$v^3 - 6.3v^2 + 10v$	$v^3 - 6v^2 + 10v$	$v^3 - 6v^2 + 10v$
$[u_T, u_H]$	[0.24365, 4.7124]	[2.9113, 5.0887]	[2.9113, 5.0887]
$[u_T^{cr}, u_H^{cr}]$	[0.38264, 4.5734]	[3.1236, 4.8764]	[3.3876, 4.6124]
$u^*$	3.0316	$Q(\bar{u}, u_2) < 0$	$Q(\bar{u}, u_2) > 0$
$I^{cr}$	$\gamma = 10$	[0.127, 0.974]	[0.093, 0.395]
	$\gamma = 50$	[0.057, 0.988]	[0.042, 0.212]
	$\gamma = 100$	[0.041, 0.992]	[0.030, 0.150]
	$\gamma = 200$	[0.029, 0.994]	[0.021, 0.106]
	$\gamma = 500$	[0.018, 0.996]	[0.013, 0.067]

Table 5.1: The admissible interval  $I^{cr}$  for three different kinetic functions. All functions are admissible, but only for the first one holds  $u^* \in [u_T^{cr}, u_H^{cr}]$ . We observe that  $I^{cr}$  is getting bigger when  $\gamma$  is increasing for the first kinetic functions, whereas it is getting smaller for the other two.

This table provides an explanation for the simulation performed in the end of Section 4.4. In Example 4.4.10 the kinetic functions  $f(u, v) = 1.4v - u$  and  $p(v) = v^3 - 6.3v^2 + 10v$  have been used. All initial conditions which have been used had a discontinuity lying in the admissible interval  $I^{cr}(200) = [0.029, 0.994]$ . Thus, all simulation showed the formation of a stable stationary solution. In Example 4.4.11 simulations for the kinetic functions  $f(u, v) = 2.5v - u$  and  $p(v) = v^3 - 6v^2 + 10v$  have been performed. Only the layer position  $\bar{x} = 0.95$  lies in the admissible interval  $I^{cr}(200) = [0.906, 0.952]$ , whereas  $\bar{x} = 0.6$  is not lying in this interval. Similarly, in Example 4.4.12 simulations for the kinetic functions  $f(u, v) = 1.6v - u$  and  $p(v) = v^3 - 6v^2 + 10v$  have been performed. The layer position  $\bar{x} = 0.1$  lies in the admissible interval  $I^{cr}(200) = [0.021, 0.106]$ , whereas  $\bar{x} = 0.4$  is not admissible and, consequently, leading to a constant stationary solution.

Next, we investigate the layer position  $\bar{x}$  and its derivative  $\frac{d}{d\bar{u}}\bar{x}$  for the missing case  $\bar{u} = u^*$  this means for  $Q(\bar{u}, u_2) = 0$ . Therefore, we need a lemma describing the asymptotic behaviour of an integral involving a small parameter to understand better the asymptotic behaviour of the time-map for  $u_0 \rightarrow 0$ , resp.  $u_e \rightarrow u_2$ .

**Notation:** We use in the following the Landau notation which is defined by

$$f \in o(g) :\Leftrightarrow \lim_{x \rightarrow a} \left| \frac{f(x)}{g(x)} \right| = 0, \quad (5.22)$$

$$f \in O(g) :\Leftrightarrow \limsup_{x \rightarrow a} \left| \frac{f(x)}{g(x)} \right| < \infty. \quad (5.23)$$

Here  $f, g$  are real functions defined on some interval containing  $a$ . We will write  $o(g)$ , respectively  $O(g)$ , to denote a function  $f$ , which is an element of  $o(g)$ , respectively  $O(g)$ .

**Lemma 5.3.4.** *Assume that  $g(u)$  is a  $C^2$  function defined on some open interval including  $[0, 1]$  and satisfying the following assumptions:*

1.  $g(0) = g'(0) = 0$ ,
2.  $g'(u) < 0$  and  $g''(u) < 0$  for  $u \in (0, 1)$ ,
3.  $g(u) < 0$  for  $u \in (0, 1]$ ,
4.  $g''(u)$  is Hölder continuous with exponent  $0 < \gamma < 1$  on the interval  $[0, 1]$  that is

$$|g''(u) - g''(v)| \leq L|u - v|^\gamma \quad \text{for } u, v \in [0, 1].$$

Define  $I(a)$  by

$$I(a) = \int_a^1 \frac{du}{\sqrt{2(g(a) - g(u))}} \quad \text{for } a \in [0, 1].$$

Then

$$I(a) = \frac{1}{\sqrt{|g''(0)|}} \log \frac{1}{a} + O(1) \quad \text{as } a \downarrow 0.$$

*Proof.* This result can be found in [Nis82] and in [Nak12].  $\square$

This Lemma allows us to deduce the following Corollary.

**Corollary 5.3.5.** *For all jumps  $\bar{u}$  the following integrals can be approximately written by*

$$\frac{1}{\sqrt{2}} \int_{u_0}^{\bar{u}} \frac{du}{\sqrt{F(h_H(u_0)) - F(h_H(u))}} = \frac{1}{\sqrt{|q'_H(0)|}} \log \frac{1}{u_0} + O(1) \quad \text{as } u_0 \downarrow 0 \quad (5.24)$$

and

$$\frac{1}{\sqrt{2}} \int_{\bar{u}}^{u_e} \frac{du}{\sqrt{F(h_T(u_e)) - F(h_T(u))}} = \frac{1}{\sqrt{|q'_T(u_2)|}} \log \frac{1}{u_2 - u_e} + O(1) \quad \text{as } u_e \uparrow u_2. \quad (5.25)$$

*Proof.* We choose  $\delta > u_0 > 0$  small enough such that  $q'_H(\delta) < 0$  holds and split the integral at  $\delta$

$$\begin{aligned} & \frac{1}{\sqrt{2}} \int_{u_0}^{\bar{u}} \frac{du}{\sqrt{F(h_H(u_0)) - F(h_H(u))}} \\ &= \frac{1}{\sqrt{2}} \int_{u_0}^{\delta} \frac{du}{\sqrt{F(h_H(u_0)) - F(h_H(u))}} + \frac{1}{\sqrt{2}} \int_{\delta}^{\bar{u}} \frac{du}{\sqrt{F(h_H(u_0)) - F(h_H(u))}}. \end{aligned}$$

The second integral is bounded, because the denominator will never be zero, i.e. it is  $O(1)$  as function of  $u_0$ .

Now, we observe that

$$g(u) := F(h_H(\delta u))$$

fulfils the assumptions of Lemma 5.3.4. We set  $a = \frac{u_0}{\delta}$  and obtain

$$I\left(\frac{u_0}{\delta}\right) = \frac{1}{\sqrt{2}} \int_{\frac{u_0}{\delta}}^1 \frac{du}{\sqrt{F(h_H(u_0)) - F(h_H(\delta u))}} = \frac{1}{\delta\sqrt{2}} \int_{u_0}^{\delta} \frac{d\tilde{u}}{\sqrt{F(h_H(u_0)) - F(h_H(\tilde{u}))}}$$

which equals by Lemma 5.3.4

$$I\left(\frac{u_0}{\delta}\right) = \frac{1}{\sqrt{|\delta^2 q'_H(0)|}} \log \frac{1}{u_0/\delta} + O(1) = \frac{1}{\delta\sqrt{|q'_H(0)|}} \log \frac{1}{u_0} + O(1) \quad \text{as } u_0 \downarrow 0.$$

Multiplying by  $\delta$ , this yields the result.

Similarly, we choose  $\delta$  such that  $q'_T(u_2 - \delta) < 0$  holds and split the integral

$$\begin{aligned} & \frac{1}{\sqrt{2}} \int_{\bar{u}}^{u_e} \frac{du}{\sqrt{F(h_T(u_e)) - F(h_T(u))}} \\ &= \frac{1}{\sqrt{2}} \int_{\bar{u}}^{u_2 - \delta} \frac{du}{\sqrt{F(h_T(u_e)) - F(h_T(u))}} + \frac{1}{\sqrt{2}} \int_{u_2 - \delta}^{u_e} \frac{du}{\sqrt{F(h_T(u_e)) - F(h_T(u))}}, \end{aligned}$$

where the first integral is  $O(1)$  as function of  $u_e$ . Then, we consider

$$g(u) := F(h_T(\delta(u_2 - u))) - Q(\bar{u}, u_2)$$

which fulfils the assumptions of Lemma 5.3.4 and therefore leads to the result.  $\square$

For the analysis of  $\frac{d}{d\bar{u}}\bar{x}$ , we also need to understand the asymptotic behaviour of the derivatives of the time-maps.

**Lemma 5.3.6.** *For  $u_0 \rightarrow 0$  it holds*

$$\frac{\partial}{\partial u_0} \left( \frac{1}{\sqrt{2}} \int_{u_0}^{\bar{u}} \frac{du}{\sqrt{F(h_H(u_0)) - F(h_H(u))}} \right) = -\frac{1}{\sqrt{|q'_H(0)|}} \frac{1}{u_0} + o(1) \quad (5.26)$$

and for  $u_e \rightarrow u_2$  it holds

$$\frac{\partial}{\partial u_e} \left( \frac{1}{\sqrt{2}} \int_{\bar{u}}^{u_e} \frac{du}{\sqrt{F(h_T(u_e)) - F(h_T(u))}} \right) = \frac{1}{\sqrt{|q'_T(u_2)|}} \frac{1}{u_2 - u_e} + o(1). \quad (5.27)$$

*Proof.* We use Corollary 5.3.5 and calculate the derivative of formula (5.24) and (5.24), respectively, with respect to  $u_0$  and with respect to  $u_e$ , respectively, to obtain equations (5.26) and (5.27).  $\square$

In the remainder of this section, we consider from now on the jump  $\bar{u} = u^*$  as fixed and the diffusion coefficient as variable. We write  $u_0(\gamma)$  for the unique solution of  $T(u^*, u_0(\gamma)) = 1$ . The function  $u_e(\gamma)$  is determined by  $Q(u^*, u_0(\gamma)) = Q(u^*, u_e(\gamma))$ .

**Lemma 5.3.7.**  *$u_e(\gamma)$  can be written in terms of  $u_0(\gamma)$  by*

$$u_2 - u_e(u_0(\gamma)) = \sqrt{\frac{q'_H(0)}{q'_T(u_2)}} u_0(\gamma) + o(u_0(\gamma)), \quad \text{as } \gamma \rightarrow \infty.$$

*Proof.* We use the Taylor development of  $q_H(u)$  near 0

$$q_H(u) = q_H(0) + q'_H(0)u + o(u) = q'_H(0)u + o(u), \quad \text{as } u \rightarrow 0$$

respectively of  $q_T(u)$  near  $u_2$

$$q_T(u) = q_T(u_2) + q'_T(u_2)(u - u_2) + o(u - u_2) = q'_T(u_2)u + o(u - u_2) \quad \text{as } u \rightarrow u_2.$$

We calculate the values of the potential near 0, respectively near  $u_2$

$$\begin{aligned} Q(u^*, u_0(\gamma)) &= \int_0^{u_0(\gamma)} q_H(u) du = \int_0^{u_0(\gamma)} (q'_H(0)u + o(u)) du \\ &= \frac{1}{2} q'_H(0) u_0(\gamma)^2 + o(u_0(\gamma)^2) \quad \text{as } \gamma \rightarrow \infty \end{aligned}$$

and

$$\begin{aligned} Q(u^*, u_e(\gamma)) &= Q(u^*, u_2) + \int_{u_2}^{u_e(\gamma)} q_T(u) du = \int_{u_2}^{u_e(\gamma)} (q'_T(u_2)(u - u_2) + o((u - u_2))) du \\ &= \frac{1}{2} q'_T(u_2) (u_e(\gamma) - u_2)^2 + o((u_e(\gamma) - u_2)^2) \quad \text{as } \gamma \rightarrow \infty, \end{aligned}$$

where we used the defining relation  $Q(u^*, u_2) = 0$  for  $u^*$ .

From  $Q(u^*, u_0(\gamma)) = Q(u^*, u_e(\gamma))$  we deduce the relation

$$\frac{1}{2} q'_H(0) u_0(\gamma)^2 + o(u_0(\gamma)^2) = \frac{1}{2} q'_T(u_2) (u_e(\gamma) - u_2)^2 + o((u_e(\gamma) - u_2)^2).$$

Hence, we found the expression which allows to consider  $u_e(\gamma)$  as function of  $u_0(\gamma)$ . We remind that both,  $q'_H(0) < 0$  and  $q'_T(u_2) < 0$  (see Lemma 2.1.9), thus their quotient is positive and we can take the squareroot.  $\square$

**Corollary 5.3.8.** *For  $\bar{u} = u^*$  it holds*

$$\frac{\partial}{\partial u_e} \left( \frac{1}{\sqrt{2}} \int_{\bar{u}}^{u_e} \frac{du}{\sqrt{F(h_T(u_e)) - F(h_T(u))}} \right) = \frac{1}{\sqrt{|q'_H(0)|}} \frac{1}{u_0} + o\left(\frac{1}{u_0}\right). \quad (5.28)$$

*Proof.* We use Lemma 5.3.7 to replace  $u_2 - u_e$  in formula (5.27) and consider now the limit for  $u_0 \rightarrow 0$

$$\begin{aligned} \frac{\partial}{\partial u_e} \left( \frac{1}{\sqrt{2}} \int_{\bar{u}}^{u_e} \frac{du}{\sqrt{F(h_T(u_e)) - F(h_T(u))}} \right) &= \frac{1}{\sqrt{|q'_T(u_2)|}} \frac{1}{\sqrt{\frac{q'_H(0)}{q'_T(u_2)} u_0 + o(u_0)}} + o(1) \\ &= \frac{1}{\sqrt{|q'_H(0)|}} \frac{1}{u_0} \frac{1}{1 + o(1)} + o(1) \\ &= \frac{1}{\sqrt{|q'_H(0)|}} \frac{1}{u_0} (1 + o(1)) + o(1) \\ &= \frac{1}{\sqrt{|q'_H(0)|}} \frac{1}{u_0} + o\left(\frac{1}{u_0}\right) \end{aligned}$$

where we used that  $\frac{1}{1+x} = 1 - x + o(x)$  for  $x \rightarrow 0$ .  $\square$

**Theorem 5.3.9.** *For the jump  $\bar{u} = u^*$ , a monotone increasing solution of the generic model (2.1) in the hysteresis case has an interior transition layer at the value which tends for  $\gamma \rightarrow \infty$  to*

$$\bar{x} = \frac{\sqrt{|q'_T(u_2)|}}{\sqrt{|q'_T(u_2)|} + \sqrt{|q'_H(0)|}}.$$

*Proof.* Let  $(U(x), V(x))$  be a monotone increasing solution with jump at  $\bar{u}$  and layer position  $\bar{x}$ . To find a more suitable representation of  $\bar{x}$  we change variables  $x \mapsto \eta = (x - \bar{x})\sqrt{\gamma}$  and set  $\tilde{U}(\eta) = U(x)$ . Hence the bounds of integration are mapped to

$$0 \mapsto -\bar{x}\sqrt{\gamma} =: -M(\gamma) \quad \text{and} \quad 1 \mapsto (1 - \bar{x})\sqrt{\gamma} =: N(\gamma).$$

We can easily calculate that the layer position is given by the relation

$$\bar{x}(\gamma) = \frac{M(\gamma)}{M(\gamma) + N(\gamma)}. \quad (5.29)$$

The values  $M(\gamma)$  and  $N(\gamma)$  can be calculated in terms of time-maps

$$M(\gamma) = \sqrt{\gamma} T_1(\bar{u}, u_0(\gamma)) = \frac{1}{\sqrt{2}} \int_{u_0(\gamma)}^{\bar{u}} \frac{du}{\sqrt{F(h_H(u_0(\gamma))) - F(h_H(u))}} \quad (5.30)$$

and

$$N(\gamma) = \sqrt{\gamma} T_2(\bar{u}, u_e(\gamma)) = \frac{1}{\sqrt{2}} \int_{\bar{u}}^{u_e(\gamma)} \frac{du}{\sqrt{F(h_T(u_e(\gamma))) - F(h_T(u))}}. \quad (5.31)$$

We are interested in the behaviour of  $N(\gamma)$  and  $M(\gamma)$  for  $\gamma \rightarrow \infty$ , which implies  $u_0(\gamma) \rightarrow 0$  and  $u_e(\gamma) \rightarrow u_2$ , because of  $Q(u^*, u_2) = 0$ . Therefore, we use Corollary 5.3.5 to write

$$M(\gamma) = \frac{1}{\sqrt{|q'_H(0)|}} \log \frac{1}{u_0(\gamma)} + O(1) \quad \text{as } \gamma \rightarrow \infty \quad (5.32)$$

and

$$N(\gamma) = \frac{1}{\sqrt{|q'_T(u_2)|}} \log \frac{1}{u_2 - u_e(\gamma)} + O(1) \quad \text{as } \gamma \rightarrow \infty. \quad (5.33)$$

We replace the expression  $u_2 - u_e(\gamma)$  in  $N(\gamma)$  by Lemma 5.3.7 which leads to

$$\begin{aligned}
\log \frac{1}{u_2 - u_e(\gamma)} &= \log \frac{1}{\left(\frac{q'_H(0)}{q'_T(u_2)}\right)^{\frac{1}{2}} u_0(\gamma) + o(u_0(\gamma))} \\
&= -\log \left( \left(\frac{q'_H(0)}{q'_T(u_2)}\right)^{\frac{1}{2}} u_0(\gamma) + o(u_0(\gamma)) \right) \\
&= -\log(u_0(\gamma)) \left(\frac{q'_H(0)}{q'_T(u_2)}\right)^{\frac{1}{2}} + o(1) \\
&= -\log u_0(\gamma) - \log \left( \left(\frac{q'_H(0)}{q'_T(u_2)}\right)^{\frac{1}{2}} + o(1) \right) \\
&= \log \frac{1}{u_0(\gamma)} + O(1), \quad \text{as } u_0(\gamma) \downarrow 0.
\end{aligned}$$

Finally, we obtain

$$\begin{aligned}
\bar{x}(\gamma) &= \frac{M(\gamma)}{M(\gamma) + N(\gamma)} = \frac{\frac{1}{\sqrt{q'_H(0)}} \log \frac{1}{u_0(\gamma)} + O(1)}{\frac{1}{\sqrt{|q'_H(0)|}} \log \frac{1}{u_0(\gamma)} + \frac{1}{\sqrt{|q'_T(u_2)|}} \log \frac{1}{u_0(\gamma)} + O(1)} \\
&= \frac{\frac{1}{\sqrt{|q'_H(0)|}} + o(1)}{\frac{1}{\sqrt{|q'_H(0)|}} + \frac{1}{\sqrt{|q'_T(u_2)|}} + o(1)} \\
&= \frac{\sqrt{|q'_T(u_2)|} + o(1)}{\sqrt{|q'_T(u_2)|} + \sqrt{|q'_H(0)|} + o(1)} \quad \text{as } \gamma \rightarrow \infty.
\end{aligned}$$

This yields the result.  $\square$

Next, we need to understand how fast  $u_0(\gamma)$  tends to 0 for  $\gamma$  tending to infinity.

**Lemma 5.3.10.** *We calculate the limit*

$$\lim_{\gamma \rightarrow \infty} \frac{q_H(u_0(\gamma))}{q_T(u_e(\gamma))} = -\sqrt{\frac{q'_H(0)}{q'_T(u_2)}}$$

*Proof.* We remark that  $\lim_{\gamma \rightarrow \infty} q_H(u_0(\gamma)) = q_H(0) = 0$  and  $\lim_{\gamma \rightarrow \infty} q_T(u_e(\gamma)) = q_T(u_2) = 0$ , thus we can use L'Hôpital's rule

$$\lim_{\gamma \rightarrow \infty} \frac{q_H(u_0(\gamma))}{q_T(u_e(\gamma))} = \lim_{\gamma \rightarrow \infty} \frac{q'_H(u_0(\gamma)) \frac{d}{d\gamma} u_0(\gamma)}{q'_T(u_e(\gamma)) \frac{d}{du_0} u_e(u_0(\gamma)) \frac{d}{d\gamma} u_0(\gamma)} = \frac{q'_H(0)}{q'_T(u_2)} \frac{1}{\lim_{\gamma \rightarrow \infty} \frac{q_H(u_0(\gamma))}{q_T(u_e(\gamma))}},$$

where we used equation (4.17). Thus, multiplying by  $\lim_{\gamma \rightarrow \infty} \frac{q_H(u_0(\gamma))}{q_T(u_e(\gamma))}$  and taking the squareroot yields the result. We have to choose the negative root, because  $\frac{q_H(u_0(\gamma))}{q_T(u_e(\gamma))}$  is negative for all  $\gamma$ .  $\square$

**Lemma 5.3.11.** *For  $\bar{u} = u^*$  we calculate the limit*

$$\lim_{\gamma \rightarrow \infty} u_0(\gamma) \sqrt{\gamma} = 0.$$

*Proof.* We multiply the relation  $T(u^*, u_0(\gamma)) = 1$  by  $\sqrt{\gamma}$  and obtain

$$\frac{1}{\sqrt{2}} \int_{u_0(\gamma)}^{u^*} \frac{du}{\sqrt{F(h_H(u_0(\gamma))) - F(h_H(u))}} + \frac{1}{\sqrt{2}} \int_{u^*}^{u_e(\gamma)} \frac{du}{\sqrt{F(h_T(u_e(\gamma))) - F(h_T(u))}} = \sqrt{\gamma}.$$

The left hand side of this equation is only implicitly depending on  $\gamma$ , thus calculating the derivative with respect to  $\gamma$  and using Lemma 5.3.6 and Corollary 5.3.8 yields

$$\begin{aligned} \frac{d}{du_0} \left( \frac{1}{\sqrt{2}} \int_{u_0(\gamma)}^{u^*} \frac{du}{\sqrt{F(h_H(u_0(\gamma))) - F(h_H(u))}} \right) \frac{d}{d\gamma} u_0(\gamma) \\ + \frac{d}{du_e} \left( \frac{1}{\sqrt{2}} \int_{u^*}^{u_e(\gamma)} \frac{du}{\sqrt{F(h_T(u_e(\gamma))) - F(h_T(u))}} \right) \frac{d}{du_0} u_e(u_0(\gamma)) \frac{d}{d\gamma} u_0(\gamma) &= \frac{1}{2\sqrt{\gamma}} \\ \left( \frac{1}{\sqrt{|q'_H(0)|}} \frac{-1}{u_0(\gamma)} + \frac{1}{\sqrt{|q'_H(0)|}} \frac{1}{u_0(\gamma)} \frac{q_H(u_0(\gamma))}{q_T(u_e(u_0(\gamma)))} + o\left(\frac{1}{u_0(\gamma)}\right) \right) \frac{d}{d\gamma} u_0(\gamma) &= \frac{1}{2\sqrt{\gamma}} \\ \left( -1 + \frac{q_H(u_0(\gamma))}{q_T(u_e(u_0(\gamma)))} + o(1) \right) \left( \frac{1}{\sqrt{|q'_H(0)|}} \frac{1}{u_0(\gamma)} \right) \frac{d}{d\gamma} u_0(\gamma) &= \frac{1}{2\sqrt{\gamma}}. \end{aligned}$$

We are interested in the behaviour of  $u_0(\gamma)$  for  $\gamma$  tending to infinity. Therefore, we calculate the limit

$$\lim_{\gamma \rightarrow \infty} \left( -1 + \frac{q_H(u_0(\gamma))}{q_T(u_e(u_0(\gamma)))} + o(1) \right) = -1 - \sqrt{\frac{q'_H(0)}{q'_T(u_2)}} = \frac{-(\sqrt{|q'_H(0)|} + \sqrt{|q'_T(u_2)|})}{\sqrt{|q'_T(u_2)|}}.$$

For large  $\gamma$  the function  $u_0(\gamma)$  is approximately given by the differential equation

$$\frac{d}{d\gamma} u_0(\gamma) = - \frac{\sqrt{|q'_H(0)|} \sqrt{|q'_T(u_2)|}}{\sqrt{|q'_H(0)|} + \sqrt{|q'_T(u_2)|}} \frac{u_0(\gamma)}{2\sqrt{\gamma}}.$$

Thus, we obtain

$$u_0(\gamma) = \exp \left( - \frac{\sqrt{|q'_H(0)|} \sqrt{|q'_T(u_2)|}}{\sqrt{|q'_H(0)|} + \sqrt{|q'_T(u_2)|}} \sqrt{\gamma} \right)$$

In particular, we calculate the limit  $\lim_{\gamma \rightarrow \infty} u_0(\gamma) \sqrt{\gamma} = 0$ . □

**Proposition 5.3.12.** *The derivative of the layer position evaluated at  $\bar{u} = u^*$  tends to minus infinity for  $\gamma$  tending to infinity.*

$$\frac{d}{d\bar{u}} \bar{x}(u^*) \rightarrow -\infty \quad \text{for } \gamma \rightarrow \infty.$$

*Proof.* We consider again  $u_0(\gamma)$  as a function of  $\gamma$  for the fixed jump  $u^*$ . We know from Proposition 5.2.1 that the derivative of the time-map at  $\bar{u} = u^*$  is given by

$$\begin{aligned} \frac{d}{d\bar{u}}\bar{x}(u^*) &= \frac{1}{\sqrt{2\gamma}} \frac{1}{\sqrt{Q(u^*, u_0(\gamma)) - Q(u^*, u^*)}} \\ &+ \frac{(q_H(u^*) - q_T(u^*)) \frac{\partial}{\partial u_e} T_2(u^*, u_e(\gamma)) \frac{\partial}{\partial u_0} T_1(u^*, u_0(\gamma))}{q_T(u_e(\gamma)) \frac{\partial}{\partial u_0} T_1(u^*, u_0(\gamma)) + q_H(u_0(\gamma)) \frac{\partial}{\partial u_e} T_2(u^*, u_e(\gamma))}. \end{aligned}$$

The limit of the first term in this expression is zero,

$$\lim_{\gamma \rightarrow \infty} \frac{1}{\sqrt{2\gamma}} \frac{1}{\sqrt{Q(u^*, u_0(\gamma)) - Q(u^*, u^*)}} = 0,$$

because  $\frac{1}{\sqrt{Q(u^*, u_0(\gamma)) - Q(u^*, u^*)}}$  is bounded by  $\frac{1}{\sqrt{-Q(u^*, u^*)}}$ . We use Lemma 5.3.6 and Corollary 5.3.8 to replace the derivatives of the time-maps in the second term.

$$\begin{aligned} &\frac{(q_H(u^*) - q_T(u^*)) \frac{\partial}{\partial u_e} T_2(u^*, u_e(\gamma)) \frac{\partial}{\partial u_0} T_1(u^*, u_0(\gamma))}{q_T(u_e(\gamma)) \frac{\partial}{\partial u_0} T_1(u^*, u_0(\gamma)) + q_H(u_0(\gamma)) \frac{\partial}{\partial u_e} T_2(u^*, u_e(\gamma))} \\ &= \frac{(q_H(u^*) - q_T(u^*)) \left( \frac{1}{\sqrt{\gamma}} \frac{1}{\sqrt{|q'_H(u_0(\gamma))|}} \frac{1}{u_0(\gamma)} + o\left(\frac{1}{\sqrt{\gamma} u_0(\gamma)}\right) \right) \left( -\frac{1}{\sqrt{\gamma}} \frac{1}{\sqrt{|q'_H(0)|}} \frac{1}{u_0(\gamma)} + o\left(\frac{1}{\sqrt{\gamma}}\right) \right)}{q_T(u_e(\gamma)) \left( -\frac{1}{\sqrt{\gamma}} \frac{1}{\sqrt{|q'_H(0)|}} \frac{1}{u_0(\gamma)} + o\left(\frac{1}{\sqrt{\gamma}}\right) \right) + q_H(u_0(\gamma)) \left( \frac{1}{\sqrt{\gamma}} \frac{1}{\sqrt{|q'_H(0)|}} \frac{1}{u_0(\gamma)} + o\left(\frac{1}{\sqrt{\gamma} u_0(\gamma)}\right) \right)} \\ &= \frac{-(q_H(u^*) - q_T(u^*)) \left( \frac{1}{\sqrt{\gamma}} \frac{1}{\sqrt{|q'_H(0)|}} \frac{1}{u_0(\gamma)} + o\left(\frac{1}{\sqrt{\gamma} u_0(\gamma)}\right) \right)^2}{(q_H(u_0(\gamma)) - q_T(u_e(\gamma))) \left( \frac{1}{\sqrt{\gamma}} \frac{1}{\sqrt{|q'_H(0)|}} \frac{1}{u_0(\gamma)} + o\left(\frac{1}{\sqrt{\gamma} u_0(\gamma)}\right) \right)} \\ &= \frac{(q_T(u^*) - q_H(u^*)) \left( \frac{1}{\sqrt{\gamma}} \frac{1}{\sqrt{|q'_H(0)|}} \frac{1}{u_0(\gamma)} + o\left(\frac{1}{\sqrt{\gamma} u_0(\gamma)}\right) \right)}{(q_H(u_0(\gamma)) - q_T(u_e(\gamma)))}. \end{aligned}$$

Finally, we use Lemma 5.3.11 to calculate the limit

$$\begin{aligned} \lim_{\gamma \rightarrow \infty} \frac{d}{d\bar{u}}\bar{x}(u^*) &= 0 + \frac{q_T(u^*) - q_H(u^*)}{\sqrt{|q'_H(0)|}} \lim_{\gamma \rightarrow \infty} \frac{1}{u_0(\gamma) \sqrt{\gamma}} \lim_{\gamma \rightarrow \infty} \frac{1}{q_H(u_0(\gamma)) - q_T(u_e(\gamma))} \\ &= \infty \cdot (-\infty) = -\infty \end{aligned}$$

□

Hence, we have confirmed which can be observed in simulations.

The steepness of the slope of  $\bar{x}(\bar{u})$  also shows that for a small interval of  $\bar{u}$  around  $u^*$ , a large range of layer positions is attained.

**Theorem 5.3.13.** *We consider the generic model in the hysteresis case with admissible kinetic functions and such that there exist the value  $u^*$ . Moreover, we require  $u^* \in (u_T^{cr}, u_H^{cr})$ . Under these conditions the following holds.*

*For every  $\delta > 0$  small, there is a diffusion coefficient  $\frac{1}{\gamma}$  such that for all*

$$\bar{x} \in (\delta, 1 - \delta)$$

*there is a unique monotone increasing and a unique monotone decreasing stationary solution with jump at  $\bar{x}$ . Moreover, these solutions are stable.*

*Proof.* We choose an  $\epsilon$ , such that  $(u^* - \epsilon, u^* + \epsilon) \subset (u_T^{cr}, u_H^{cr})$  holds.  $\bar{x}(u^* - \epsilon)$  tends to 1 and  $\bar{x}(u^* + \epsilon)$  tends to 0 for  $\gamma \rightarrow \infty$  (Theorem 5.3.1). Therefore, let  $\gamma_1$  such that  $\bar{x}(u^* - \epsilon) > 1 - \delta$  for all  $\gamma > \gamma_1$ . Similarly, let  $\gamma_2$  such that  $\bar{x}(u^* + \epsilon) < \delta$  for all  $\gamma > \gamma_2$ . For  $\gamma > \max\{\gamma_1, \gamma_2\}$  we obtain that  $(\delta, 1 - \delta) \subset I^{cr}(\gamma)$ , which leads to the result because of Theorem 5.2.3.  $\square$

## 5.4 Irregular solutions

So far, we have considered only monotone stationary solutions. But, in Figure 4.5d we observed the formation of a nonmonotone stationary solution.

In this section, we use the monotone solutions to construct all stationary solutions of the generic model in the hysteresis case.

At first, we construct solutions, which are periodic in space.

**Corollary 5.4.1.** *For the generic model in the hysteresis case, there are exactly two nonhomogeneous stationary solution  $(U(x), V(x))$ , which are periodic with  $k$  modes for all diffusion coefficients  $\frac{1}{\gamma}$ . Restricted to the interval  $[0, \frac{1}{k}]$  one of them is monotone increasing, whereas the other one is monotone decreasing.*

*Proof.* The proof of existence is identically to the one in the bistable case, compare Corollary 3.1.2. The uniqueness follows from the uniqueness of the monotone increasing solution.  $\square$

**Corollary 5.4.2.** *A periodic solution  $(U(x), V(x))$  with  $k$  modes and jump at  $\bar{u}$  has  $k$  layer positions  $\bar{x}^1, \dots, \bar{x}^k$ , where the first one is given by*

$$\bar{x}^1 = \begin{cases} T_1(\bar{u}, u_0) & \text{if } u_0 < \bar{u} \\ T_2(\bar{u}, u_0) & \text{if } u_0 > \bar{u} \end{cases}$$

where  $u_0 := U(0)$ . The other layer positions are given by

$$\bar{x}^i = \begin{cases} \frac{i}{k} - \bar{x}^1 & \text{for } i \text{ even} \\ \frac{i-1}{k} + \bar{x}^1 & \text{for } i \text{ odd.} \end{cases}$$

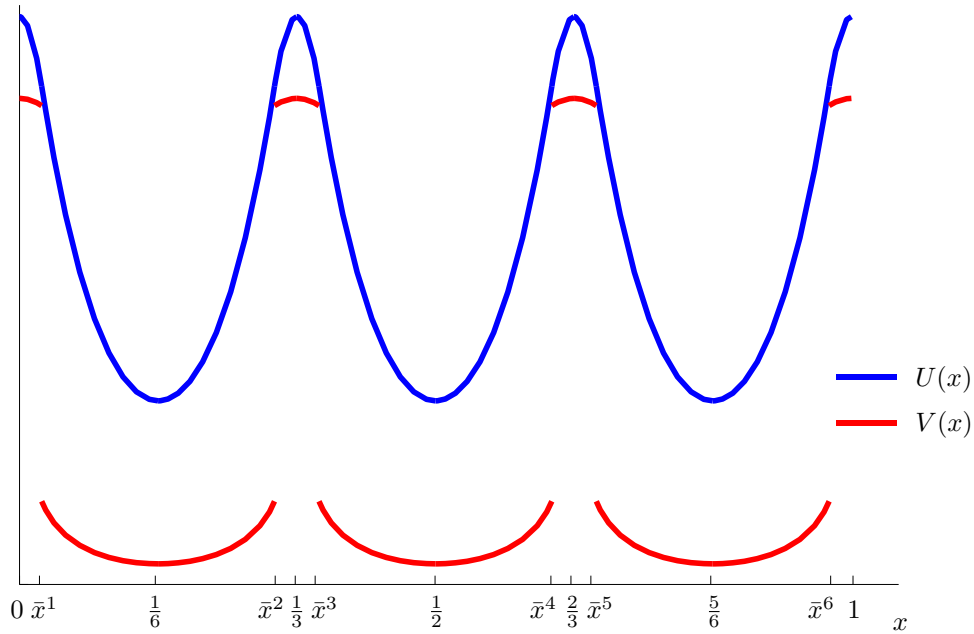


Figure 5.6: A periodic stationary solution  $(U(x), V(x))$  with six modes, which is decreasing on  $(0, \frac{1}{6})$ . We observe that the layer positions are determined by  $\bar{x}^1 + \bar{x}^2 = \frac{1}{3}$ ,  $\bar{x}^3 = \bar{x}^1 + \frac{1}{3}$ ,  $\bar{x}^4 = \bar{x}^2 + \frac{1}{3}$ ,  $\bar{x}^5 = \bar{x}^1 + \frac{2}{3}$  and  $\bar{x}^6 = \bar{x}^2 + \frac{2}{3}$ .

*Proof.* For a periodic solution the first layer position is calculated using the results for monotone solutions. The second one is then given by  $\frac{2}{k} - \bar{x}^1$  because for a periodic solution with  $k$  modes  $U(x) = U(\frac{2}{k} - x)$  holds for  $x \in [\frac{1}{k}, \frac{2}{k}]$ . All other can be calculated by adding successively  $\frac{2}{k}$ , which yields the formula stated above.  $\square$

Additionally to the periodic pattern, in the model with hysteresis there exists another class of stationary solutions. It is a consequence from the fact that the phase planes of  $\frac{1}{\gamma}U_{xx} + q_H(U) = 0$  and  $\frac{1}{\gamma}U_{xx} + q_T(U) = 0$  are overlapping. For a periodic solution the switch between these phase planes takes always place at the same value  $\bar{u}$ , as one can see for the blue trajectory in Figure 5.7. However, a similar construction of discontinuous patterns can be performed with switches at different values  $\bar{u}^1, \bar{u}^2, \dots$  as one can see for the red trajectory in Figure 5.7. Then there exist subintervals of  $[0, 1]$  such that the solution restricted to them is monotone stationary solution with jump at  $\bar{u}^1, \bar{u}^2, \dots$  respectively.

We remind that the time-map  $T(\bar{u}, u_0)$  is defined as the time a monotone stationary solution with jump at  $\bar{u}$  needs to connect  $u_0$  with  $u_e(u_0, \bar{u})$ . This time is the same for monotone increasing and decreasing solutions. Thus,  $T(\bar{u}, u_0)$  is defined for  $u_0 < \bar{u}$

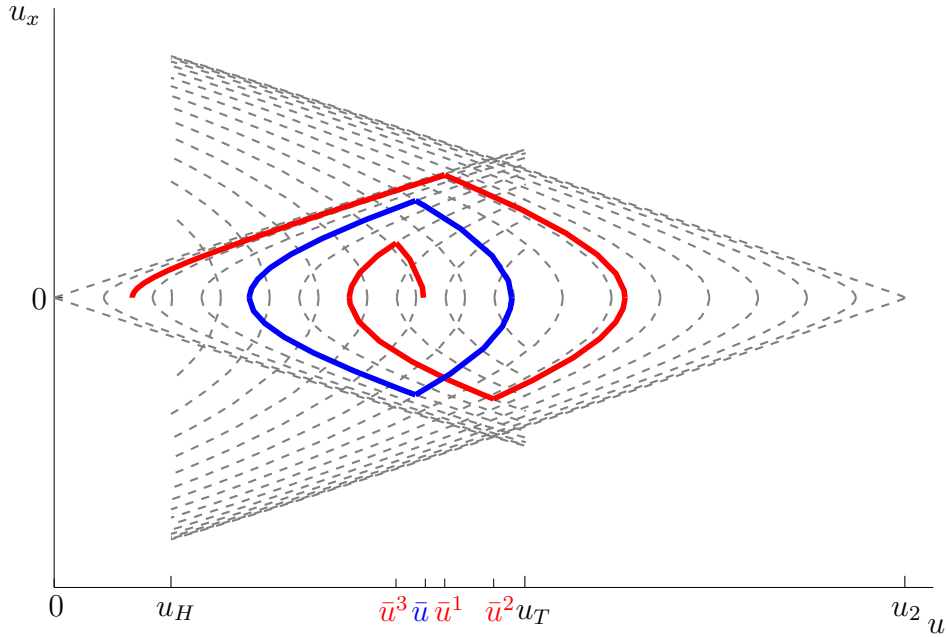


Figure 5.7: The phase planes of  $\frac{1}{\gamma}U_{xx} + q_H(U) = 0$  and  $\frac{1}{\gamma}U_{xx} + q_T(U) = 0$  are overlapping. In blue we see a periodic solution with jump at  $\bar{u}$ . We cannot determine the mode of a periodic solution in the phase plane. It corresponds to how often the trajectory has been traveled through. In red we see a irregular solution with three different jumps.

as well as for  $u_0 > \bar{u}$  (see Remark 4.3.3). However,  $T_1(\bar{u}, u_0)$  is only defined for  $u_0 < \bar{u}$  and  $T_2(\bar{u}, u_e)$  is only defined for  $u_e > \bar{u}$ .

**Definition:** A pair of functions  $(U(x), V(x)) \in C^1([0, 1]) \cap H_N^2(0, 1) \times L^\infty(0, 1)$  is called **irregular stationary solution** with jumps at  $\bar{u}^1, \bar{u}^2, \dots, \bar{u}^k$  of system (2.1) in the hysteresis case, if there are values

$$x^0 = 0 < x^1 < \dots < x^i < x^{i+1} < \dots < x^{k-1} < 1 = x^k$$

and jumps  $\bar{u}^i \in (u_T, \min(u_H, u_2))$ , for  $i = 1, \dots, k$ , such that the restriction of  $U$  to the intervals  $[x^{i-1}, x^i]$  are alternately monotone increasing and monotone decreasing. Thereby,  $U|_{[x^{i-1}, x^i]}$  is given by

$$U(x) := \tilde{U}^i\left(\frac{x - x^{i-1}}{x^i - x^{i-1}}\right) \quad \text{for } x \in [x^{i-1}, x^i], \tag{5.34}$$

where  $\tilde{U}^i(x)$  is a monotone increasing (resp. decreasing) weak solution of the equa-

tion

$$\frac{1}{(x^i - x^{i-1})^2 \gamma} \tilde{U}_{xx}^i(\tilde{x}) + q_{\tilde{u}^i}(\tilde{U}^i(\tilde{x})) = 0, \quad (5.35)$$

for  $\tilde{x} \in [0, 1]$  and with the boundary condition  $\tilde{U}_x^i(0) = \tilde{U}_x^i(1) = 0$ . We denote the start and end values of each such solution by

$$\tilde{U}^i(0) =: u_0^i \quad \text{and} \quad \tilde{U}^i(1) =: u_e^i. \quad (5.36)$$

The  $V$ -component of an irregular solution is given by

$$V(x) = \begin{cases} h_H(U(x)) & \text{for } x \in [x^{i-1}, x^i] \text{ if } U(x) \leq \bar{u}^i \\ h_T(U(x)) & \text{for } x \in [x^{i-1}, x^i] \text{ if } U(x) > \bar{u}^i. \end{cases} \quad (5.37)$$

**Proposition 5.4.3.** *Let  $(U(x), V(x))$  be an irregular solution with jumps at  $\bar{u}^1, \bar{u}^2, \dots, \bar{u}^k$ . Then, it holds*

$$u_e^i = u_0^{i+1} \quad (5.38)$$

for all  $i = 0, \dots, k-1$ .

Moreover, the time-maps have to fulfil the relation

$$\sum_{i=1}^k T(\bar{u}^i, u_0^i) = 1. \quad (5.39)$$

*Proof.* The function  $U(x)$  has to be continuously differentiable, therefore the solutions constructed on each subinterval  $[x^{i-1}, x^i]$  have to be connected to each other. By definition (5.36) and equation (5.34),  $u_e^i$  is the value of  $U(x^i) = \tilde{U}^i(1)$ . But,  $U(x^i)$  is also given by  $\tilde{U}^{i+1}(0)$  which leads to the condition (5.38).

The relation (5.39) has to be fulfilled, because an irregular solution has to be a solution on the interval  $[0, 1]$ .  $\square$

**Proposition 5.4.4.** *There are at most two irregular stationary solutions with jumps at  $\bar{u}^1, \dots, \bar{u}^k$ . Restricted to the first subinterval  $[0, x^1]$  one of them is monotone increasing and the other one is monotone decreasing.*

*Proof.* At first, we remark that for a given partition of the interval  $0, x^1, \dots, x^{k-1}, 1$  of the interval  $[0, 1]$  and fixed monotonicity of the interval  $[0, x^1]$  an irregular solution with jumps at  $\bar{u}^1, \dots, \bar{u}^k$  is unique. This is clear as  $U|_{[x^{i-1}, x^i]}$  is given by formula (5.34) and the function  $\tilde{U}^i$  is the unique monotone increasing (resp. decreasing) solution of equation (5.35). Now, observe that

$$\frac{1}{\gamma} U_{xx}(x) = \frac{1}{(x^i - x^{i-1})^2 \gamma} \tilde{U}_{xx}^i \left( \frac{x^{i-1} - x}{x^{i-1} - x^i} \right)$$

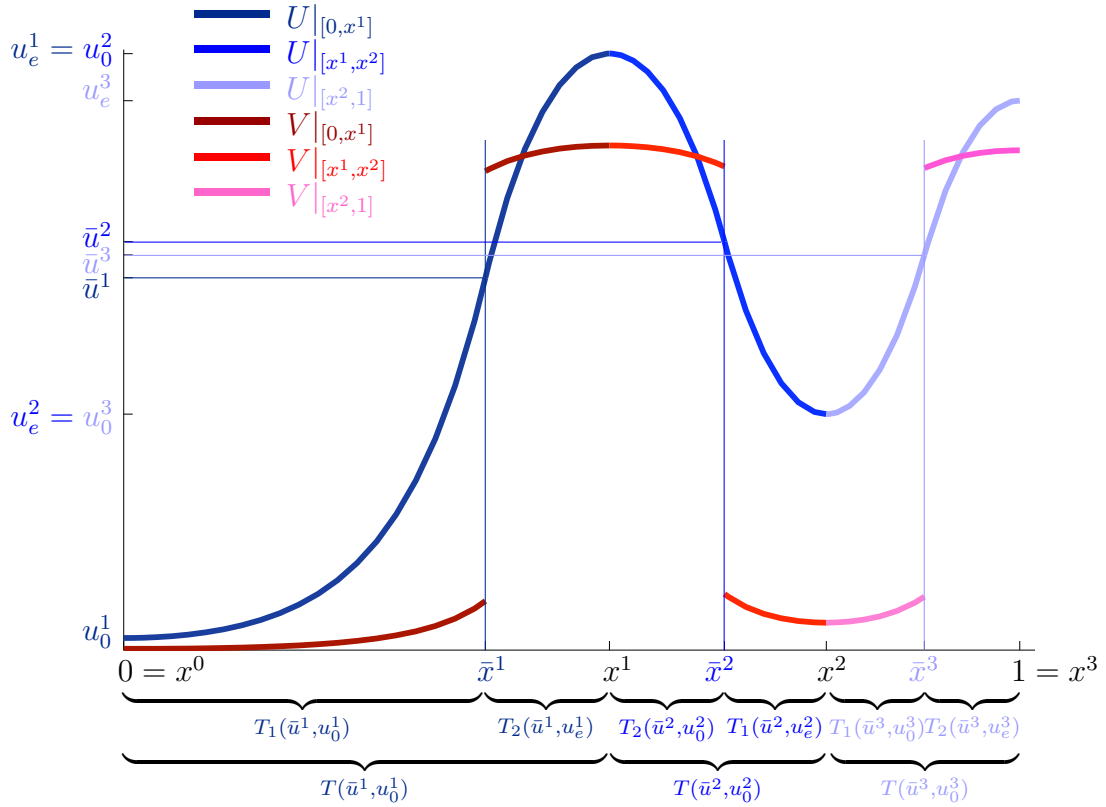


Figure 5.8: An irregular solution  $(U(x), V(x))$  with three jumps  $\bar{u}^1, \bar{u}^2, \bar{u}^3$ , which is monotone increasing restricted to  $[0, x^1]$ . We see that for continuity of  $U(x)$  we need to have  $u_e^1 = u_0^2$  and  $u_e^2 = u_0^3$  fulfilled. Furthermore, we see how the partition of the interval is determined:  $x^1 = T(\bar{u}^1, u_0^1), x^2 = x^1 + T(\bar{u}^2, u_0^2)$  and  $1 = x^2 + T(\bar{u}^3, u_0^3)$ . And the layer positions are given by  $\bar{x}^1 = T_1(\bar{u}^1, u_0^1)$  and  $\bar{x}^3 = x^2 + T_1(\bar{u}^3, u_0^3)$ , because  $U(x)$  is increasing on the corresponding subintervals and  $\bar{x}^2 = x^1 + T_2(\bar{u}^2, u_0^2) = x^2 - T_1(\bar{u}^2, u_0^3)$ .

holds, which yields the scaling of the diffusion coefficient and shows that  $U|_{[x^{i-1}, x^i]}$  is a solution of system (4.1) with jump at  $\bar{u}^i$  restricted to the interval  $[x^{i-1}, x^i]$ .

Thus, for proving the proposition, it will be enough to show that for a fixed set of jumps  $\bar{u}^1, \dots, \bar{u}^k$  and prescribed monotonicity on the first subinterval, there is only one possible partition of the interval  $[0, 1]$ .

Looking at the phase plane (Compare Figure 5.7), we see that an irregular solution which is increasing on  $[x^{i-1}, x^i]$  has to be decreasing on  $[x^i, x^{i+1}]$  and vice versa. Therefore, if  $u_0^i < \bar{u}^i$ , then  $u_0^{i+1} > \bar{u}^{i+1}$  and vice versa. Moreover, using the relation

$u_e^i = u_0^{i+1}$ , there is the connection

$$Q(\bar{u}^i, u_0^i) = Q(\bar{u}^i, u_0^{i+1}) \quad (5.40)$$

between two consecutive values  $u_0^i$ . Fixing the value  $u_0^1$ , this successively determines  $u_0^i$  for  $i = 2, \dots, k$ . Hence, the following sum of time-maps is well-defined

$$T(\bar{u}^1, \dots, \bar{u}^k, u_0^1) := T(\bar{u}^1, u_0^1) + T(\bar{u}^2, u_0^2) + \dots + T(\bar{u}^k, u_0^k).$$

We observe that in this sum all values  $u_0^i$  which are larger than the corresponding  $\bar{u}^i$  can be replaced by  $u_0^{i+1} < \bar{u}^i$ . This follows from the condition  $u_e^i = u_0^{i+1}$  and equation (5.40). Therefore, it holds

$$T(\bar{u}^i, u_0^i) = T(\bar{u}^i, u_0^{i+1})$$

if  $u_0^i > \bar{u}^i$ .

In the case that  $U_{[0,x^1]}$  is monotone increasing, the sum of the time-maps can be rewritten as

$$T(\bar{u}^1, \dots, \bar{u}^k, u_0^1) = T(\bar{u}^1, u_0^1) + T(\bar{u}^2, u_0^3) + T(\bar{u}^3, u_0^3) + T(\bar{u}^4, u_0^5) + T(\bar{u}^5, u_0^5) + \dots$$

Now, we set the index  $i$  in equation (5.40) to 1 and 2, and derivate the equality with respect to  $u_0^1$ . We obtain the relations

$$q_H(u_0^1) = \frac{d}{du_0^1}(u_0^2) \cdot q_T(u_0^2) \quad \text{and} \quad \frac{d}{du_0^1}(u_0^2) \cdot q_T(u_0^2) = \frac{d}{du_0^1}(u_0^3) \cdot q_H(u_0^3),$$

which yields

$$\frac{d}{du_0^1}u_0^3 = \frac{q_H(u_0^1)}{q_H(u_0^3)} > 0.$$

Repeating this procedure for increasing indices, we obtain for all odd  $i$  that it holds

$$\frac{d}{du_0^1}u_0^i = \frac{q_H(u_0^1)}{q_H(u_0^i)} > 0. \quad (5.41)$$

Finally, we calculate the derivative of the time-map

$$\begin{aligned} \frac{\partial}{\partial u_0^1}T(\bar{u}^1, \dots, \bar{u}^k, u_0^1) &= \frac{\partial}{\partial u_0^1}T(\bar{u}^1, u_0^1) + \frac{\partial}{\partial u_0^1}T(\bar{u}^2, u_0^3) + \frac{\partial}{\partial u_0^1}T(\bar{u}^3, u_0^3) + \dots \\ &= \frac{\partial}{\partial u_0^1}T(\bar{u}^1, u_0^1) + \frac{q_H(u_0^1)}{q_H(u_0^3)} \frac{\partial}{\partial u_0^3}T(\bar{u}^2, u_0^3) + \frac{q_H(u_0^1)}{q_H(u_0^3)} \frac{\partial}{\partial u_0^3}T(\bar{u}^3, u_0^3) + \dots < 0, \end{aligned}$$

which is negative using Theorem 4.3.10 and the positivity of relation (5.41).

This result yields the uniqueness of a value  $u_0^1$  such that

$$T(\bar{u}^1, \dots, \bar{u}^k, u_0^1) = 1$$

holds, which in turn determines uniquely the partition of the interval  $[0, 1]$ . Indeed the subintervals  $[x^{i-1}, x^i]$  are given by

$$x^i = \sum_{j=1}^i T(\bar{u}^j, u_0^j). \tag{5.42}$$

This proves the uniqueness of an irregular solution having jumps at  $\bar{u}^1, \bar{u}^2, \dots, \bar{u}^k$  which is monotone increasing on  $[0, x^1]$ .

In the case that  $U_{[0, x^1]}$  is monotone decreasing the sum of the time-maps is given by

$$T(\bar{u}^1, \dots, \bar{u}^k, u_0^2) = T(\bar{u}^1, u_0^2) + T(\bar{u}^2, u_0^2) + T(\bar{u}^3, u_0^4) + T(\bar{u}^4, u_0^4) + \dots$$

Using again equation (5.40), we show that all  $u_0^i$  are determined by  $u_0^2$  and that

$$\frac{d}{du_0^2} u_0^i = \frac{q_H(u_0^2)}{q_H(u_0^i)} > 0.$$

holds for all even  $i$ . This yields

$$\frac{\partial}{\partial u_0^2} T(\bar{u}^1, \dots, \bar{u}^k, u_0^2) < 0$$

and we accomplish the proof in the same way as we did in the case of an irregular solution which is monotone increasing in  $[0, x^1]$ . □

**Corollary 5.4.5.** *An irregular solution with jumps at  $\bar{u}^1, \bar{u}^2, \dots, \bar{u}^k$  has  $k$  layer positions  $\bar{x}^1, \bar{x}^2, \dots, \bar{x}^k$ . They are given by the formula*

$$\bar{x}^i = \begin{cases} x^{i-1} + T_1(\bar{u}^i, u_0^i) & \text{if } u_0^i < \bar{u}^i, \\ x^i - T_1(\bar{u}^i, u_0^{i+1}) & \text{if } u_0^i > \bar{u}^i. \end{cases}$$

*Proof.* There is exactly one layer position  $\bar{x}^i$  in every subinterval  $[x^{i-1}, x^i]$ . Depending on the monotonicity of  $U|_{[x^{i-1}, x^i]}$  the layer position is given by  $x^{i-1} + T_1(\bar{u}^i, u_0^i)$  and  $x^{i-1} + T_2(\bar{u}^i, u_0^i)$ , resp. We observe that by definition and because of formula (5.42)

$$\begin{aligned} x^i &= x^{i-1} + T(\bar{u}^i, u_0^i) = x^{i-1} + T_1(\bar{u}^i, u_0^i) + T_2(\bar{u}^i, u_0^i), \\ &= x^{i-1} + T_1(\bar{u}^i, u_0^{i+1}) + T_2(\bar{u}^i, u_0^i) \end{aligned}$$

holds. Thus, if  $U|_{[x^{i-1}, x^i]}$  is monotone decreasing the layer condition is given by

$$\bar{x}^i = x^{i-1} + T_2(\bar{u}^i, u_0^i) + T_1(\bar{u}^i, u_0^{i+1}) - T_1(\bar{u}^i, u_0^{i+1}) = x^i - T_1(\bar{u}^i, u_0^{i+1}).$$

□

Having showed the uniqueness of irregular solutions, we now turn our attention to their existence. The proof is not as obvious as it might seem. Actually there is not necessarily for every set of jumps and every diffusion coefficient  $\frac{1}{\gamma}$  an irregular solution. To see the problem that occurs we consider the following situation.

**Example 5.4.6.** *We consider kinetic functions, such that there is  $u^*$  with  $Q(u^*, u_2) = 0$ . We choose jumps  $\bar{u}^1 < u^* < \bar{u}^2$  and, therefore, it holds*

$$Q(\bar{u}^1, u_2) > 0 \quad \text{and} \quad Q(\bar{u}^2, u_2) < 0.$$

*We remind that to construct an irregular solution with jumps  $\bar{u}^1$  and  $\bar{u}^2$  we need to find values  $u_0^1, u_e^1, u_0^2$  and  $u_e^2$  fulfilling*

$$\tilde{U}^1(0) = u_0^1, \quad \tilde{U}^1(1) = u_e^1, \quad \tilde{U}^2(0) = u_0^2 \quad \text{and} \quad \tilde{U}^2(1) = u_e^2,$$

*where  $\tilde{U}^1$  and  $\tilde{U}^2$  are monotone solutions of equation (5.35). We require  $U(x)$  to be continuously differentiable and therefore the condition*

$$u_e^1 \stackrel{!}{=} u_0^2$$

*has to be fulfilled.*

*Here, we require  $U|_{[0, x^1]}$  to be monotone increasing, then  $\tilde{U}^1$  has to be increasing and  $\tilde{U}^2$  decreasing. Hence, the possible ranges for  $u_e^1$  and  $u_0^2$  are given by*

$$\bar{u}^1 < u_e^1 < u_{\max}^1 < u_2 \quad \text{and} \quad \bar{u}^2 < u_0^2 < u_2$$

*where  $u_{\max}^1 = u_{\max}(\bar{u}^1) < u_2$ , because of the assumption  $Q(\bar{u}^1, u_2) > 0$  (See Proposition 5.1.3).*

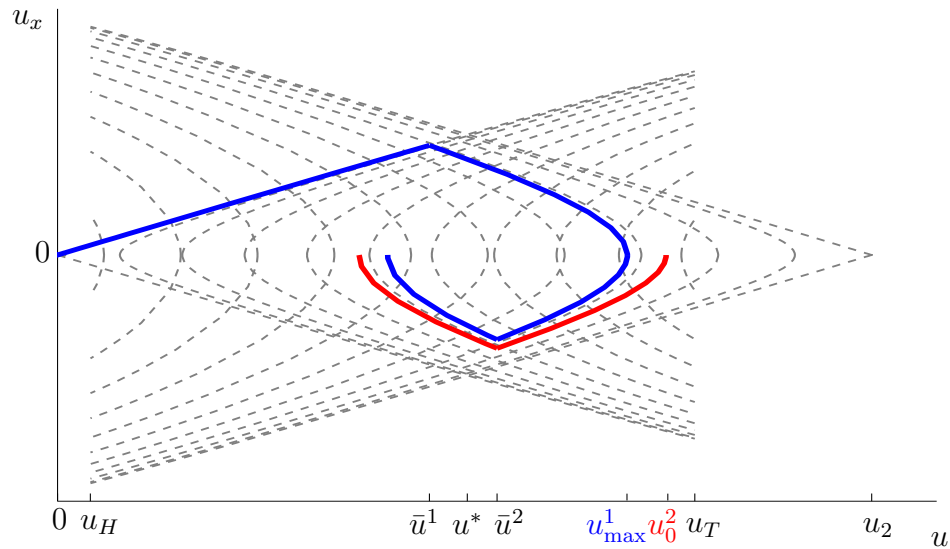
*For  $\gamma$  small, it is possible to find these values. But, for  $\gamma$  increasing the value  $u_0^2$  tends towards  $u_2$ , whereas  $u_e^1$  is bounded by  $u_{\max}^1$ . Hence, there will be a value  $\gamma_{\max}^1(\bar{u}^1, \bar{u}^2)$  such that an irregular solution with jumps at  $\bar{u}^1, \bar{u}^2$  which is monotone increasing on  $[0, x^1]$  does not exist for diffusion coefficients  $\frac{1}{\gamma}$ , with  $\gamma > \gamma_{\max}^1(\bar{u}^1, \bar{u}^2)$ . Compare Figure 5.9a for the phase plane of this situation.*

**Example 5.4.7.** *We consider again kinetic functions, such that there is  $u^*$ . The same kind of problem as described in example 5.4.6 occurs when we want to construct an irregular solution with jumps  $\bar{u}^1$  and  $\bar{u}^2$  which is monotone decreasing on  $[0, x^1]$ . In this situation the possible ranges for  $u_e^1$  and  $u_0^2$  are*

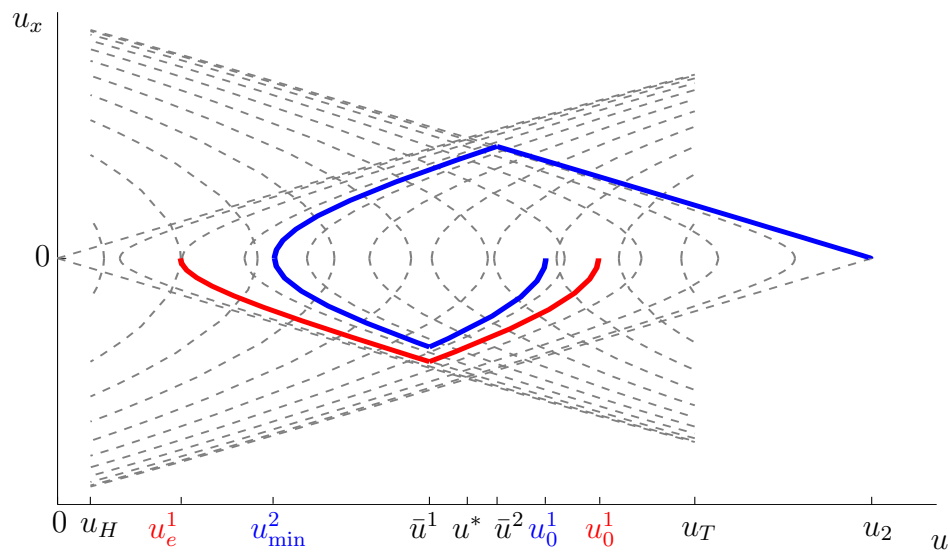
$$0 < u_e^1 < \bar{u}^1 \quad \text{and} \quad 0 < u_{\min}^2 < u_0^2 < \bar{u}^2,$$

*where  $0 < u_{\min}^2 = u_{\min}(\bar{u}^2)$ .*

*Thus, for  $\gamma$  increasing the value  $u_e^1$  tends to zero, whereas  $u_0^2$  is bounded from below by  $u_{\min}^2$ . Hence, there is a value  $\gamma_{\max}^2(\bar{u}^1, \bar{u}^2)$ , such that there is no irregular solution with jumps at  $\bar{u}^1$  and  $\bar{u}^2$ , which is monotone decreasing on  $[0, x^1]$  for diffusion coefficients  $\frac{1}{\gamma}$ , where  $\gamma > \gamma_{\max}^2(\bar{u}^1, \bar{u}^2)$ . Compare Figure 5.9b.*



(a) The phase plane shows a trajectory with jumps at  $\bar{u}^1, \bar{u}^2$ , such that  $U|_{[0,x^1]}$  is monotone increasing. It starts at  $u_0^1 = 10^{-6}$  and  $u_e^1$  is close to  $u_{\max}^1$ . For  $\gamma > \gamma_{\max}^1(\bar{u}^1, \bar{u}^2)$ , the solution  $(U(x), V(x))$  restricted to the interval  $[x^1, 1]$  corresponds to the red trajectory which cannot be connected with the upper part of the blue one, because  $u_0^2 > u_{\max}^1$ .



(b) The phase plane shows a trajectory with jumps at  $\bar{u}^1, \bar{u}^2$ , such that  $U|_{[0,x^1]}$  is monotone decreasing. If it starts at  $u_0^1 > \bar{u}^1$ , then the trajectory reaches  $u_e^1 < u_{\min}^2$  and can be connected with  $U|_{[x^1,1]}$ . For growing  $\gamma$  the solution restricted to the interval  $[0, x^1]$  corresponds to the red trajectory starting at  $u_0^1$  closer to  $u_2$ , which cannot be connected with a trajectory with a jump at  $\bar{u}^2$ , because here  $u_e^1 < u_{\min}^2$ .

Figure 5.9: Overlapping phase planes of  $\frac{1}{\gamma}U_{xx} + q_H(U) = 0$  and  $\frac{1}{\gamma}U_{xx} + q_T(U) = 0$  with trajectories which cannot be connected.

**Example 5.4.8.** Now, we compare the situation described in example 5.4.6 and 5.4.7 to the case where  $\bar{u}^1 < \bar{u}^2 < u^*$  and, therefore,

$$Q(\bar{u}^1, u_2) > Q(\bar{u}^2, u_2) > 0 \quad (5.43)$$

holds. For an irregular solution which is monotone increasing on  $[0, x^1]$  the same problem as before occurs. The ranges for  $u_e^1$  and  $u_0^2$  are given by

$$\bar{u}^1 < u_e^1 < u_{\max}^1 < u_2 \quad \text{and} \quad \bar{u}^2 < u_0^2 < u_{\max}^2 < u_2$$

The order  $u_{\max}(\bar{u}^1) = u_{\max}^1 < u_{\max}^2 = u_{\max}(\bar{u}^2)$  holds, because Proposition 5.1.1 shows that  $u_{\max}(\bar{u})$  is a monotone increasing function for  $\bar{u} < u^*$ . Again for  $\gamma$  sufficiently large  $u_0^2$  has to be closer to  $u_2$  then it is possible for  $u_e^1$ .

Nevertheless, an irregular solution which is monotone decreasing on  $[0, x^1]$  can always be constructed, because in this case  $u_e^1$  and  $u_0^2$  are both allowed to tend to zero.

**Definition:** We define the sets

$$\Gamma^1(\bar{u}^1, \bar{u}^2, \dots, \bar{u}^k) = \left\{ \gamma \mid \text{Problem (4.1) with diffusion coefficient } \frac{1}{\gamma} \text{ admits an irregular solution with jumps at } \bar{u}^1, \bar{u}^2, \dots, \bar{u}^k, \text{ which is monotone increasing on } [0, x^1]. \right\}$$

$$\Gamma^2(\bar{u}^1, \bar{u}^2, \dots, \bar{u}^k) = \left\{ \gamma \mid \text{Problem (4.1) with diffusion coefficient } \frac{1}{\gamma} \text{ admits an irregular solution with jumps at } \bar{u}^1, \bar{u}^2, \dots, \bar{u}^k, \text{ which is monotone decreasing on } [0, x^1]. \right\}$$

and denote the supremum of these sets by

$$\gamma_{\max}^1(\bar{u}^1, \bar{u}^2, \dots, \bar{u}^k) := \sup \Gamma^1(\bar{u}^1, \bar{u}^2, \dots, \bar{u}^k)$$

$$\gamma_{\max}^2(\bar{u}^1, \bar{u}^2, \dots, \bar{u}^k) := \sup \Gamma^2(\bar{u}^1, \bar{u}^2, \dots, \bar{u}^k).$$

We call these values **maximal diffusion coefficients**.

**Proposition 5.4.9.** If all  $\bar{u}^i = \bar{u}$  are equal, then the maximal diffusion coefficient is infinite.

$$\gamma_{\max}^2(\bar{u}, \bar{u}, \dots, \bar{u}) = \infty \quad \text{and} \quad \gamma_{\max}^1(\bar{u}, \bar{u}, \dots, \bar{u}) = \infty.$$

*Proof.* If all  $\bar{u}^i$  are equal, an irregular solution is a periodic solution, which exists for all diffusion coefficients. Compare Corollary 5.4.1.  $\square$

**Proposition 5.4.10.** *We consider the generic model in the hysteresis case and two jumps  $\bar{u}^1, \bar{u}^2 \in (u_T, \min(u_H, u_2))$ , which are not equal. If the jumps are such that  $Q(\bar{u}^1, u_2) \leq 0$  and  $Q(\bar{u}^2, u_2) \leq 0$ , then it holds*

$$\gamma_{\max}^1(\bar{u}^1, \bar{u}^2) = \infty,$$

*otherwise if the potential  $Q(\bar{u}^i, u_2)$  is positive at least for  $\bar{u}^1$  or  $\bar{u}^2$ , then*

$$\gamma_{\max}^1(\bar{u}^1, \bar{u}^2) < \infty.$$

*If  $\bar{u}^1$  and  $\bar{u}^2$  are such that  $Q(\bar{u}^1, u_2) \geq 0$  and  $Q(\bar{u}^2, u_2) \geq 0$ , then it holds*

$$\gamma_{\max}^2(\bar{u}^1, \bar{u}^2) = \infty,$$

*otherwise if the potential  $Q(\bar{u}^i, u_2)$  is negative at least for  $\bar{u}^1$  or  $\bar{u}^2$ , then*

$$\gamma_{\max}^2(\bar{u}^1, \bar{u}^2) < \infty.$$

*Proof.* We start by showing the construction of an irregular solution with jumps  $\bar{u}^1$  and  $\bar{u}^2$ , which is monotone increasing on  $[0, x^1]$ , when  $Q(\bar{u}^1, u_2) \leq 0$  and  $Q(\bar{u}^2, u_2) \leq 0$ . When  $U|_{[0, x^1]}$  is monotone increasing, we have the ranges  $\bar{u}^1 < u_e^1 < u_{\max}(\bar{u}^1)$  and  $\bar{u}^2 < u_0^2 < u_{\max}(\bar{u}^2)$  for the values  $u_e^1$ , resp.  $u_0^2$ . When  $Q(\bar{u}^1, u_2) \leq 0$  and  $Q(\bar{u}^2, u_2) \leq 0$  holds, then  $u_{\max}(\bar{u}^1) = u_{\max}(\bar{u}^2) = u_2$ . Thus, for all diffusion coefficients  $\frac{1}{\gamma}$  it is possible to find suitable values  $u_e^1 = u_0^2$  and to connect the solutions on the subintervals  $[0, x^1]$  and  $[x^1, 1]$ .

If at least for  $\bar{u}^1$  or  $\bar{u}^2$  it holds  $Q(\bar{u}^i, u_2) > 0$ , then  $\min\{u_{\max}(\bar{u}^1), u_{\max}(\bar{u}^2)\} < u_2$  and we obtain

$$\gamma_{\max}^1(\bar{u}^1, \bar{u}^2) = \sup\{\gamma > 0 \mid u_e^1(\gamma) = u_0^2(\gamma) < \min\{u_{\max}(\bar{u}^1), u_{\max}(\bar{u}^2)\}\}.$$

This supremum is finite. Indeed when we assume that  $\bar{u}^1 < \bar{u}^2$  then it holds  $u_{\max}(\bar{u}^1) < u_{\max}(\bar{u}^2)$ , because of Proposition 5.1.3. Therefore,  $u_e^1$  tends to  $u_{\max}(\bar{u}^2)$  for  $\gamma$  tending to infinity and reaches  $u_{\max}(\bar{u}^1)$  for some finite  $\gamma$ . For  $\bar{u}^1 > \bar{u}^2$ , we argue similarly.

Next, we show that we can always construct solutions with jumps  $\bar{u}^1$  and  $\bar{u}^2$  which is monotone decreasing on  $[0, x^1]$ , if  $Q(\bar{u}^1, u_2) \geq 0$  and  $Q(\bar{u}^2, u_2) \geq 0$ . When  $U|_{[0, x^1]}$  is monotone decreasing, we have the range  $u_{\min}(\bar{u}^1) < u_e^1 < \bar{u}^1$  and  $u_{\max}(\bar{u}^1) < u_0^2 < \bar{u}^2$  for the values  $u_e^1$  resp.  $u_0^2$ , which have to be equal. When  $Q(\bar{u}^1, u_2) \geq 0$  and  $Q(\bar{u}^2, u_2) \geq 0$  holds, then  $u_{\min}(\bar{u}^1) = u_{\min}(\bar{u}^2) = 0$ . Thus, there is a solution for all  $\gamma$ .

If  $Q(\bar{u}^1, u_2) < 0$  or  $Q(\bar{u}^2, u_2) < 0$ , then  $\max\{u_{\min}(\bar{u}^1), u_{\min}(\bar{u}^2)\} > 0$  and we obtain

$$\gamma_{\max}^2(\bar{u}^1, \bar{u}^2) = \sup\{\gamma > 0 \mid u_e^1(\gamma) = u_0^2(\gamma) > \max\{u_{\min}(\bar{u}^1), u_{\min}(\bar{u}^2)\}\},$$

which is finite using similar arguments as before. □

**Remark 5.4.11.** *The functions  $u_{\min}(\bar{u})$  and  $u_{\max}(\bar{u})$  are continuous because of Proposition 5.1.3. Therefore,  $\gamma_{\max}^1(\bar{u}^1, \bar{u}^2)$  and  $\gamma_{\max}^1(\bar{u}^1, \bar{u}^2)$  are bigger the more  $\bar{u}^1$  and  $\bar{u}^2$  are close to each other.*

*The most interesting case for us is when  $\bar{u}^1$  and  $\bar{u}^2$  are close to  $u^*$ , if it exists. Then both  $\gamma_{\max}^1(\bar{u}^1, \bar{u}^2)$  and  $\gamma_{\max}^1(\bar{u}^1, \bar{u}^2)$  are big, because  $u_{\min}$  is zero or close to it, whereas  $u_{\max}$  is  $u_2$  or close to it. Moreover, for  $\bar{u}^i$  close to  $u^*$  the corresponding layer position is in the interval  $[x^{i-1} + \delta, x^i - \delta]$  for some small  $\delta$  (Theorem 5.3.13). Thus, we have the biggest variety of irregular solutions if we choose all  $\bar{u}^i$  close to  $u^*$ .*

Next, we investigate the maximal diffusion coefficient for irregular solutions with more than two jumps.

**Proposition 5.4.12.** *It holds the following rule for changing the order of the jumps*

$$\gamma_{\max}^1(\bar{u}^1, \bar{u}^2, \dots, \bar{u}^k) = \begin{cases} \gamma_{\max}^1(\bar{u}^k, \bar{u}^{k-1}, \dots, \bar{u}^1) & \text{if } k \text{ is even,} \\ \gamma_{\max}^2(\bar{u}^k, \bar{u}^{k-1}, \dots, \bar{u}^1) & \text{if } k \text{ is odd} \end{cases}$$

and

$$\gamma_{\max}^2(\bar{u}^1, \bar{u}^2, \dots, \bar{u}^k) = \begin{cases} \gamma_{\max}^2(\bar{u}^k, \bar{u}^{k-1}, \dots, \bar{u}^1) & \text{if } k \text{ is even,} \\ \gamma_{\max}^1(\bar{u}^k, \bar{u}^{k-1}, \dots, \bar{u}^1) & \text{if } k \text{ is odd.} \end{cases}$$

*Proof.* We observe that if  $(\tilde{U}(x), \tilde{V}(x))$  is an irregular solution with jumps at  $\bar{u}^1, \bar{u}^2, \dots, \bar{u}^k$ , then we obtain an irregular solution  $(U(x), V(x))$  with jumps at  $\bar{u}^k, \bar{u}^{k-1}, \dots, \bar{u}^1$  by setting

$$U(x) := \tilde{U}(1-x) \quad \text{and} \quad V(x) := \tilde{V}(1-x).$$

Thus, if for a certain diffusion coefficient  $\frac{1}{\gamma}$  the solution  $(\tilde{U}(x), \tilde{V}(x))$  exists, also  $(U(x), V(x))$  exists. Now, we need to figure out if  $U(x)|_{[0, x^1]}$  is increasing or decreasing, thus the sign of  $U|_{[0, x^1]}$ . First, we observe that by definition  $U_x(x) = -\tilde{U}_x(1-x)$  holds. Thus, if  $k$  is even then

$$\text{sgn } U_x|_{[0, x^1]} = -\text{sgn } \tilde{U}_x|_{[x^{k-1}, 1]} = -(-\text{sgn } \tilde{U}_x|_{[0, x^1]})$$

holds, because an irregular solution is alternately monotone increasing and decreasing on consecutive subintervals  $[x^i, x^{i+1}]$ . Therefore, the sets  $\Gamma^{1/2}(\bar{u}^1, \bar{u}^2, \dots, \bar{u}^k)$  and  $\Gamma^{1/2}(\bar{u}^k, \bar{u}^{k-1}, \dots, \bar{u}^1)$  are equal.

Similarly, if  $k$  is odd then

$$\text{sgn } U_x|_{[0, x^1]} = -\text{sgn } \tilde{U}_x|_{[x^{k-1}, 1]} = -\text{sgn } \tilde{U}_x|_{[0, x^1]}$$

holds. Therefore,  $\Gamma^{1/2}(\bar{u}^1, \bar{u}^2, \dots, \bar{u}^k) = \Gamma^{2/1}(\bar{u}^k, \bar{u}^{k-1}, \dots, \bar{u}^1)$  holds.  $\square$

**Proposition 5.4.13.** *If  $k \geq 3$  we calculate*

$$\gamma_{\max}^j(\bar{u}^1, \dots, \bar{u}^k) = \min_{2 \leq i \leq k} \left\{ \frac{\gamma_{\max}^{\text{ind}(i,j)}(\bar{u}^{(i-1)}, \bar{u}^i)}{(x^i - x^{i-2})^2} \right\}$$

where  $j \in \{1, 2\}$  indicates the monotonicity on the first subinterval and

$$\text{ind}(i, j) = \begin{cases} 1 & \text{if } i + j \text{ is odd,} \\ 2 & \text{if } i + j \text{ is even.} \end{cases}$$

*Proof.* At first we remind that for a solution with jumps at  $\bar{u}^1, \dots, \bar{u}^k$  the partition  $0, x^1, \dots, x^{k-1}, 1$  of the interval  $[0, 1]$  is unique (Proposition 5.4.4). If the solution  $(U(x), V(x))$  with jumps at  $\bar{u}^1, \bar{u}^2, \dots, \bar{u}^k$  exists for a certain diffusion coefficient  $\frac{1}{\gamma}$ , then its restriction to the interval  $[x^{i-2}, x^i]$  equals

$$U(x) = \tilde{U}^{(i-2,i)}\left(\frac{x^{i-2} - x}{x^{i-2} - x^i}\right) \quad \text{for } x \in [x^{i-2}, x^i]. \quad (5.44)$$

The function  $\tilde{U}^{(i-2,i)}(x)$  is an irregular solution with jumps at  $\bar{u}^{i-1}$  and  $\bar{u}^i$  of the equation

$$\begin{aligned} 0 &= \frac{1}{(x^i - x^{i-2})^2 \gamma} \tilde{U}_{xx}^{(i-2,i)}(\tilde{x}) + f(\tilde{U}^{(i-2,i)}(\tilde{x}), \tilde{V}^{(i-2,i)}(\tilde{x})), \\ 0 &= g(\tilde{U}^{(i-2,i)}(\tilde{x}), \tilde{V}^{(i-2,i)}(\tilde{x})), \end{aligned} \quad (5.45)$$

for  $\tilde{x} \in [0, 1]$  and with the boundary condition  $\tilde{U}_x^{(i-2,i)}(0) = \tilde{U}_x^{(i-2,i)}(1) = 0$ . Thus, we obtain that the diffusion coefficient  $\frac{1}{\gamma}$  fulfils  $(x^i - x^{i-2})^2 \gamma < \gamma_{\max}^1(\bar{u}^i, \bar{u}^{i+1})$  or  $(x^i - x^{i-2})^2 \gamma < \gamma_{\max}^2(\bar{u}^i, \bar{u}^{i+1})$ , depending on the monotonicity of the solution on  $[0, x^1]$ , because this is the condition for the existence of  $(\tilde{U}^{(i-2,i)}(x), \tilde{V}^{(i-2,i)}(x))$ . This shows that

$$\gamma_{\max}^j(\bar{u}^1, \dots, \bar{u}^k) \leq \frac{\gamma_{\max}^{\text{ind}(i,j)}(\bar{u}^{i-1}, \bar{u}^i)}{(x^i - x^{i-2})^2} \quad (5.46)$$

holds for all  $i \in \{2, \dots, k\}$ .

On the other hand, if for for all  $i = 2, \dots, k$  a solution with jumps at  $\bar{u}^{i-1}$  and  $\bar{u}^i$  and suitable monotonicity of equation (5.45) exists, then they can be composed by equation (5.44) to the unique solution  $(U(x), V(x))$ . We have to show that the definition of  $U$  agrees on the interval  $[x^i, x^{i+1}]$ . This means that

$$\tilde{U}^{(i-2,i)}\left(\frac{x^{i-2} - x}{x^{i-2} - x^i}\right) = \tilde{U}^{(i-1,i+1)}\left(\frac{x^{i-1} - x}{x^{i-1} - x^{i+1}}\right) \quad \text{for } x \in [x^{i-1}, x^i].$$

But this is true, because the restrictions of  $\tilde{U}^{(i-2,i)}$  and  $\tilde{U}^{(i-1,i+1)}$  to the interval  $[x^{i-1}, x^i]$  are both given by a solution of equation (5.35) with diffusion coefficient

$\frac{1}{\gamma(x^i - x^{i-1})^2}$ . Therefore, we obtain the opposite inequality of equation (5.46) and thus equality.

The value of  $\text{ind}(i, j)$  follows from the fact that the restrictions of  $U(x)$  are alternately increasing and decreasing.  $\square$

**Remark 5.4.14.** *The more jumps an irregular solution has the bigger the maximal diffusion coefficient will usually get. This follows from the fact that in formula (5.46) the denominator is a square of a value smaller than one. For example, we have*

$$\gamma_{\max}^1(\bar{u}^1, \bar{u}^2, \bar{u}^3) = \min \left\{ \frac{\gamma_{\max}^1(\bar{u}^1, \bar{u}^2)}{(x^2)^2}, \frac{\gamma_{\max}^2(\bar{u}^2, \bar{u}^3)}{(1-x^1)^2} \right\}.$$

We assume that  $x^1 \approx \frac{1}{3}$  and  $x^2 \approx \frac{2}{3}$ , then the denominator is approximately  $\frac{4}{9}$  and  $\gamma_{\max}^1(\bar{u}^1, \bar{u}^2, \bar{u}^3)$  is almost twice as big as the smaller value of  $\gamma_{\max}^1(\bar{u}^1, \bar{u}^2)$  and  $\gamma_{\max}^2(\bar{u}^2, \bar{u}^3)$ .

We now perform simulations to calculate irregular solutions with jumps  $\bar{u}^1, \dots, \bar{u}^5$ . We choose three different kinetic functions which are the same as in example 4.4.10, 4.4.11 and 4.4.12. We write  $T_i$  for a certain quintuple of jumps

$$T_i = (\bar{u}^1, \bar{u}^2, \bar{u}^3, \bar{u}^4, \bar{u}^5).$$

Motivated by Remark 5.4.11, we compare irregular solutions for jumps which are all close to  $u^*$  to those where the jumps are more distant from  $u^*$ . Moreover, we vary the diffusion coefficients  $\frac{1}{\gamma}$  to see the impact of these variations on the shape of the solutions.

For all plots, we use the same color code. The  $U$ -component of the irregular solution is plotted in blue, whereas the  $V$ -component is red. Moreover, the ticks on the  $x$ -axis always correspond to  $0, \bar{x}^1, x^1, \bar{x}^2, x^2, \bar{x}^3, x^3, \bar{x}^4, x^4, \bar{x}^5, 1$ .

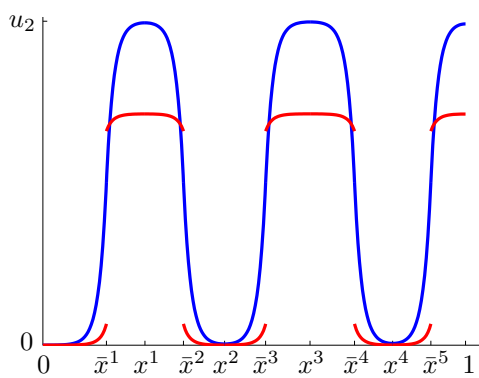
**Example 5.4.15.** *We consider the generic model for the kinetic functions  $f(u, v) = 1.4v - u$  and  $p(v) = v^3 - 6.3v^2 + 10v$ . In this situation  $u^*$  is given by 3.0316,  $u_2 = 6.02$  and  $[u_T, u_H] = [0.24365, 4.7124]$ . In Figure 5.10 we see plots of irregular solutions having jumps at the elements of the quintuples  $T_1, T_2$  and  $T_3$  for two different diffusion coefficients  $\frac{1}{\gamma}$ .*

$$T_1 = (3.03155, 3.03159, 3.03165, 3.0317, 3.0315)$$

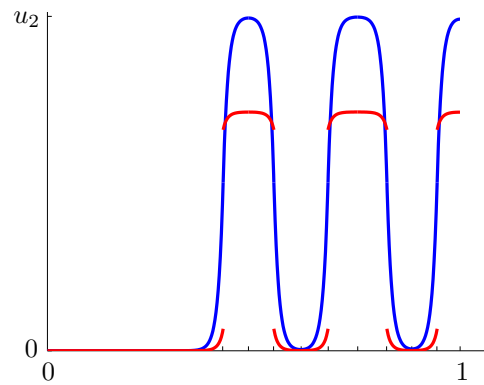
$$T_2 = (3.02, 3.04, 3.05, 3.03, 3.02)$$

$$T_3 = (2.5, 3, 3.5, 3, 2.5)$$

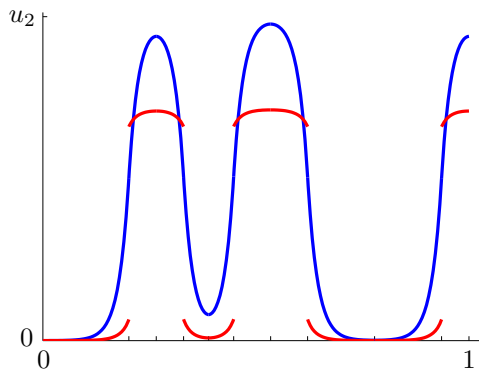
For the elements of  $T_1$  the variation around  $u^*$  is of order  $10^{-4}$ . We observe that the values  $u_0^i$  and  $u_e^i$  are close to 0 and  $u_2$ , respectively, depending on the sign of



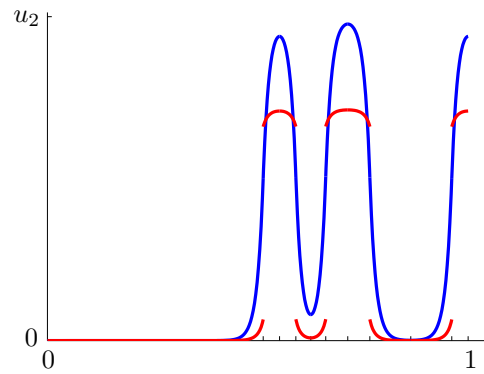
(a) jumps at the elements of  $T_1$  and  $\gamma = 3910$



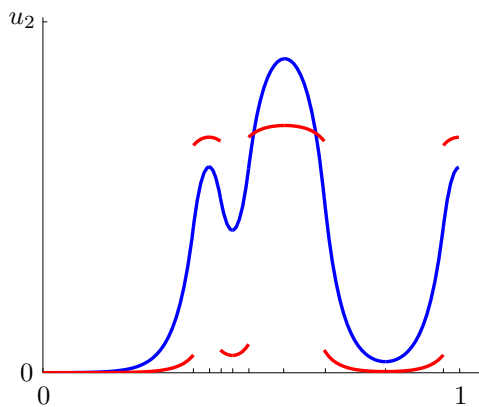
(b) jumps at the elements of  $T_1$  for  $\gamma = 8626$



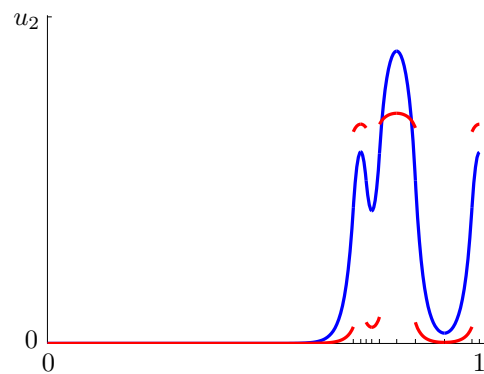
(c) jumps at the elements of  $T_2$  and  $\gamma = 2171$



(d) jumps at the elements of  $T_2$  and  $\gamma = 5948$

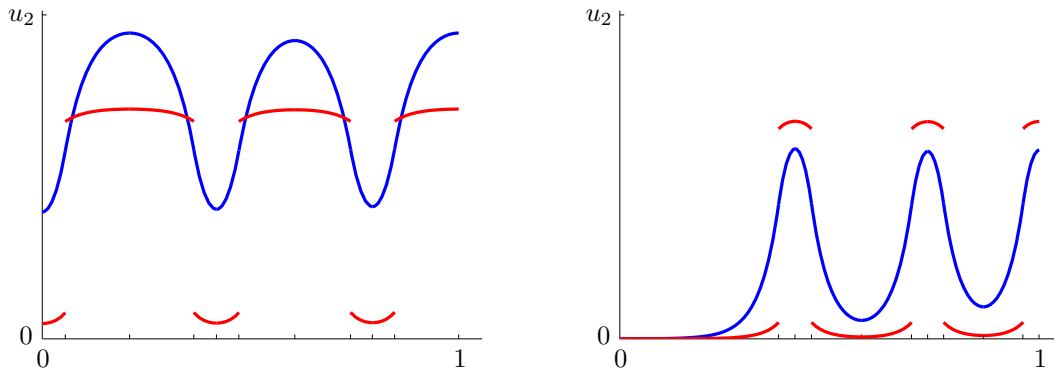


(e) jumps at the elements of  $T_3$  and  $\gamma = 646$



(f) jumps at the elements of  $T_3$  and  $\gamma = 3088$

Figure 5.10: Irregular solutions  $(U(x), V(x))$  with jumps  $\bar{u}^1, \dots, \bar{u}^5$  for the kinetic functions  $f(u, v) = 1.4v - u$  and  $p(v) = v^3 - 6.3v^2 + 10v$  (cf. Example 5.4.15). The diffusion coefficient is  $\frac{1}{\gamma}$  and the jumps  $\bar{u}^i$  vary near  $u^* = 3.0316$ .



(a) jumps at the elements of  $T_4$  and  $\gamma = 351$       (b) jumps at the elements of  $T_5$  and  $\gamma = 590$

Figure 5.11: Irregular solutions  $(U(x), V(x))$  with jumps  $\bar{u}^1, \dots, \bar{u}^5$  for the kinetic functions  $f(u, v) = 1.4v - u$  and  $p(v) = v^3 - 6.3v^2 + 10v$  (cf. Example 5.4.15). The jumps  $\bar{u}^i$  vary near near 2.5 and near 3.5, respectively.

$U_x|_{[x^i, x^{i+1}]}$ . For  $\gamma = 3910$  the solution seems periodic on the first glance, but for  $\gamma = 8626$  it is obviously not periodic.

For the elements of  $T_2$  and  $T_3$  the variation of the jumps around  $u^*$  is of order  $10^{-2}$  and 0.1, respectively. Therefore, we observe that the values  $u_0^i$  and  $u_e^i$  are more distant from 0 and  $u_2$ , respectively, compared to those in  $T_1$ . Moreover, the length of the subintervals  $[x^i, x^{i+1}]$  differ more.

In Figure 5.11 we see irregular solutions having jumps at the elements of the quintuples  $T_4$  and  $T_5$ .

$$T_4 = (3.49, 3.51, 3.5, 3.52, 3.53)$$

$$T_5 = (2.5, 2.51, 2.49, 2.51, 2.52)$$

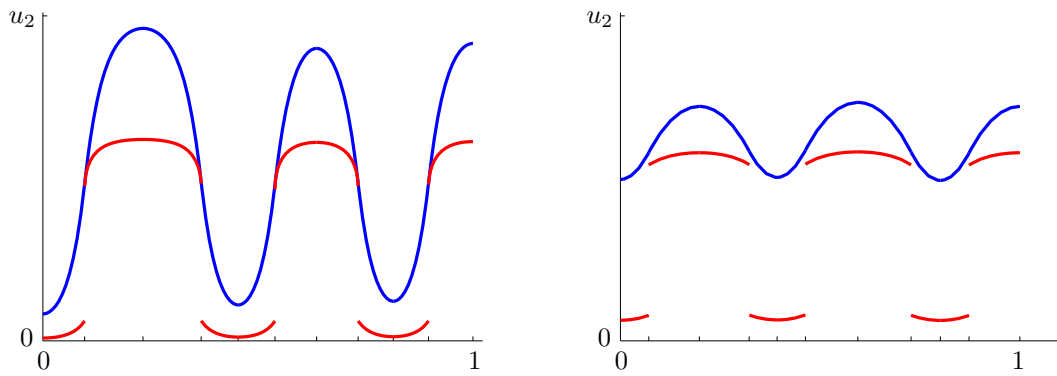
For all jumps in  $T_4$  it holds  $Q(\bar{u}^i, u_2) < 0$  for all  $\bar{u}^i$ . Now, all  $u_0^i$  and  $u_e^i$  which are smaller than  $\bar{u}^i$  are far away from 0, whereas those above  $\bar{u}^i$  are close to  $u_2$ .

For all jumps in  $T_5$  it holds  $Q(\bar{u}^i, u_2) > 0$  for all  $\bar{u}^i$ . All  $u_0^i$  and  $u_e^i$  which are smaller than  $\bar{u}^i$  are close to 0, whereas those above  $\bar{u}^i$  are away from  $u_2$ .

**Example 5.4.16.** We consider the kinetic functions  $f(u, v) = 1.6v - u$  and  $p(v) = v^3 - 6v^2 + 10v$ . In this situation there is no  $u^*$ . The potential  $Q(\bar{u}, u_2)$  is negative for all  $\bar{u}$ . The interval for  $\bar{u}$  is given by  $[u_T, u_H] = [2.9113, 5.0887]$  and  $u_2 = 6.0394$ . In Figure 5.12 we see irregular solutions having jumps at the elements of the quintuples

$$T_6 = (2.92, 2.94, 2.91, 2.92, 2.93)$$

$$T_7 = (3.5, 3.52, 3.54, 3.51, 3.49)$$



(a) jumps at the elements of  $T_6$  and  $\gamma = 765$       (b) jumps at the elements of  $T_7$  and  $\gamma = 81$

Figure 5.12: Irregular solutions  $(U(x), V(x))$  with jumps  $\bar{u}^1, \dots, \bar{u}^5$  for the kinetic functions  $f(u, v) = 1.6v - u$  and  $p(v) = v^3 - 6v^2 + 10v$  (cf. Example 5.4.16). In this situation  $Q(\bar{u}, u_2) < 0$  for all  $\bar{u}$ .

In  $T_6$  the jumps are close to  $u_T$  and vary of order  $10^{-2}$ , whereas in  $T_7$  they are more distant from  $u_T$ , but vary also of order  $10^{-2}$ . The solutions resemble those for jumps in  $T_4$  of Example 5.4.15, because it holds  $Q(\bar{u}, u_2) < 0$  in both cases. The more the jumps are away from  $u_T$  the smaller is the amplitude of the solution, because  $u_{\min}(\bar{u})$  is getting bigger.

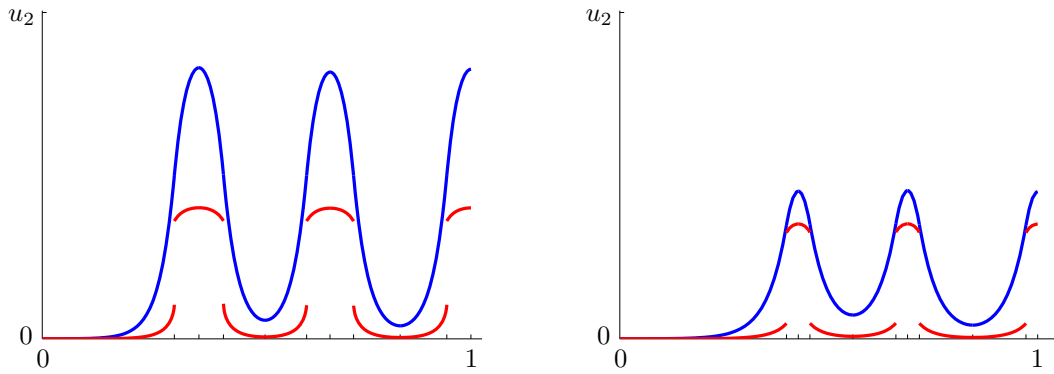
**Example 5.4.17.** We consider the kinetic functions  $f(u, v) = 2.5v - u$  and  $p(v) = v^3 - 6v^2 + 10v$ . In this situation there is no  $u^*$ . The potential  $Q(\bar{u}, u_2)$  is positive for all  $\bar{u}$ . The interval for  $\bar{u}$  is given by  $[u_T, u_H] = [2.9113, 5.0887]$  and  $u_2 = 10.04$ . In Figure 5.13 we see irregular solutions having jumps at the elements of the quintuples

$$T_8 = (5.04, 5.06, 5.03, 5.02, 5.04)$$

$$T_9 = (3.5, 3.53, 3.54, 3.52, 3.5)$$

In  $T_8$  the jumps are close to  $u_H$  and vary of order  $10^{-2}$ , whereas in  $T_9$  they are more distant from  $u_H$ , but vary also of order  $10^{-2}$ . The solutions resemble those for jumps in  $T_5$  in Example 5.4.15, because it holds  $Q(\bar{u}, u_2) > 0$  in both cases. The more the jumps are away from  $u_H$  the smaller is the amplitude of the solution, because  $u_{\max}(\bar{u})$  is getting smaller.

We observe that for jumps  $\bar{u}^i$  such that  $Q(\bar{u}^i, u_2) < 0$  the layer positions are close to the  $x^i$ , which correspond to the local minima of the irregular solution  $(U(x), V(x))$ . Descriptively speaking, the solution has broad peaks and narrow valleys. If all jumps  $\bar{u}^i$  are such that  $Q(\bar{u}^i, u_2) > 0$  the layer positions are close to the local maxima of the irregular solution which then have broad valleys and narrow peaks.



(a) jumps at the elements of  $T_8$  and  $\gamma = 1188$       (b) jumps at the elements of  $T_9$  and  $\gamma = 652$

Figure 5.13: Irregular solutions  $(U(x), V(x))$  with jumps  $\bar{u}^1, \dots, \bar{u}^5$  for the kinetic functions  $f(u, v) = 2.5v - u$  and  $p(v) = v^3 - 6v^2 + 10v$  (cf. Example 5.4.17). In this situation  $Q(\bar{u}, u_2) > 0$  for all  $\bar{u}$ .

We see clearly that for kinetic function such that there exist the value  $u^*$  fulfilling  $Q(u^*, u_2) = 0$ , we can produce a huge variety of irregular solutions, including those which can be produced by kinetic functions such that there is no  $u^*$ .

Finally, we turn our attention to the stability of irregular solutions.

**Theorem 5.4.18.** *We consider the generic model in the hysteresis case with admissible kinetic functions. Let  $(U(x), V(x))$  be an irregular solution with jumps  $\bar{u}^1, \dots, \bar{u}^k$  which are all admissible, then  $(U(x), V(x))$  is asymptotically stable.*

*Proof.* The proof is the same as for Corollary 4.4.9. □

In time-dependent simulations we are able to set up the layer positions by our choice of initial condition, but we do not know the jumps of an irregular solution. We would like to obtain a theorem similar to Theorem 5.2.3. But, as the critical interval depends on the diffusion coefficient, we also need to know the partition  $0, x^1, \dots, x^{k-1}, 1$  of the interval  $[0, 1]$  which is not possible. However, we derive a connection between  $x^{i-1}, x^i$  and  $\bar{x}^i$ .

**Proposition 5.4.19.** *We consider the generic model in the hysteresis case with admissible kinetic functions. An irregular solution  $(U(x), V(x))$  with layer positions  $\bar{x}^1 < \dots < \bar{x}^k$  is a stable solution of the generic model (2.1) for the diffusion coefficient  $\frac{1}{\gamma}$ , requiring that for the partition  $0 = x^0, x^1, \dots, x^{k-1}, 1 = x^k$  it holds:*

$$\frac{\bar{x}^i - x^{i-1}}{x^i - x^{i-1}} \in I^{cr}(\gamma \cdot (x^i - x^{i-1})^2), \quad (5.47)$$

when  $U|_{[x^{i-1}, x^i]}$  is monotone increasing and

$$1 - \frac{\bar{x}^i - x^{i-1}}{x^i - x^{i-1}} \in I^{cr}(\gamma \cdot (x^i - x^{i-1})^2), \tag{5.48}$$

when  $U|_{[x^{i-1}, x^i]}$  is monotone decreasing.

*Proof.* For an irregular solution the restriction  $U|_{[x^{i-1}, x^i]}$  is determined by  $U(x) = \tilde{U}^i\left(\frac{x-x^{i-1}}{x^i-x^{i-1}}\right)$ . The function  $\tilde{U}^i(x)$  is monotone solution of the scaled equation (5.35).

An irregular solution is stable if all  $\tilde{U}^i$  are stable.

The layer position of  $\tilde{U}^i$  is given by  $\frac{\bar{x}^i - x^{i-1}}{x^i - x^{i-1}}$  or  $1 - \frac{\bar{x}^i - x^{i-1}}{x^i - x^{i-1}}$  depending on the monotonicity. The diffusion coefficient of the scaled problem is  $\frac{1}{(x^i - x^{i-1})^2 \gamma}$ . Therefore,  $\tilde{U}^i$  is stable, if its layer position lies in the critical interval  $I^{cr}(\gamma \cdot (x^i - x^{i-1})^2)$ .  $\square$

Now, we perform simulations of the generic model in the hysteresis case with initial conditions, such that we expect the formation of an irregular stationary solution. For determined positions  $0 < \tilde{x}_1 < \tilde{x}_2 < \tilde{x}_3 < \tilde{x}_4 < 1$  we consider initial conditions of type

$$u_0(x) = \begin{cases} 0.2 & \text{for } x \leq \tilde{x}_1 \\ 6 & \text{for } \tilde{x}_1 < x \leq \tilde{x}_2 \\ 0.5 & \text{for } \tilde{x}_2 < x \leq \tilde{x}_3 \\ 5 & \text{for } \tilde{x}_3 < x \leq \tilde{x}_4 \\ 0 & \text{for } \tilde{x}_4 < x \end{cases} \quad \text{and} \quad v_0(x) = \begin{cases} 1.3 & \text{for } x \leq \tilde{x}_1 \\ 5 & \text{for } \tilde{x}_1 < x \leq \tilde{x}_2 \\ 1 & \text{for } \tilde{x}_2 < x \leq \tilde{x}_3 \\ 6 & \text{for } \tilde{x}_3 < x \leq \tilde{x}_4 \\ 0.2 & \text{for } \tilde{x}_4 < x \end{cases}. \tag{5.49}$$

The diffusion coefficient equals  $\frac{1}{\gamma} = \frac{1}{1000}$  for all simulations. We perform simulations for three different choices of kinetic functions. We remark that for all choices the points  $(0.2, 1.3)$ ,  $(0.5, 1)$  and  $(0, 0.2)$  are attracted by the steady state  $S_0$ , whereas  $(6, 5)$  and  $(5, 6)$  are attracted by  $S_2$ .

The discontinuities of the initial condition are given by a quadruple  $L_i = (\tilde{x}_1, \tilde{x}_2, \tilde{x}_3, \tilde{x}_4)$ . For all choices of kinetic functions we use the same six quadruples which are given by

$$\begin{aligned} L_1 &= (0.2, 0.4, 0.6, 0.8) \\ L_2 &= (0.1, 0.4, 0.6, 0.95) \\ L_3 &= (0.2, 0.3, 0.8, 0.9) \\ L_4 &= (0.2, 0.3, 0.4, 0.8) \\ L_5 &= (0.1, 0.15, 0.25, 0.3) \\ L_6 &= (0.3, 0.4, 0.45, 0.55). \end{aligned}$$

For all plots we use the same color code which is in accordance with the one used for irregular solutions (cf. Examples 5.4.15-5.4.15). The  $u$ -component of a solution at a certain time is blue, whereas the  $v$ -component is red. The initial condition  $(u(0, x), v(0, x)) = (u_0(x), v_0(x))$  is indicated by dotted lines and the solution

$(u(t_{end}, x), v(t_{end}, x))$  is indicated by continuous bold lines. Here,  $t_{end}$  is a sufficiently big timepoint, such that the solution  $(u(t, x), v(t, x))$  does not change in time anymore.

**Example 5.4.20.** *We consider the admissible kinetic functions  $f(u, v) = 1.4v - u$  and  $p(v) = v^3 - 6.3v^2 + 10v$ . It holds  $u^* \in (u_T^{cr}, u_H^{cr})$ . For all initial conditions of type (5.49) with discontinuities at  $L_i$  for  $i = 1, \dots, 6$ , we observe the formation of a stable nonhomogeneous stationary solution (cf. Figure 5.14). These stationary solutions are irregular and have layer positions exactly at the discontinuities of the initial condition.*

**Example 5.4.21.** *We consider the admissible kinetic functions  $f(u, v) = 1.6v - u$  and  $p(v) = v^3 - 6v^2 + 10v$ . It holds  $Q(\bar{u}, u_2) < 0$  for all  $\bar{u}$ . For initial conditions with discontinuities at  $L_3, L_5$  and  $L_6$  we observe the formation of the constant stationary solution  $S_0 = (0, 0)$ . For discontinuities at  $L_4$  we obtained a solution with two layer positions, whereas for discontinuities at  $L_1$  and  $L_2$  we observe the formation of a stable irregular solution with four layer positions exactly at the discontinuities of the initial condition. (cf. Figure 5.15).*

*In Example 5.4.16 we have investigated how irregular solutions for these kinetic functions look like. We observed that they all have broad peaks. Therefore, in time-dependent simulations, we remark that narrow peaks which have been set up by the initial conditions disappear.*

**Example 5.4.22.** *We consider the admissible kinetic functions  $f(u, v) = 2.5v - u$  and  $p(v) = v^3 - 6v^2 + 10v$ . It holds  $Q(\bar{u}, u_2) > 0$  for all  $\bar{u}$ . For initial conditions with discontinuities at  $L_1, L_2, L_3, L_4$  and  $L_6$  we observe the formation of the constant stationary solution  $S_2 = (u_2, v_2)$  (cf. Figure 5.16a) for a plot of the solution  $(u(t, x), v(t, x))$  for  $t \in [0, t_{end}]$  for the initial condition with discontinuities at  $L_4$ . For discontinuities at  $L_5$  we observe the formation of a stable irregular solution with four layer positions exactly at the discontinuities of the initial condition (cf. Figure 5.16b)).*

*In Example 5.4.17 we have investigated how irregular solutions for these kinetic functions look like. We observed that they all have narrow peaks. Therefore, in time-dependent simulations, we remark that the initial condition with discontinuities at  $L_5$  leads to peaks which are more narrow than for all other initial conditions.*

To sum up, the simulations show that a solution of the generic model in the hysteresis case strongly depends on the initial condition. When there exists a stable stationary solution with layer positions where it has been prescribed by the initial condition, we observe that the time-dependent solution is quickly approaching this stationary solution. When there is no such stable stationary solution, we observe a moving front finally leading to a constant solution or a stationary solution with less layer position than prescribed by the initial condition.

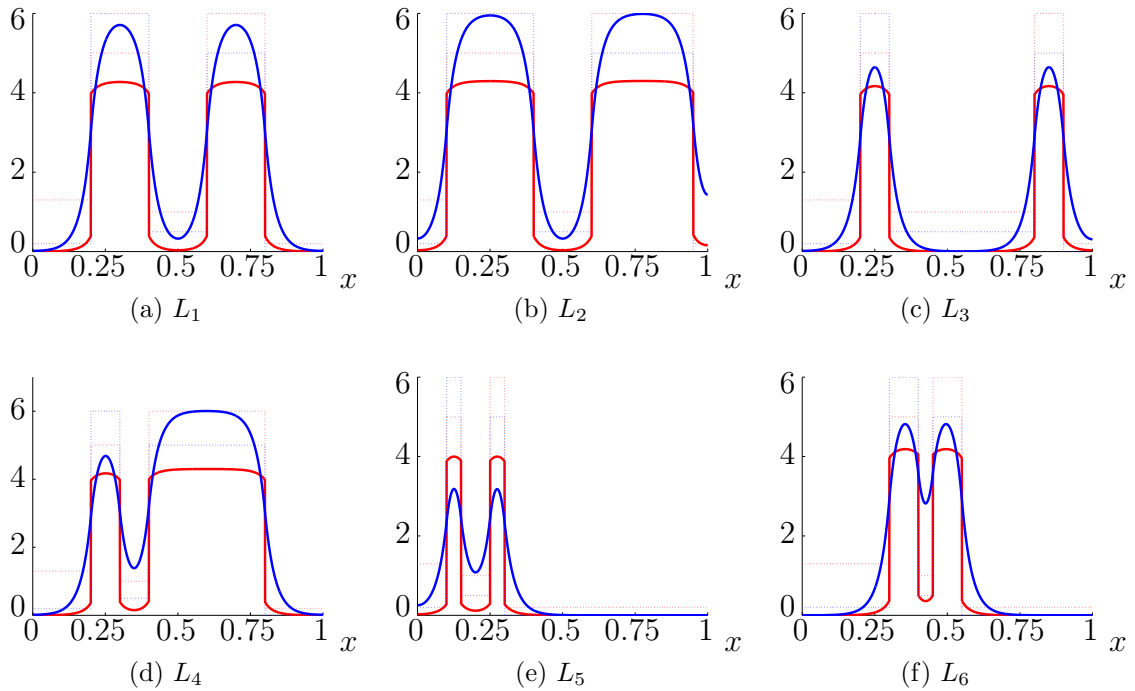


Figure 5.14: Simulations of the generic model in the hysteresis case for admissible kinetic functions  $f(u, v) = 1.4v - u$  and  $p(v) = v^3 - 6.3v^2 + 10v$ , diffusion coefficient  $\frac{1}{\gamma} = \frac{1}{1000}$  and initial conditions of type (5.49) having discontinuities at  $L_i$  (cf. Example 5.4.20).

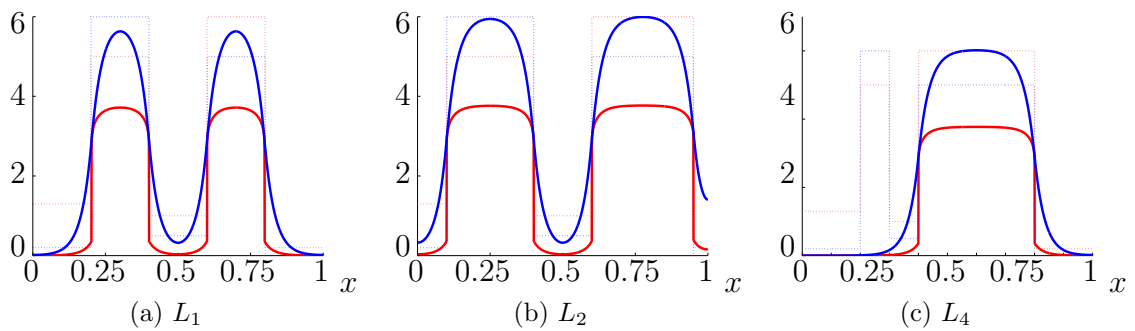


Figure 5.15: Simulations of the generic model in the hysteresis case for admissible kinetic functions  $f(u, v) = 1.6v - u$  and  $p(v) = v^3 - 6v^2 + 10v$ , diffusion coefficient  $\frac{1}{\gamma} = \frac{1}{1000}$  and initial conditions of type (5.49) having discontinuities at  $L_i$  (cf. Example 5.4.21)

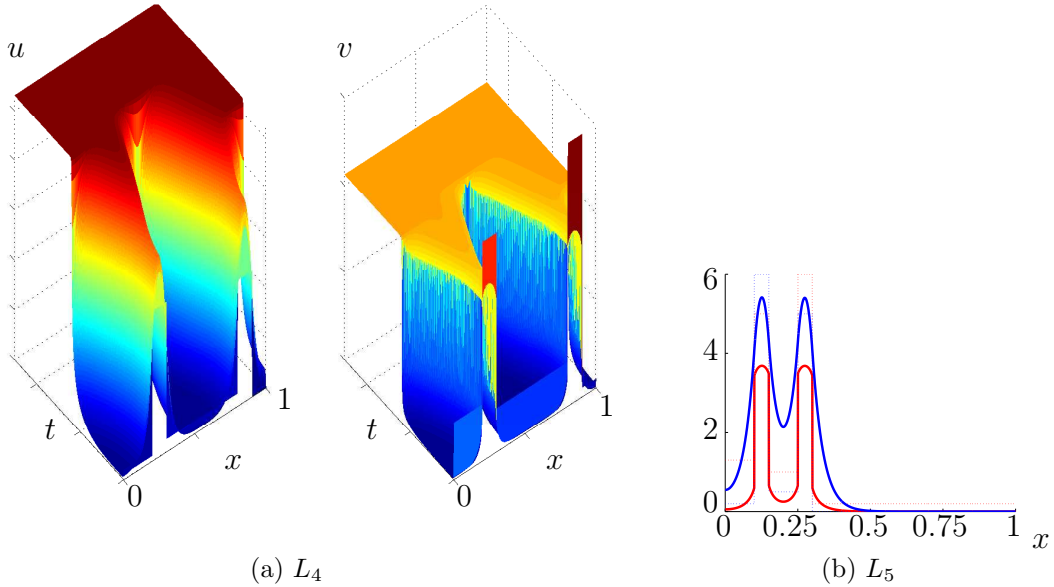


Figure 5.16: Simulations of the generic model in the hysteresis case for admissible kinetic functions  $f(u, v) = 2.5v - u$  and  $p(v) = v^3 - 6v^2 + 10v$ , diffusion coefficient  $\frac{1}{\gamma} = \frac{1}{1000}$  and initial conditions of type (5.49) having discontinuities at  $L_i$  (cf. Example 5.4.22)

We never observed a moving front leading to a stable stationary solution with layer positions at positions different from those prescribed by the initial condition.

We clearly see in the simulations that the most favorable situation to obtain a big variety of stable stationary solutions are kinetic functions which meet the following requirements:

- the kinetic functions are admissible, that means that  $u_T^{cr} < u_H^{cr}$  and
- there is a jump fulfilling  $Q(u^*, u_2) = 0$  which lies in the interval  $u^* \in [u_T^{cr}, u_H^{cr}]$ .

This is in accordance with Theorem 5.3.13 for monotone increasing stationary solutions.

The kinetic functions  $f(u, v) = 1.4v - u$  and  $p(v) = v^3 - 6.3v^2 + 10v$  meet these requirement and, indeed, for all initial conditions used in this thesis, we obtained a stable nonhomogeneous stationary solution (cf. Example 4.4.10 and 4.4.1 for more simulations of the model for these kinetic functions). We can also show that these functions are suitable to explain the outcome of grafting experiments in Hydra. We assume that the concentration of the ligands is given by  $U(x)$ , such that  $(U(x), V(x))$  is a monotone increasing stationary solution of the generic model with layer position at  $\bar{x} = 0.8$ .

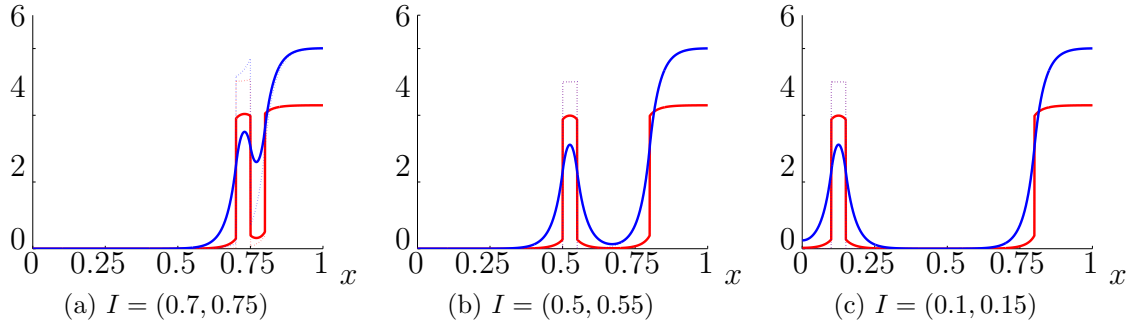


Figure 5.17: Simulations of the generic model in the hysteresis case which simulate the grafting experiments for Hydra. The kinetic functions are  $f(u, v) = 1.4v - u$  and  $p(v) = v^3 - 6.3v^2 + 10v$  and diffusion coefficient  $\frac{1}{\gamma} = \frac{1}{200}$

To simulate the grafting experiments, we use initial conditions

$$u_0(x) = U(x) + 5\chi_I(x) \quad \text{and} \quad v_0(x) = V(x) + 5\chi_I(x),$$

for intervals  $I \subset [0, 1]$  of length 0.05. We observe in Figure 5.17 the formation of irregular stationary solutions for the intervals  $I = (0.7, 0.75)$ ,  $I = (0.5, 0.55)$  and  $I = (0.1, 0.15)$ . The different choices of  $I$  correspond to different positions of the transplantation.

Finally, we describe here heuristically how the nullclines of kinetic functions meeting the requirements look like. First, the polynomial  $p(v) = a_2v^3 + a_1v^2 + a_0v$  has to be curved and not only slightly bend. This is the case, when the coefficients fulfil  $\frac{a_1^2}{a_0a_2}$  is close to 4 (cf. Lemma 2.1.2). Moreover, the straight line  $f(u, v) = \alpha v - \beta u$  has to cut the “S” described by  $p(v)$  in the middle.

## 5.5 Summary

In this chapter, we addressed the problem, how the layer position of a monotone stationary solution depends on the jump and the diffusion coefficient. We proved that for admissible jumps  $\bar{u} \in [u_H^{cr}, u_T^{cr}]$  the layer position depends continuously on the jump and is monotone decreasing. Therefore, for a value  $\bar{x} \in [\bar{x}_{\min}^{cr}, \bar{x}_{\max}^{cr}]$  there is a unique monotone increasing stationary solution with layer position  $\bar{x}$  which is stable.

Moreover, we investigated the dependence of the layer positions on the diffusion coefficient  $\frac{1}{\gamma}$ . We showed that for the jump  $u^*$  defined by  $Q(u^*, u_2) = 0$ , there is an interior transition layer. For all other jumps the layer position is close to the boundary. For  $\gamma$  tending to infinity the layer position approaches 1 for  $\bar{u} < u^*$  and

0 for  $\bar{u} > u^*$  with a steep slope at  $u^*$ . The length of the interval  $[\bar{x}_{\min}^{cr}, \bar{x}_{\max}^{cr}]$  also depends on the diffusion coefficient and, requiring that  $u^* \in [u_T^{cr}, u_H^{cr}]$ , it contains  $(\delta, 1 - \delta)$  with  $\delta$  decreasing for  $\gamma$  increasing.

In the last section of this chapter, we constructed all stationary solutions of the generic model in the hysteresis case. Besides monotone and periodic solutions there are also so-called irregular solutions. Irregular solutions restricted to some subintervals are given by monotone stationary solutions. Restricted to certain subintervals an irregular solution is monotone. The value of the jumps may be different on each of the subintervals. We showed the uniqueness of these solutions for a prescribed set of jumps and their existence for all diffusion coefficients  $\frac{1}{\gamma}$  with  $\gamma$  below a value depending on the jumps.

The most interesting case is when all jumps are near  $u^*$ , because this yields a big maximal  $\gamma$  and the highest variety of behaviour of the irregular solutions. If, moreover, the kinetic functions are admissible and  $u^* \in [u_T^{cr}, u_H^{cr}]$  holds, then all irregular solutions with jumps at  $\bar{u}^i \in [u_T^{cr}, u_H^{cr}]$  are stable.

# Chapter 6

## Summary and Outlook

Mechanisms for pattern formation are an important topic in developmental biology. We presented in this thesis a top-down approach to biological pattern formation inspired by a model for head formation and regeneration in Hydra from Marciniak-Czochra. It has been our aim to analyse under which conditions a model consisting of one reaction-diffusion equation coupled with one ordinary differential equation can describe patterning processes. We included bistability and hysteresis in the kinetic functions and supplemented the model with homogeneous Neumann boundary conditions, nonnegative, uniformly bounded and possibly discontinuous initial conditions. The choice of kinetic functions is heuristic and allowed us to perform analytical investigations and not only numerical ones. Thus, we have obtained mathematical insights which would have been impossible with more realistic, consequently more complicated kinetics.

We distinguished between two cases of the model. In the “bistable case” the model includes bistability in the kinetics, but not the hysteresis effect. The “hysteresis case” refers to the model with hysteresis and also with bistability. Our aim was to compare the abilities to form patterns of these two models.

### Common properties of both cases of the model

We described the parameter spaces for the model in the bistable and the hysteresis case and examined stability properties of spatially homogeneous steady states. The kinetic system possesses two stable steady states and one saddle in both cases. Moreover, these steady states are also stable as solutions of the reaction-diffusion system. Therefore, the model does not exhibit diffusion-driven instability, thus, pattern formation is not due to the Turing mechanism. Furthermore, the stable manifold of the saddle serves as a separatrix for the kinetic system.

We addressed the problems of existence, positiveness and boundedness of time-dependent solutions of the model for both cases. Existence was shown by a direct

proof based on the theory of evolution equations [Bre10] and on Banach's fixed point theorem.

To sum up, on the level of the kinetic systems the model in the bistable and in the hysteresis case exhibits the same dynamics.

## The bistable case

We investigated stationary solutions in the bistable case and showed existence of a finite number of monotone and space periodic solutions for every diffusion coefficient smaller than some critical one. All stationary solutions are classical solutions of a partial differential equation of elliptic type.

But, we also proved the instability of all spatially inhomogeneous stationary solutions. Therefore, the model without hysteresis in the kinetic functions is not able to explain pattern formation.

## The hysteresis case

In the hysteresis case the situation is more complicated and thus more interesting. The steady state equation reduces to one differential equation of elliptic type with discontinuous right hand side. The discontinuity is at the "jump"  $\bar{u}$ , which can be each value in the interval  $(u_T, \min(u_H, u_2))$ . For every jump and every diffusion coefficient we proved the uniqueness of a monotone increasing stationary solution. Therefore, in the hysteresis case, there is an infinite number of stationary solutions for every positive diffusion coefficient. There is no upper bound for the diffusion coefficient like in the bistable case, which has been proved by analysing the time-map associated to the system.

Stationary solutions in the hysteresis case have properties which are different compared to those in the bistable case. The  $u$ -component of the solution is continuously differentiable, whereas the  $v$ -component has a discontinuity at the "layer position"  $\bar{x}$ .

For the stability analysis we defined critical values  $u_H^{cr}$  and  $u_T^{cr}$  which are related to the derivatives of the kinetic functions. They always exist and their relative position is important. The kinetic functions are called admissible when  $u_T^{cr} < u_H^{cr}$  holds.

For stationary solutions of the generic model in the hysteresis case with admissible kinetic functions and having the jump in the interval  $\bar{u} \in [u_T^{cr}, u_H^{cr}]$ , we proved stability with respect to small perturbations in the  $L^\infty(0, 1)$  norm. The stability is not in  $L^2(0, 1)$ , which means in particular that shifting the layer position leads to a different stationary solution. If the kinetic functions are admissible then an infinite number of stationary solutions is stable in  $L^\infty(0, 1)$ .

We observed in simulations that the final outcome of a simulation of the generic model in the hysteresis case strongly depends on the initial condition. The layer positions are set up by the values where the initial condition changes from one side of the separatrix, the stable manifold at  $S_1$ , to the other one. Therefore, we analysed how the layer position depends on the jump  $\bar{u}$  to understand which choice of initial conditions leads to a stable stationary solution. We proved that for  $\bar{u} \in [u_T^{cr}, u_H^{cr}]$  the layer position is monotone decreasing as a function of the jump. This shows that there is an interval of layer positions such that for every prescribed layer position in this interval there is a unique monotone increasing stationary solution, which is stable. We defined the jump  $u^*$  as the one fulfilling  $Q(u^*, u_2) = 0$  and showed that for admissible kinetic functions with  $u^* \in [u_H^{cr}, u_T^{cr}]$ , the interval of layer positions leading to stable stationary solutions is the biggest. This interval is getting bigger for increasing  $\gamma$ .

Finally, we constructed all stationary solutions of the model in the hysteresis case. Besides monotone and periodic solutions, there are so-called irregular solutions. The restriction of an irregular solution to certain subintervals are given by monotone stationary solutions with possibly different jumps.

We proved the uniqueness of irregular solutions for a prescribed set of jumps and their existence for all diffusion coefficients  $\frac{1}{\gamma}$  with  $\gamma$  below a value depending on the jumps.

The biggest variety of irregular solutions exists when all jumps are near  $u^*$ . On the one hand the maximal  $\gamma$  is bigger, when all jumps are close to each other, on the other hand for  $\bar{u}$  close to  $u^*$  the layer position can achieve a big range of values.

In simulations of the generic model in the hysteresis case, we justified that admissible kinetic functions for which the value  $u^*$  exists and lies in the interval  $[u_H^{cr}, u_T^{cr}]$  are the most favorable for pattern formation. For a huge amount of initial conditions, we observed the formation of a stable stationary solution with layer positions where it has been prescribed by the initial condition.

The generic model in the hysteresis case is able to explain pattern formation triggered by some external signal which yields a sufficiently strong initial perturbation. Therefore, such mechanisms can explain grafting experiments for Hydra. It explains pattern formation for different sizes of the transplant, bigger than a minimal size.

## Outlook

The next step of our work is to apply the hysteresis-driven mechanism for pattern formation in more realistic situations. It is well-known that the Wnt-pathway plays a pivotal role in the head formation and regeneration in Hydra [HPA<sup>+</sup>10] [HRea00] [BGRB05]. The head activator is assumed to be a molecule in this pathway and

could play the role of the diffusing molecule in our model. A detailed analysis of the pathway may lead to a more realistic production rate which exhibits the hysteresis effect. The hysteresis-driven mechanism might explain the inducing capacities of the hypostome.

In combination with equations for the head organizer which should be based on mechanism which is able to explain the self-organising capacities, for example the Turing mechanism, this may lead to a full description of the patterning processes in Hydra.

# Appendix A

## Models for pattern formation in Hydra

### A.1 Activator-inhibitor model

The activator-inhibitor model proposed by Gierer and Meinhardt in [GM72] reads

$$\begin{aligned}\frac{\partial}{\partial t}a &= D_a \frac{\partial^2}{\partial x^2}a + \rho \frac{a^2}{h} + \rho_a - \mu_a a, \\ \frac{\partial}{\partial t}h &= D_h \frac{\partial^2}{\partial x^2}h + \rho a^2 + \rho_h - \mu_h h.\end{aligned}$$

Here,  $a$  denotes the concentration of the activator and  $h$  the concentration of the inhibitor.

### A.2 Receptor-based models

A receptor-based model for pattern formation in Hydra proposed by Marciniak-Czochra in [MC03] reads

$$\begin{aligned}\frac{\partial}{\partial t}r_f &= -\mu_f r_f + p_r(r_b) - br_f l + dr_b, \\ \frac{\partial}{\partial t}r_b &= -\mu_b r_b + br_f l - dr_b, \\ \frac{\partial}{\partial t}l &= d_l \frac{\partial^2}{\partial x^2}l - \mu_l l - br_f l + p_l(r_b) + dr_b - b_e l e, \\ \frac{\partial}{\partial t}e &= d_e \frac{\partial^2}{\partial x^2}e - \mu_e e + p_e(l, r_b),\end{aligned}$$

Here,  $r_f$  denotes the concentration of free receptors,  $r_b$  the concentration of bound receptors,  $l$  the concentration of ligands and  $e$  the concentration of an enzyme.  $p_r$ ,  $p_l$  and  $p_e$  are production rates which have been modelled by a Hill function.

For the receptor-based model with hysteresis, the production rates for ligands and enzyme have been modelled by two ordinary differential equations:

$$\begin{aligned}\frac{\partial}{\partial t} p_l &= -\delta_l \frac{p_l}{1+p_l^2} + \frac{m_2 l r_b}{(1+\sigma_l p_l^2 - \beta_l p_l)(1+\alpha_l r_b)}, \\ \frac{\partial}{\partial t} p_e &= -\delta_e \frac{p_e}{1+p_e^2} + \frac{m_3 l e}{(1+\sigma_e p_e^2 - \beta_e p_e)(1+\alpha_e r_b)}.\end{aligned}$$

# Bibliography

- [AFS04] D. Angeli, J. E. Ferrell, and E. D. Sontag. Detection of multistability, bifurcations, and hysteresis in a large class of biological positive-feedback systems. *PNAS*, 101:1822–1827, 2004.
- [Arn06] V. I. Arnold. *Mathematical methods of classical mechanics*. Springer, New York, 2. ed. edition, 2006.
- [ATH84] D.G. Aronson, A. Tesei, and H. Weinberger. A density-dependent diffusion system with stable discontinuous stationary solutions. *Annali di Matematica Pura ed Applicata*, 152:259–280, 1988(4).
- [Bal12] P. Ball. Pattern formation in nature: Physical constraints and self-organising characteristics. *Architectural Design*, 82(2):22–27, 2012.
- [BB02] M. Broun and H. R. Bode. Characterization of the head organizer in hydra. *Development*, 129:875–884, 2002.
- [BGRB05] M. Broun, L. Gee, B. Reinhardt, and H. R. Bode. Formation of the head organizer in hydra involves the canonical wnt pathway. *Development*, 132:2907–2916, 2005.
- [Bre10] H. Brezis. *Functional Analysis, Sobolev Spaces and Partial Differential Equations*. Springer, 2010.
- [Chi00] C. Chicone. *Ordinary Differential Equations with Applications*. Springer, 2000.
- [Eva08] L. C. Evans. *Partial differential equations*. Graduate studies in mathematics. American Mathematical Society, Providence, RI, 2008.
- [Fer08] J. E. Ferrell. Feedback regulation of opposing enzymes generates robust, all-or-none bistable responses. *Current Biology*, 18(6):244–245, 2008.
- [For10] O. Forster. *Analysis 2*. Vieweg+Teubner, Wiesbaden, 2010.

- [FX01] J. E. Ferrell and W. Xiong. Bistability in cell signalling: How to make continuous processes discontinuous, and reversible processes irreversible. *Chaos*, 11:227–236, 2001.
- [Gal12] B. Galliot. Hydra, a fruitful model system for 270 years. *International Journal of Developmental Biology*, 56:411–423, 2012.
- [GM72] A. Gierer and H. Meinhardt. A theory of biological pattern formation. *Biological Cybernetics*, 12:30–39, 1972.
- [Gri91] P. Grindrod. *Patterns and waves*. Oxford applied mathematics and computing science series. Clarendon Press, Oxford, 1991.
- [GT12] P. Gurevich and S. Tikhomirov. Uniqueness of transverse solutions for reaction-diffusion equations with spatially distributed hysteresis. *Non-linear Analysis*, 75:6610–6619, 2012.
- [GTDR10] T. G.W. Graham, S.M. A. Tabei, A. R. Dinner, and I. Rebay. Modelling bistable cell-fate choices in the drosophila eye: qualitative and quantitative perspectives. *Development*, 137:2265–2278, 2010.
- [GWM<sup>+</sup>07] T. Gregor, E. F. Wieschaus, A. P. McGregor, W. Bialek, and D. W. Tank. Stability and nuclear dynamics of the bicoid morphogen gradient. *Cell*, 130(1):141–152, 2007.
- [Ham12] H. Hamada. In search of turing in vivo: Understanding nodal and lefty behavior. *Developmental Cell*, 22:911–912, 2012.
- [Hen93] D. Henry. *Geometric theory of semilinear parabolic equations*. Number 840 in Lecture notes in mathematics. Springer, Berlin ; Heidelberg [u.a.], 1993.
- [HJ80] F. Hoppensteadt and W. Jäger. Pattern formation in bacteria. In S. Levin, editor, *Lecture Notes in Biomathematics: Biological growth and spread*, pages 69–81. Springer, 1980.
- [HJP83] F. Hoppensteadt, W. Jäger, and C. Pöppe. A hysteresis model for bacterial growth pattern. In S. Levin, editor, *Lecture Notes in Biomathematics: Modelling of Pattern in Space and Time*, pages 123–134. Springer, 1983.
- [HPA<sup>+</sup>10] B. Hobmayer, I. Philipp, R. Aufschnaiter, M.-K. Eder, and M. Jenewein. Wnts in der Achsenbildung und Morphogenese bei Hydra. *BIOspektrum*, 7:746–748, 2010.

- [HRea00] B. Hobmayer, F. Rentzsch, and K. Kuhn et al. Wnt signaling molecules act in axis formation in the diploblastic metazoan hydra. *Nature*, 407:186–189, 2000.
- [JK99] J. Jaros and T. Kusano. A picone type identity for second order half-linear differential equations. *Acta Mathematica Universitatis Comenianae*, 68:137–151, 1999.
- [KA95] S. Kondo and R. Asai. A reaction-diffusion wave on the skin of the marine angelfish pomacanthus. *Nature*, 376:765–768, 1995.
- [Kle98] C. Klein. Hysteresis-driven structure formation in biochemical networks. *Journal of theoretical biology*, 194:263–274, 1998.
- [KM10] S. Kondo and T. Miura. Reaction-diffusion model as a framework for understanding biological pattern formation. *Science*, 329:1616–1620, 2010.
- [KW07] M. Kerszberg and L. Wolpert. Specifying positional information in the embryo: Looking beyond morphogens. *Cell*, 130:205–209, 2007.
- [Lan11] A. D. Lander. Pattern, growth, and control. *Cell*, 144:955–969, 2011.
- [Lew08] J. Lewis. From signals to patterns: Space, time, and mathematics in developmental biology. *Science*, 322:399–403, 2008.
- [LK99] M. Laurent and N. Kellershohn. Multistability: a major means of differentiation and evolution in biological systems. *Trends in Biochemical Sciences*, 24:418–422, 1999.
- [Lou59] W. Loud. Periodic solutions of  $x'' + cx' + g(x) = \epsilon f(t)$ . *Memoirs of the American Mathematical Society*, 31:58, 1959.
- [LVH<sup>+</sup>08] F. J.P. Lopes, F. M.C. Vieira, D. M. Holloway, P. M. Bisch, and A. V. Spirov. Spatial bistability generates hunchback expression sharpness in the drosophila embryo. *PLOS Computational Biology*, 4, 2008.
- [MC03] A. Marciniak-Czochra. Receptor-based models with diffusion-driven instability for pattern formation in hydra. *Journal of Biological Systems*, 11 (3):293–324, 2003.
- [MC04] A. Marciniak-Czochra. *Developmental models with cell surface receptor densities defining morphological position*. PhD thesis, Universität Heidelberg, Fakultät für Mathematik und Informatik, 2004.

- [MC06] A. Marciniak-Czochra. Receptor-based models with hysteresis for pattern formation in hydra. *Mathematical biosciences*, 199(1):97–119, 2006.
- [MCK13] A. Marciniak-Czochra and A. Köthe. Multistability and hysteresis-based mechanism of pattern formation in biology. In V. Capasso, M. Gromov, and N. Morozova, editors, *Pattern Formation in Morphogenesis-problems and their Mathematical Formalization*, volume 15 of *Springer Proceedings in Mathematics*, pages 153–173, 2013.
- [MCKS13] A. Marciniak-Czochra, G. Karch, and K. Suzuki. Unstable patterns in autocatalytic reaction-diffusion-ode systems. *arXiv:1301.2002 [math.AP]*, 2013.
- [MU78] T. Myint-U. *Ordinary Differential Equations*. Elsevier North-Holland, 1978.
- [Mur03] J. D. Murray. *Spatial models and biomedical applications*. Interdisciplinary applied mathematics. Springer, New York ; Berlin ; Heidelberg, 2003.
- [Nak12] M. Nakayama. *Mathematical analysis of a system of diffusive and non-diffusive species modeling pattern formation in Hydra*. PhD thesis, Tohoku University, Sendai, Japan, 2012.
- [Nie01] C. Niehrs. The Spemann organizer and embryonic head induction. *The EMBO Journal*, 20:631–637, 2001.
- [Nis82] Y. Nishiura. Global structure of bifurcating solutions of some reaction-diffusion systems. *Siam journal mathematical analysis*, 13:555–593, 1982.
- [Paz83] A. Pazy. *Semigroups of linear operators and applications to partial differential equations*. Number 44 in Applied mathematical sciences. Springer, New York ; Heidelberg [u.a.], 1983.
- [PSJ03] J. R. Pomeroy, E. D. Sontag, and J. E. Ferrell Jr. Building a cell cycle oscillator: hysteresis and bistability in the activation of *cdc2*. *Nature Cell Biology*, 5(4):346–251, 2003.
- [QX10] K. Qin and C. Xiang. Hysteresis modeling for calcium-mediated ciliary beat frequency in airway epithelial cells. *Mathematical biosciences*, 229:101–108, 2010.
- [RHL77] N. Rouche, P. Habets, and M. Laloy. *Stability Theory by Liapunov's Direct Method*. Springer, 1977.

- [Sch90] R. Schaaf. *Global solution branches of two point boundary value problems*. Springer, 1990.
- [SMC<sup>+</sup>03] W. Sha, J. Moore, K. Chen, A. D. Lassaletta, C.-S. Yi, and J. J. Tyson. Hysteresis drives cell-cycle transitions in xenopus laevis egg extracts. *PNAS*, 100:975–980, 2003.
- [SMJ95] J. A. Sherrat, P.K. Maini, and W. Jäger. A receptor based model for pattern formation in hydra. *Forma*, 10:77–95, 1995.
- [Smo83] J. Smoller. *Shock waves and reaction-diffusion equations*. Number 258 in Die Grundlehren der mathematischen Wissenschaften in Einzeldarstellungen ; 258. Springer, New York ; Heidelberg ; Berlin, 1983.
- [TA07] C. J. Tomlin and J. D. Axelrod. Biology by numbers: mathematical modelling in developmental biology. *Nature Reviews*, 8:331–340, 2007.
- [Tur51] A.M. Turing. The chemical basis of morphogenesis. *Philosophical Transactions of the Royal Society of London B*, 237:37–72, 1951.
- [USOO06] D. M. Umulis, M. Serpe, M. B. O’Connor, and H.G. Othmer. Robust, bistable patterning of the dorsal surface of the drosophila embryo. *PNAS*, 103:11613–11618, 2006.
- [Ver10] F. Verhulst. *Nonlinear differential equations and dynamical systems*. Universitext. Springer, Berlin ; Heidelberg[u.a.], 2010.
- [WF05] Y.-C. Wang and E. L. Ferguson. Spatial bistability of dpp-receptor interactions during drosophila dorsal-ventral patterning. *Nature*, 434:229–234, 2005.
- [Wil09] T. Wilhelm. The smallest chemical reaction system with bistability. *BMC Systems Biology*, 3:90, 2009.